INFORMATION TO USERS

This manuscript has been reproduced from the microfilm master. UMI films the text directly from the original or copy submitted. Thus, some thesis and dissertation copies are in typewriter face, while others may be from any type of computer printer.

The quality of this reproduction is dependent upon the quality of the copy submitted. Broken or indistinct print, colored or poor quality illustrations and photographs, print bleedthrough, substandard margins, and improper alignment can adversely affect reproduction.

In the unlikely event that the author did not send UMI a complete manuscript and there are missing pages, these will be noted. Also, if unauthorized copyright material had to be removed, a note will indicate the deletion.

Oversize materials (e.g., maps, drawings, charts) are reproduced by sectioning the original, beginning at the upper left-hand corner and continuing from left to right in equal sections with small overlaps.

Photographs included in the original manuscript have been reproduced xerographically in this copy. Higher quality 6" x 9" black and white photographic prints are available for any photographs or illustrations appearing in this copy for an additional charge. Contact UMI directly to order.

Bell & Howell Information and Learning
300 North Zeeb Road, Ann Arbor, MI 48106-1346 USA
800-521-0600

UMI®

UNIVERSITY OF CALIFORNIA

Los Angeles

Control of Nonlinear Differential Difference Equation Systems: Theory and Application to Chemical Processes

A thesis submitted in partial satisfaction of the requirements for the degree Doctor of Philosophy in Chemical Engineering

by

Charalambos Ioanni Antoniades

2000

The thesis of Charalambos Ioanni Antoniades is approved.

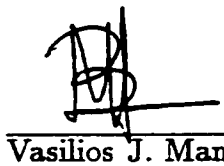

Vasilios J. Manousiouthakis

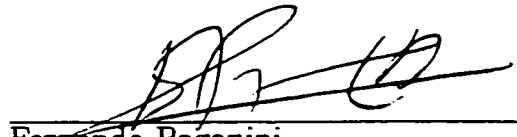

Fernando Paganini

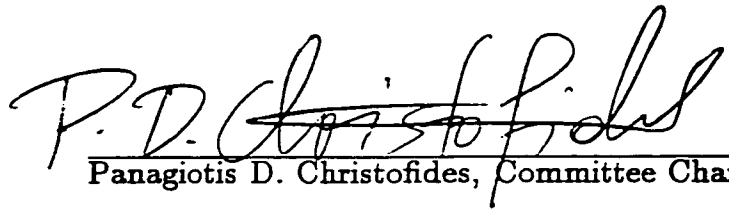

Panagiotis D. Christofides, Committee Chair

University of California, Los Angeles

2000

Contents

List of Figures

List of Tables

ACKNOWLEDGMENTS

I am grateful to my advisor, Prof. Panagiotis Christofides, for his guidance and support in the course of this project.

I would like to thank Prof. Vasilios J. Manousiouthakis, Prof. James C. Liao and Prof. Fernando Paganini for agreeing to participate in my examination committee.

Special acknowledgments to my family in Cyprus, for their constant support, encouragement, and dedication.

VITA

December 28, 1969	Born, Famagusta, Cyprus
1987-89	Military Service
1989	Five-year scholarship for studies at National Technical University of Athens from the Government of Cyprus
1993-94	Field work as Environmental Engineer Ministry o Labor, Department of Industrial Inspection Nicosia, Cyprus
1995	Diploma, Chemical Engineering National Technical University Athens, Greece
1995	Associate Consultant Planning AE Consulting Company Athens, Greece
1995-96	Environmental Engineer Hydrotech Water and Environmental Engineering Limassol, Cyprus
1996	Post Graduate Diploma, Management Mediterranean Institute of Management Nicosia, Cyprus
1996	Full scholarship for graduate studies at University of California at Los Angeles from the Fulbright Commission
1997-98	Teaching Assistant Department of Chemical Engineering University of California at Los Angeles
1998	M.S., Chemical Engineering University of California Los Angeles, California
1998-2000	Teaching Assistant Coordinator Department of Chemical Engineering University of California at Los Angeles

PUBLICATIONS AND PRESENTATIONS

Christofides, P. D. and C. Antoniades, "Control of Nonlinear Differential Difference Equation Systems", AIChE Annual Meeting, paper 191i, Los Angeles, California, 1997.

Christofides, P. D. and C. Antoniades, "Control of Nonlinear Differential Difference Equation Systems," *Proceedings of Mathematical Theory of Networks and Systems-98 Conference*, 41-44, Padova, Italy, 1998.

Antoniades, C. and P. D. Christofides, "Robust State Estimation and Control of Nonlinear Time Delay Processes", AIChE Annual Meeting, paper 228c, Miami, Florida, 1998.

Antoniades, C. and P. D. Christofides, "Feedback Control of Nonlinear Differential Difference Equation Systems", *Chem. Eng. Sci.*, Vol. **54**(23), 5677-5709, 1999.

Antoniades, C. and P. D. Christofides, "Robust Control of Nonlinear Time-Delay Systems", *Appl. Math. & Comp. Sci.*, Vol. **9**(4), 101-127, 1999.

Antoniades, C. and P. D. Christofides, "Analyzing the Interaction of Design and Control in Transport-Reaction Processes", AIChE Annual Meeting, paper 219a, Dallas, Texas, 1999.

Antoniades, C. and P. D. Christofides, "Computation of Optimal Actuator Locations for Nonlinear Controllers in Transport-Reaction Processes", *Comp. & Chem. Eng.*, Vol. **24**(2-7), 577-583, 2000.

Antoniades, C. and P. D. Christofides, "Nonlinear Feedback Control of Parabolic Partial Differential Difference Equation Systems", *Int. J. Contr.*, Vol. **54**, 1572-1591, 2000.

Antoniades, C. and P. D. Christofides, "Studies on Nonlinear Dynamics and Control of Tubular Reactors with Recycle", Third World Congress of Nonlinear Analysis, Catania, Italy, 2000.

Antoniades, C. and P. D. Christofides, "Optimal Actuator/Sensor Placement of Robust Controllers in Uncertain Transport-Reaction Processes", AIChE Annual Meeting, paper 256b, Los Angeles, California, 2000.

Armaou, A. and Antoniades, C. and P. D. Christofides, "Real Time Control of a PECVD Reactor", AIChE Annual Meeting, paper 260i, Los Angeles, California, 2000.

Antoniades, C. and P. D. Christofides, "Studies on Nonlinear Dynamics and Control of a Tubular Reactor with Recycle," *Nonlinear Analysis: Theory, Methods & Applications*, to appear.

ABSTRACT OF THE DISSERTATION

Control of Nonlinear
Differential Difference Equation Systems:
Theory and Application to Chemical Processes

by

Charalambos Ioanni Antoniades
Doctor of Philosophy in Chemical Engineering
University of California, Los Angeles, 2000

Professor Panagiotis D. Christofides, Chair

The dynamic models of many chemical engineering processes involve severe nonlinearities and significant time delays and are naturally described by nonlinear differential difference equation (DDE) systems. Nonlinearities usually arise from complex reaction mechanisms and Arrhenius dependence of reaction rates on temperature, while time delays often occur due to transportation lag such as in flow through pipes, dead times associated with measurement sensors (measurement delays) and control actuators (manipulated input delays), and approximation of high-order dynamics. Typical examples of processes which involve nonlinearities and time delays include chemical reactors with recycle loops, fluidized catalytic cracking units, distillation columns, chemical vapor deposition processes to name a few.

While the co-presence of nonlinearities and time-delays in several chemical processes is well-known, the existing approach to control nonlinear time-delay systems

is to neglect the presence of time delays and address the controller design problem on the basis of the resulting nonlinear ordinary differential equation (ODE) systems. Clearly, such an approach limits the achievable control quality and may lead to severe degradation of the desired performance, or even to destabilization of the closed-loop system in the presence of significant time delays. Furthermore, most general methods for the design of controllers for time-delay processes require that the process model used for controller design is linear. At this stage, there is no rigorous, yet practical, method for the design of nonlinear controllers for *nonlinear* DDE systems with state, manipulated input and measured output delays.

Motivated by the above, this doctoral thesis presents a general and practical framework for the synthesis of nonlinear and robust controllers for broad classes of nonlinear DDE systems that include time-delays in the states, manipulated input and measured output. The proposed controller designs are based on novel integrations of geometric, Lyapunov and spectral decomposition techniques, and the resulting controllers use measurements of process output to enforce stability, output tracking and uncertainty attenuation in the closed-loop system, independently of the size of the delays. The proposed methods are applied to chemical processes of industrial interest and their effectiveness and advantages with respect to control methods that do not account for the effect of time delays is documented through detailed computer simulations.

Chapter 1

Introduction

The dynamic models of many chemical engineering processes involve severe nonlinearities and significant time delays and are naturally described by nonlinear differential difference equation (DDE) systems. Nonlinearities usually arise from complex reaction mechanisms and Arrhenius dependence of reaction rates on temperature, while time delays often occur due to transportation lag such as in flow through pipes, dead times associated with measurement sensors (measurement delays) and control actuators (manipulated input delays), and approximation of high-order dynamics. Typical examples of processes which involve nonlinearities and time delays include chemical reactors with recycle loops, fluidized catalytic cracking units, distillation columns, chemical vapor deposition processes to name a few.

Motivated by the inherently nonlinear nature of physical and chemical processes, in the last decade, a flourishing research activity has emerged towards the development of feedback control methods for nonlinear lumped parameter processes (i.e. processes described by nonlinear ordinary differential equations (ODEs)). Differential geometry has proven to be a natural framework for the analysis and control of such systems. Within this framework, key aspects of nonlinear dynamics and

important control-theoretic properties have been well-understood. Furthermore, basic control problems, including the modification of the input/output behavior, the elimination of measurable disturbances, and the attenuation of unmeasured disturbances and unknown parameters have been successfully addressed. Specifically, in this area, important contributions include the synthesis of state feedback controllers (e.g., [69, 83, 85]), the design of state estimators [75, 136] and output feedback controllers (e.g., [53, 52, 135, 94, 37]), the design of robust [86, 16, 2, 48, 41] controllers for nonlinear systems with uncertainty, the synthesis of well-conditioned controllers for nonlinear multiple-time-scale systems [43, 47, 90, 34], and the synthesis of controllers for nonlinear constrained systems [95, 76, 73, 139, 32]. Successful experimental applications of the above nonlinear control methods to lumped parameter chemical processes have been also reported including control of distillation columns [100], polymerization reactors [131, 137, 138], pH neutralization processes [154, 155, 115] and activated sludge processes [123]. Excellent reviews of results in the area of nonlinear process control can be found in [84, 85, 82, 21, 1, 121, 97].

The conventional approach to control linear/nonlinear DDE systems is to neglect the presence of time delays and address the controller design problem on the basis of the resulting linear/nonlinear ODE systems, employing standard control methods for ODE systems. However, it is well-known (see, for example, [140]) that such an approach may pose unacceptable limitations on the achievable control quality and cause serious problems in the behavior of the closed-loop system including poor performance (e.g., sluggish response, oscillations) and instability. Motivated by these limitations, significant research efforts have focused on the development of control methods for linear DDE systems that compensate for the effect of time delays. Research initially focused on linear systems with a single manipulated input delay which are described

by transfer function models, in which the presence of the time delay prevents the use of large controller gains (i.e., the proportional gain of a proportional-integral controller should be sufficiently small in order to avoid destabilization of the closed-loop system), thereby leading to sluggish closed-loop response. To overcome this problem, O. J. M. Smith [133] proposed a control structure, known as Smith predictor, which completely eliminates the time delay from the characteristic polynomial of the closed-loop system, allowing the use of larger controller gains. Since then many researchers have proposed alternatives or modifications of the Smith predictor structure (e.g., [147]), extensions to control structures for linear systems including inferential control [28] and internal model control [60], other predictor structures such as the analytical predictor [111, 151] and established connections of the Smith predictor with other predictors [152]. The Smith predictor structure has also been extended to linear multivariable systems with multiple input and output delays which are described by transfer function models, leading to multi-delay compensators [114, 71]. Excellent reviews of results on Smith and other predictor structures can be found in [71, 152].

Even though the above works provided powerful methods for dealing with control actuator and measurement dead time in linear systems, they do not explicitly account for the effect of time delays in the process state variables. This motivates research on the design of controllers for DDE systems with state delays. In this direction, the application of classical optimal control approaches to DDE systems in order to design optimal distributed parameter (infinite-dimensional) controllers was initially studied (e.g., [134, 122]). Then, the distributed parameter nature of the developed controllers motivated research on the problem of model reduction of linear DDE systems. This problem is the one of finding a linear low-dimensional ODE system that accurately reproduces the solutions of a linear DDE system. Approaches to

address this problem include balanced approximation based on controllability and observability gramians [103], frequency response analysis [62], and approximations using Fourier-Laguerre models [118, 148] to name a few. An alternative approach for the synthesis of controllers for linear DDE systems with state delays that stabilize the closed-loop system independently of the size of the delays is based on the method of Lyapunov functionals [63]. The central idea of this approach is to synthesize a linear controller so that the time-derivative of an appropriate Lyapunov functional calculated along the trajectories of the closed-loop DDE system is negative definite, independently of the size of the delays. The method of Lyapunov functionals has been used in the design of linear stabilizing controllers for linear DDE systems in [126, 113].

Despite the abundance of results on control of linear DDE systems, most of the research on nonlinear DDE systems has focused on the derivation of conditions for existence and uniqueness of solutions, the understanding of qualitative and geometric properties of the solutions (see the book [63] for results and reference lists), and stability analysis through Razumikhin-type theorems and nonlinear small-gain theorem techniques (e.g., [156, 143]). Very few results are available on control of nonlinear DDE systems, with the exception of optimal control methods [79, 122]. For nonlinear systems represented by input-output models, extensions of the Smith predictor have been proposed in [153, 20]. The existing approach to control nonlinear time-delay systems is to neglect the presence of time delays and address the controller design problem on the basis of the resulting nonlinear ODE systems. It is well-accepted that such an approach limits the achievable control quality and may lead to severe degradation of the desired performance, or even to destabilization of the closed-loop system in the presence of significant time delays. To our knowledge, within a state-

space framework, the only available results on controller synthesis are for single-input single-output nonlinear systems with a single manipulated input delay, for which a nonlinear Smith predictor structure was proposed in [87] under the assumption of open-loop stability, and further extended to open-loop unstable systems in [65]. At this stage, there is no rigorous, yet practical, method for the design of nonlinear controllers for *nonlinear* DDE systems with state, manipulated input and measured output delays.

Motivated by the fact that many industrially-important chemical processes involve nonlinearities and time-delays, and the lack of general nonlinear and robust control methods for nonlinear DDE systems, the objectives of the present thesis are:

- to present general nonlinear and robust control methods for nonlinear DDE systems, and
- to illustrate the application of the proposed methods to chemical processes of industrial interest and document their effectiveness and advantages with respect to control methods that do not account for the effect of time delays.

The rest of the thesis is structured as follows.

Chapter 2 focuses on nonlinear control on a class of nonlinear DDE systems which include time delays in the states, the control actuator and the measurement sensor. For such systems, a novel integration of geometric, Lyapunov and spectral decomposition techniques is proposed for the synthesis of nonlinear output feedback controllers that enforce stability and output tracking in the closed-loop system, independently of the size of the state delays.

In Chapter 3, the developed control method is applied to an exothermic reactor-separator process with recycle and a fluidized catalytic cracker and is shown to out-

perform nonlinear controller designs that do not account for the presence of dead time associated with the recycle loop and the pipes transferring material from the reactor to the regenerator and vice versa, respectively.

Chapter 4 focuses on nonlinear DDE systems of the type studied in Chapter 2, which also include time-varying uncertain variables. Utilizing a combination of geometric control concepts and Lyapunov's direct method, a general method is presented for the synthesis of robust nonlinear controllers that guarantees boundedness of the state and achieves asymptotic output tracking with arbitrary degree of asymptotic attenuation of the effect of uncertain variables on the output of the closed-loop system, independently of the size of the state delays. The developed control method is applied to a fluidized catalytic cracker with time-delays and uncertain time-varying variables.

In Chapter 5, we turn to nonlinear control of quasi-linear parabolic partial differential difference equation (PDDE) systems whose dynamics can be separated into slow and fast ones, for which the manipulated, controlled and measured variables are also distributed in space. Taking advantage of the low-dimensional nature of the dominant dynamics of such systems, we develop a procedure, based on a combination of Galerkin's method with approximate inertial manifolds, for the construction of low-order DDE systems that accurately reproduce the dominant dynamics of the PDDE systems. These DDE systems are used as the basis for the synthesis of nonlinear output feedback controllers that guarantee stability and enforce output tracking in the closed-loop system by utilizing the method proposed in Chapter 2.

In Chapter 6, the methodology is successfully employed to control the temperature profile of a non-isothermal tubular reactor with recycle around an unstable steady-state and is shown to outperform controller designs which do not account for the

recycle loop dead-time.

Chapter 7 proposes a general and practical methodology for the integration of nonlinear output feedback control with optimal placement of control actuators and measurement sensors for transport-reaction processes described by a broad class of quasi-linear parabolic partial differential equations (PDEs). Initially, Galerkin's method is employed to derive finite-dimensional approximations of the PDE system which are used for the synthesis of stabilizing nonlinear state feedback controllers via geometric techniques. The optimal actuator location problem is subsequently formulated as the one of minimizing a meaningful cost functional that includes penalty on the response of the closed-loop system and the control action and is solved by using standard unconstrained optimization techniques. Then, under the assumption that the number of measurement sensors is equal to the number of slow modes, we employ a procedure proposed in [40] for obtaining estimates for the states of the approximate finite-dimensional model from the measurements. The optimal location of the measurement sensors is also computed. The proposed methodology is successfully applied to a diffusion-reaction process and a non-isothermal packed-bed reactor with recycle to derive nonlinear output feedback controllers and compute optimal actuator/sensor locations for stabilization of unstable steady-states.

Finally, Chapter 8 presents the main conclusions of this thesis. The proofs of all the results are given in the appendices.

Chapter 2

Feedback Control of Nonlinear Differential Difference Equation Systems

2.1 Introduction

This chapter proposes a methodology for the synthesis of nonlinear output feedback controllers for single-input single-output nonlinear DDE systems which include time delays in the states, the control actuator and the measurement sensor. Initially, DDE systems which only include state delays are considered and a novel combination of geometric and Lyapunov-based techniques is employed for the synthesis of nonlinear state feedback controllers that guarantee stability and enforce output tracking in the closed-loop system, independently of the size of the state delays. Then, the problem of designing nonlinear distributed state observers, which reconstruct the state of the DDE system while guaranteeing that the discrepancy between the actual and the estimated state tends exponentially to zero, is addressed and solved by using spectral decomposition techniques for DDE systems. The state feedback controllers

and the distributed state observers are combined to yield distributed output feedback controllers that enforce stability and output tracking in the closed-loop system, independently of the size of the state delays. For DDE systems with state, control actuator and measurement delays, distributed output feedback controllers are synthesized on the basis of an auxiliary output constructed within a Smith-predictor framework.

2.2 Differential difference equation systems

2.2.1 Description of nonlinear DDE systems

We consider single-input single-output systems of nonlinear differential difference equations with the following state-space description:

$$\begin{aligned} \dot{\bar{x}} &= A\bar{x}(\bar{t}) + \sum_{\kappa=1}^{q} B_\kappa \bar{x}(\bar{t}-\bar{\alpha}_\kappa) + f(\bar{x}(\bar{t}), \bar{x}(\bar{t}-\bar{\alpha}_1), \ldots, \bar{x}(\bar{t}-\bar{\alpha}_q)) \\ &\quad + g(\bar{x}(\bar{t}), \bar{x}(\bar{t}-\bar{\alpha}_1), \ldots, \bar{x}(\bar{t}-\bar{\alpha}_q))u(\bar{t}-\hat{\alpha}_1), \\ &\quad \bar{x}(\xi) = \bar{\eta}(\xi), \ \xi \in [-\bar{\alpha}, 0), \ \ \bar{x}(0) = \bar{\eta}_0 \\ y &= h(\bar{x}(\bar{t}-\hat{\alpha}_2)) \end{aligned} \tag{2.1}$$

where $\bar{x} \in \mathbb{R}^n$ denotes the vector of state variables, $u \in \mathbb{R}$ denotes the manipulated input, and $y \in \mathbb{R}$ denotes the controlled output (whose on-line measurements are assumed to be available). $\bar{\alpha}_\kappa$, $\kappa = 1, \ldots, q$, denotes the κ−th state delay, $\bar{\alpha} = \max\{\bar{\alpha}_1, \ldots, \bar{\alpha}_q\}$, $\hat{\alpha}_1$ denotes the manipulated input delay (control actuator dead time) and $\hat{\alpha}_2$ denotes the measured output delay (measurement sensor dead time). $A, B_1, \ldots, B_q$ are constant matrices of dimension $n \times n$, $f(\bar{x}(\bar{t}), \bar{x}(\bar{t}-\bar{\alpha}_1), \ldots, \bar{x}(\bar{t}-\bar{\alpha}_q))$, $g(\bar{x}(\bar{t}), \bar{x}(\bar{t}-\bar{\alpha}_1), \ldots, \bar{x}(\bar{t}-\bar{\alpha}_q))$ are locally Lipschitz nonlinear vector functions, $h(\bar{x}(\bar{t}-\hat{\alpha}_2))$ is a locally Lipschitz nonlinear scalar function, $\bar{\eta}(\xi)$ is a smooth vector function defined in the interval $[-\bar{\alpha}, 0)$ and $\bar{\eta}_0$ is a constant vector. We will assume that the vector function $f(\bar{x}(\bar{t}), \bar{x}(\bar{t}-\bar{\alpha}_1), \ldots, \bar{x}(\bar{t}-\bar{\alpha}_q))$ includes only nonlinear terms

and satisfies $f(0,0,\ldots,0) = 0$ which implies that $x(t) \equiv 0$ is an equilibrium solution for the open-loop (i.e., $u(\bar{t} - \hat{\alpha}_1) \equiv 0$) system of Eq.2.1.

There are many chemical engineering processes whose dynamic models involve time delays in the state variables and are naturally described by nonlinear DDE systems of the form of Eq.2.1. Example of such processes include chemical reactors with recycle loops (where the state delays occur due to transportation lag in the recycle loops), fluidized catalytic cracking reactors (where the state delays occur due to dead time in pipes transferring material from the regenerator to the reactor and vice versa) and distillation columns (where the state delays occur due to dead time in reboiler and condenser recycle loops). Furthermore, control actuator and measurement sensor dead times are also very common sources of time delays in chemical process control, and they are explicitly accounted for in the DDE system of Eq.2.1. The linear appearance of the manipulated input u in the system of Eq.2.1 is also typical in most practical applications, where inlet flow rates, inlet temperatures and concentrations are typically chosen as manipulated inputs. Finally, the assumption that the controlled output is identical to the measured output is done in order to simplify the notation of this work and can be readily relaxed (i.e., the extension of the proposed theory to systems in which the controlled output is different from the measured output is conceptually straightforward)

To simplify the presentation of the results of this work, we will transform the DDE system of Eq.2.1 into an equivalent DDE system which includes state and measurement delays and does not include manipulated input delay. We will also focus on DDE systems with a single state delay (the generalization of the results of this chapter to the case of DDE systems with multiple state delays is conceptually straightforward and will not be presented here for reasons of brevity). To this end, we set $\bar{\alpha} = \hat{\alpha}_1 + \hat{\alpha}_2$,

$t = \bar{t} - \hat{\alpha}_1$, $q = 1$, $B_1 = B$, $\bar{\alpha} = \tilde{\alpha}_1$, $\alpha = \hat{\alpha}_1 + \tilde{\alpha}$, $x(t) = \bar{x}(t + \hat{\alpha}_1)$ and obtain the following system (which will be used in our development):

$$\begin{aligned} \dot{x} &= Ax(t) + Bx(t-\alpha) + f(x(t), x(t-\alpha)) + g(x(t), x(t-\alpha))u(t), \\ & \quad x(\xi) = \bar{\eta}(\xi),\ \xi \in [-\alpha, 0),\ \ x(0) = \bar{\eta}_0 \\ y &= h(x(t-\tilde{\alpha})) \end{aligned} \tag{2.2}$$

Remark 2.1: In order to compare the proposed approach for control of nonlinear DDE systems with existing approaches for control of linear DDE systems, we set $f(x(t), x(t-\alpha)) = 0$, $g(x(t), x(t-\alpha)) = c$ and $h(x(t-\tilde{\alpha})) = wx(t-\tilde{\alpha})$, where c, w are constant vectors, in the system of Eq.2.2 to derive the following linear DDE system:

$$\begin{aligned} \dot{x} &= Ax(t) + Bx(t-\alpha) + cu(t), \quad x(\xi) = \bar{\eta}(\xi), \quad \xi \in [-\alpha, 0), \quad x(0) = \bar{\eta}_0 \\ y &= wx(t-\tilde{\alpha}) \end{aligned} \tag{2.3}$$

which will be used to synthesize linear state feedback controllers and state observers.

In the next subsection, a typical chemical process example [114] is given in order to illustrate modeling of a chemical process in the form of Eq.2.2.

2.2.2 Example of a chemical process modeled by a nonlinear DDE system

Consider the cascade of two perfectly-mixed chemical reactors with recycle loop, which is shown in Figure 2.1. A first-order irreversible reaction of the form $A \rightarrow B$ takes place in the reactors. The process possesses an inherent state delay due to the transportation lag in the recycle loop. Under standard modeling assumptions, the dynamic model of the process can be derived from mass and energy balances and consists of the following system of four nonlinear differential difference equations:

$$\begin{aligned} \frac{dC_1}{dt} &= \frac{F_1}{V_1}C_{1f} - \frac{(F_1+R)}{V_1}C_1 + \frac{R}{V_1}C_2(t-\alpha) - k_0 e^{-\frac{E}{RT_1}}C_1 \\ \frac{dT_1}{dt} &= \frac{F_1}{V_1}T_{1f} - \frac{(F_1+R)}{V_1}T_1 + \frac{R}{V_1}T_2(t-\alpha) - \frac{(-\Delta H)}{\rho c_p}k_0 e^{-\frac{E}{RT_1}}C_1 \end{aligned}$$

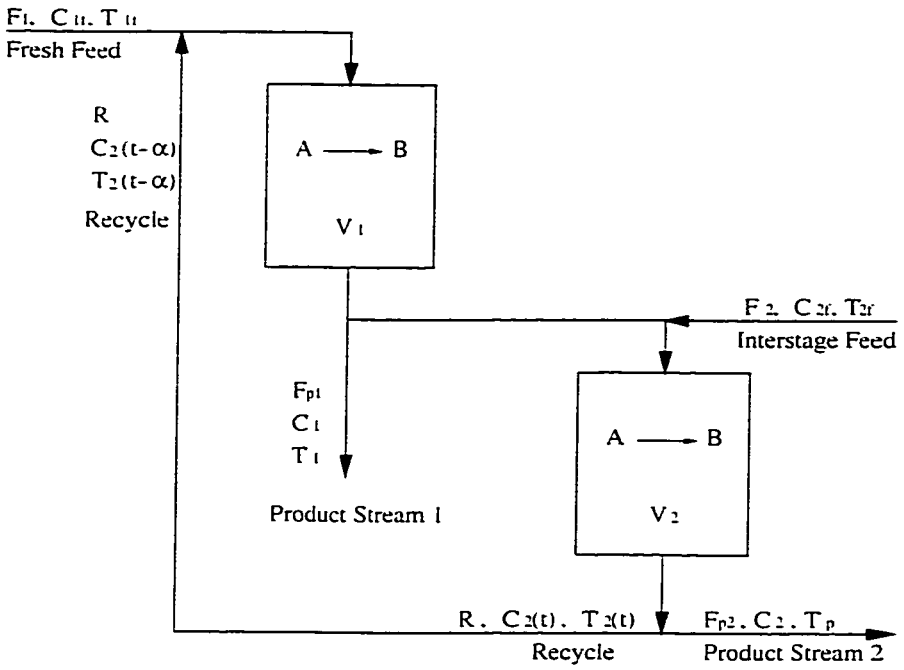

Figure 2.1: Two chemical reactors with recycle loop.

$$\begin{aligned}
\frac{dC_2}{dt} &= \frac{F_2}{V_2}C_{2f} - \frac{(F_{p2}+R)}{V_2}C_2 + \frac{(F_1+R-F_{p1})}{V_2}C_1 - k_0 e^{-\frac{E}{RT_2}}C_2 \\
\frac{dT_2}{dt} &= \frac{F_2}{V_2}T_{2f} - \frac{(F_{p2}+R)}{V_2}T_2 + \frac{(F_1+R-F_{p1})}{V_2}T_1 - \frac{(-\Delta H)}{\rho c_p}k_0 e^{-\frac{E}{RT_2}}C_2
\end{aligned} \tag{2.4}$$

where F_1, F_2 denote the flow rates of the inlet streams to the two reactors, V_1, V_2 denote the volumes of the two reactors, R denotes the recycle (from the second to the first reactor) flow rate, F_{p1}, F_{p2} denote the flow rate of the product streams from the two reactors, C_{1f}, C_{2f} denote the concentration of species A in the inlet streams to the reactors, C_1, C_2 denote the concentration of species A in the reactors, T_{1f}, T_{2f} denote the temperature of the inlet streams to the two reactors, T_1, T_2 denote the temperature in the two reactors, k_0, E, ΔH denotes the pre-exponential constant, the activation energy and the enthalpy of the reaction, c_p, ρ denote the heat capacity and the density of the reacting liquid, and α denotes the recycle loop dead time.

A typical control problem for this process can be formulated as the one of regulating the concentration of species A in the first reactor, C_1, by manipulating the feed concentration of A in the first reactor, C_{1f}. Setting:

$$x_1 = C_1, \;\; x_2 = C_2, \; x_3 = T_1, \;\; x_4 = T_2, \;\; u = C_{1f}, \;\; y = C_1$$

the original set of equations can be put in the form of Eq.2.2.

2.3 Mathematical properties of DDE systems

The objective of this section is to present the basic mathematical properties of DDE systems that will be used in our development. We will begin with the spectral properties of DDE systems, and we will continue with stability concepts and results.

2.3.1 Spectral properties

In this subsection, we formulate the system of Eq.2.2 as an infinite dimensional system in an appropriate Banach space and provide the statement and solution of the eigenvalue problem for the linear delay operator (see Eq.2.7 below). The solution of the eigenvalue problem will be utilized in the design of nonlinear distributed state observers in Section 2.7. We formulate the system of Eq.2.2 in the Banach space $\mathcal{C}([-\alpha, 0], \mathbb{R}^n)$ of continuous n-vector valued functions defined in the interval $[-\alpha, 0]$ with inner product and norm:

$$\begin{aligned} (\tilde{\omega}_1, \tilde{\omega}_2) &= \tilde{\omega}_1(0)\tilde{\omega}_2(0) + \int_{-\alpha}^{0} \tilde{\omega}_1(z+\alpha) B \tilde{\omega}_2(z) dz, \\ ||\tilde{\omega}_1||_2 &= (\tilde{\omega}_1, \tilde{\omega}_1)^{\frac{1}{2}} \end{aligned} \tag{2.5}$$

where $\tilde{\omega}_1$ is an element of $\mathcal{C}^*([-\alpha, 0], \mathbb{R}^{n^*})$, $\mathbb{R}^{n^*}$ is the n-dimensional vector space of row vectors, and $\tilde{\omega}_2 \in \mathcal{C}$. On $\mathcal{C}$, the state function x of the system of Eq.2.2 is defined as:

$$x_t(\xi) = x(t+\xi), \;\; t \geq 0, \;\; \xi \in [-\alpha, 0], \tag{2.6}$$

the operator $\mathcal{A}$ as:

$$\mathcal{A}\phi(\xi) = \left\{ \begin{array}{ll} \dfrac{d\phi(\xi)}{d\xi}, & \xi \in [-\alpha, 0) \\ \\ A\phi(0) + B\phi(-\alpha), & \xi = 0 \end{array} \right\} \tag{2.7}$$

$$\phi(\xi) \in D(\mathcal{A}) \;=\; \left\{\phi \in C^*([-\alpha, 0], \mathbb{R}^{n^*}) : \dot{\phi} \in C, \dot{\phi}(0) = A\phi(0) + B\phi(-\alpha)\right\} \tag{2.8}$$

and the output as:

$$y(t) \;=\; h(Px_t) \tag{2.9}$$

where $P : C \rightarrow \mathbb{R}^n$ is defined by $Px_t = x_t(0)$. $D(\mathcal{A})$ is a dense subset of C. If $\eta \in D(\mathcal{A})$, then the system of Eq.2.2 can be equivalently written as:

$$\begin{array}{rcl} \dfrac{dx_t}{dt} & = & \mathcal{A}x_t + f(Px_t, Qx_t) + g(Px_t, Qx_t)u, \;\; x_0(\xi) = \bar{\eta}, \;\; x_0(0) = \bar{\eta}_0 \\ y(t) & = & h(Px_t) \end{array} \tag{2.10}$$

where $Qx_t = x_t(-\alpha)$.

The eigenvalue problem for the operator $\mathcal{A}$ is defined as:

$$\mathcal{A}\phi_j = \lambda_j \phi_j, \;\; j = 1, \ldots, \infty \tag{2.11}$$

where λ_j denotes an eigenvalue and ϕ_j denotes an eigenfunction (note that ϕ_j is a vector of dimension n); the eigenspectrum of $\mathcal{A}$, $\sigma(\mathcal{A})$, is defined as the set of all eigenvalues of $\mathcal{A}$, i.e., $\sigma(\mathcal{A}) = \{\lambda_1, \lambda_2, \ldots, \}$ and is given by [63]:

$$\sigma(\mathcal{A}) \;=\; \left\{\lambda : det(\lambda I - A - Be^{-\lambda\alpha}) = 0\right\} \tag{2.12}$$

The eigenfunctions can be directly computed from the formula $\phi_\lambda = e^{\lambda\xi}\phi_\lambda(0)$, where $\phi_\lambda(0)$ satisfies the equation $(\lambda I - A - Be^{-\lambda\alpha})\phi_\lambda(0) = 0$. The adjoint of operator $\bar{\mathcal{A}}\psi$ of $\mathcal{A}$ is defined from the relation $(\mathcal{A}\phi, \psi) = (\phi, \bar{\mathcal{A}}\psi)$, where $(,)$ denotes the inner product of Eq.2.5, and its eigenspectrum, $\sigma(\bar{\mathcal{A}})$, satisfies $\sigma(\bar{\mathcal{A}}) = \sigma(\mathcal{A})$.

Remark 2.2: Regarding the properties of the eigenspectrum of $\mathcal{A}$, several comments are in order [63, 106]: a) the eigenspectrum $\sigma(\mathcal{A})$ is a point spectrum consisting

of eigenvalues, $\lambda \in \sigma(\mathcal{A})$, of finite multiplicity, $\kappa(\lambda)$, b) the number of eigenvalues of $\sigma(\mathcal{A})$ which have positive real part (i.e., they are located in the right-half of the complex plane) is always finite, c) the real parts of all the eigenvalues are bounded from above (i.e., there exists a positive real number β such that $|Re\ \lambda_i| \leq \beta$ for all $i = 1, \ldots, \infty$), and d) the eigenvalues are asymptotically distributed along nearly vertical asymptotes in the complex plane.

Remark 2.3: To illustrate the formulation of a DDE system in an infinite dimensional Banach space, and the formulation and solution of the corresponding eigenvalue problem for the delay operator, we consider the following numerical example:

$$\dot{x} = \begin{bmatrix} -2.0 & 3.5 \\ 3.0 & -3.0 \end{bmatrix} x(t) + \begin{bmatrix} -2.0 & 0.0 \\ 0.0 & 0.0 \end{bmatrix} x(t-3) + \begin{bmatrix} 4x_1x_2 - 3x_1^2 - x_2^2 \\ 0 \end{bmatrix} \quad (2.13)$$

For the above system, the solution $(x_1, x_2) = (0, 0)$ is the unique equilibrium solution, the Banach space is $\mathcal{C}([-3, 0], \mathbb{R}^2)$ and the operator $\mathcal{A}$ takes the form:

$$\mathcal{A}\phi(\xi) = \left\{ \begin{array}{ll} \dfrac{d\phi(\xi)}{d\xi}, & \xi \in [-3, 0) \\ \begin{bmatrix} -2.0 & 3.5 \\ 3.0 & -3.0 \end{bmatrix} \phi(0) + \begin{bmatrix} -2.0 & 0.0 \\ 0.0 & 0.0 \end{bmatrix} \phi(-3), & \xi = 0 \end{array} \right\} \quad (2.14)$$

$$\begin{aligned} \phi(\xi) \in D(\mathcal{A}) \ = \ & \Big\{ \phi \in \mathcal{C}^*([-3, 0], \mathbb{R}^{2^*}) : \dot{\phi} \in \mathcal{C}, \\ & \dot{\phi}(0) = \begin{bmatrix} -2.0 & 3.5 \\ 3.0 & -3.0 \end{bmatrix} \phi(0) + \begin{bmatrix} -2.0 & 0.0 \\ 0.0 & 0.0 \end{bmatrix} \phi(-3) \Big\} \end{aligned} \quad (2.15)$$

The eigenvalue problem for $\mathcal{A}$ was solved numerically by using the mathematical software MAPLE and was found that $\sigma(\mathcal{A})$ includes two unstable eigenvalues $\lambda_1 = 0.58$, $\lambda_2 = 0.21$ and infinitely many stable eigenvalues; this implies that the equilibrium solution $(0, 0)$ of the system of Eq.2.13 is unstable.

We finally note that even though the solution $(x_1, x_2) = (0, 0)$ of the DDE system

of Eq.2.13 is unstable, the origin of the *undelayed* system:

$$\dot{x} = \begin{bmatrix} -4.0 & 3.5 \\ 3.0 & -3.0 \end{bmatrix} x(t) + \begin{bmatrix} 4x_1x_2 - 3x_1^2 - x_2^2 \\ 0 \end{bmatrix} \tag{2.16}$$

is globally asymptotically stable (the linearization of the above system around the origin possesses two stable eigenvalues: $\lambda_1 = -6.78$, $\lambda_2 = -0.22$ and $(x_1, x_2) = (0, 0)$ is the unique equilibrium point).

2.3.2 Stability concepts and results

From the analysis of the previous subsection, it is evident that DDE systems of the form of Eq.2.2 possess fundamentally different properties from ODE systems. The main difference is that the state-space of a DDE system is infinite dimensional, while the state-space of an ODE system is finite dimensional. Therefore, the rigorous analysis of the stability properties of the system of Eq.2.2 requires the use of stability concepts and results for DDE systems. In what follows, we review the definitions of asymptotic stability and input-to-state stability for DDE systems as well as a basic theorem that provides sufficient conditions for assessing asymptotic stability. The reader may refer to the classic book [63] for a complete treatment of stability issues for nonlinear differential difference equations.

Consider the following system of nonlinear differential difference equations:

$$\dot{x}(t) = f(x(t), x(t-\alpha), \theta(t), \theta(t-\alpha)), \quad x(\xi) = \bar{\eta}(\xi), \ \xi \in [-\alpha, 0), \quad x(0) = \bar{\eta}_0 \tag{2.17}$$

where $x \in \mathbb{R}^n$, $\theta \in \mathbb{R}^m$, and suppose that $f(0,0,0,0) = 0$. Now, given a function $\theta : [-\alpha, \infty) \to \mathbb{R}^m$ and $t \in [0, \infty)$, $\theta_t(\xi)$ represents a function from $[-\alpha, 0]$ to $\mathbb{R}^m$ defined by $\theta_t(\xi) := \theta(t + \xi)$. We also define $|\theta_t(\xi)| := \max_{t-\alpha \le \xi \le t} |\theta_t(\xi)|$, $||\theta_t|| := sup_{s \ge 0} |\theta_s(\xi)|$ and $||\theta_t||_T := sup_{0 \le s \le T} |\theta_s(\xi)|$. Finally, $|\cdot|_{\mathbb{R}^n}$ denotes the standard Euclidean norm in $\mathbb{R}^n$. Definition 2.1 that follows provides a rigorous statement of the concept of

input-to-state stability for the system of Eq.2.17.

Definition 2.1 [143]: *Let γ be a function of class-$\mathcal{Q}$ (see definition of class-$\mathcal{Q}$ function in the appendix) and δ_x, δ_θ be positive real numbers. The zero solution of Eq.2.17 is said to be input-to-state stable if $|x_0(\xi)| \leq \delta_x$ and $||\theta_t|| \leq \delta_\theta$ imply that the solution of the system of Eq.2.17 is defined for all times and satisfies:*

$$|x_t(\xi)| \leq \beta(|x_0(\xi)|, t) + \gamma(||\theta_t||), \ \forall\, t \geq 0 \tag{2.18}$$

The above definition, when $\theta(t) \equiv 0$, $\forall\, t \geq 0$ reduces to the definition of asymptotic stability for the zero solution of the DDE system of Eq.2.17. Furthermore, when $\alpha = 0$, Definition 2.1 reduces to the standard definition of input-to-state stable for nonlinear ODE systems with external inputs (see, for example, [78]). Finally, we note that from the definition of $|x_t(\xi)|$ and Eq.2.18, it follows that $|x(t)|_{\mathbb{R}^n} \leq |x_t(\xi)| \leq \beta(|x_0(\xi)|, t) + \gamma(||\theta_t||)$, $\forall\, t \geq 0$.

The following theorem provides sufficient conditions for the stability of the zero solution of the system of Eq.2.17, expressed in terms of a suitable functional, and consists a natural generalization of the direct method of Lyapunov for ordinary differential equations. The result of this theorem will be directly used in the solution of the state feedback control problem in Section 2.5 below.

Theorem 2.1 [63]: *Consider the system of Eq.2.17 with $\theta(t) \equiv 0$ and let $\gamma_1, \gamma_2, \gamma_3$ be functions of class Q. If $\gamma_1(s), \gamma_2(s) > 0$ for $s > 0$ and there is a continuous functional $V : \mathcal{C} \to R_{\geq 0}$ such that:*

$$\begin{aligned} \gamma_1(|x(t)|_{\mathbb{R}^n}) \leq V(x_t(\xi)) \leq \gamma_2(|x_t(\xi)|) \\ \dot{V}(x_t(\xi)) \leq -\gamma_3(|x(t)|_{\mathbb{R}^n}) \end{aligned} \tag{2.19}$$

then the solution $x = 0$ is stable. If $\gamma_3(s) > 0$ for $s > 0$, then the solution $x = 0$ is locally asymptotically stable. If $\gamma_1(s) \to \infty$ as $s \to \infty$ and $\gamma_3(s) > 0$ for $s > 0$, then the solution $x = 0$ is globally asymptotically stable.

Remark 2.4: Even though, at this stage, there is no systematic way for selecting the form of the functional $V(x_t(\xi))$ which is suitable for a particular application, a choice for $V(x_t(\xi))$, which is frequently used to show local exponential stability of a DDE system of the form of Eq.2.17 via Theorem 2.1, is:

$$V(x_t(\xi)) = x(t)^T C x(t) + a^2 \int_{t-\alpha}^{t} x(s)^T E x(s) ds \tag{2.20}$$

where E, C are symmetric positive definite matrices and a is a positive real number. Clearly, the functional of Eq.2.20 satisfies $K_1 |x(t)|^2_{\mathbb{R}^n} \leq V(x_t(\xi)) \leq K_2 |x_t(\xi)|^2$ for some positive K_1, K_2.

2.4 Nonlinear control of DDE systems with small time delays

In order to motivate the need for accounting for the presence of time delays in the controller design, we will now establish that a direct application of any nonlinear control method to DDE systems without accounting for the presence of time delays, will lead to the design of controllers that enforce stability and output tracking in the closed-loop system, provided that the time delays are sufficiently small.

We assume that there exists a nonlinear output feedback controller of the form:

$$\begin{aligned} \dot{\omega} &= \mathcal{F}(\omega, y, v) \\ u &= \mathcal{P}(\omega, y, t) \end{aligned} \tag{2.21}$$

where $\mathcal{F}(\omega, y, v)$ is a vector function, $\mathcal{P}(\omega, y, t)$ is a scalar function, and v is the set point, which has been designed on the basis of the system:

$$\begin{aligned} \dot{x} &= Ax(t) + Bx(t) + f(x(t), x(t)) + g(x(t), x(t))u(t), \;\; x(0) = x_0 \\ y &= h(x(t)) \end{aligned} \tag{2.22}$$

so that the closed-loop system:

$$\begin{aligned} \dot{\omega} &= \mathcal{F}(\omega, y, v), \ \ \omega(0) = \omega_0 \\ \dot{x} &= Ax(t) + Bx(t) + f(x(t), x(t)) + g(x(t), x(t))\mathcal{P}(\omega, y, t), \ \ x(0) = x_0 \\ y &= h(x(t)) \end{aligned} \tag{2.23}$$

is locally exponentially stable (see [78] for stability definitions for ODE systems) and the discrepancy between y and v is asymptotically zero (i.e., $\lim_{t\to\infty} |y - v|_{\mathbb{R}^n} = 0$).

Theorem 2.2 that follows establishes that if the controller of Eq.2.21 enforces local exponential stability and asymptotic output tracking in the closed-loop system of Eq.2.23, then it also enforces these properties in the closed-loop system of Eqs.2.2-2.21, provided that the state and measurement delays are sufficiently small (the proof of the theorem can be found in Appendix A).

Theorem 2.2: *If the ODE system of Eq.2.23 is locally exponentially stable, then the nonlinear DDE system of Eq.2.2 under the nonlinear output feedback controller of Eq.2.21 is locally exponentially stable and the discrepancy between y and v tends asymptotically to zero (i.e., $\lim_{t\to\infty} |y - v|_{\mathbb{R}^n} = 0$), provided that α and $\bar{\alpha}$ are sufficiently small.*

Remark 2.5: Even though the result of the theorem clearly indicates the need for accounting for the presence of time delays in the controller design, it is worth mentioning that Theorem 2.2 establishes a very important robustness property of any nonlinear controller with respect to small time delays. This property may also be useful in many practical applications, because it could lead to simplifications in the controller design task, which, for DDE systems with small time delays, could be addressed on the basis of an ODE system instead of a DDE one.

2.5 Nonlinear control of DDE systems with large time delays

2.5.1 Problem statement

Since the application of controller design methods which do not account for the presence of time delays is limited to DDE systems with small time delays, we address, in this paper, the problem of synthesizing nonlinear output feedback controllers of the general form:

$$\begin{aligned} \dot{\omega} &= A\omega(t) + B\omega(t-\alpha) + f(\omega(t),\omega(t-\alpha)) \\ &\quad +g(\omega(t),\omega(t-\alpha))\mathcal{A}(\omega(t),\bar{v}(t),\omega(t-\alpha),\bar{v}(t-\alpha)) + \mathcal{I}(y(t)-h(\omega(t))) \\ u &= \mathcal{A}(\omega(t),\bar{v}(t),\omega(t-\alpha),\bar{v}(t-\alpha)) \end{aligned} \tag{2.24}$$

where $\mathcal{I}(\cdot)$ is a nonlinear integral operator, $\mathcal{A}(\omega(t),\bar{v}(t),\omega(t-\alpha),\bar{v}(t-\alpha))$ is a nonlinear scalar function, $\bar{v}(s) = [v(s)\ v^{(1)}(s)\ \cdots\ v^{(r-1)}(s)]^T$, $s \in [t-\alpha, t]$ and $v^{(k)}$ denotes the $k-$th time-derivative of the reference input $v \in \mathbb{R}$, that enforce exponential stability, asymptotic output tracking and time-delay compensation in the closed-loop system, *independently of the size of the state and measurement delays.*

2.5.2 Methodological framework

To develop a comprehensive method for the synthesis of controllers of the form of Eq.2.24 that enforce the requested properties in the closed-loop system, we will employ a methodology which involves the following steps:

1. Synthesis of nonlinear state feedback controllers that enforce stability and output tracking in the closed-loop system, independently of the size of the state delay.

2. Design of nonlinear distributed state observers (i.e., the observer itself is a system of nonlinear integro-differential equations) that produce estimates of the

unknown state variables of the process with guaranteed asymptotic convergence of the error between the actual and estimated states to zero.

3. Synthesis of distributed nonlinear output feedback controllers through combination of the developed state feedback controllers with the distributed state observers.

Initially, nonlinear state feedback controllers will be synthesized for DDE systems which only include state delays by employing a novel combination of geometric control concepts with the method of Lyapunov functionals (i.e., the controllers will be synthesized in such a way so that the time-derivative of an appropriate Lyapunov-functional calculated along the trajectories of the closed-loop system is negative definite). Then, nonlinear distributed state observers will be constructed for DDE systems which only include state delays by using spectral decomposition techniques. Finally, for DDE systems with state and measurement delays, the output feedback controller will be synthesized on the basis of an auxiliary output constructed within a Smith-predictor framework.

2.6 Nonlinear state feedback control for DDE systems with state delays

In this section, we consider systems of the form of Eq.2.2 without measurement delay, i.e., $\tilde{\alpha} = 0$, (this assumption will be removed below) and assume that measurements of the states are available (i.e., $x(s)$ for $s \in [t-\alpha, t]$, $t \in [0, \infty)$ is known). For these systems, we address the problem of synthesizing nonlinear static state feedback control laws of the general form:

$$u = \mathcal{A}(x(t), \bar{v}(t), x(t-\alpha), \bar{v}(t-\alpha)) \tag{2.25}$$

where $\mathcal{A}(x(t), \bar{v}(t), x(t-\alpha), \bar{v}(t-\alpha))$ is a nonlinear scalar function, that: a) guarantee local exponential stability, b) force the output to asymptotically follow the reference input (i.e., ensure that $\lim_{t\to\infty} |y - v|_{\mathbb{R}^n} = 0$), and c) compensate for the effect of the time delay on the output, in the closed-loop system. The structure of the control law of Eq.2.25 is motivated by available results on stabilization of linear DDE systems (e.g., [126, 113]) and the requirement of output tracking.

In order to proceed with the explicit synthesis of the control law of Eq.2.25, we will need to make certain assumptions on the structure and stability properties of the system of Eq.2.2. To simplify the statement of these assumptions, we introduce the notation $f(x(t), x(t-\alpha)) = f_1(x(t)) + f_2(x(t), x(t-\alpha))$, $\bar{f}(x(t)) = Ax(t) + f_1(x(t))$, and $\bar{p}(x(t), x(t-\alpha)) = Bx(t-\alpha) + f_2(x(t), x(t-\alpha))$, which allows us to rewrite the system of Eq.2.2 in the following form:

$$\begin{aligned} \dot{x} &= \bar{f}(x(t)) + g(x(t), x(t-\alpha))u + \bar{p}(x(t), x(t-\alpha)) \\ y &= h(x) \end{aligned} \tag{2.26}$$

The first assumption is motivated by the requirement of output tracking and will play a crucial role in the synthesis of the controller.

Assumption 2.1: *Referring to the system of Eq.2.26, there exists an integer r and a change of variables:*

$$\begin{bmatrix} \zeta(s) \\ \eta(s) \end{bmatrix} = \begin{bmatrix} \zeta_1(s) \\ \zeta_2(s) \\ \vdots \\ \zeta_r(s) \\ \eta_1(s) \\ \vdots \\ \eta_{n-r}(s) \end{bmatrix} = \mathcal{X}(x(s)) = \begin{bmatrix} h(x) \\ L_{\bar{f}}h(x(s)) \\ \vdots \\ L_{\bar{f}}^{r-1}h(x(s)) \\ \chi_1(x(s)) \\ \vdots \\ \chi_{n-r}(x(s)) \end{bmatrix} \tag{2.27}$$

where $s \in [t-\alpha, t]$ and $\chi_1(x(s)), \cdots, \chi_{n-r}(x(s))$ are scalar functions such that the

system of Eq.2.26 takes the form:

$$\begin{aligned}
\dot{\zeta}_1 &= \zeta_2(t) + p_1(\zeta(t),\eta(t),\zeta(t-\alpha),\eta(t-\alpha)) \\
&\vdots \\
\dot{\zeta}_{r-1} &= \zeta_r(t) + p_{r-1}(\zeta(t),\eta(t),\zeta(t-\alpha),\eta(t-\alpha)) \\
\dot{\zeta}_r &= L_{\tilde{f}}^r h(\mathcal{X}^{-1}(\zeta(t),\eta(t))) + L_g L_{\tilde{f}}^{r-1} h(\mathcal{X}^{-1}(\zeta(t),\eta(t)))u \\
&\quad + p_r(\zeta(t),\eta(t),\zeta(t-\alpha),\eta(t-\alpha)) \\
\dot{\eta}_1 &= \Psi_1(\zeta(t),\eta(t),\zeta(t-\alpha),\eta(t-\alpha)) \\
&\vdots \\
\dot{\eta}_{n-r} &= \Psi_{n-r}(\zeta(t),\eta(t),\zeta(t-\alpha),\eta(t-\alpha)) \\
y &= \zeta_1
\end{aligned} \tag{2.28}$$

where $p_1(\zeta(t),\eta(t),\zeta(t-\alpha),\eta(t-\alpha)),\ldots,p_r(\zeta(t),\eta(t),\zeta(t-\alpha),\eta(t-\alpha))$, $\Psi_1(\zeta(t),\eta(t),\zeta(t-\alpha),\eta(t-\alpha)),\ldots,\Psi_{n-r}(\zeta(t),\eta(t),\zeta(t-\alpha),\eta(t-\alpha))$ *are nonlinear Lipschitz functions and* $L_g L_{\tilde{f}}^{r-1} h(x) \neq 0$ *for all* $x(s) \in \mathbb{R}^n$ *and* $s \in [t-\alpha, t]$.

Assumption 2.1 provides the explicit form of a coordinate change (which is independent of the state delay present in the system of Eq.2.2) that transforms the nonlinear DDE system of Eq.2.2 into an interconnection of two subsystems, the ζ-subsystem which describes the input/output dynamics of the system of Eq.2.2 and the η-subsystem which includes the dynamics of the system of Eq.2.2 which are unobservable from the output. Specifically, the interconnection of Eq.2.28 is obtained by considering the change of variables of Eq.2.27 with $s = t$, differentiating it with respect to time, and using that $x(t) = \mathcal{X}^{-1}(\zeta(t),\eta(t))$ and $x(t-\alpha) = \mathcal{X}^{-1}(\zeta(t-\alpha),\eta(t-\alpha))$ (note that this is possible because the coordinate change of Eq.2.27 is assumed to be valid for $s \in [t-\alpha, t]$). The coordinate transformation of Eq.2.27 is not restrictive from an application point of view (one can easily verify that Assumption 2.1 holds for the two chemical reactors with recycle of Subsection 2.1.2 and the two applications studied in Chapter 3). The assumption that $L_g L_{\tilde{f}}^{r-1} h(x) \neq 0$ for all $x(s) \in \mathbb{R}^n$ and $s \in [t-\alpha, t]$ is necessary in order to guarantee that the controller which will be synthesized is well-posed in the sense that it does not generate infinite control action for

any values of the states of the process (compare with the structure of the controller given in Theorem 2.3).

To proceed with the controller design, we need to impose the following stability requirement on the $\eta-$subsystem of the system of Eq.2.28 which will allow addressing the controller synthesis task on the basis of the low-order ζ-subsystem.

Assumption 2.2: *The dynamical system:*

$$\begin{aligned} \dot{\eta}_1 &= \Psi_1(\zeta(t), \eta(t), \zeta(t-\alpha), \eta(t-\alpha)) \\ &\vdots \\ \dot{\eta}_{n-r} &= \Psi_{n-r}(\zeta(t), \eta(t), \zeta(t-\alpha), \eta(t-\alpha)) \end{aligned} \tag{2.29}$$

is input-to-state stable (see Definition 2.1 for a precise statement of this concept) with respect to the input $\zeta_t(\xi)$.

Loosely speaking, the above assumption states that if the state of the $\zeta-$subsystem is bounded, then the state of the $\eta-$subsystem will also remain bounded (see Remark 2.8 for an interpretation of the η-subsystem). In practice, Assumption 2.2 can be verified by linearizing the system of Eq.2.29 with $\zeta_t(\xi) = 0$ around the operating steady-state and computing the eigenvalues of the resulting linear system. If all of these eigenvalues are in the left-half of the complex plane, then [143] Assumption 2.2 is satisfied locally (i.e., for sufficiently small initial conditions and $\zeta_t(\xi)$). An application of this approach for checking Assumption 2.2 is discussed in Subsection 3.2.2.

Using Assumption 2.2, the controller synthesis problem can be now addressed on the basis of the $\zeta-$subsystem. Specifically, applying the following preliminary feedback law:

$$u = \frac{1}{L_g L_{\tilde{f}}^{r-1} h(\mathcal{X}^{-1}(\zeta, \eta))} (\tilde{u} - L_{\tilde{f}}^r h(\mathcal{X}^{-1}(\zeta, \eta)) - p_r(\zeta(t), \eta(t), \zeta(t-\alpha), \eta(t-\alpha))) \tag{2.30}$$

where $\tilde{u}$ is an auxiliary input, to the system of Eq.2.28 in order to cancel all the nonlinear terms that can be cancelled by using a feedback which utilizes measurements of $x(s)$ for $s \in [t-\alpha, t]$, we obtain the following modified system:

$$\begin{aligned}
\dot{\zeta}_1 &= \zeta_2 + p_1(\zeta(t), \eta(t), \zeta(t-\alpha), \eta(t-\alpha)) \\
&\vdots \\
\dot{\zeta}_{r-1} &= \zeta_r + p_{r-1}(\zeta(t), \eta(t), \zeta(t-\alpha), \eta(t-\alpha))) \\
\dot{\zeta}_r &= \tilde{u} \\
\dot{\eta}_1 &= \Psi_1(\zeta(t), \eta(t), \zeta(t-\alpha), \eta(t-\alpha)) \\
&\vdots \\
\dot{\eta}_{n-r} &= \Psi_{n-r}(\zeta(t), \eta(t), \zeta(t-\alpha), \eta(t-\alpha)) \\
y &= \zeta_1
\end{aligned} \tag{2.31}$$

Introducing the notation:

$$\begin{aligned}
\tilde{A} &= \begin{bmatrix} 0 & 1 & 0 & \cdots & 0 & 0 \\ 0 & 0 & 1 & \cdots & 0 & 0 \\ 0 & 0 & 0 & \cdots & 0 & 0 \\ \vdots & \vdots & \vdots & \ddots & \vdots & \vdots \\ 0 & 0 & 0 & \cdots & 0 & 0 \end{bmatrix}, \quad b = \begin{bmatrix} 0 \\ 0 \\ 0 \\ \vdots \\ 1 \end{bmatrix}, \\
p(\zeta(t), \eta(t), \zeta(t-\alpha), \eta(t-\alpha)) &= \begin{bmatrix} p_1(\zeta(t), \eta(t), \zeta(t-\alpha), \eta(t-\alpha)) \\ p_2(\zeta(t), \eta(t), \zeta(t-\alpha), \eta(t-\alpha)) \\ \vdots \\ p_{r-1}(\zeta(t), \eta(t), \zeta(t-\alpha), \eta(t-\alpha)) \\ 0 \end{bmatrix}
\end{aligned} \tag{2.32}$$

the ζ-subsystem of the system of Eq.2.31 can be written in the following compact form:

$$\begin{aligned}
\dot{\zeta} &= \tilde{A}\zeta + b\tilde{u} + p(\zeta(t), \eta(t), \zeta(t-\alpha), \eta(t-\alpha)) \\
y &= \zeta_1
\end{aligned} \tag{2.33}$$

The controller synthesis task has been now reduced to the one of synthesized $\tilde{u}$ to stabilize the ζ-subsystem and force the output y to asymptotically follow the reference input, v. To develop a solution to this problem, we will need to make the following assumption on the growth of the vector $p(\zeta(t), \eta(t), \zeta(t-\alpha), \eta(t-\alpha))$.

Assumption 2.3: *Let* $\bar{e}(s) = [(h(x(s)) - v(s)) \; (L_{\tilde{f}}h(x(s)) - v^{(1)}(s)) \; \cdots \; (L_{\tilde{f}}^{r-1}h(x(s)) - v^{(r-1)}(s))]^T$, $s \in [t-\alpha, t]$ *where* $v^{(k)}$ *denotes the* $k-th$ *time-derivative of the reference*

input v. There exist positive real numbers a_1, a_2 such that the following bound can be written:

$$|p(\bar{e}(t)+\bar{v}(t),\eta(t),\bar{e}(t-\alpha)+\bar{v}(t-\alpha),\eta(t-\alpha))|^2_{\mathbb{R}^n} \leq a_1\bar{e}^2(t)+a_2\bar{e}^2(t-\alpha) \tag{2.34}$$

The above assumption on the growth of the vector $p(\bar{e}(t)+\bar{v}(t),\eta(t),\bar{e}(t-\alpha)+\bar{v}(t-\alpha),\eta(t-\alpha))$ does not need to hold globally (i.e., for any $\bar{e}(t),\eta(t)$), and thus, it is satisfied by most practical problems (see, for example, the applications studied in Chapter 3). Furthermore, Assumption 2.3 will allow us to synthesize a linear auxiliary feedback law of the form $\bar{u}=K\bar{e}$ to stabilize the ζ-subsystem and enforce output tracking. The synthesis of such a $\bar{u}$ will be performed by using the method of Lyapunov functionals. Specifically, $\bar{u}$ will be designed so that the time-derivative of the following Lyapunov functional:

$$V(\bar{e}_t(\xi)) \;=\; \bar{e}^T P\bar{e}+a^2\int_{t-\alpha}^{t}\bar{e}^T(s)\bar{e}(s)ds \tag{2.35}$$

where a is a positive real number, calculated along the state of the closed-loop $\zeta-$subsystem is negative definite. The incorporation of the integral term $\int_{t-\alpha}^{t}\bar{e}^T(s)\bar{e}(s)ds$ in the functional of Eq.2.35 allows accounting for the distributed parameter (delayed) nature of the system of Eq.2.2 in the controller design stage and synthesizing a controller that enforces the requested properties in the closed-loop system independently of the size of the state delay.

We are now in a position to state the main controller synthesis result of this section. Theorem 2.3 that follows provides the formula of the controller and conditions under which stability and output tracking is guaranteed in the closed-loop system (the proof of the theorem can be found in Appendix A).

Theorem 2.3: *Consider the system of nonlinear differential difference equations of*

Eq.2.2 with $\tilde{\alpha} = 0$, for which Assumptions 2.1, 2.2 and 2.3 hold. Then, if the matrix equation:

$$\tilde{A}^T P + P\tilde{A} - 2P^T b R_2^{-1} b^T P + (a^2 + a_1)I + P^2 = -R_1 \tag{2.36}$$

where $a^2 > a_2$, and R_1, R_2 are positive definite matrices, has a unique positive definite solution for P, the nonlinear state feedback controller:

$$\begin{aligned} u &= \mathcal{A}(x(t), \bar{v}(t), x(t-\alpha), \bar{v}(t-\alpha)) \\ &:= \frac{1}{L_g L_f^{r-1} h(x)} \Big(-R_2^{-1} b^T P \bar{e}(t) + v^{(r)}(t) - L_f^r h(x) \\ &\quad -p_r(x(t), \bar{v}(t), x(t-\alpha), \bar{v}(t-\alpha)) \Big) \end{aligned} \tag{2.37}$$

enforces: a) local exponential stability, and b) asymptotic output tracking in the closed-loop system, independently of the size of the state delay.

Remark 2.6: Regarding the structure, implementation and closed-loop properties of the nonlinear state feedback controller of Eq.2.37, several remarks are in order: a) it uses measurements of the states of the process at t and $t - \alpha$ (i.e., $x(t)$ and $x(t-\alpha)$), and thus, it belongs to the class of the requested control laws of Eq.2.25, b) its practical implementation requires the use of memory lines to store the values of x in the time interval $[t-\alpha, t]$, and c) it enforces stability and asymptotic output tracking in the closed-loop system *independently of the size of the state delay.*

Remark 2.7: In order to apply the result of Theorem 2.3 to a chemical process application, one has to initially verify Assumptions 2.1, 2.2 and 2.3 of the theorem on the basis of the process model and compute the parameters a_1 and a_2. Then, a, R_1, R_2 should be chosen so that $a^2 > a_2$ and the matrices R_1, R_2 are positive definite to ensure that Eq.2.36 has a unique positive definite solution for P. Regarding the role of R_1, R_2 on closed-loop properties, we note that R_1 determines the speed of the closed-loop output response (namely, "larger" (in terms of the smallest eigenvalue) R_1 means faster response), while R_2 determines the penalty that should be imposed

on the manipulated input in achieving stabilization and output tracking ("larger" R_2 means larger penalty on the control action). If these assumptions are satisfied, the synthesis formula of Eq.2.37 can be directly used to derive the explicit form of the controller (see Chapter 3 for the application of this procedure to two chemical process examples).

Remark 2.8: In analogy to the case of nonlinear ODE systems (see, for example, [69, 82]), one can show that the η-subsystem of Eq.2.29 represents the inverse dynamics of the DDE system of Eq.2.2. Moreover, the η-subsystem of Eq.2.29 with $\zeta_t(\xi) = 0$, i.e.:

$$\begin{aligned} \dot{\eta}_1 &= \Psi_1(0, \eta(t), 0, \eta(t-\alpha)) \\ &\vdots \\ \dot{\eta}_{n-r} &= \Psi_{n-r}(0, \eta(t), 0, \eta(t-\alpha)) \end{aligned} \tag{2.38}$$

represents the zero dynamics of the DDE system of Eq.2.2 (i.e., the dynamics of Eq.2.2 when the output is set identically equal to zero). Linearizing the zero dynamics of Eq.2.38 around the zero solution, one can show that the eigenvalues of the resulting linear system are identical to the zeros (which are infinite) of the linear DDE system of Eq.2.3.

Remark 2.9: Applying the proposed method for the synthesis of state feedback controllers for DDE systems to linear systems of the form of Eq.2.3 with $\bar{\alpha} = 0$, we end up with the following controller synthesis formula:

$$u = [wA^{r-1}c]^{-1}\left(-R_2^{-1}b^T P\bar{e}(t) + v^{(r)}(t) - wA^r x(t) - wA^{r-1}Bx(t-\alpha)\right) \tag{2.39}$$

where P is the solution of Eq.2.36. The linear controller of Eq.2.39 can be thought of as an extension of linear control laws of the form:

$$u = F_1 x(t) + F_2 x(t-\alpha) \tag{2.40}$$

where F_1, F_2 are constant vectors of appropriate dimensions, which were considered in

the context of stabilization of linear DDE systems (e.g., [126, 113]), to the problems of stabilization with output tracking. We note that the usual approach followed in the literature for the design of the vectors F_1, F_2 is based on the method of Lyapunov functionals.

Remark 2.10: A control problem which has attracted significant attention in the area of nonlinear process control is the one of specifying the explicit formula of a controller that enforces a linear response between the controlled output and the reference input in the closed-loop system. This problem was solved in [83] for systems of nonlinear ODEs, and more recently, in [42] for systems of nonlinear hyperbolic PDEs. In this remark, we formally pose this problem for DDE systems of the form of Eq.2.2 with $\tilde{\alpha} = 0$ and show that it leads to the synthesis of a nonlinear feedback controller which is non-realizable, and thus, it cannot be implemented in practice. Specifically, we seek to design a nonlinear feedback controller that enforces the following linear input/output response:

$$\gamma_r \frac{d^r y}{dt^r} + \cdots + \gamma_1 \frac{dy}{dt} + y = v \tag{2.41}$$

where r is the 'relative order' of the system of Eq.2.2 (i.e., the smallest derivative of y which depends explicitly on the manipulated input u) and $\gamma_1, \gamma_2, \cdots, \gamma_r$ are adjustable parameters, in the closed-loop system. Calculating the time-derivatives of the output y, up to order r, in the system of Eq.2.2, we obtain the following expressions:

$$\begin{aligned}
y &= h(x) \\
\frac{dy}{dt} &= \psi_1(x(t), x(t-\alpha)) \\
\frac{d^2y}{dt^2} &= \psi_2(x(t), x(t-\alpha), x(t-2\alpha)) \\
&\vdots \\
\frac{d^ry}{dt^r} &= \psi_r(x(t), x(t-\alpha), \ldots, x(t-r\alpha)) + \phi(x(t), x(t-\alpha), \ldots, x(t-r\alpha))u
\end{aligned} \tag{2.42}$$

where $\psi_1(x(t), x(t-\alpha)), \ldots, \psi_r(x(t), x(t-\alpha), \ldots, x(t-r\alpha)), \phi(x(t), x(t-\alpha), \ldots, x(t-r\alpha))$ are smooth nonlinear functions whose specific form is omitted for brevity. Substituting the expressions for the time-derivatives of y in Eq.2.41, assuming that the term $\phi(x(t), x(t-\alpha), \ldots, x(t-r\alpha)) \neq 0$ and solving for u, we obtain the following expression for the controller that enforces the linear response of Eq.2.41 in the closed-loop system:

$$\begin{aligned} u(t) &= \frac{1}{\phi(x(t), x(t-\alpha), \ldots, x(t-r\alpha))} \Big((v - h(x(t)) \\ &\quad - \sum_{\nu=1}^{r} \gamma_\nu \psi_\nu(x(t), x(t-\alpha), \ldots, x(t-\nu\alpha)) \Big) \end{aligned} \tag{2.43}$$

The above controller clearly uses measurements of $x(t-\nu\alpha)$ with $2 \leq \nu \leq r$ which may not be available, and thus, it cannot be implemented in practice. To illustrate this point, we consider the representation of the controller of Eq.2.43 for $t = 0$ i.e.:

$$\begin{aligned} u(0) &= \frac{1}{\phi(x(0), x(-\alpha), \ldots, x(-r\alpha))} \Big((v - h(x(0)) \\ &\quad - \sum_{\nu=1}^{r} \gamma_\nu \psi_\nu(x(0), x(-\alpha), \ldots, x(-\nu\alpha)) \Big) \end{aligned} \tag{2.44}$$

Clearly, the calculation of the initial control action, $u(0)$, requires values of the state, such as $x(-2\alpha), \ldots, x(-r\alpha)$, which are not included in the initial data of the system of Eq.2.2, and thus, $u(0)$, cannot be realized. We finally note that an extension of the initial conditions in the past as a remedy to this problem is not meaningful, since, from a mathematical point of view, it leads to an ill-defined DDE system, while, from a practical point of view, it may require past knowledge of the state at an *arbitrarily large* time interval which, in general, there is no guarantee that exists.

2.7 Nonlinear state observer design for DDE systems with state delay

In this section, we consider nonlinear DDE systems of the form of Eq.2.2 with $\tilde{\alpha} = 0$ and focus on the design of nonlinear state observers that use measurements of process output, $y(s)$, for $s \in [t-\alpha, t]$ to produce estimates of the state variables $x(t)$, with guaranteed exponential convergence of the error between the actual and the estimated values of $x(t)$ to zero. Specifically, we consider the design of state observers with the following general state-space description:

$$\begin{aligned} \dot{\omega} &= A\omega(t) + B\omega(t-\alpha) + f(\omega(t), \omega(t-\alpha)) + g(\omega(t), \omega(t-\alpha))u \\ &\quad + \mathcal{I}(y(t) - h(\omega(t))), \\ &\quad \omega(\xi) = \bar{\omega}(\xi),\ \xi \in [-\alpha, 0),\ \ \omega(0) = \bar{\omega}_0 \end{aligned} \tag{2.45}$$

where $\omega \in \mathbb{R}^n$ is the observer state, $\bar{\omega}(\xi)$ is a smooth vector function defined in $\xi \in [-\alpha, 0)$, $\bar{\omega}_0$ is a constant vector and $\mathcal{I}(\cdot)$ is a bounded nonlinear integral operator, mapping $\mathbb{R}$ into C. The system of Eq.2.45 consists of a replica of the system of Eq.2.2 and the term $\mathcal{I}(y(t) - h(\omega(t)))$ which will be designed so that the system of Eq.2.45 is locally exponentially stable and the discrepancy between $x(t)$ and $\omega(t)$ tends exponentially to zero. The derivation of the explicit form of the integral operator $\mathcal{I}(\cdot)$ will be performed by working with the infinite dimensional formulation, Eq.2.10, of the nonlinear DDE system of Eq.2.2 presented in Section 3.1, and using a spectral decomposition of the DDE system and nonlinear observer design results for finite-dimensional systems.

We initially transform the system of Eq.2.10 into an interconnection of a finite-dimensional system that describes the dynamics of the eigenmodes of $\mathcal{A}$ corresponding to the unstable eigenvalues of $\sigma(\mathcal{A})$, and an infinite-dimensional system that describes the dynamics of the remaining eigenmodes of $\mathcal{A}$. Let $H = \{\lambda : \lambda \in \sigma(\mathcal{A}) \text{ and } Re\lambda \geq 0\}$ and assume, in order to simplify the development, that $\kappa(\lambda) = 1$ for each $\lambda \in \sigma(\mathcal{A})$

(i.e., the multiplicity of all the eigenvalues is assumed to be one; the usual case in most practical applications). Let m be the number of eigenvalues included in H (note that m is always finite). Also, let the elements of H be ordered as $(\lambda_1, \lambda_2, \ldots, \lambda_m)$, where $Re\lambda_1 \geq Re\lambda_2 \geq \cdots Re\lambda_m$. Clearly, the eigenfunctions (column vectors) in the $n \times m$ matrix $\Phi_H = [\phi_1, \phi_2, \ldots, \phi_m]$ form a basis in $C_{\lambda \geq 0}$. Also, let $\Psi_H = [\psi_1, \psi_2, \ldots, \psi_m]^T$ be the basis in $C^*_{\lambda \geq 0}$ chosen so that $(\Psi_H, \Phi_H) = I$, where $(\Psi_H, \Phi_H) = [(\psi_i, \phi_j)]$, ψ_i and ϕ_j being the i-th element and j-th element of Ψ_H and Φ_H, respectively. Defining the orthogonal projection operators P_p and P_n such that $x_t^p = P_p x_t$, $x_t^n = P_n x_t$ (note that $x_t^p = \Phi_H(\Psi_H, x_t)$), the state x_t of the system of Eq.2.10 can be decomposed as:

$$x_t = x_t^p + x_t^n = P_p x_t + P_n x_t \tag{2.46}$$

Applying P_p and P_n to the system of Eq.2.10 and using the above decomposition for x_t, the system of Eq.2.10 can be equivalently written in the following form:

$$\begin{aligned}
\frac{dx_t^p}{dt} &= \mathcal{A}_p x_t^p + f_p(P(x_t^p + x_t^n), Q(x_t^p + x_t^n)) + g_p(P(x_t^p + x_t^n), Q(x_t^p + x_t^n))u \\
\frac{\partial x_t^n}{\partial t} &= \mathcal{A}_n x_t^n + f_n(P(x_t^p + x_t^n), Q(x_t^p + x_t^n)) + g_n(P(x_t^p + x_t^n), Q(x_t^p + x_t^n))u \\
y &= h(P(x_t^p + x_t^n)) \\
x_t^p(0) &= P_p x(0) = P_p \bar{\eta}, \quad x_t^n(0) = P_n x(0) = P_n \bar{\eta}
\end{aligned} \tag{2.47}$$

where $\mathcal{A}_p = P_p \mathcal{A} P_p$, $g_p = P_p g$, $f_p = P_p f$, $\mathcal{A}_n = P_n \mathcal{A} P_n$, $g_n = P_n g$ and $f_n = P_n f$ and the notation $\frac{\partial x_t^n}{\partial t}$ is used to denote that the state x_t^n belongs in an infinite-dimensional space. In the above system, $\mathcal{A}_p = \Phi_H A_p$, where A_p is a matrix of dimension $m \times m$ whose eigenvalues are the ones included in H, f_p and f_n are Lipschitz vector functions, and $\mathcal{A}_n$ is an infinite range matrix which is stable (this follows from the fact that H includes all the eigenvalues of, $\sigma(\mathcal{A})$, which are in the closed right half of the complex plane). Neglecting the x_n-subsystem, the following finite-dimensional system

is obtained:

$$\begin{aligned} \frac{dx_t^p}{dt} &= \mathcal{A}_p x_t^p + f_p(Px_t^p, Qx_t^p) + g_p(Px_t^p, Qx_t^p)u \\ y_p &= h(Px_t^p) \end{aligned} \tag{2.48}$$

where the subscript p in y_p denotes that the output is associated with an approximate finite dimensional system.

Assumption 2.4 that follows states that the system of of Eq.2.48 is observable and is needed in order to design a nonlinear state observer for the system of Eq.2.2 (the reader may refer to [136] for a precise definition of the concept of observability for nonlinear finite-dimensional systems; see also [27] for definitions and characterizations of observability for linear DDE systems).

Assumption 2.4: *The pair* $[h(x_t^p)\ \mathcal{A}_p x_t^p + f_p(x_t^p, 0)]$ *is locally observable in the sense that there exists a nonlinear gain column vector* $L(x_t^p)$ *of dimension* m *(where* m *is the number of unstable eigenvalues of* $\mathcal{A}$*) so that the finite-dimensional dynamical system:*

$$\frac{d\omega_t^p}{dt} = \mathcal{A}_p\omega_t^p + f_p(P\omega_t^p, Q\omega_t^p) + L(\omega_t^p)(y_p - h(P\omega_t^p)) \tag{2.49}$$

is locally exponentially stable.

Theorem 2.4 that follows provides a nonlinear distributed state observer (the proof of the theorem can be found in Appendix A).

Theorem 2.4: *Referring to the system of Eq.2.10 with* $u(t) \equiv 0$ *and suppose that Assumption 2.4 holds. Then, if there exists a positive real number* a_1 *such that* $||\bar{\omega} - \bar{\eta}||_2 \leq a_1$*, the nonlinear infinite-dimensional dynamical system:*

$$\begin{aligned} \frac{d\omega_t}{dt} &= \mathcal{A}\omega_t + f(P\omega_t, Q\omega_t) + \Phi_H L(\Psi_H, \omega_t)(y(t) - h(P\omega_t)), \\ & \omega_0(\xi) = \bar{\omega}, \quad \omega_0(0) = \bar{\omega}_0 \end{aligned} \tag{2.50}$$

is a local exponential observer for the system of Eq.2.10 in the sense that the estimation error, $e_t = \omega_t - x_t$*, tends exponentially to zero.*

The abstract dynamical system of Eq.2.50 can be simplified by utilizing a procedure based on the method of characteristics for first-order hyperbolic PDE systems (this procedure is detailed in Appendix A of this dissertation) to obtain the following nonlinear integro-differential equation system representation for the state observer:

$$\begin{aligned}\dot{\omega} &= A\omega(t) + B\omega(t-\alpha) + f(\omega(t),\omega(t-\alpha)) + g(\omega(t),\omega(t-\alpha))u \\ &\quad +\Phi_H(0)L(\Psi_H,\bar{\omega}(\xi,t))(y(t)-h(\omega(t))) \\ &\quad +B\int_0^{\alpha}\Phi_H(\xi-\alpha)L(\Psi_H,\bar{\omega}(\xi,t))[y(t-\xi)-h(\omega(t-\xi))]d\xi, \\ &\quad \omega(\xi)=\bar{\omega}(\xi),\ \xi\in[-\alpha,0),\ \ \omega(0)=\bar{\omega}_0\end{aligned} \tag{2.51}$$

Remark 2.11: Referring to the state observer of Eq.2.51, it is worth noting that: a) it includes an integral of the observer error, which is expected because the proposed observer design method accounts explicitly for the distributed parameter nature of the time-delay system of Eq.2.2, and b) it consists of a replica of the process model and a nonlinear integral gain acting on the discrepancy between the actual and the estimated output, and thus, it can be thought of as the analogue of nonlinear Luenberger-type observers (e.g., [75, 136]) developed for nonlinear ODE systems in the case of nonlinear DDE systems.

Remark 2.12: For open-loop *stable* systems, the nonlinear gain $L(\Psi_H,\bar{\omega}(\xi,t))$ can be set identically equal to zero and the distributed state observer of Eq.2.51 reduces to an open-loop DDE observer of the form:

$$\dot{\omega} = A\omega(t) + B\omega(t-\alpha) + f(\omega(t),\omega(t-\alpha)) + g(\omega(t),\omega(t-\alpha))u \tag{2.52}$$

Remark 2.13: For open-loop *unstable* systems, the practical implementation of the state observer of Eq.2.51 involves the design of a nonlinear gain, $L(\Psi_H,\bar{\omega}(\xi,t))$, on the basis of a nonlinear finite dimensional system (Assumption 2.4). However, in most practical applications, the construction of a nonlinear gain requires performing

extensive computations (for example, series solutions of nonlinear partial differential equations [75]), and thus, it cannot be easily performed. A computationally efficient way to address this problem is to design a constant gain, L, on the basis of a linear DDE system resulting from the linearization of the nonlinear DDE system around an operating steady-state and evaluating its validity through computer simulations (see the implementation of the observer of Eq.2.51 in the reactor-separator system studied in Section 2.9). We note that the only computations needed to design a constant observer gain are: a) the computation of the eigenvalues of the characteristic equation $det(\lambda I - A - Be^{-\lambda\alpha}) = 0$ which are in the right-half of the complex plane (this can be done by using standard algorithms, for example, [105, 106]) and b) the computation of the eigenfunctions from the formula $\phi_\lambda = e^{\lambda\xi}\phi_\lambda(0)$, where $\phi_\lambda(0)$ satisfies the equation $(\lambda I - A - Be^{-\lambda\alpha})\phi_\lambda(0) = 0$.

Remark 2.14: To illustrate the application of the result of Theorem 2.4, consider the numerical DDE example of Remark 2.3 (Eq.2.13) with $y = x_2$ as the output. The eigenvectors $\phi_j(\xi)$ corresponding to the two unstable eigenvalues of the delay operator of Eq.2.14 are:

$$\phi_1(\xi) = \begin{bmatrix} -0.78 \\ 0.62 \end{bmatrix} e^{0.58\xi}, \quad \phi_2(\xi) = \begin{bmatrix} -0.68 \\ -0.73 \end{bmatrix} e^{0.21\xi} \tag{2.53}$$

The following constant observer gain:

$$L = \begin{bmatrix} -1.0 \\ -16.0 \end{bmatrix} \tag{2.54}$$

was found to satisfy Assumption 2.4 and yields the following nonlinear state observer:

$$\begin{aligned} \dot{\omega} = & \begin{bmatrix} -2.0 & 3.5 \\ 3.0 & -3.0 \end{bmatrix} \omega(t) + \begin{bmatrix} -2.0 & 0.0 \\ 0.0 & 0.0 \end{bmatrix} \omega(t-3) + \begin{bmatrix} 4\omega_1\omega_2 - 3\omega_1^2 - \omega_2^2 \\ 0 \end{bmatrix} \\ & + \begin{bmatrix} -0.78 & -0.68 \\ 0.62 & -0.73 \end{bmatrix} \begin{bmatrix} -1.0 \\ -16.0 \end{bmatrix} (x_2 - \omega_2) \end{aligned}$$

$$+\begin{bmatrix} -2.0 & 0.0 \\ 0.0 & 0.0 \end{bmatrix}\int_0^3 \begin{bmatrix} -0.78e^{0.58(\xi-3.0)} & -0.68e^{0.21(\xi-3.0)} \\ 0.62e^{0.58(\xi-3.0)} & -0.73e^{0.21(\xi-3.0)} \end{bmatrix} \times \begin{bmatrix} -1.0 \\ -16.0 \end{bmatrix}(x_2(t-\xi)-\omega_2(t-\xi))d\xi \tag{2.55}$$

Remark 2.15: Applying the proposed observer design method to linear DDE systems of the form of Eq.2.3 with $\bar{\alpha} = 0$, we obtain the following linear state observer:

$$\begin{aligned} \dot{\omega} &= A\omega(t) + B\omega(t-\alpha) + cu + \Phi_H(0)L(wx(t) - w\omega(t)) \\ &\quad + B\int_0^{\alpha} \Phi_H(\xi-\alpha)L[wx(t-\xi) - w\omega(t-\xi)]d\xi, \\ &\quad \omega(\xi) = \bar{\omega}(\xi),\ \xi \in [-\alpha, 0),\ \ \omega(0) = \bar{\omega}_0 \end{aligned} \tag{2.56}$$

2.8 Nonlinear output feedback control of DDE systems with state delay

In this section, we consider DDE systems of the form of Eq.2.2 with $\bar{\alpha} = 0$ and address the problem of synthesizing distributed output feedback controllers that enforce local exponential stability and asymptotic output tracking in the closed-loop system, independently of the size of the state delay. The requisite output feedback controllers will be synthesized employing combination of the developed distributed state feedback controllers with distributed state observers.

Theorem 2.5 that follows provides a state-space realization of the distributed output feedback controller and the properties that it enforces in the closed-loop system (the proof of the theorem can be found in Appendix A).

Theorem 2.5: *Consider the system of nonlinear differential difference equations of Eq.2.2 with $\bar{\alpha} = 0$, for which the Assumptions 2.1, 2.2, 2.3 and 2.4 hold. Then, if there exists a positive real number a_0 such that $||\bar{\omega} - \bar{\eta}||_2 \leq a_0$ and the matrix equation of Eq.2.36 has a unique positive definite solution for P, the distributed output feedback*

controller:

$$
\begin{aligned}
\dot{\omega} &= A\omega(t) + B\omega(t-\alpha) + f(\omega(t),\omega(t-\alpha)) \\
&\quad +\Phi_H(0)L(\Psi_H,\tilde{\omega}(\xi,t))(y(t)-h(\omega(t))) \\
&\quad +B\int_0^{\alpha}\Phi_H(\xi-\alpha)L(\Psi_H,\tilde{\omega}(\xi,t))[y(t-\xi)-h(\omega(t-\xi))]d\xi \\
&\quad +g(\omega(t),\omega(t-\alpha))\times\frac{1}{L_gL_{\tilde{f}}^{r-1}h(\omega)}\left(-R_2^{-1}b^TP\bar{e}(t)+v^{(r)}(t)-L_{\tilde{f}}^{r}h(\omega)\right. \\
&\quad \left.-p_r(\omega(t),\bar{v}(t),\omega(t-\alpha),\bar{v}(t-\alpha))\right) \\
&\quad \omega(\xi)=\bar{\omega}(\xi),\ \xi\in[-\alpha,0),\ \ \omega(0)=\bar{\omega}_0 \\
u &= \frac{1}{L_gL_{\tilde{f}}^{r-1}h(\omega)}\left(-R_2^{-1}b^TP\bar{e}(t)+v^{(r)}(t)-L_{\tilde{f}}^{r}h(\omega)\right. \\
&\quad \left.-p_r(\omega(t),\bar{v}(t),\omega(t-\alpha),\bar{v}(t-\alpha))\right)
\end{aligned}
\tag{2.57}
$$

where $\bar{e}=[(h(\omega)-v)\ (L_{\tilde{f}}h(\omega)-v^{(1)})\ \cdots\ (L_{\tilde{f}}^{r-1}h(\omega)-v^{(r-1)})]^T$, *a) guarantees local exponential stability of the closed-loop system, and b) enforces asymptotic output tracking, independently of the size of the state delay.*

Remark 2.16: For open-loop stable systems, $L(\Psi_H,\tilde{\omega}(\xi,t))$ can be set equal to zero and the distributed output feedback controller of Eq.2.57 can be simplified to:

$$
\begin{aligned}
\dot{\omega} &= A\omega(t)+B\omega(t-\alpha)+f(\omega,\omega(t-\alpha))+g(\omega(t),\omega(t-\alpha)) \\
&\quad \times\frac{1}{L_gL_{\tilde{f}}^{r-1}h(\omega)}\left(-R_2^{-1}b^TP\bar{e}(t)+v^{(r)}(t)-L_{\tilde{f}}^{r}h(\omega)\right. \\
&\quad \left.-p_r(\omega(t),\bar{v}(t),\omega(t-\alpha),\bar{v}(t-\alpha))\right) \\
\bar{u} &= \frac{1}{L_gL_{\tilde{f}}^{r-1}h(\omega)}\left(-R_2^{-1}b^TP\bar{e}(t)+v^{(r)}(t)-L_{\tilde{f}}^{r}h(\omega)\right. \\
&\quad \left.-p_r(\omega(t),\bar{v}(t),\omega(t-\alpha),\bar{v}(t-\alpha))\right)
\end{aligned}
\tag{2.58}
$$

Remark 2.17: Referring to the result of Theorem 2.5, we note that no consistent initialization requirement has been imposed on the observer states in order to prove local exponential stability and asymptotic output tracking in the closed-loop system (i.e., it is not necessary that $\bar{\omega}(\xi)=\bar{\eta}(\xi)$, $\xi\in[-\alpha,0)$ and $\bar{\omega}_0=\bar{\eta}_0$).

Remark 2.18: The exponential stability of the closed-loop system guarantees that in the presence of small modeling errors (i.e., unknown model parameters and external disturbances) and initialization errors of the observer states, the states of the closed-loop system will remain bounded. Furthermore, it is possible to implement a linear error feedback controller around the $(y - v)$ loop to ensure asymptotic offsetless output tracking in the closed-loop system, in the presence of *constant* parametric uncertainty, external disturbances and initialization errors. In this case, one can use calculations similar to the ones in [52] to derive a mixed-error and output feedback controller, which possesses integral action, (i.e., a controller of the form of Eq.2.57 with $\bar{e} = [(y(t) - v)\ (L_{\bar{f}}h(\omega) - v^{(1)})\ \cdots\ (L_{\bar{f}}^{r-1}h(\omega) - v^{(r-1)})]^T$), that enforces exponential stability and asymptotic offsetless output tracking in the closed-loop system in the presence of constant modeling errors and disturbances.

2.9 Nonlinear output feedback control for DDE systems with state and measurement delay

In this section, we consider DDE systems of the form of Eq.2.2 with $\tilde{\alpha} > 0$ and address the problem of synthesizing distributed output feedback controllers that enforce local exponential stability and asymptotic output tracking in the closed-loop system, independently of the size of the state delay. In order to account for the presence of the measurement delay in the controller design, the requisite output feedback controller will be obtained by working within a Smith Predictor framework [87, 65]. Within this framework, the state feedback controller is synthesized on the basis of an auxiliary output $\bar{y}$, which represents the prediction of the output if there were no dead-time on the output, and can be obtained by adding a corrective signal δy to the on-line

measurement of the actual output y:

$$\bar{y} = y + \delta y$$

Assuming that the open-loop DDE system is observable, the corrective signal, δy, is obtained through a *closed-loop* Smith-type predictor; which for the problem in question is a nonlinear DDE system driven by the manipulated input, that simulates the difference in the responses between the process model without output dead-time and the process model with output dead-time:

$$\begin{aligned}
\dot{\omega} \;=\; & A\omega(t) + B\omega(t-\alpha) + f(\omega(t),\omega(t-\alpha)) + g(\omega(t),\omega(t-\alpha))u \\
& + \Phi_H(0) L(\Psi_H, \tilde{\omega}(\xi,t))(y(t-\tilde{\alpha}) - h(\omega(t-\tilde{\alpha}))) \\
& + B\int_0^{\alpha-\tilde{\alpha}} \Phi_H(\xi-\alpha) L(\Psi_H, \tilde{\omega}(\xi,t))[y(t-\xi-\tilde{\alpha}) - h(\omega(t-\xi-\tilde{\alpha}))]d\xi, \\
& \omega(\xi) = \bar{\omega}(\xi),\ \xi \in [-\alpha, 0),\ \ \omega(0) = \bar{\omega}_0
\end{aligned} \tag{2.59}$$

The resulting output feedback controller and the properties that it enforces in the closed-loop system are given in Theorem 2.6 below (the proof of the theorem is similar to the one of theorem of Theorem 2.5 and will be omitted for brevity).

Theorem 2.6: *Consider the nonlinear DDE system of Eq.2.2 with $\tilde{\alpha} > 0$, for which Assumptions 2.1, 2.2, and 2.3 hold, and an observability property similar to the one of Assumption 2.4 holds for $0 \leq \tilde{\alpha} \leq \alpha$. Then, if there exists a positive real number a_0 such that $||\bar{\omega} - \bar{\eta}||_2 \leq a_0$ and the matrix equation of Eq.2.36 has a unique positive definite solution for P, the distributed output feedback controller:*

$$\begin{aligned}
\dot{\omega} \;=\; & A\omega(t) + B\omega(t-\alpha) + f(\omega(t),\omega(t-\alpha)) \\
& + \Phi_H(0) L(\Psi_H, \tilde{\omega}(\xi,t))(y(t-\tilde{\alpha}) - h(\omega(t-\tilde{\alpha}))) \\
& + B\int_0^{\alpha-\tilde{\alpha}} \Phi_H(\xi-\alpha) L(\Psi_H, \tilde{\omega}(\xi,t))[y(t-\xi-\tilde{\alpha}) - h(\omega(t-\xi-\tilde{\alpha}))]d\xi \\
& + g(\omega(t),\omega(t-\alpha)) \times \frac{1}{L_g L_{\tilde{f}}^{r-1} h(\omega)} \Big(-R_2^{-1} b^T P \bar{e} + v^{(r)}(t) - L_{\tilde{f}}^r h(\omega) - \\
& - p_r(\omega(t), \bar{v}(t), \omega(t-\alpha), \bar{v}(t-\alpha)) \Big) \\
& \omega(\xi) = \bar{\omega}(\xi),\ \xi \in [-\alpha, 0),\ \ \omega(0) = \bar{\omega}_0
\end{aligned}$$

$$\begin{aligned}\bar{u} &= \frac{1}{L_g L_{\tilde{f}}^{r-1} h(\omega)} \Big(-R_2^{-1} b^T P \bar{e} + v^{(r)}(t) - L_{\tilde{f}}^r h(\omega) - \\ &\quad - p_r(\omega(t), \bar{v}(t), \omega(t-\alpha), \bar{v}(t-\alpha))\Big)\end{aligned} \tag{2.60}$$

where $\bar{e} = [(y(t-\tilde{\alpha}) - v + h(\omega(t)) - h(\omega(t-\tilde{\alpha}))) \; (L_{\tilde{f}} h(\omega) - v^{(1)}) \; \cdots \; (L_{\tilde{f}}^{r-1} h(\omega) - v^{(r-1)})]^T$, *enforces: a) local exponential stability, and b) asymptotic output tracking in the closed-loop system, independently of the size of the state delay.*

Remark 2.19: We note that no restrictions have been imposed on the stability properties of the open-loop DDE system (e.g., open-loop stable system) in order to derive the result of Theorem 2.6. This is because the predictor of Eq.2.59 which is used to produce values of the corrective signal δy is a closed-loop one (we remark that the use of an open-loop predictor would require to assume that the open-loop DDE system is stable).

Remark 2.20: For open-loop stable DDE systems with measurement delay but no state delay (i.e., $\tilde{\alpha} > 0$ and $\alpha = 0$), the output feedback controller of Eq.2.60 simplifies to:

$$\begin{aligned}\dot{\omega} &= A\omega(t) + B\omega(t) + f(\omega(t), \omega(t)) + g(\omega(t), \omega(t)) \\ &\quad \times \frac{1}{L_g L_{\tilde{f}}^{r-1} h(\omega)} \Big(-R_2^{-1} b^T P \bar{e} + v^{(r)}(t) - L_{\tilde{f}}^r h(\omega) - p_r(\omega(t), \bar{v}(t), \omega(t), \bar{v}(t))\Big) \\ \bar{u} &= \frac{1}{L_g L_{\tilde{f}}^{r-1} h(\omega)} \Big(-R_2^{-1} b^T P \bar{e} + v^{(r)}(t) - L_{\tilde{f}}^r h(\omega) - p_r(\omega(t), \bar{v}(t), \omega(t), \bar{v}(t))\Big)\end{aligned} \tag{2.61}$$

where $\bar{e} = [(y(t-\tilde{\alpha}) - v + h(\omega(t)) - h(\omega(t-\tilde{\alpha}))) \; (L_{\tilde{f}} h(\omega) - v^{(1)}) \; \cdots \; (L_{\tilde{f}}^{r-1} h(\omega) - v^{(r-1)})]^T$. The above controller is a Smith-predictor based open-loop output feedback controller similar to the one developed in [87].

Remark 2.21: The nonlinear distributed output feedback of Eqs.2.57-2.60 are infinite dimensional ones, due to the infinite dimensional nature of the observers of Eqs.2.51-2.59, respectively. Therefore, finite-dimensional approximation of these con-

trollers have to be derived for on-line implementation. This task can be performed utilizing standard discretization techniques such as finite differences. We note that it is well-established (e.g., [134]) that as the number of discretization points increases, the closed-loop system resulting from the DDE model plus an approximate finite-dimensional controller converges to the closed-loop system resulting from the DDE model plus the infinite-dimensional controller, guaranteeing the well-posedness of the approximate finite-dimensional controller.

2.10 Conclusions

In this chapter, we introduced a methodology for the synthesis of nonlinear output feedback controllers for nonlinear DDE systems which include time delays in the states, the control actuator and the measurement sensor. Initially, DDE systems with state delays were considered and a novel combination of geometric and Lyapunov-based techniques was employed for the synthesis of nonlinear state feedback controllers that guarantee stability and enforce output tracking in the closed-loop system, independently of the size of the state delay. Then, the problem of designing nonlinear distributed state observers, which reconstruct the state of the DDE system while guaranteeing that the discrepancy between the actual and the estimated state tends exponentially to zero, was addressed and solved by using spectral decomposition techniques for DDE systems. The state feedback controllers and the distributed state observers were combined to yield distributed output feedback controllers that enforce stability and asymptotic output tracking in the closed-loop system, independently of the size of the time-delay. For DDE systems with state, control actuator and measurement delays, the output feedback controller was synthesized on the basis of an auxiliary output constructed within a Smith-predictor framework.

Chapter 3

Simulation studies

In this chapter, the nonlinear control method presented in the previous chapter is applied to an exothermic reactor-separator process with recycle and a fluidized catalytic cracker and is shown to outperform nonlinear controller designs that do not account for the presence of dead time associated with the recycle loop and the pipes transferring material from the reactor to the regenerator and vice versa, respectively.

3.1 Application to a reactor-separator system with recycle

3.1.1 Process description - Control problem formulation

Consider the process, shown in Figure 3.1, which consists of a reactor and a separator [98]. An irreversible reaction of the form $A \rightarrow B$, where A is the reactant species and B is the product species, takes place in the reactor. The reaction is exothermic and a cooling jacket is used to remove heat from the reactor. The reaction rate is assumed to be of first-order and is given by:

$$r = k_0 exp\left(-\frac{E}{RT}\right) C_A$$

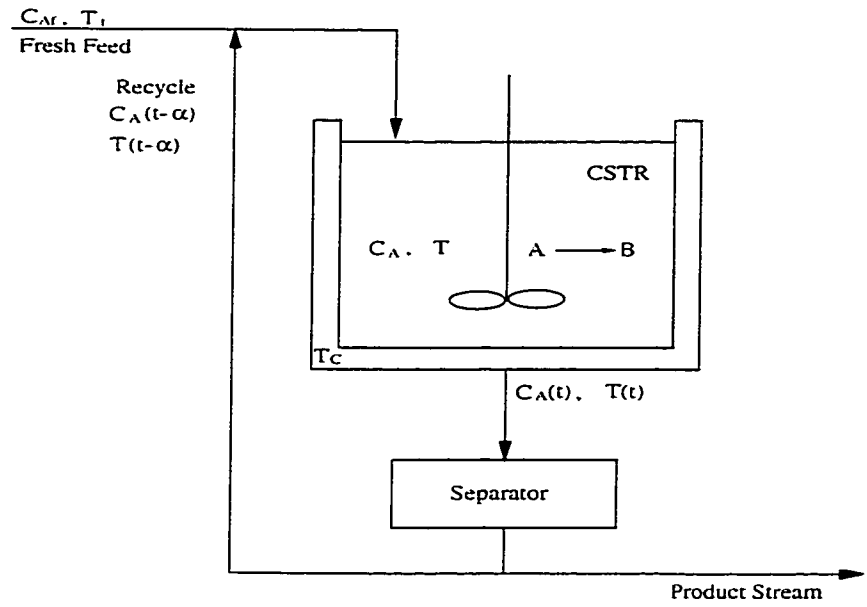

Figure 3.1: A reactor-separator process with recycle.

where k_0 and E denote the pre-exponential constant and activation energy of the reaction, and T and C_A denote the temperature and concentration of species A in the reactor. The outlet of the reactor is fed to a separator where the unreacted species A is separated from the product B. The unreacted amount of species A is fed back to the reactor through a recycle loop; this allows increasing the overall conversion of the reaction and minimizing reactant wastes. The inlet stream to the reactor consists of a fresh feed of pure A, at flow-rate λF, concentration C_{Af} and temperature T_f, and of the recycle stream at flow-rate $(1-\lambda)F$, concentration $C_A(t-\alpha)$ and temperature $T(t-\alpha)$, where F is the total reactor flow-rate, λ is the recirculation coefficient (it varies from zero to one, with zero corresponding to total recycle and zero fresh feed and one corresponding to no recycle) and α is the recycle loop dead time. Under the assumptions of constant volume of the reacting liquid, V, negligible heat loses, constant density, ρ, and heat capacity, c_p, of the reacting liquid, and constant jacket temperature, T_c, a process dynamic model can be derived from mass and energy

Table 3.1: Process parameters of the reactor-separator system.

V	=	0.10	m^3
F	=	13.3330×10^{-3}	$m^3\ sec^{-1}$
C_{Af}	=	0.7090	$kmol\ m^{-3}$
λ	=	0.25	
E	=	1.20×10^4	$kcal\ kmol^{-1}$
k_0	=	1.0×10^7	sec^{-1}
R	=	1.987	$kcal\ kmol^{-1}\ K^{-1}$
ΔH_0	=	5.0×10^4	$kcal\ kmol^{-1}$
c_p	=	0.001	$kcal\ kg^{-1}\ K^{-1}$
ρ	=	1000.0	$kg\ m^{-3}$
T_f	=	300.0	K
T_c	=	295.0	K
U	=	30.0	$kcal\ m^{-2}\ sec^{-1}\ K^{-1}$
A	=	1.0	m^2

balances and consists of the following two nonlinear differential difference equations:

$$\begin{aligned}
\frac{dC_A}{dt} &= \frac{\lambda F}{V}C_{Af} - \frac{F}{V}C_A + \frac{(1-\lambda)F}{V}C_A(t-\alpha) - k_0 exp\Big(-\frac{E}{RT}\Big)C_A \\
\frac{dT}{dt} &= \frac{\lambda F}{V}T_f - \frac{F}{V}T + \frac{(1-\lambda)F}{V}T(t-\alpha) + \frac{(-\Delta H)}{\rho c_p}k_0 exp\Big(-\frac{E}{RT}\Big)C_A \\
&\quad -\frac{UA}{V\rho c_p}(T-T_c)
\end{aligned} \tag{3.1}$$

where ΔH denotes the enthalpy of the reaction, U denotes the heat transfer coefficient, and A denotes the heat transfer area. The values of the process parameters are given in Table 3.1. For these values the corresponding steady-state is:

$$C_{As} = 0.5000\ mol/L, \quad T_s = 296.16^o K, \quad C_{Afs} = 0.7090\ mol/L \tag{3.2}$$

where the subscript s denotes the steady-state value. It was verified, through computation of the eigenvalues of the open-loop system, that this steady-state is a stable one.

The control objective for the process is formulated as the one of regulating the temperature of the reactor, T, by manipulating the inlet concentration of the fresh

feed C_{Af}. Setting $x_1 = C_A$, $x_2 = T$, $y = x_2$ and $u = C_{Af} - C_{Afs}$, the process model of Eq.3.1 can be written in the form of Eq.2.26 with:

$$\tilde{f}(x(t)) = \begin{bmatrix} \frac{\lambda F}{V} C_{Afs} - \frac{F}{V} x_1 - k_0 exp\Big(-\frac{E}{Rx_2}\Big) x_1 \\ \frac{\lambda F}{V} T_f - \frac{F}{V} x_2 + \frac{(-\Delta H)}{\rho c_p} k_0 exp\Big(-\frac{E}{Rx_2}\Big) x_1 - \frac{UA}{V \rho c_p}(x_2 - T_c) \end{bmatrix}, \quad (3.3)$$

$$g(x(t), x(t-\alpha)) = \begin{bmatrix} \frac{\lambda F}{V} \\ 0 \end{bmatrix}, \quad \bar{p}(x(t), x(t-\alpha)) = \begin{bmatrix} \frac{(1-\lambda)F}{V} x_1(t-\alpha) \\ \frac{(1-\lambda)F}{V} x_2(t-\alpha) \end{bmatrix} \quad (3.4)$$

3.1.2 State feedback controller design

For the system of Eq.3.1, Assumption 2.1 is satisfied with $r = 2$ and the coordinate transformation of Eq.2.27 takes the form:

$$\begin{aligned} \begin{bmatrix} \zeta_1 \\ \zeta_2 \end{bmatrix} &= \mathcal{X}(x) = \begin{bmatrix} h(x) \\ L_{\tilde{f}} h(x) \end{bmatrix} \\ &= \begin{bmatrix} x_2 \\ \frac{\lambda F}{V} T_f - \frac{F}{V} x_2 + \frac{(-\Delta H)}{\rho c_p} k_0 exp\Big(-\frac{E}{Rx_2}\Big) x_1 - \frac{UA}{V \rho c_p}(x_2 - T_c) \end{bmatrix} \end{aligned} \quad (3.5)$$

Using the above coordinate change, the process dynamic model can be equivalently written as:

$$\begin{aligned} \dot{\zeta}_1 &= \zeta_2 + \frac{(1-\lambda)F}{V} \zeta_1(t-\alpha) \\ \dot{\zeta}_2 &= L_{\tilde{f}}^2 h(x) + L_g L_{\tilde{f}} h(x) u + p_2(\zeta_1(t), \zeta_2(t), \zeta_1(t-\alpha), \zeta_2(t-\alpha)) \\ y &= \zeta_1 \end{aligned} \quad (3.6)$$

where the explicit form of the term $p_2(\zeta_1(t), \zeta_2(t), \zeta_1(t-\alpha), \zeta_2(t-\alpha))$ is omitted for brevity. For the above system Assumption 2.2 is trivially satisfied, while Assumption 2.3 is satisfied with $p(\bar{e}(t) + \bar{v}(t), \bar{e}(t-\alpha) + \bar{v}(t-\alpha)) = [0.1 e_1(t-\alpha) \quad 0]^T$, $a_1 = 0$ and $a_2 = 0.01$. Utilizing the result of Theorem 2.3, the following matrix equation can be formed:

$$\tilde{A}^T P + P\tilde{A} - 2P^T b R_2^{-1} b^T P + a^2 I + P^2 = -R_1 \quad (3.7)$$

with $R_2 = 1.0$, $a = 0.101$ ($a^2 > a_2$), and

$$\tilde{A} = \begin{bmatrix} 0 & 1 \\ 0 & 0 \end{bmatrix}, \quad b = \begin{bmatrix} 0 \\ 1 \end{bmatrix}, \quad R_1 = \begin{bmatrix} 0.001 & 0 \\ 0 & 0.001 \end{bmatrix} \tag{3.8}$$

Eq.3.7 has a unique positive definite solution for P of the form:

$$P = \begin{bmatrix} 0.055 & -0.119 \\ -0.119 & 0.513 \end{bmatrix} \tag{3.9}$$

which leads to the following nonlinear state feedback controller:

$$\begin{aligned} u = \frac{1}{L_g L_{\tilde{f}} h(x)} \big(& -0.119(x_2 - v) - 0.513(L_{\tilde{f}} h(x) + 0.1v(t-\alpha)) \\ & - L_{\tilde{f}}^2 h(x) - p_2(x(t), \bar{v}(t), x(t-\alpha), \bar{v}(t-\alpha)) \big) \end{aligned} \tag{3.10}$$

3.1.3 State observer and output feedback controller design

In order to avoid the lengthy computations involved in the design of a nonlinear observer gain, we will design a nonlinear state observer of the form of Eq.2.51 with a constant observer gain, L, for the system of Eq.3.1 (see also discussion in Remark 2.13). Computing the linearization of the system of Eq.3.1 around the unstable steady state, $C_{A_s} = 2.36\ mol/L$, $T_s = 320.0^o K$ ($v = 320.0^o K$ will be the new value of the reference input in the simulations discussed in the next subsection), we obtain the following linear DDE system:

$$\dot{x} = Ax(t) + Bx(t-\alpha) \tag{3.11}$$

with:

$$A = \begin{bmatrix} -0.1970 & -0.00885 \\ 3181.8 & 142.23 \end{bmatrix}, \quad B = \begin{bmatrix} 0.1 & 0 \\ 0 & 0.1 \end{bmatrix} \tag{3.12}$$

The system of Eq.3.11 was found to possess two real unstable eigenvalues, $\lambda_1 = 142.036$ and $\lambda_2 = 0.031$ and infinitely many stable eigenvalues. The eigenfunctions corresponding to the unstable eigenvalues were found to be:

$$\phi_1(\xi) = \begin{bmatrix} 0.00006 \\ -1.0 \end{bmatrix} e^{\lambda_1 \xi}, \quad \phi_2(\xi) = \begin{bmatrix} -0.0447 \\ 1.0 \end{bmatrix} e^{\lambda_2 \xi} \tag{3.13}$$

The following constant observer gain:

$$L = \begin{bmatrix} -361.0 \\ -50.0 \end{bmatrix} \tag{3.14}$$

was found to satisfy Assumption 2.4 and yields the following nonlinear output feedback controller:

$$\begin{aligned} \dot{\omega} &= \tilde{f}(\omega(t), \omega(t-\alpha)) + g(\omega, \omega(t-\alpha))u + \bar{p}(\omega(t), \omega(t-\alpha)) \\ &\quad + \Phi_H(0)L(y(t) - h(\omega(t))) + B\int_0^{\alpha} \Phi_H(\xi - \alpha)L[y(t-\xi) - h(\omega(t-\xi))]d\xi \\ u &= \frac{1}{L_g L_{\tilde{f}} h(\omega)} \Big(-0.119(y(t) - v) - 0.513(L_{\tilde{f}} h(\omega) + 0.1v(t-\alpha)) \\ &\quad - L_{\tilde{f}}^2 h(\omega) - p_2(\omega(t), \bar{v}(t), \omega(t-\alpha), \bar{v}(t-\alpha))\Big) \end{aligned} \tag{3.15}$$

where $\Phi_H(\xi) = [\phi_1(\xi)\ \phi_2(\xi)]$. When both state and measurement delays are included in the system of Eq.3.1, the following nonlinear output feedback controller was employed in the simulations described in the next subsection:

$$\begin{aligned} \dot{\omega} &= \tilde{f}(\omega(t), \omega(t-\alpha)) + g(\omega, \omega(t-\alpha))u + \bar{p}(\omega(t), \omega(t-\alpha)) \\ &\quad + \Phi_H(0)L(y(t) - h(\omega(t))) \\ &\quad + B\int_0^{\alpha-\tilde{\alpha}} \Phi_H(\xi - \alpha)L[y(t-\xi-\tilde{\alpha}) - h(\omega(t-\xi-\tilde{\alpha}))]d\xi \\ u &= \frac{1}{L_g L_{\tilde{f}} h(\omega)} \Big(-0.119(y(t-\tilde{\alpha}) - v + \omega_2(t) - \omega_2(t-\tilde{\alpha}))) - 0.513(L_{\tilde{f}} h(\omega) \\ &\quad + 0.1v(t-\alpha)) - L_{\tilde{f}}^2 h(\omega) - p_2(\omega(t), \bar{v}(t), \omega(t-\alpha), \bar{v}(t-\alpha))\Big) \end{aligned} \tag{3.16}$$

Note that according to the discussion of Remark 2.18, the controllers of Eq.3.15 and Eq.3.16 possess integral action.

3.1.4 Closed-loop system simulations

We performed several sets of simulation runs to evaluate the stabilization and output tracking capabilities of the output feedback controllers of Eqs.3.15-3.16 and compare their performance with nonlinear controllers that do not account for the presence of

recycle loop dead time in the model of Eq.3.1. In all the simulation runs, the process was initially assumed to be at the steady state of Eq.3.2 and the user-friendly software package SIMULINK was used to simulate the closed-loop DDE system (SIMULINK is a toolbox of the mathematical software MATLAB that includes a delay function which can be readily used to simulate differential equations with time delays). The computation of the integrals in the controllers of Eqs.3.15-3.16 was performed by discretizing the interval $[-\alpha, 0)$ into ten equispaced intervals using finite differences (further increase on the number of discretization intervals was found to lead to negligible differences on the results). In the first two sets of simulation runs, a $8.84^{o}K$ increase in the reference input value (i.e., $v = 305.0^{o}K$) was imposed at time $t = 0sec.$ The new reference input value corresponds to a stable steady state. In the first set of simulation runs, we initially considered the process of Eq.3.1 with $\alpha = 40sec$ and $\tilde{\alpha} = 0sec$ under the output feedback controller of Eq.3.15 with $L = 0$ (due to operation at a stable region). Figure 3.2 shows the closed-loop output and manipulated input profiles (solid lines). It is clear that the proposed controller drives quickly the output to the new reference input value, achieving an excellent transient response. For the sake of comparison, we also implemented on the process the same output feedback controller with $\alpha = 0sec.$ The closed-loop output and manipulated input profiles under this controller are also displayed in Figure 3.2 (dashed lines). This controller yields a very poor transient response driving the output (dashed line) to the new reference input value very slowly.

In the second set of simulation runs, we initially considered the process of Eq.3.1 with $\alpha = 40sec$ and $\tilde{\alpha} = 12sec$ under the output feedback controller of Eq.3.16 with $L = 0$. The resulting closed-loop output and manipulated input profiles are presented in Figure 3.3 (solid lines). The proposed controller, after the initial delay in the

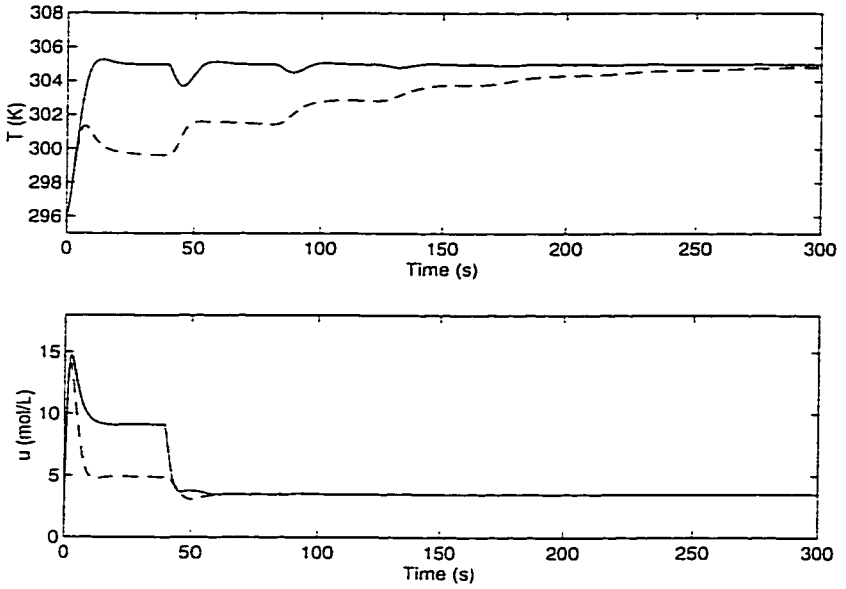

Figure 3.2: Closed-loop output and manipulated input profiles with $\alpha = 40sec$ and $\tilde{\alpha} = 0sec$ under the controller of Eq.3.15 with $L = 0$(solid lines) and the controller of Eq.3.15 with $L = 0$ and $\alpha = 0sec$ (dashed lines) - operation in stable region.

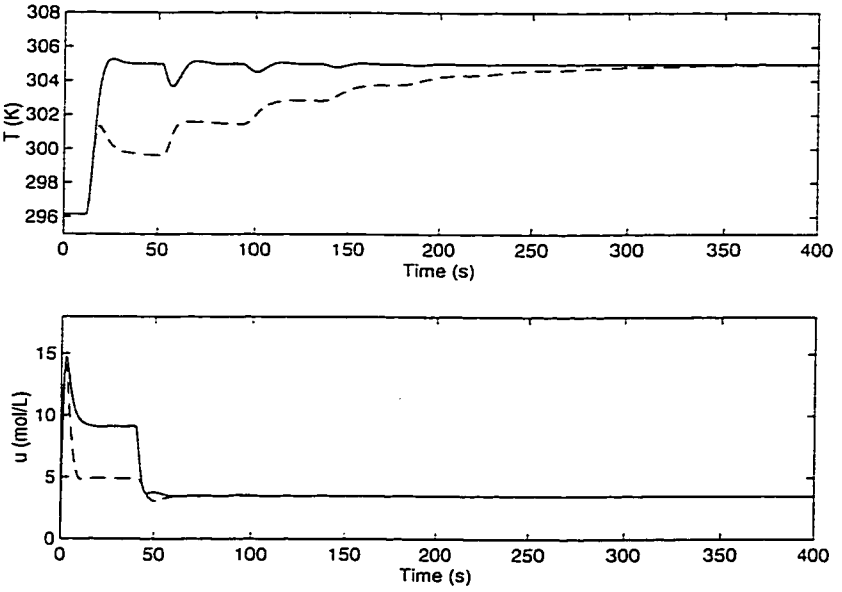

Figure 3.3: Closed-loop output and manipulated input profiles with $\alpha = 40sec$ and $\tilde{\alpha} = 12sec$ under the controller of Eq.3.16 with $L = 0$ (solid lines) and the controller of Eq.3.16 with $L = 0$, $\alpha = 0sec$ and $\tilde{\alpha} = 12sec$ (dashed lines) - operation in stable region.

output of $t = 12sec$, which is caused by the presence of measurement delay, regulates successfully the output to the new reference input value. We also implemented on the process the same controller with $\alpha = 0sec$. The closed-loop output and manipulated input profiles are also shown in Figure 3.3 (dashed lines). The transient performance of the closed-loop system is clearly inferior to the one obtained by the proposed controller.

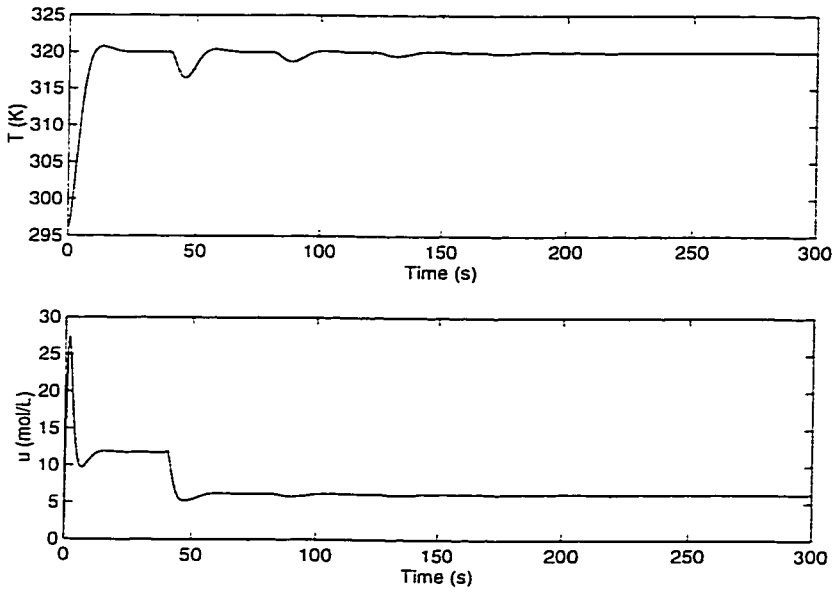

Figure 3.4: Closed-loop output and manipulated input profiles with $\alpha = 40sec$ and $\tilde{\alpha} = 0sec$ under the controller of Eq.3.15 - operation in unstable region.

In the next three sets of simulation runs, a 23.84^oK increase in the reference input value (i.e., $v = 320.0^oK$) was imposed at time $t = 0sec$. The new reference input value corresponds to an unstable steady state. We initially considered the process of Eq.3.1 with $\alpha = 40sec$ and $\tilde{\alpha} = 0sec$ under the controller of Eq.3.15. Figure 3.4 shows the closed-loop output and manipulated input profiles. It is clear that the proposed controller drives quickly the output to the new reference input value. For the sake of comparison, we also implemented on the process the same output feedback controller

with $\alpha = 0sec$. This controller led to an unstable closed-loop system (see the closed-loop output and manipulated input profiles in Figure 3.5). Then, the process of Eq.3.1

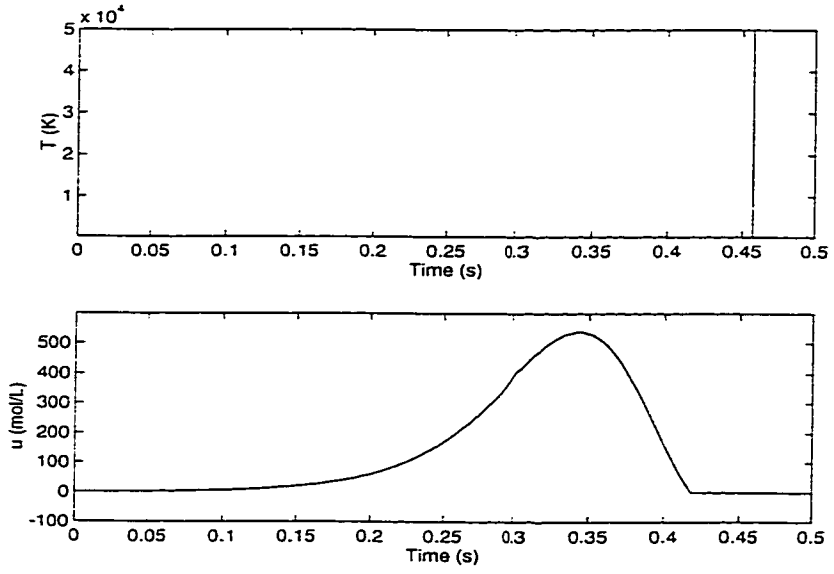

Figure 3.5: Closed-loop output and manipulated input profiles with $\alpha = 40sec$ and $\tilde{\alpha} = 0sec$ under the controller of Eq.3.15 with $\alpha = 0sec$ - operation in unstable region.

with $\alpha = 40sec$ and $\tilde{\alpha} = 12sec$ was considered under the output feedback controller of Eq.3.16 and Figure 3.6 shows the resulting closed-loop output and manipulated input profiles. The proposed controller, after the initial delay in the output of $t = 12sec$, which is caused by the measurement delay, regulates successfully the output to the new reference input value. The same controller with $\alpha = 0sec$ was also implemented on the process. Again, this controller led to an unstable closed-loop system. Finally, we considered the process of Eq.3.1 with $\alpha = 40sec$ and $\tilde{\alpha} = 12sec$ and studied the robustness properties of the controller of Eq.3.15 in the presence of a $5°K$ increase in the value of the temperature of the fresh feed. Figure 3.7 shows the closed-loop output and manipulated input profiles. Despite the presence of a significant disturbance and operation in unstable region, the controller drives the output of the closed-loop system close to the reference input value, exhibiting very good robustness properties.

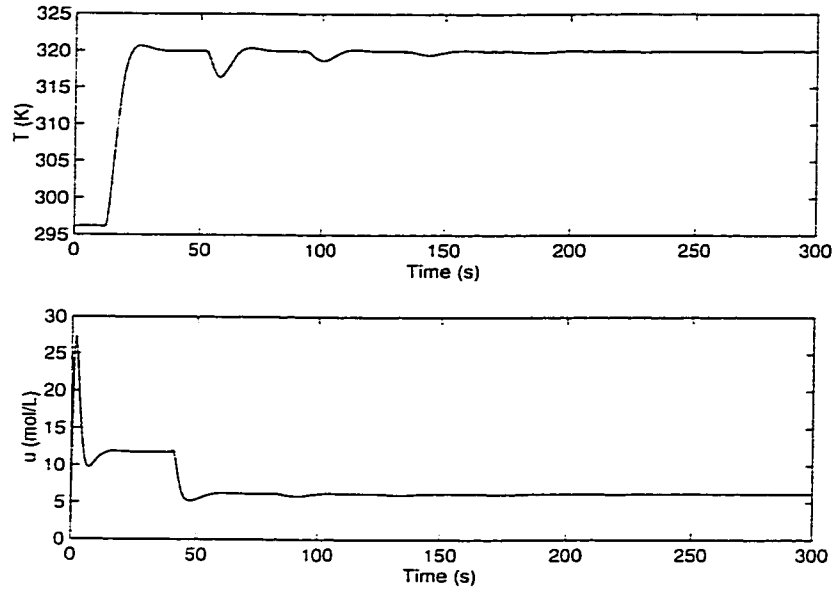

Figure 3.6: Closed-loop output and manipulated input profiles with $\alpha = 40sec$ and $\tilde{\alpha} = 12sec$ under the the controller of Eq.3.16 - operation in unstable region.

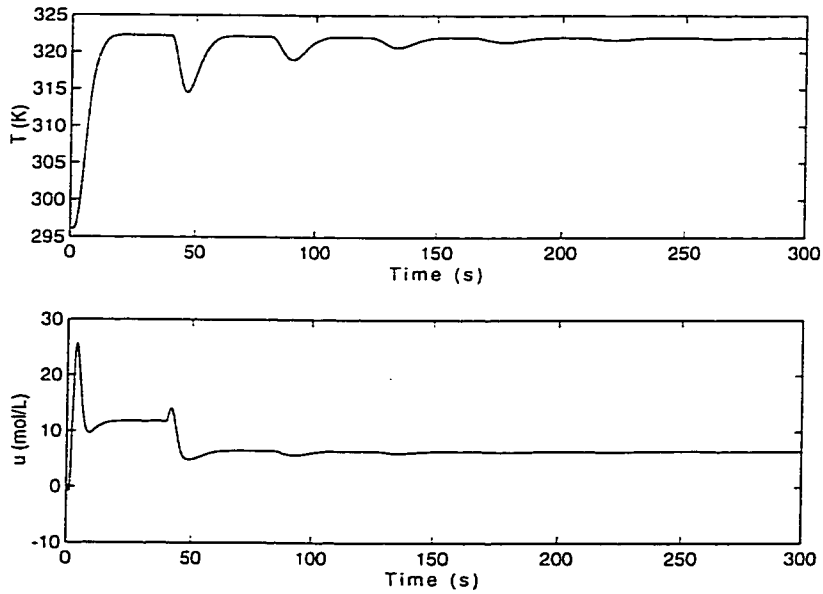

Figure 3.7: Closed-loop output and manipulated input profiles with $\alpha = 40sec$ and $\tilde{\alpha} = 0sec$ under the controller of Eq.3.15 in the presence of modeling error - operation in unstable region.

3.2 Application to a fluidized catalytic cracker

3.2.1 Process modeling - Control problem formulation

In this section, we illustrate the implementation of the developed control methodology on another important chemical engineering process, the fluidized catalytic cracking (FCC) unit shown in Figure 3.8. The FCC unit consists of a cracking reactor, where the cracking of high boiling gas oil fractions into lighter hydrocarbons (e.g., gasoline) and the carbon formation reactions (undesired reactions) take place and a regenerator, where the carbon removal reactions take place. The reader may refer to: a) [55, 108, 14] for a detailed discussion of the features of the FCC unit, b) [15] for an analysis of the issue of the control structure and c) [109, 67] and [47] for application of linear and nonlinear control methods to the FCC unit, respectively. Unfortunately, in all of these studies, the dead-time associated with the pipes transferring material from the reactor to the regenerator and vice versa were not accounted for both in modeling and controller design.

Under the standard modeling assumptions, of well-mixed reactive catalyst in the reactor, small-size catalyst particles, constant solid holdup in reactor and regenerator, uniform and constant pressure in reactor and regenerator, the process dynamic model takes the form [55]:

$$
\begin{aligned}
V_{ra}\frac{dC_{cat}}{dt} &= -60F_{rc}C_{cat}(t) + 50R_{cf}(C_{cat}(t), C_{rc}(t-\alpha_1), T_{ra}) \\
V_{ra}\frac{dC_{sc}}{dt} &= 60F_{rc}[C_{rc}(t-\alpha_1) - C_{sc}(t)] + 50R_{cf}(C_{cat}(t), C_{rc}(t-\alpha_1), T_{ra}) \\
V_{ra}\frac{dT_{ra}}{dt} &= 60F_{rc}[T_{rg}(t-\alpha_1) - T_{ra}(t)] + 0.875\frac{S_f}{S_c}D_{tf}R_{tf}[T_{fp} - T_{ra}(t)] \\
&\quad +0.875\frac{(-\Delta H_{fv})}{S_c}D_{tf}R_{tf} + 0.5\frac{(-\Delta H_{cr})}{S_c}R_{oc}(C_{cat}(t), C_{rc}(t-\alpha_1), T_{ra}) \\
V_{rg}\frac{dC_{rc}}{dt} &= 60F_{rc}[C_{sc}(t-\alpha_2) - C_{rc}(t)] - 50R_{cb}(C_{rc}(t), T_{rg}(t))
\end{aligned}
$$

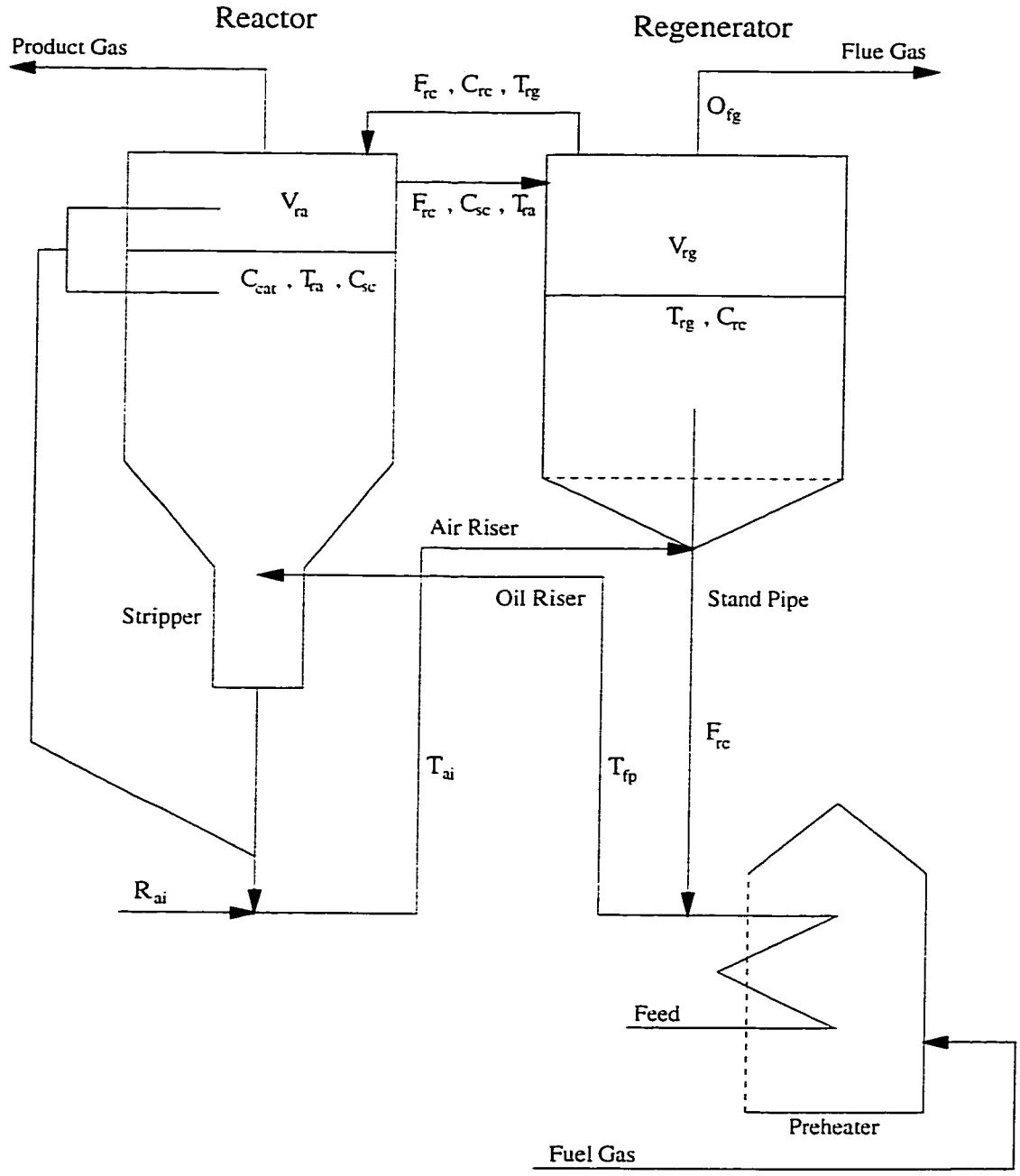

Figure 3.8: A fluidized catalytic cracking unit.

$$V_{rg}\frac{dT_{rg}}{dt} = 60F_{rc}[T_{ra}(t-\alpha_2) - T_{rg}(t)] + 0.5\frac{S_a}{S_c}R_{ai}[T_{ai} - T_{rg}(t)] \\ -0.5\frac{(-\Delta H_{rg})}{S_c}R_{cb}(C_{rc}(t), T_{rg}(t)) \tag{3.17}$$

where C_{cat}, C_{sc}, C_{rc} denote the concentrations of catalytic carbon on spent catalyst, the total carbon on spent catalyst, and carbon on regenerated catalyst, T_{ra}, T_{rg} denote the temperatures in the reactor and the regenerator, R_{ai} is the air flow rate in the regenerator, R_{tf} is the total feed flow rate, D_{tf} is the density of total feed, V_{ra}, V_{rg} denote the catalyst holdup of the reactor and the regenerator, $\Delta H_{rg}, \Delta H_{cr}$ are the heat of regeneration and cracking, ΔH_{fv} is the heat of feed vaporization, F_{rc} denotes the circulation flow rate of catalyst from reactor to regenerator and vice-versa, S_a, S_c, S_f denote specific heats of the air, the catalyst, and the feed, T_{fp}, T_{ai} denote the inlet temperatures of the feed in the reactor and of the air in the regenerator, and R_{cf}, R_{oc}, R_{cb} denote the reaction rates of total carbon forming, of gas-oil cracking, and of coke burning. The analytic expressions for the reaction rates R_{cf}, R_{oc}, R_{cb} can be found in [55].

The presence of time delay in the terms $C_{rc}(t-\alpha_1), T_{rg}(t-\alpha_1)$ is due to dead-time in the pipes transferring regenerated catalyst from the regenerator to the reactor, and the time delay in the terms $C_{sc}(t-\alpha_2), T_{ra}(t-\alpha_2)$ is due to dead time in pipes transferring spent catalyst from the reactor to the regenerator. Even though the proposed method can be readily applied to the case where $\alpha_1 \neq \alpha_2$, we pick in order to simplify our development, $\alpha_1 = \alpha_2 = \alpha = 0.3\ hr$. The values of the remaining process parameters and the corresponding steady-state values are given in Table 3.2.

The control objective is formulated as the one of regulating the temperature in the regenerator, T_{rg}, by manipulating the temperature of the inlet air in the regenerator, T_{ai}. By setting $x = [x_1\ x_2\ x_3\ x_4\ x_5]^T = [T_{rg}\ C_{rc}\ T_{ra}\ C_{sc}\ C_{cat}]^T$, $u = T_{ai} - T_{ais}$, $y = T_{rg}$,

Table 3.2: Process parameters of the fluidized catalytic cracking unit.

E_{cc}	=	18000.0	$Btu\ lb^{-1}\ mole^{-1}$
E_{cr}	=	27000.0	$Btu\ lb^{-1}\ mole^{-1}$
E_{or}	=	63000.0	$Btu\ lb^{-1}\ mole^{-1}$
k_{cc}	=	8.59	$Mlb\ hr^{-1}\ psia^{-1} ton^{-1}(wt\%)^{-1.06}$
k_{cr}	=	11600	$Mbbl\ day^{-1}\ psia^{-1} ton^{-1}(wt\%)^{-1.15}$
k_{or}	=	$3,5 \times 10^{10}$	$Mlb\ hr^{-1}\ psia^{-1} ton^{-1}$
V_{rg}	=	200.0	ton
V_{ra}	=	60.0	ton
F_{rc}	=	40.0	$ton\ hr^{-1}$
T_{fps}	=	744.0	F
T_{ai}	=	175.0	F
P_{rg}	=	25.0	$psia$
P_{ra}	=	40.0	$psia$
ΔH_{fv}	=	60.0	$Btu\ lb^{-1}$
ΔH_{cr}	=	77.3	$Btu\ lb^{-1}$
ΔH_{rg}	=	10561.0	$Btu\ lb^{-1}$
S_a	=	0.3	$Btu\ lb^{-1} F^{-1}$
S_c	=	0.3	$Btu\ lb^{-1} F^{-1}$
S_f	=	0.7	$Btu\ lb^{-1} F^{-1}$
R_{tf}	=	100.0	$Mbbl/day$
D_{tf}	=	7.0	$lb\ gal^{-1}$
α	=	0.3	hr
R_{ai}	=	400.0	$Mlb\ min^{-1}$
$(C_{cat})_{s1}$	=	0.8723	$wt\%$
$(C_{sc})_{s1}$	=	1.5696	$wt\%$
$(C_{rc})_{s1}$	=	0.6973	$wt\%$
$(T_{ra})_{s1}$	=	930.62	F
$(T_{rg})_{s1}$	=	1155.96	F

the process model of Eq.3.17 can be written in the form of Eq.2.26 with:

$$\tilde{f}(x(t)) = \begin{bmatrix} \tilde{f}_1 \\ \tilde{f}_2 \\ \tilde{f}_3 \\ \tilde{f}_4 \\ \tilde{f}_5 \end{bmatrix} = \begin{bmatrix} \frac{0.5 S_a R_{ai}}{S_c V_{rg}} T_{ais} - \left(\frac{60 F_{rc}}{V_{rg}} + 0.5 \frac{S_a R_{ai}}{S_c V_{rg}} \right) T_{rg}(t) \\ -0.5 \frac{(-\Delta H_{rg,n})}{S_c V_{rg}} R_{cb}(C_{rc}(t), T_{rg}(t)) \\ -\frac{60 F_{rc}}{V_{rg}} C_{rc}(t) - \frac{50}{V_{rg}} R_{cb}(C_{rc}(t), T_{rg}(t)) \\ -\frac{60 F_{rc}}{V_{ra}} T_{ra}(t) + 0.875 \frac{S_f}{S_c V_{ra}} D_{tf} R_{tf} [T_{fp} - T_{ra}(t)] \\ +0.875 \frac{(-\Delta H_{fv})}{S_c V_{ra}} D_{tf} R_{tf} \\ -\frac{60 F_{rc}}{V_{ra}} C_{sc}(t) \\ -\frac{60 F_{rc}}{V_{ra}} C_{cat}(t) \end{bmatrix} \tag{3.18}$$

$$\bar{p}(x(t), x(t-\alpha)) = \begin{bmatrix} \bar{p}_1 \\ \bar{p}_2 \\ \bar{p}_3 \\ \bar{p}_4 \\ \bar{p}_5 \end{bmatrix} = \begin{bmatrix} \frac{60 F_{rc}}{V_{rg}} T_{ra}(t-\alpha) \\ \frac{60 F_{rc}}{V_{rg}} C_{sc}(t-\alpha) \\ \frac{60 F_{rc}}{V_{ra}} T_{rg}(t-\alpha) \\ +0.5 \frac{(-\Delta H_{cr})}{S_c V_{ra}} R_{oc}(C_{cat}(t), C_{rc}(t-\alpha), T_{ra}(t)) \\ \frac{60 F_{rc}}{V_{ra}} C_{rc}(t-\alpha) \\ +\frac{50}{V_{ra}} R_{cf}(C_{cat}(t), C_{rc}(t-\alpha), T_{ra}(t)) \\ \frac{50}{V_{ra}} R_{cf}(C_{cat}(t), C_{rc}(t-\alpha), T_{ra}(t)) \end{bmatrix} \tag{3.19}$$

$$g(x(t), x(t-\alpha)) = \begin{bmatrix} g_1 \\ g_2 \\ g_3 \\ g_4 \\ g_5 \end{bmatrix} = \begin{bmatrix} \frac{0.5 S_a R_{ai}}{S_c V_{rg}} \\ 0 \\ 0 \\ 0 \\ 0 \end{bmatrix} \tag{3.20}$$

3.2.2 State feedback controller design

For the system of Eq.3.17, Assumption 2.1 is satisfied with $r = 1$, and the coordinate transformation of Eq.2.27 takes the form $[\zeta \ \eta_1 \ \eta_2 \ \eta_3 \ \eta_4]^T = [T_{rg} \ C_{rc} \ T_{ra} \ C_{sc} \ C_{cat}]^T$ and yields the following system:

$$\begin{aligned} \dot{\zeta} &= L_{\tilde{f}} h(\mathcal{X}^{-1}(\zeta, \eta)) + L_g h(\mathcal{X}^{-1}(\zeta, \eta)) u(t) + p_1(\zeta(t), \eta(t), \zeta(t-\alpha), \eta(t-\alpha)) \\ \dot{\eta} &= \Psi(\zeta(t), \eta(t), \zeta(t-\alpha), \eta(t-\alpha)) \end{aligned} \tag{3.21}$$

where the explicit form of $\Psi(\zeta(t), \eta(t), \zeta(t-\alpha), \eta(t-\alpha))$ is omitted for brevity. To verify Assumption 2.2, we consider the η-subsystem of Eq.3.21 with $\zeta(t) = \zeta(t-\alpha) = \zeta_s = 1155.96^o F$ i.e., the system:

$$\dot{\eta} = \begin{bmatrix} \dot{\eta}_1 \\ \dot{\eta}_2 \\ \dot{\eta}_3 \\ \dot{\eta}_4 \end{bmatrix} = \begin{bmatrix} -\frac{60 F_{rc}}{V_{rg}} \eta_1 - \frac{50}{V_{rg}} R_{cb}(\eta_1, \zeta_s) + \frac{60 F_{rc}}{V_{rg}} \eta_3(t-\alpha) \\ -\frac{60 F_{rc}}{V_{ra}} \eta_2 + 0.875 \frac{S_f}{S_c V_{ra}} D_{tf} R_{tf} [T_{fp} - \eta_2] + 0.875 \frac{(-\Delta H_{fv})}{S_c V_{ra}} D_{tf} R_{tf} \\ \quad + 0.5 \frac{(-\Delta H_{cr})}{S_c V_{ra}} R_{oc}(\eta_4, \eta_1(t-\alpha), \eta_2) \\ -\frac{60 F_{rc}}{V_{ra}} \eta_3 + \frac{60 F_{rc}}{V_{ra}} \eta_1(t-\alpha) + \frac{50}{V_{ra}} R_{cf}(\eta_4, \eta_1(t-\alpha), \eta_2) \\ -\frac{60 F_{rc}}{V_{ra}} \eta_4 + \frac{50}{V_{ra}} R_{cf}(\eta_4, \eta_1(t-\alpha), \eta_2) \end{bmatrix} \tag{3.22}$$

The linearization of the above system around the steady-state

$$C_{rc} = 0.6973\ wt\%\ ,\ \ T_{ra} = 930.62^{o}F\ ,\ \ C_{sc} = 1.5696\ wt\%\ ,\ \ C_{cat} = 0.8723\ wt\% \tag{3.23}$$

was found to be exponentially stable, which implies that the η-subsystem of Eq.3.21 possesses a local input-to-state stability property with respect to $\zeta_t(\xi)$. Therefore, Assumption 2.2 holds and the controller synthesis problem can be addressed on the basis of the ζ-subsystem which is given below:

$$\begin{aligned}\dot{\zeta} \;=\; & -\left(\frac{60F_{rc}}{V_{rg}} + \frac{0.5S_aR_{ai}}{S_cV_{rg}}\right)\zeta(t) - 0.5\frac{(-\Delta H_{rg,n})}{S_cV_{rg}}R_{cb}(\eta_1(t),\zeta(t)) \\ & + \left(\frac{0.5S_aR_{ai}}{S_cV_{rg}}\right)u(t) + \left(\frac{60F_{rc}}{V_{rg}}\right)\eta_2(t-\alpha)\end{aligned} \tag{3.24}$$

Setting $e = \zeta - v$ where v is the desired set point and using a preliminary control law of the form of Eq.2.30, the above system becomes:

$$\dot{e}(t) \;=\; -R_2^{-1}b^TPe(t) \tag{3.25}$$

For the above system, Assumption 2.4 is trivially satisfied since $p(x(t), x(t-\alpha)) = 0$. Utilizing the results of Theorem 2.3, the following equation can be formed:

$$\tilde{A}^TP + P\tilde{A} - 2P^TbR_2^{-1}b^TP + a^2 + P^2 = -R_1 \tag{3.26}$$

with $R_2 = 1.0$, $a^2 = 0.5$ ($a^2 > a_2 = 0$), and

$$\tilde{A} \;=\; 0\ ,\qquad b \;=\; 1\ ,\qquad R_1 \;=\; 0.5 \tag{3.27}$$

Eq.3.26 has a unique positive definite solution for P of the form:

$$P \;=\; 1.0 \tag{3.28}$$

which leads to the following nonlinear state feedback controller:

$$u \;=\; \frac{1}{L_gh(x(s))}\Big(-(x_1 - v) - L_{\tilde{f}}h(x(s)) - p_1(x(t), x(t-\alpha))\Big) \tag{3.29}$$

3.2.3 State observer and output feedback controller design

Since the open-loop process is stable, we set the observer gain L equal to zero and derive the following nonlinear output feedback controller using the result of Theorem 2.5:

$$\begin{aligned} \dot{\omega} &= \tilde{f}(\omega(t)) + g(\omega, \omega(t-\alpha))u + \bar{p}(\omega(t), \omega(t-\alpha)) \\ u &= \frac{1}{L_g h(\omega)} \left(-(y(t)-v) - L_{\tilde{f}} h(\omega) - p_1(\omega(t), \bar{v}(t), \omega(t-\alpha), \bar{v}(t-\alpha))\right) \end{aligned} \tag{3.30}$$

When both state and measurement delays are included in the system of Eq.3.17, the following nonlinear output feedback controller was derived by using the result of Theorem 2.6 and employed in the simulations described in the next subsection:

$$\begin{aligned} \dot{\omega} &= \tilde{f}(\omega(t)) + g(\omega, \omega(t-\alpha))u + \bar{p}(\omega(t), \omega(t-\alpha)) \\ u &= \frac{1}{L_g h(\omega)} \Big(-(y(t-\tilde{\alpha}) - v + \omega_1(t) - \omega_1(t-\tilde{\alpha})) - L_{\tilde{f}} h(\omega) \\ &\quad -p_1(\omega(t), \bar{v}(t), \omega(t-\alpha), \bar{v}(t-\alpha))\Big) \end{aligned} \tag{3.31}$$

Note that the controllers of Eq.3.30 and Eq.3.31 possess integral action.

3.2.4 Closed-loop system simulations

We performed several sets of simulation runs to evaluate the performance of the output feedback controllers of Eqs. 3.30-3.31 and compare their performance with nonlinear controllers that do not account for the presence of time delays in the model of Eq.3.17. In all the simulation runs, the process was initially ($t = 0.0\ hr$) assumed to be at the steady-state shown in Table 3.2 and the MATLAB toolbox SIMULINK was used to simulate the closed-loop DDE system.

In the first simulation run, we considered the process of Eq.3.17 with $\alpha = 0.3\ hr$ and $\tilde{\alpha} = 0\ hr$ (i.e., no measurement delay is present) under the output feedback controller of Eq.3.30. Figure 3.9 shows the output and manipulated input profiles, for a $44^o F$ increase in the reference input. It is clear that the proposed controller drives

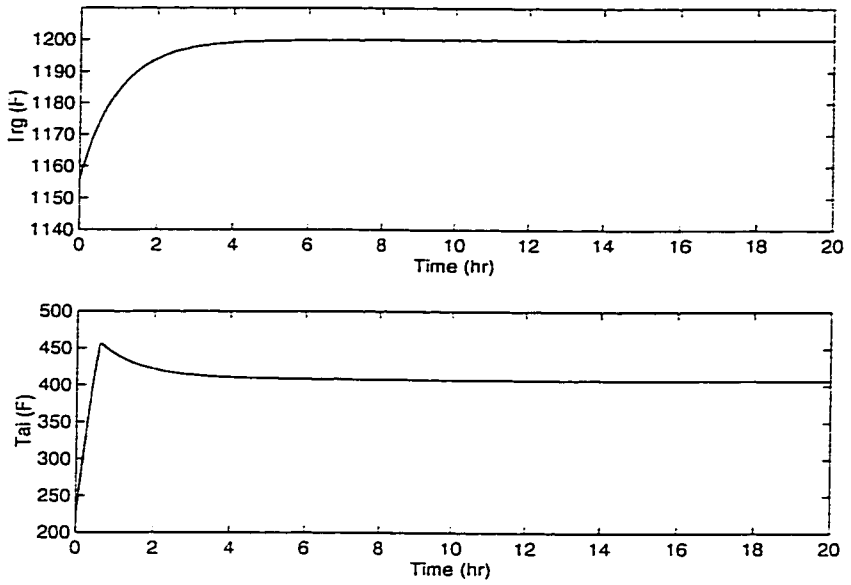

Figure 3.9: Closed-loop output and manipulated input profiles with $\alpha = 0.3hr$ and $\tilde{\alpha} = 0hr$ under the controller of Eq.3.30.

quickly the output to the new reference input value, compensating for the effect of the dead times associated with the pipes transferring material from the reactor to the regenerator and vice versa. For the sake of comparison, we also implemented on the process the same output feedback controller with $\alpha = 0\ hr$ and $\tilde{\alpha} = 0\ hr$ (i.e., we did not account for the presence of time delays in the design of the controller). Figure 3.10 shows the output and manipulated input profiles; this controller leads to an unstable closed-loop system because it does not compensate for the detrimental effect of the time delays.

In the next simulation run, we considered the process of Eq.3.17 with $\alpha = 0.3\ hr$ and $\tilde{\alpha} = 0.05\ hr$ (i.e., significant measurement delay is present) under the output feedback controller of Eq.3.31. Figure 3.11 shows the output and manipulated input profiles, for a 44^oF increase in the reference input. Clearly, the controller of Eq.3.31 drives the output of the closed-loop system, after an initial delay caused by the

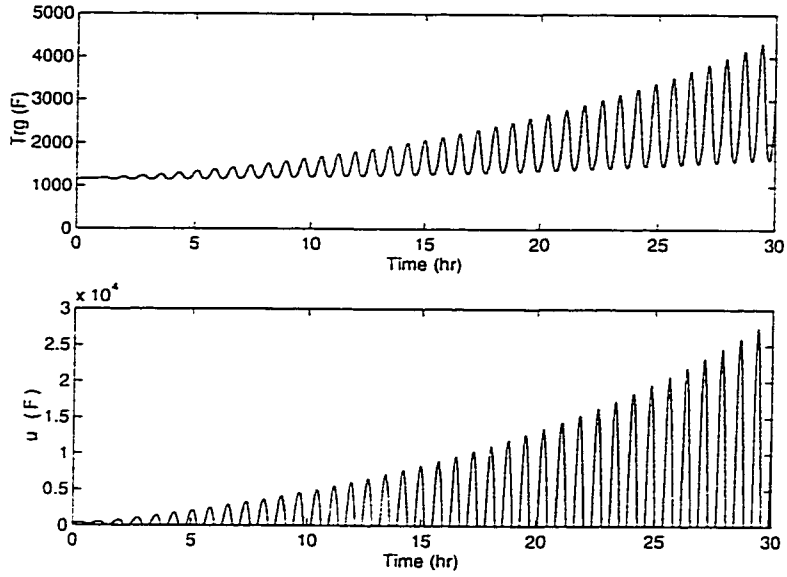

Figure 3.10: Closed-loop output and manipulated input profiles with $\alpha = 0.3hr$ and $\tilde{\alpha} = 0hr$ under the controller of Eq.3.30 with $\tilde{\alpha} = 0.05hr$.

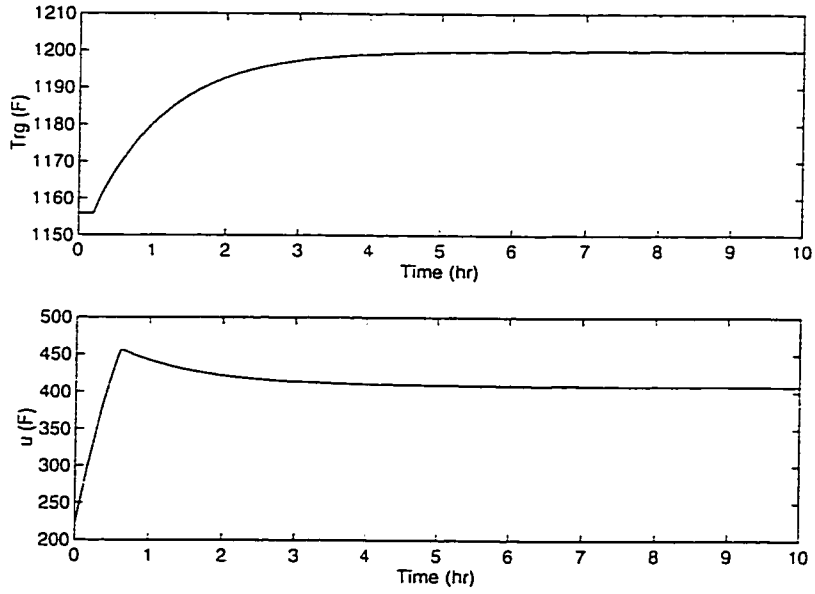

Figure 3.11: Closed-loop output and manipulated input profiles with $\alpha = 0.3hr$ and $\tilde{\alpha} = 0.05hr$ under the controller of Eq.3.31.

measurement dead time, to the new reference input value.

Finally, we considered the process of Eq.3.17 with $\alpha = 0.3\ hr$ and $\tilde{\alpha} = 0.05\ hr$ and studied the robustness properties of the controller of Eq.3.29 in the presence of modeling errors. In particular we simultaneously considered 5% error in the values of: a) the catalyst circulation rate, F_{rc}, b) the temperature of the feed in the reactor, T_{fp}, and c) the inflow air rate in the regenerator, R_{ai}. Figure 3.12 shows the output and

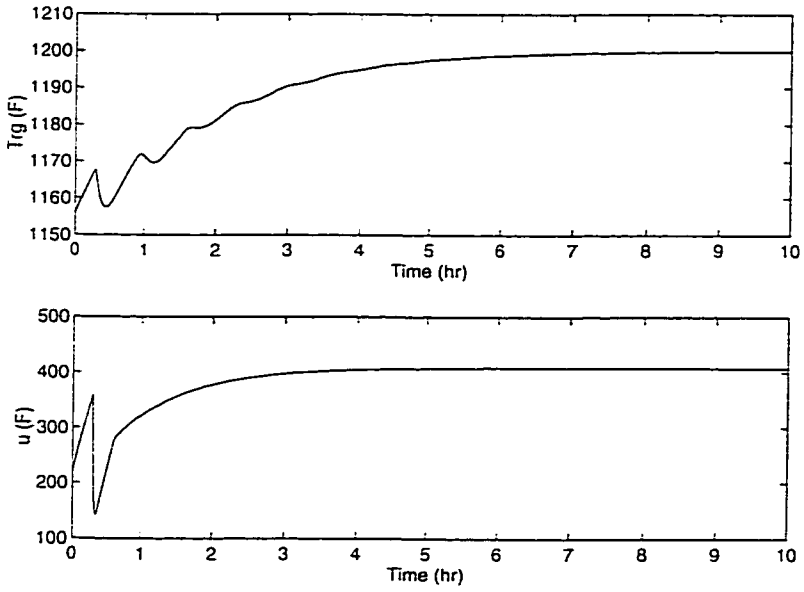

Figure 3.12: Closed-loop output and manipulated input profiles with $\alpha = 0.3hr$ and $\tilde{\alpha} = 0.05hr$ under the controller of Eq.3.31 in the presence of modeling errors.

manipulated input profiles, for a $44^o F$ increase in the reference input. Despite the presence of a significant modeling errors the proposed controller drives the output of the closed-loop system to the new reference input value, exhibiting very good robustness properties.

Summarizing, the results of both simulation studies clearly show that it is necessary to compensate for the effect dead-time associated with pipes transferring material from one unit to an other, as well as that the proposed control methodology is a very

efficient tool for this purpose.

Remark 3.1: We finally note that even though the FCC unit exhibits two-time-scale behavior [55, 47] owing to the significantly different hold ups of the regenerator and reactor (i.e., the reactor dynamics are significantly faster than the regenerator dynamics), which, in general, may cause controller ill-conditioning (see, for example, [47] for a discussion on this issue), in the present study, the presence of time-scale multiplicity in the FCC process model was not taken into account in the controller design problem addressed in Subsections 3.2.2 and 3.2.3 because the control problem that we formulated does not lead to the synthesis of an ill-conditioned controller.

3.3 Conclusions

In this chapter, the nonlinear control method proposed in Chapter 2 was successfully applied to an exothermic reactor-separator process with recycle and a fluidized catalytic cracker and was shown to outperform nonlinear controller designs that do not account for the presence of dead time associated with the recycle loop and the pipes transferring material from the reactor to the regenerator and vice versa, respectively.

Chapter 4

Robust Control of Nonlinear Time-Delay Systems

4.1 Introduction

The dynamic models of many chemical engineering processes involve nonlinearities, time delays and uncertain variables and are naturally described by nonlinear DDE systems. Time delays often occur due to transportation lag such as in flow through pipes, dead times associated with measurement sensors (measurement delays) and control actuators (manipulated input delays), and approximation of high-order dynamics. On the other hand, uncertain variables usually arise from unknown or partially known process parameters (e.g., heat transfer coefficients, kinetic constants, etc.) and external disturbances (e.g., concentration, temperature, and flow of inlet streams). Representative examples of processes which involve nonlinearities and time delays include chemical reactors with recycle loops, fluidized catalytic cracking units, distillation columns, chemical vapor deposition processes, etc. The presence of time-delays and uncertain variables, if it is not appropriately accounted for in the design of the controller, may pose unacceptable limitations on the achievable control quality

and may cause serious problems in the behavior of the closed-loop system including poor performance (e.g., sluggish response) and instability (e.g., oscillations).

The problem of synthesizing linear and nonlinear controllers for uncertain systems that enforce output tracking with attenuation of the effect of the uncertain variables on the output has received considerable attention in the past. Specifically, research initially focused on the development of robust control methods to address this problem for linear systems in both frequency-domain and state-space domain including H_∞, μ-synthesis, etc. (e.g., [56]). In the context of nonlinear systems, adaptive control techniques were employed to solve this problem locally (i.e., for sufficiently small initial conditions and uncertain variables) [129, 72, 142] and globally [107, 88] for certain classes of nonlinear systems with constant uncertain variables. For nonlinear systems with time-varying uncertain variables that satisfy the so-called matching condition, robust state feedback controllers have been designed via Lyapunov's direct method to solve this problem locally (see the papers [50, 99] for a review of results in this area). More recently, robust state [48] and output [77] feedback controllers were designed that solve this problem for arbitrarily large initial conditions and uncertainty (semi-global result). Although these works provided powerful methods for adaptive and robust controller design for several classes of nonlinear systems, a direct application of these methods to nonlinear systems with uncertainty and time-delays may lead to poor performance and/or closed-loop instability.

In the area of control of systems with time-delays, research initially focused on linear systems with a manipulated input delay which are described by transfer function models, in which the presence of the time delay prevents the use of large controller gains (i.e., the proportional gain of a proportional-integral controller should be sufficiently small in order to avoid destabilization of the closed-loop system), thereby

leading to sluggish closed-loop response. To overcome this problem, many researchers proposed various predictor schemes which completely eliminate the time delay from the characteristic polynomial of the closed-loop system, allowing the use of larger controller gains (see, for example, [133, 28, 71]). These results were extended to certain classes of nonlinear systems in [87, 65, 160]. For DDE systems with state, measurement and manipulated input delays, a general method based on a novel integration of geometric concepts, Lyapunov functionals and predictor schemes was proposed in [38, 39, 7] for the synthesis of nonlinear output feedback controllers. Research on control of uncertain DDE systems has mainly focused on linear systems where important contributions include robust control using the concept of quadratic stabilization [119, 102, 29] and linear matrix inequalities [146]. In the context of nonlinear uncertain DDE systems, results include stabilization via variable structure control [130, 145] and dynamic disturbance decoupling [110].

This chapter [5, 8] focuses on single-input single-output nonlinear DDE systems with uncertain variables. For such systems, we propose a general methodology for the synthesis of robust nonlinear state feedback controllers that guarantee boundedness of the states and ensure that the ultimate discrepancy between the output and the external reference input in the closed-loop system can be made arbitrarily small by an appropriate choice of controller parameters. The controllers are synthesized by using a novel combination of geometric and Lyapunov-based techniques and enforce the aforementioned properties in the closed-loop system independently of the size of the state delay. The proposed control method is successfully applied to a FCC unit with a time-varying uncertain variable.

4.2 Notation

- $L_f h$ denotes the Lie derivative of a scalar field h with respect to the vector field f. $L_f^k h$ denotes the k-th order Lie derivative and $L_g L_f^{k-1} h$ denotes the mixed Lie derivative.

- A function $W : \mathbb{R}^n \to \mathbb{R}_{\geq 0}$ is said to be positive definite if $W(x)$ is positive for all nonzero x and is zero at zero.

- A function $W : \mathbb{R}^n \to \mathbb{R}_{\geq 0}$ is said to be proper if $W(x)$ tends to $+\infty$ as $\|x\|_{\mathbb{R}^n}$ tends to $+\infty$, where $\|\cdot\|_{\mathbb{R}^n}$ denotes the standard Euclidean norm in $\mathbb{R}^n$.

- A function $\gamma : \mathbb{R}_{\geq 0} \to \mathbb{R}_{\geq 0}$ is said to be of class $\mathcal{Q}$ if it is continuous, nondecreasing and zero at zero. It is of class $\mathcal{K}$ if it is continuous, strictly increasing and is zero at zero. It is of class $\mathcal{K}_\infty$, if in addition, it is proper.

- A function $\beta : \mathbb{R}_{\geq 0} \times \mathbb{R}_{\geq 0} \to \mathbb{R}_{\geq 0}$ is said to be of class $\mathcal{KL}$ if, for each fixed t, the function $\beta(\cdot, t)$ is of class $\mathcal{K}$ and, for each fixed s, the function $\beta(s, \cdot)$ is nonincreasing and tends to zero at infinity.

4.3 Preliminaries

We consider single-input single-output nonlinear DDE systems with uncertain variables with the following state-space description:

$$\begin{aligned} \dot{x} &= f(x(t), x(t-\alpha), \theta(t-\alpha_\theta)) + g(x(t), x(t-\alpha))u(t) \\ x(\xi) &= \bar{\eta}(\xi), \quad \xi \in [-\alpha, 0] \\ y(t) &= h(x(t)) \end{aligned} \tag{4.1}$$

where $x(t) \in \mathbb{R}^n$ denotes the vector of the state variables, $u(t) \in \mathbb{R}$ denotes the manipulated input, $\theta(t-\alpha_\theta) = [\theta_1(t-\alpha_{\theta 1}) \cdots \theta_q(t-\alpha_{\theta q})] \in \mathbb{R}^q$ denotes the vector of the time-varying uncertain variables, $y(t) \in \mathbb{R}$ denotes the controlled output,

α denotes the state delay, $f(x(t), x(t-\alpha)), \theta(t-\alpha_\theta))$, $g(x(t), x(t-\alpha))$ are locally Lipschitz nonlinear vector functions, $h(x(t))$ is a locally Lipschitz nonlinear scalar function and $\bar{\eta}(\xi)$ is a smooth vector function defined in the interval $[-\alpha, 0]$. We will assume that the vector function $f(x(t), x(t-\alpha), \theta(t-\alpha_\theta))$ satisfies $f(0,0,0) = 0$ which implies that $x(t) \equiv 0$ is an equilibrium solution for the open-loop system of Eq.4.1 (i.e., system of Eq.4.1 with $u(t) \equiv 0$).

There are many chemical engineering processes whose dynamic models involve uncertain variables and time delays in the state variables, and are naturally described by nonlinear DDE systems of the form of Eq.4.1. Uncertain variables typically arise from unknown or partially known process parameters (e.g., activation energies, heat of reaction, heat transfer coefficients) and external disturbances (e.g., upsets in inlet concentrations, temperatures). On the other hand, state delays usually occur due to dead-time in pipes used to transfer material among process units including fluidized catalytic cracking units (where the state delays occur due to dead time in pipes transferring material from the regenerator to the reactor and vice-versa) and distillation columns (where the state delays occur due to dead time in reboiler and condenser recycle loops). The linear appearance of the manipulated input u in the system of Eq.4.1 is also typical in most practical applications, where inlet flow rates, inlet temperatures and concentrations are typically chosen as manipulated inputs.

In the remainder of this section, we review several stability concepts and theorems for DDE systems which will be used in our development (the reader may refer to [63] for more details).

We begin with some notation. Given a function $\theta : [-\alpha, \infty) \to \mathbb{R}^m$ and $t \in [0, \infty)$, $\theta_t(\xi)$ represents a function from $[-\alpha, 0]$ to $\mathbb{R}^m$ defined by $\theta_t(\xi) := \theta(t+\xi)$. We also define $|\theta_t(\xi)| := \max_{-\alpha \le \xi \le 0} \|\theta_t(\xi)\|_{\mathbb{R}^m}$, $||\theta_t|| := \sup_{s \ge 0} |\theta_s(\xi)|$ and $||\theta_t||_T := \sup_{0 \le s \le T} |\theta_s(\xi)|$.

Definition 4.1 that follows provides a rigorous statement of the concept of input-to-state stability for the system of Eq.4.1.

Definition 4.1 [143]: *Let β be a function of class-$\mathcal{KL}$, γ be a function of class-$\mathcal{Q}$ and δ_x, δ_θ be positive real numbers. The zero solution of Eq.4.1 with $u(t) = 0$ is said to be input-to-state stable if $|x_0(\xi)| \leq \delta_x$ and $||\theta_t|| \leq \delta_\theta$ imply that the solution of the system of Eq.4.1 is defined for all times and satisfies:*

$$|x_t(\xi)| \leq \beta(|x_0(\xi)|, t) + \gamma(||\theta_t||), \quad \forall\, t \geq 0 \tag{4.2}$$

The above definition, when $\theta(t) \equiv 0$, $\forall\, t \geq 0$ reduces to the definition of asymptotic stability for the zero solution of the DDE system of Eq.4.1. Furthermore, when $\alpha = 0$, Definition 4.1 reduces to the standard definition of input-to-state stability for nonlinear ODE systems with external inputs (see, for example, [78]). Finally, we note that from the definition of $|x_t(\xi)|$ and Eq.4.2, it follows that $\|x(t)\|_{\mathbb{R}^n} \leq |x_t(\xi)| \leq \beta(|x_0(\xi)|, t) + \gamma(||\theta_t||)$, $\forall\, t \geq 0$.

The following theorem provides sufficient conditions for uniform ultimate boundedness of the system of Eq.4.1, expressed in terms of a suitable functional. The result of this theorem will be directly used in the solution of the state feedback control problem in Section 4.4 below.

Theorem 4.1 [63]: *Consider the system of Eq.4.1 with $u(t) \equiv 0$ and let γ_1 be a function of class-$\mathcal{K}_\infty$ and $\gamma_2, \gamma_3, \gamma_4$ be functions of class-$\mathcal{Q}$. If there is a continuous functional $V : C \to R_{\geq 0}$ such that:*

$$\begin{aligned} \gamma_1(\|x(t)\|_{\mathbb{R}^n}) &\leq V(x_t(\xi)) \leq \gamma_2(|x_t(\xi)|) \\ \dot{V}(x_t(\xi)) &\leq -\gamma_3(\|x(t)\|_{\mathbb{R}^n}), \\ \|x(t)\|_{\mathbb{R}^n} &\geq \gamma_4(||\theta_t||) \end{aligned} \tag{4.3}$$

then the solutions of Eq.4.1 satisfy Eq.4.2.

Remark 4.1: Even though, at this stage, there is no systematic way for selecting the form of the functional $V(x_t(\xi))$ which is suitable for a particular application, a choice for $V(x_t(\xi))$, which is frequently used to show local exponential stability of a DDE system of the form of Eq.4.1 via Theorem 4.1, is:

$$V(x_t(\xi)) \;=\; x(t)^T C x(t) + a^2 \int_{t-\alpha}^{t} x(s)^T E x(s) ds \tag{4.4}$$

where E, C are symmetric positive definite matrices and a is a positive real number. Clearly, the functional of Eq.4.4 satisfies $K_1 \|x(t)\|^2_{\mathbb{R}^n} \leq V(x_t(\xi)) \leq K_2 |x_t(\xi)|^2$ for some positive K_1, K_2.

4.4 Robust nonlinear controller synthesis

We consider systems of the form of Eq.4.1 and address the problem of synthesizing nonlinear static state feedback control laws of the general form:

$$u(t) \;=\; \mathcal{R}(x(t), \bar{v}(t), x(t-\alpha), \bar{v}(t-\alpha)) \tag{4.5}$$

where $\mathcal{R}(x(t), \bar{v}(t), x(t-\alpha), \bar{v}(t-\alpha))$ is a nonlinear scalar function, $\bar{v}(s) = [v(s) \;\; v^{(1)}(s) \;\; \cdots \;\; v^{(r-1)}(s)]^T$, $s \in [t-\alpha, t]$ and $v^{(k)}$ denotes the $k-$th time-derivative of the reference input $v \in \mathbb{R}$. The controllers enforce the following properties in the closed-loop system: a) boundedness of the trajectories, b) robust output tracking for changes in the reference input with arbitrary degree of asymptotic attenuation of the effect of the uncertainty on the output, and c) compensate for the effect of the time delay on the output, *independently of the size of the state delays.* The structure of the control law of Eq.4.5 is motivated by available results on stabilization of linear DDE systems (e.g., [126, 113]) and the requirement of output tracking with attenuation of the effect of the uncertainty on the output. The controllers will be synthesized by employing a novel combination of geometric control concepts with the method of

Lyapunov functionals.

In order to proceed with the explicit synthesis of the control law of Eq.4.5, we will need to make certain assumptions on the structure and stability properties of the system of Eq.4.1. To simplify the statement of these assumptions, we introduce the notation:

$$\begin{aligned} f(x(t), x(t-\alpha), \theta(t-\alpha_\theta)) &= f_{nom}(x(t), x(t-\alpha)) + \delta(x(t), x(t-\alpha), \theta(t-\alpha_\theta)) \\ f_{nom}(x(t), x(t-\alpha)) &= \tilde{f}_{nom}(x(t)) + p(x(t), x(t-\alpha)) \\ \tilde{p}(x(t), x(t-\alpha), \theta(t-\alpha_\theta)) &= \delta(x(t), x(t-\alpha), \theta(t-\alpha_\theta)) + p(x(t), x(t-\alpha)) \end{aligned} \tag{4.6}$$

which allows us to rewrite the system of Eq.4.1 in the following form:

$$\begin{aligned} \dot{x} &= \tilde{f}_{nom}(x(t)) + g(x(t), x(t-\alpha))u + \tilde{p}(x(t), x(t-\alpha), \theta(t-\alpha_\theta)) \\ y &= h(x) \end{aligned} \tag{4.7}$$

The first assumption is motivated by the requirement of output tracking with the attenuation of the effect of the uncertainty on the output and will play a crucial role in the synthesis of the controller.

Assumption 4.1 : *Referring to the system of Eq.4.7, there exists an integer r and a change of variables:*

$$\begin{bmatrix} \zeta(s) \\ \eta(s) \end{bmatrix} = \begin{bmatrix} \zeta_1(s) \\ \zeta_2(s) \\ \vdots \\ \zeta_r(s) \\ \eta_1(s) \\ \vdots \\ \eta_{n-r}(s) \end{bmatrix} = \mathcal{X}(x(s)) = \begin{bmatrix} h(x(s)) \\ L_{\tilde{f}_{nom}} h(x(s)) \\ \vdots \\ L^{r-1}_{\tilde{f}_{nom}} h(x(s)) \\ \chi_1(x(s)) \\ \vdots \\ \chi_{n-r}(x(s)) \end{bmatrix} \tag{4.8}$$

where $s \in [t-\alpha, t]$, $t \in [0, \infty)$ and $\chi_1(x(s)), \cdots, \chi_{n-r}(x(s))$ are nonlinear scalar functions such that the system of Eq.4.7 takes the form:

$$\begin{aligned} \dot{\zeta}_1 &= \zeta_2(t) + \tilde{p}_1(\zeta(t), \eta(t), \zeta(t-\alpha), \eta(t-\alpha), \theta(t-\alpha_\theta)) \\ &\vdots \\ \dot{\zeta}_{r-1} &= \zeta_r(t) + \tilde{p}_{r-1}(\zeta(t), \eta(t), \zeta(t-\alpha), \eta(t-\alpha), \theta(t-\alpha_\theta)) \end{aligned}$$

$$
\begin{aligned}
\dot{\zeta}_r &= L^r_{\bar{f}_{nom}} h(\mathcal{X}^{-1}(\zeta(t),\eta(t)) + L_g L^{r-1}_{\bar{f}_{nom}} h(\mathcal{X}^{-1}(\zeta(t),\eta(t))u(t) \\
&\quad + p_r(\zeta(t),\eta(t),\zeta(t-\alpha),\eta(t-\alpha)) \\
&\quad + \delta_r(\zeta(t),\eta(t),\zeta(t-\alpha),\eta(t-\alpha),\theta(t-\alpha_\theta)) \\
\dot{\eta}_1 &= \Psi_1(\zeta(t),\eta(t),\zeta(t-\alpha),\eta(t-\alpha),\theta(t-\alpha_\theta)) \\
&\vdots \\
\dot{\eta}_{n-r} &= \Psi_{n-r}(\zeta(t),\eta(t),\zeta(t-\alpha),\eta(t-\alpha),\theta(t-\alpha_\theta)) \\
y &= \zeta_1(t)
\end{aligned}
\tag{4.9}
$$

where $p_r(\zeta(t),\eta(t),\zeta(t-\alpha),\eta(t-\alpha)) + \delta_r(\zeta(t),\eta(t),\zeta(t-\alpha),\eta(t-\alpha),\theta(t-\alpha_\theta)) = \bar{p}_r(\zeta(t),\eta(t),\zeta(t-\alpha),\eta(t-\alpha),\theta(t-\alpha_\theta))$ *and* $L_g L^{r-1}_{\bar{f}_{nom}} h(x) \neq 0$ *for all* $x(s) \in \mathbb{R}^n$, $s \in [t-\alpha, t]$. *Moreover, for each* $\theta(s) \in \mathbb{R}^q$, $s \in [t-\alpha_\theta, t]$, *the states* $\zeta(s)$ *and* $\eta(s)$, $s \in [t-\alpha, t]$, *are bounded if and only if the state* $x(s) \in \mathbb{R}^n$, $s \in [t-\alpha, t]$ *is bounded.*

Assumption 4.1 provides the explicit form of a coordinate change (which is independent of the state delay present in the system of Eq.4.1) that transforms the nonlinear DDE system of Eq.4.1 into an interconnection of two subsystems, the ζ-subsystem which describes the input/output dynamics of the system of Eq.4.1 and the η-subsystem which describes the dynamics of the system of Eq.4.1 which are unobservable from the output. Specifically, the interconnection of Eq.4.9 is obtained by considering the change of variables of Eq.4.8 with $s = t$, differentiating it with respect to time, and using that $x(t) = \mathcal{X}^{-1}(\zeta(t),\eta(t))$, $x(t-\alpha) = \mathcal{X}^{-1}(\zeta(t-\alpha),\eta(t-\alpha))$ (note that this is possible because the coordinate change of Eq.4.8 is assumed to be valid for $s \in [t-\alpha, t]$). The assumption that $L_g L^{r-1}_{\bar{f}_{nom}} h(x) \neq 0$ is necessary in order to guarantee that the resulting controller is well-posed in the sense that the controller does not generate infinite control action for any values of the states of the process (compare with the structure of the controller given in Theorem 4.2).

The coordinate transformation of Eq.4.8 is not restrictive from an application point of view (one can easily verify that Assumption 4.1 holds for the FCC unit of Section

4.5), and it significantly facilitates the controller synthesis task which will be now addressed on the basis of the low-order partially-linear ζ-subsystem.

To proceed with the controller design, we need to impose the following stability requirement on the $\eta-$subsystem of the system of Eq.4.9.

Assumption 4.2: *The dynamical system:*

$$\begin{aligned} \dot{\eta}_1 &= \Psi_1(\zeta(t), \eta(t), \zeta(t-\alpha), \eta(t-\alpha), \theta(t-\alpha_\theta)) \\ &\vdots \\ \dot{\eta}_{n-r} &= \Psi_{n-r}(\zeta(t), \eta(t), \zeta(t-\alpha), \eta(t-\alpha), \theta(t-\alpha_\theta)) \end{aligned} \tag{4.10}$$

is input-to-state stable with respect to the inputs $\zeta_t(\xi)$ and $\theta_t(\xi)$.

The above assumption states that if the states of the $\zeta-$subsystem, $\zeta_t(\xi)$ and the uncertainty $\theta_t(\xi)$, are bounded, then the states of the $\eta-$subsystem will also remain bounded. In practice, Assumption 4.2 can be verified by linearizing the system of Eq.4.10 with $\zeta_t(\xi) = \theta_t(\xi) = 0$ around the operating steady-state and computing the eigenvalues of the resulting linear DDE system (this can be done by using standard algorithms, for example [105, 106]). If all of these eigenvalues are in the left-half of the complex plane, then [143] Assumption 4.2 is satisfied locally (i.e., for sufficiently small initial conditions, $||\zeta_t(\xi)||$, and $||\theta_t(\xi)||$).

Assumption 4.2 allows addressing the controller synthesis problem on the basis of the $\zeta-$subsystem. Specifically, applying the following preliminary feedback law:

$$\begin{aligned} u(t) = \frac{1}{L_g L_{\tilde{f}_{nom}}^{r-1} h(\mathcal{X}^{-1}(\zeta,\eta))} &(\tilde{u}(t) - L_{\tilde{f}_{nom}}^{r} h(\mathcal{X}^{-1}(\zeta,\eta)) \\ &-p_r(\zeta(t), \eta(t), \zeta(t-\alpha), \eta(t-\alpha))) \end{aligned} \tag{4.11}$$

where $\tilde{u}(t)$ is an auxiliary input, to the system of Eq.4.9 in order to cancel all the nonlinear terms that are known and can be cancelled by using a feedback which utilizes measurements of $x(s)$ for $s \in [t-\alpha, t]$, we obtain the following modified system:

$$
\begin{aligned}
\dot{\zeta}_1 &= \zeta_2(t) + \tilde{p}_1(\zeta(t), \eta(t), \zeta(t-\alpha), \eta(t-\alpha), \theta(t-\alpha_\theta)) \\
&\vdots \\
\dot{\zeta}_{r-1} &= \zeta_r(t) + \tilde{p}_{r-1}(\zeta(t), \eta(t), \zeta(t-\alpha), \eta(t-\alpha), \theta(t-\alpha_\theta)) \\
\dot{\zeta}_r &= \tilde{u} + \delta_r(\zeta(t), \eta(t), \zeta(t-\alpha), \eta(t-\alpha), \theta(t-\alpha_\theta)) \\
\dot{\eta}_1 &= \Psi_1(\zeta(t), \eta(t), \zeta(t-\alpha), \eta(t-\alpha), \theta(t-\alpha_\theta)) \\
&\vdots \\
\dot{\eta}_{n-r} &= \Psi_{n-r}(\zeta(t), \eta(t), x(t-\alpha), \eta(t-\alpha), \theta(t-\alpha_\theta)) \\
y &= \zeta_1(t)
\end{aligned}
\tag{4.12}
$$

where $\zeta_k(t) = L_{\tilde{f}_{nom}}^{k-1} h(x)$, $k = 1, \ldots, r$.

Introduce the notation:

$$
\tilde{A} = \begin{bmatrix} 0 & 1 & 0 & \cdots & 0 & 0 \\ 0 & 0 & 1 & \cdots & 0 & 0 \\ 0 & 0 & 0 & \cdots & 0 & 0 \\ \vdots & \vdots & \vdots & \ddots & \vdots & \vdots \\ 0 & 0 & 0 & \cdots & 0 & 0 \end{bmatrix}, \qquad b = \begin{bmatrix} 0 \\ 0 \\ 0 \\ \vdots \\ 1 \end{bmatrix},
$$

$$
\bar{p}(\zeta(t), \eta(t), \zeta(t-\alpha), \eta(t-\alpha), \theta(t-\alpha_\theta)) = \tag{4.13}
$$

$$
\begin{bmatrix} \tilde{p}_1(\zeta(t), \eta(t), \zeta(t-\alpha), \eta(t-\alpha), \theta(t-\alpha_\theta)) \\ \tilde{p}_2(\zeta(t), \eta(t), \zeta(t-\alpha), \eta(t-\alpha), \theta(t-\alpha_\theta)) \\ \vdots \\ \tilde{p}_{r-1}(\zeta(t), \eta(t), \zeta(t-\alpha), \eta(t-\alpha), \theta(t-\alpha_\theta)) \\ 0 \end{bmatrix}
$$

Let $\bar{e}(s) = [(h(x(s)) - v(s)) \ (L_{\tilde{f}_{nom}} h(x(s)) - v^{(1)}(s)) \ \cdots \ (L_{\tilde{f}_{nom}}^{r-1} h(x(s)) - v^{(r-1)}(s))]^T$ and $\bar{v}(s) = [v(s) \ v^{(1)}(s) \ \cdots \ v^{(r-1)}(s)]^T$, $s \in [t-\alpha, t]$ where $v^{(k)}$ denotes the k-th time-derivative of the reference input v, the ζ-subsystem of the system of Eq.4.12 can be written in the following compact form:

$$
\begin{aligned}
\dot{\bar{e}} &= \tilde{A}\bar{e}(t) + b\tilde{u}(t) + \bar{p}(\bar{e}(t) + \bar{v}(t), \eta(t), \bar{e}(t-\alpha) + \bar{v}(t-\alpha), \eta(t-\alpha), \theta(t-\alpha_\theta)) \\
&\quad + b\delta_r(\bar{e}(t) + \bar{v}(t), \eta(t), \bar{e}(t-\alpha) + \bar{v}(t-\alpha), \eta(t-\alpha), \theta(t-\alpha_\theta)) \\
y &= \bar{e}_1(t)
\end{aligned}
\tag{4.14}
$$

The controller synthesis task has been now reduced to the one of synthesizing the auxiliary input $\tilde{u}(t)$ to achieve the asymptotic attenuation of the effect of the un-

certainties of the $\bar{e}$-subsystem of Eq.4.14, on the output. Specifically, the synthesis of $\bar{u}(t)$ will be performed by using the method of Lyapunov functionals, so that the time-derivative of the following Lyapunov functional:

$$V = \bar{e}^T(t)P\bar{e}(t) + a^2\int_{t-\alpha}^{t}\bar{e}^T(s)\bar{e}(s)ds \tag{4.15}$$

where a is a positive real number, calculated along the state of the closed-loop $\bar{e}$—subsystem is negative definite. The incorporation of the integral term $\int_{t-\alpha}^{t}\bar{e}^T(s)\bar{e}(s)ds$ in the functional of Eq.4.15 allows accounting for the distributed parameter (delayed) nature of the system of Eq.4.1 in the controller design stage and synthesizing a controller that enforces the requested properties in the closed-loop system independently of the size of the state delay.

To explicitly synthesize $\bar{u}(t)$, we need to assume the existence of known state-dependent, possibly time varying, upper bound that capture the size of the uncertainty for all times (such bounds are usually obtained from physical considerations, preliminary simulations, experimental data, etc.). Assumptions 4.3 and 4.4 formalize our requirements.

Assumption 4.3: *There exists a known function* $\bar{c}_0(\bar{e}(t)+\bar{v}(t),\eta(t),\bar{e}(t-\alpha)+\bar{v}(t-\alpha),\eta(t-\alpha),t)$ *such that the following condition holds:*

$$\begin{aligned}|\delta_r(\bar{e}(t)+\bar{v}(t),\eta(t),\bar{e}(t-\alpha)+\bar{v}(t-\alpha),\eta(t-\alpha),\theta(t-\alpha_\theta))|_{\mathbb{R}} \leq \\ \bar{c}_0(\bar{e}(t)+\bar{v}(t),\eta(t),\bar{e}(t-\alpha)+\bar{v}(t-\alpha),\eta(t-\alpha),t)\end{aligned} \tag{4.16}$$

where $|\cdot|_{\mathbb{R}}$ *denotes the absolute value of a scalar, for all* $\bar{e}(s)\in\mathbb{R}^r$, $s\in[t-\alpha,t]$, $\theta(s)\in\mathbb{R}^q$ $s\in[t-\alpha_\theta,t]$, $\bar{v}(s)\in\mathbb{R}^r$, $s\in[t-\alpha,t]$, $\eta(s)\in\mathbb{R}^{n-r}$, $s\in[t-\alpha,t]$.

Assumption 4.4: *There exist positive real numbers* a_1,a_2 *such that the following bound can be written:*

$$\begin{aligned}\|\bar{p}(\bar{e}(t)+\bar{v}(t),\eta(t),\bar{e}(t-\alpha)+\bar{v}(t-\alpha),\eta(t-\alpha),\theta(t-\alpha_\theta))\|^2_{\mathbb{R}^r} \leq \\ a_1\bar{e}^2(t)+a_2\bar{e}^2(t-\alpha)\end{aligned} \tag{4.17}$$

for all $\bar{e}(s) \in \mathbb{R}^r$, $s \in [t-\alpha, t]$, $\theta(s) \in \mathbb{R}^q$ $s \in [t-\alpha_\theta, t]$, $\bar{v}(s) \in \mathbb{R}^r$, $s \in [t-\alpha, t]$, $\eta(s) \in \mathbb{R}^{n-r}$, $s \in [t-\alpha, t]$. The above assumption on the growth of the vector $\bar{p}(\bar{e}(t)+\bar{v}(t), \eta(t), \bar{e}(t-\alpha)+\bar{v}(t-\alpha), \eta(t-\alpha), \theta(t-\alpha_\theta))$ does not need to hold globally (i.e., for any $\bar{e}(t), \eta(t)$), and thus, it is satisfied by most practical problems (see for example the fluidized catalytic cracking unit of Section 4.5).

We are now in a position to state the main controller synthesis result of this chapter in the form of a theorem (the proof of this theorem can be found in Appendix B).

Theorem 4.2: *Consider the nonlinear DDE system of Eq.4.1 for which Assumptions 4.1, 4.2, 4.3 and 4.4 hold. Suppose that the matrix equation*

$$\tilde{A}^T P + P\tilde{A} - 2P^T b R_2^{-1} b^T P + (a^2 + a_1) I_{n\times n} + P^2 = -R_1 \tag{4.18}$$

where $a^2 > a_2$, *and* R_1 *is a positive definite matrix, has a unique positive definite solution for* P, *and consider the closed-loop system under the robust nonlinear state feedback controller:*

$$\begin{aligned} u &= \mathcal{R}(x(t), x(t-\alpha), t) \\ &= \frac{1}{L_g L_{\tilde{f}}^{r-1} h(x(t))} \Big(-R_2^{-1} b^T P \bar{e}(t) + v^r(t) - \bar{\chi}\bar{c}_0(x(t), x(t-\alpha), t) w(\bar{e}(t), \phi) \\ &\quad - L_{\tilde{f}_{nom}}^r h(x(t)) - p_r(x(t), x(t-\alpha)) \Big) \end{aligned} \tag{4.19}$$

where $w(\bar{e}(t), \phi)$ *is a scalar function and is given by*

$$w(\bar{e}(t), \phi) = \frac{b^T P \bar{e}(t)}{|b^T P \bar{e}(t)|_{\mathbb{R}} + \phi} \tag{4.20}$$

and $\bar{\chi}, \phi$ *are adjustable parameters with* $\bar{\chi} > 1$ *and* $\phi > 0$. *Then, there exist positive real numbers* δ, d, ϕ^* *such that if* $\max\{|x_0(\xi)|, ||\bar{v}_t||, ||\theta_t||\} \leq \delta$ *and* $\phi \in (0, \phi^*]$, *the output of the closed-loop system satisfies a relation of the form*

$$\lim_{t\to\infty} sup\, |y(t) - v(t)|_{\mathbb{R}} \leq d \tag{4.21}$$

independently of the size of the state delays.

Remark 4.2: Regarding the structure, implementation and closed-loop properties of the nonlinear state feedback controller of Eq.4.19, several remarks are in order: a) it uses measurements of the states of the process evaluated at t and $t-\alpha$ (i.e., $x(t)$ and $x(t-\alpha)$), and thus, it belongs to the class of the requested control laws of Eq.4.5, b) its practical implementation requires the use of memory lines to store the values of x in the time interval $[t-\alpha, t]$, and c) it enforces stability and asymptotic output tracking in the closed-loop system *independently of the size of the state delay.*

Remark 4.3: In order to apply the result of Theorem 4.2 to a chemical process application, one has to initially verify Assumptions 4.1, 4.2 and 4.3 of the theorem on the basis of the process model and compute the parameters a_1 and a_2 and the function $\tilde{c}_0(x(t), x(t-\alpha), t)$. Then, a, R_1, R_2 should be chosen so that $a^2 > a_2$ and the matrices R_1, R_2 are positive definite to ensure that the matrix Eq.4.18 has a unique positive definite solution for P. Note that R_1 determines the speed of the closed-loop output response (namely, "larger" (in terms of the smallest eigenvalue) R_1 means faster response), while R_2 determines the penalty that should be imposed on the manipulated input in achieving stabilization and output tracking ("larger" R_2 means larger penalty on the control action). If these assumptions are satisfied, the synthesis formula of Eq.4.19 can be directly used to derive the explicit form of the controller (see Section 4.5 for an application of this procedure to a chemical process example).

Remark 4.4: The robust nonlinear controller of Eq.4.19 possesses a robustness property with respect to fast and exponentially stable unmodeled dynamics (i.e., the controller enforces boundedness of the state and output tracking with uncertainty attenuation in the closed-loop system despite the presence of additional dynamics in the process, as long as they are exponentially stable and sufficiently fast). This

property of the controller of Eq.4.19 can be rigorously established by analyzing the closed-loop system with the unmodeled dynamics using singular perturbations and is of particular importance for many practical applications where unmodeled dynamics often occur due to actuator and sensor dynamics, fast process dynamics, etc..

4.5 Application to a fluidized catalytic cracker

In this section, we illustrate the implementation of the developed control methodology on the FCC unit shown before in Figure 3.8. The FCC unit consists of a cracking reactor, where the cracking of high boiling gas oil fractions into lighter hydrocarbons (e.g., gasoline) and the carbon formation reactions (undesired reactions) take place and a regenerator, where the carbon removal reactions take place. The reader may refer to: a) [55, 108, 14] for a detailed discussion of the features of the FCC unit, b) [15] for an analysis of the issue of control structure selection and c) [109, 67] and [47, 7] for application of linear and nonlinear control methods to the FCC unit, respectively.

Under the assumptions of well-mixed reactive catalyst in the reactor, small-size catalyst particles, constant solid holdup in reactor and regenerator, uniform and constant pressure in reactor and regenerator, the dynamic model for the FCC unit can be derived and takes the form [55, 7]:

$$
\begin{aligned}
V_{ra}\frac{dC_{cat}}{dt} &= -60F_{rc}C_{cat}(t) + 50R_{cf}(C_{cat}(t), C_{rc}(t-\alpha_1), T_{ra}) \\
V_{ra}\frac{dC_{sc}}{dt} &= 60F_{rc}[C_{rc}(t-\alpha_1) - C_{sc}(t)] + 50R_{cf}(C_{cat}(t), C_{rc}(t-\alpha_1), T_{ra}) \\
V_{ra}\frac{dT_{ra}}{dt} &= 60F_{rc}[T_{rg}(t-\alpha_1) - T_{ra}(t)] + 0.875\frac{S_f}{S_c}D_{tf}R_{tf}[T_{fp} - T_{ra}(t)] \\
&\quad +0.875\frac{(-\Delta H_{fv})}{S_c}D_{tf}R_{tf} + 0.5\frac{(-\Delta H_{cr})}{S_c}R_{oc}(C_{cat}(t), C_{rc}(t-\alpha_1), T_{ra}) \\
V_{rg}\frac{dC_{rc}}{dt} &= 60F_{rc}[C_{sc}(t-\alpha_2) - C_{rc}(t)] - 50R_{cb}(C_{rc}(t), T_{rg}(t))
\end{aligned}
$$

$$V_{rg}\frac{dT_{rg}}{dt} = 60F_{rc}[T_{ra}(t-\alpha_2) - T_{rg}(t)] + 0.5\frac{S_a}{S_c}R_{ai}[T_{ai} - T_{rg}(t)] \\ -0.5\frac{(-\Delta H_{rg})}{S_c}R_{cb}(C_{rc}(t), T_{rg}(t)) \tag{4.22}$$

where C_{cat}, C_{sc}, C_{rc} denote the concentrations of catalytic carbon on spent catalyst, the total carbon on spent catalyst, and carbon on regenerated catalyst, T_{ra}, T_{rg} denote the temperatures in the reactor and the regenerator, R_{ai} is the air flow rate in the regenerator, R_{tf} is the total feed flow rate, D_{tf} is the density of total feed, V_{ra}, V_{rg} denote the catalyst holdup of the reactor and the regenerator, $\Delta H_{rg}, \Delta H_{cr}$ are the heat of regeneration and cracking, ΔH_{fv} is the heat of feed vaporization, F_{rc} denotes the circulation flow rate of catalyst from reactor to regenerator and vice-versa, S_a, S_c, S_f denote specific heats of the air, the catalyst, and the feed, T_{fp}, T_{ai} denote the inlet temperatures of the feed in the reactor and of the air in the regenerator, and R_{cf}, R_{oc}, R_{cb} denote the reaction rates of total carbon forming, of gas-oil cracking, and of coke burning. The analytic expressions for the reaction rates R_{cf}, R_{oc}, R_{cb} can be found in [55].

The presence of time delay in the terms $C_{rc}(t-\alpha_1), T_{rg}(t-\alpha_1)$ is due to dead-time in the pipes transferring regenerated catalyst from the regenerator to the reactor, and the time delay in the terms $C_{sc}(t-\alpha_2), T_{ra}(t-\alpha_2)$ is due to dead time in the pipes transferring spent catalyst from the reactor to the regenerator. Even though the proposed method can be readily applied to the case where $\alpha_1 \neq \alpha_2$, we pick in order to simplify our development, $\alpha_1 = \alpha_2 = \alpha = 0.3\ hr$. The values of the remaining process parameters and the corresponding steady-state values are given earlier in Table 3.2.

The control objective is the regulation of the temperature in the regenerator, T_{rg}, by manipulating the temperature of the inlet air in the regenerator, T_{ai}. The heat

of combustion in the regeneration is assumed to be the uncertain variable, $\Delta H_{rg} = \Delta H_{rg,n} + \theta(t)$, where $\Delta H_{rg,n}$ is the nominal value of the heat of combustion and $\theta(t)$ is the time-varying uncertainty. Setting $x = [x_1\ x_2\ x_3\ x_4\ x_5]^T = [T_{rg}\ C_{rc}\ T_{ra}\ C_{sc}\ C_{cat}]^T$, $u = T_{ai}$, $y = T_{rg}$, the process model of Eq.4.22 can be written in the form of Eq.4.7 with:

$$\tilde{f}(x(t)) = \begin{bmatrix} \tilde{f}_1 \\ \tilde{f}_2 \\ \tilde{f}_3 \\ \tilde{f}_4 \\ \tilde{f}_5 \end{bmatrix} = \begin{bmatrix} \dfrac{0.5 S_a R_{ai}}{S_c V_{rg}} T_{ais} - \left(\dfrac{60 F_{rc}}{V_{rg}} + 0.5 \dfrac{S_a R_{ai}}{S_c V_{rg}} \right) T_{rg}(t) \\ -0.5 \dfrac{(-\Delta H_{rg,n})}{S_c V_{rg}} R_{cb}(C_{rc}(t), T_{rg}(t)) \\ -\dfrac{60 F_{rc}}{V_{rg}} C_{rc}(t) - \dfrac{50}{V_{rg}} R_{cb}(C_{rc}(t), T_{rg}(t)) \\ -\dfrac{60 F_{rc}}{V_{ra}} T_{ra}(t) + 0.875 \dfrac{S_f}{S_c V_{ra}} D_{tf} R_{tf} [T_{fp} - T_{ra}(t)] \\ +0.875 \dfrac{(-\Delta H_{fv})}{S_c V_{ra}} D_{tf} R_{tf} \\ -\dfrac{60 F_{rc}}{V_{ra}} C_{sc}(t) \\ -\dfrac{60 F_{rc}}{V_{ra}} C_{cat}(t) \end{bmatrix} \tag{4.23}$$

$$\bar{p}(x(t), x(t-\alpha)) = \begin{bmatrix} \bar{p}_1 \\ \bar{p}_2 \\ \bar{p}_3 \\ \bar{p}_4 \\ \bar{p}_5 \end{bmatrix} = \begin{bmatrix} \dfrac{60 F_{rc}}{V_{rg}} T_{ra}(t-\alpha) - 0.5 \dfrac{(-\theta(t))}{S_c V_{rg}} R_{cb}(C_{rc}(t), T_{rg}(t)) \\ \dfrac{60 F_{rc}}{V_{rg}} C_{sc}(t-\alpha) \\ \dfrac{60 F_{rc}}{V_{ra}} T_{rg}(t-\alpha) \\ +0.5 \dfrac{(-\Delta H_{cr})}{S_c V_{ra}} R_{oc}(C_{cat}(t), C_{rc}(t-\alpha), T_{ra}(t)) \\ \dfrac{60 F_{rc}}{V_{ra}} C_{rc}(t-\alpha) \\ +\dfrac{50}{V_{ra}} R_{cf}(C_{cat}(t), C_{rc}(t-\alpha), T_{ra}(t)) \\ \dfrac{50}{V_{ra}} R_{cf}(C_{cat}(t), C_{rc}(t-\alpha), T_{ra}(t)) \end{bmatrix} \tag{4.24}$$

$$g(x(t), x(t-\alpha)) = \begin{bmatrix} g_1 \\ g_2 \\ g_3 \\ g_4 \\ g_5 \end{bmatrix} = \begin{bmatrix} \frac{0.5 S_a R_{ai}}{S_c V_{rg}} \\ 0 \\ 0 \\ 0 \\ 0 \end{bmatrix} \tag{4.25}$$

For the system of Eq.4.22, Assumption 4.1 is satisfied with $r = 1$, the coordinate transformation of Eq.4.8 takes the form $[\zeta_1\ \eta_1\ \eta_2\ \eta_3\ \eta_4]^T = [T_{rg}\ C_{rc}\ T_{ra}\ C_{sc}\ C_{cat}]^T$ and yields the following system:

$$\begin{aligned} \dot{\zeta} &= L_{\tilde{f}_{nom}} h(\mathcal{X}^{-1}(\zeta,\eta)) + L_g h(\mathcal{X}^{-1}(\zeta,\eta))u(t) + \tilde{p}_1(\zeta(t), \eta(t), \zeta(t-\alpha), \eta(t-\alpha), \theta(t)) \\ \dot{\eta} &= \Psi(\zeta(t), \eta(t), \zeta(t-\alpha), \eta(t-\alpha)) \end{aligned} \tag{4.26}$$

whose explicit form is given below in Eqs.4.27 and 4.29. To verify Assumption 4.2, we consider the η-subsystem of Eq.4.26 with $\zeta(t) = \zeta(t-\alpha) = \zeta_s = 1155.96$ i.e., the system:

$$\dot{\eta} = \begin{bmatrix} \dot{\eta}_1 \\ \dot{\eta}_2 \\ \dot{\eta}_3 \\ \dot{\eta}_4 \end{bmatrix} = \begin{bmatrix} -\frac{60F_{rc}}{V_{rg}}\eta_1 - \frac{50}{V_{rg}} R_{cb}(\eta_1, \zeta_s) + \frac{60F_{rc}}{V_{rg}}\eta_3(t-\alpha) \\ -\frac{60F_{rc}}{V_{ra}}\eta_2 + 0.875\frac{S_f}{S_c V_{ra}} D_{tf} R_{tf}[T_{fp} - \eta_2] + 0.875\frac{(-\Delta H_{fv})}{S_c V_{ra}} D_{tf} R_{tf} \\ \quad +0.5\frac{(-\Delta H_{cr})}{S_c V_{ra}} R_{oc}(\eta_4, \eta_1(t-\alpha), \eta_2) \\ -\frac{60F_{rc}}{V_{ra}}\eta_3 + \frac{60F_{rc}}{V_{ra}}\eta_1(t-\alpha) + \frac{50}{V_{ra}} R_{cf}(\eta_4, \eta_1(t-\alpha), \eta_2) \\ -\frac{60F_{rc}}{V_{ra}}\eta_4 + \frac{50}{V_{ra}} R_{cf}(\eta_4, \eta_1(t-\alpha), \eta_2) \end{bmatrix} \tag{4.27}$$

The linearization of the above system around the steady-state

$$C_{rc} = 0.6973\ wt\%\ ,\ T_{ra} = 930.62\ F\ ,\ C_{sc} = 1.5696\ wt\%\ ,\ C_{cat} = 0.8723\ wt\% \tag{4.28}$$

was found, through simulations, to be exponentially stable, which implies that the η-subsystem of Eq.4.26 possesses a local input-to-state stability property with respect to $\zeta_t(\xi)$. Therefore, Assumption 4.2 holds and the controller synthesis problem can be addressed on the basis of the ζ-subsystem which is given below:

$$\begin{aligned}\dot{\zeta} &= -\left(\frac{60F_{rc}}{V_{rg}} + \frac{0.5S_aR_{ai}}{S_cV_{rg}}\right)\zeta(t) - 0.5\frac{(-\Delta H_{rg,n})}{S_cV_{rg}}R_{cb}(\eta_1(t),\zeta(t)) \\ &\quad + \left(\frac{0.5S_aR_{ai}}{S_cV_{rg}}\right)u(t) + \left(\frac{60F_{rc}}{V_{rg}}\right)\eta_2(t-\alpha_2) + 0.5\frac{\theta(t)}{S_cV_{rg}}R_{cb}(\eta_1(t),\zeta(t))\end{aligned} \tag{4.29}$$

Setting $e(t) = \zeta(t) - v$ where v is the desired set point and implementing a preliminary control law of the form of Eq.4.11, the above system becomes:

$$\begin{aligned}\dot{e} &= -R_2^{-1}b^TPe(t) - \bar{\chi}\bar{c}_0(\bar{e}(t)+\bar{v}(t),\eta(t),\bar{e}(t-\alpha)+\bar{v}(t-\alpha),\eta(t-\alpha),t) \\ &\quad \times w(e(t),\phi) + 0.5\frac{\theta(t)}{S_cV_{rg}}R_{cb}(\eta_1(t),e(t)+\bar{v}(t))\end{aligned} \tag{4.30}$$

Assumption 4.4 is trivially satisfied since $\bar{p}(\bar{e}(t)+\bar{v}(t),\eta(t),\bar{e}(t-\alpha)+\bar{v}(t-\alpha),\eta(t-\alpha)) = 0$ and the functions $\bar{c}_0(\bar{e}(t)+\bar{v}(t),\eta(t),\bar{e}(t-\alpha)+\bar{v}(t-\alpha),\eta(t-\alpha),t)$ and $w(e(t),\phi)$ take the form:

$$\begin{aligned}\bar{c}_0(\bar{e}(t)+\bar{v}(t),\eta(t),\bar{e}(t-\alpha)+\bar{v}(t-\alpha),\eta(t-\alpha),t) &= 0.5\frac{\theta_b}{S_cV_{rg}}R_{cb}(\eta_1(t),e(t)+v) \\ w(e(t),\phi) &= \frac{Pe(t)}{|Pe(t)|_{\mathbb{R}}+\phi}\end{aligned} \tag{4.31}$$

where θ_b denotes the upper bound on the size of the uncertain variable and ϕ is an adjustable parameter. Utilizing the result of Theorem 4.2, the following matrix

equation can be formed:

$$\tilde{A}^T P + P\tilde{A} - 2P^T b R_2^{-1} b^T P + a^2 I_{n\times n} + P^2 = -R_1 \tag{4.32}$$

with $R_2 = \frac{1}{3}$, $a^2 = 2.5$ $(a^2 > a_2 = 0)$, and

$$\tilde{A} = 0\,, \quad b = 1\,, \quad R_1 = 2.5 \tag{4.33}$$

Eq.4.32 has a unique positive definite solution for P of the form:

$$P = 1.0 \tag{4.34}$$

which leads to the following nonlinear state feedback controller:

$$u = \frac{1}{L_g h(x(s))}\left[-3(x_1(t)-v) - \bar{\chi}0.5\frac{\theta_b}{S_c V_{rg}} R_{cb}(x_2(t), x_1(t))\left(\frac{x_1(t)-v}{|x_1(t)-v|_{\mathbb{R}}+\phi}\right)\right.$$
$$\left. -L_{\tilde{f}_{nom}} h(x(s)) - p_1(x(t), x(t-\alpha))\right] \tag{4.35}$$

We performed several sets of simulation runs to evaluate the performance and the robustness properties of the controller of Eq.4.35 and compare them with the ones of: a) a nonlinear controller that does not account for the time-varying uncertain variables (i.e. controller of Eq.4.35 with $\tilde{c}_0(x(t), x(t-\alpha), t) = 0$), b) a PI controller, and c) a robust nonlinear controller that does not account for the presence of dead-times associated with the pipes transferring material from the regenerator to reactor and vice versa (i.e., controller of Eq.4.35 with $\alpha = 0$). The user-friendly software package SIMULINK was used to carry out all the simulation runs (SIMULINK is a toolbox of the mathematical software MATLAB that includes a delay function which can be readily used to simulate differential equations with time delays). In all the simulation runs, the process was initially $(t = 0.0\ hr)$ assumed to be at the steady-state shown in Table 3.2 and a time-varying uncertain variable of the form:

$$\theta(t) = 300.0 * cos(0.5\ t) \tag{4.36}$$

was considered. The upper bound on the uncertainty was taken to be $\theta_b = 300.0$. The controller of Eq.4.35 was implemented with $\phi = 0.05$ and $\bar{\chi} = 1.1$ to guarantee that the output of the closed-loop system satisfies a relation of the form:

$$\lim_{t\to\infty} sup\,|y - v|_{\mathbb{R}} \leq 1.0 \tag{4.37}$$

In the first set of simulation runs, we tested the ability of the controller to maintain the output at the steady-state despite the presence of uncertainty. The output profile and the corresponding manipulated input profile are given in Figure 4.1. Clearly,

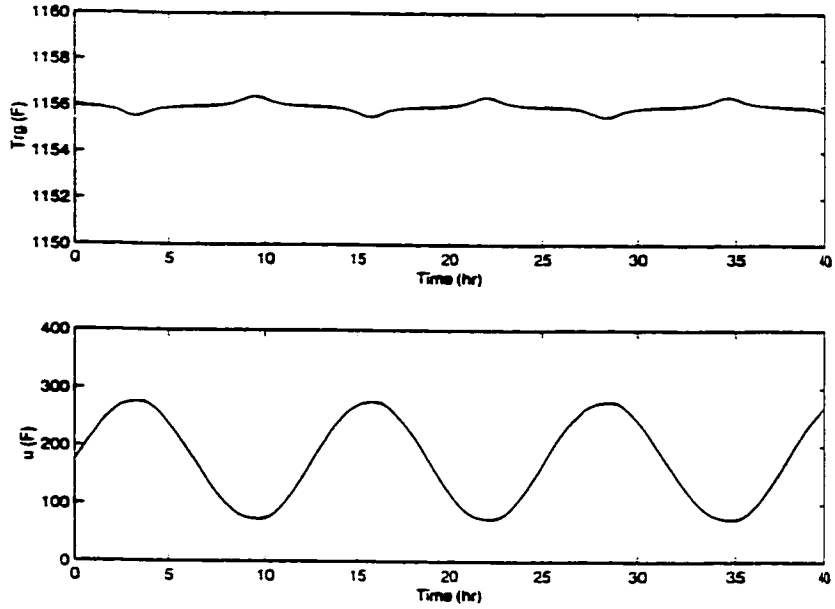

Figure 4.1: Closed-loop output and manipulated input profiles under the controller of Eq.4.35.

the controller regulates the output at the operating steady-state compensating for the effect of the uncertainty and satisfying the requirement of Eq.4.37. For the sake of comparison, we also implemented the nonlinear controller of Eq.4.35 with $\tilde{c}_0(x(t), x(t-\alpha), t) = 0$ and a PI controller with $K_c = 10$ and $\tau_I = 0.1$. Figure 4.2 shows the output profiles and the corresponding manipulated inputs of all three controllers; the performance of the proposed controller is clearly superior to the ones

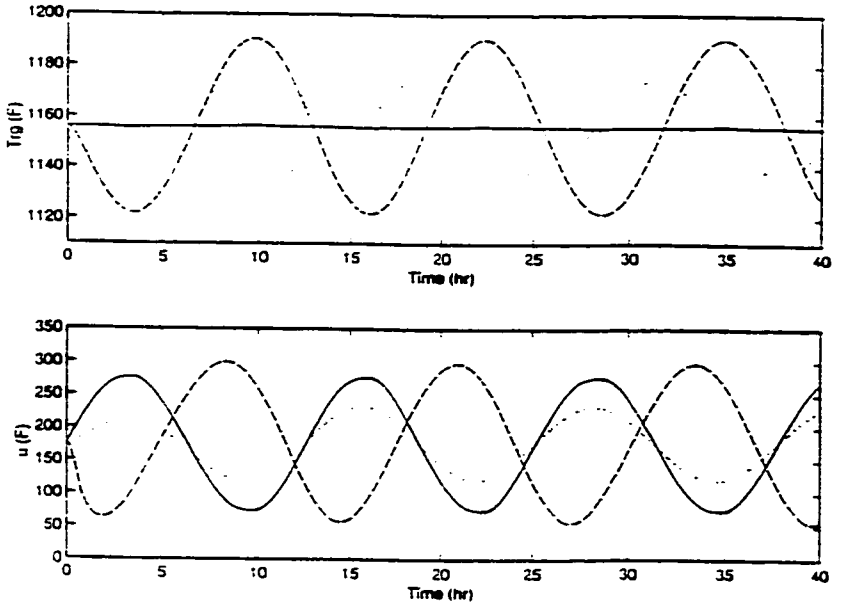

Figure 4.2: Closed-loop output and manipulated input profiles under the controller of Eq.4.35 (solid line), the controller of Eq.4.35 without accounting for the uncertainty (dashed line), and a PI controller (dotted line).

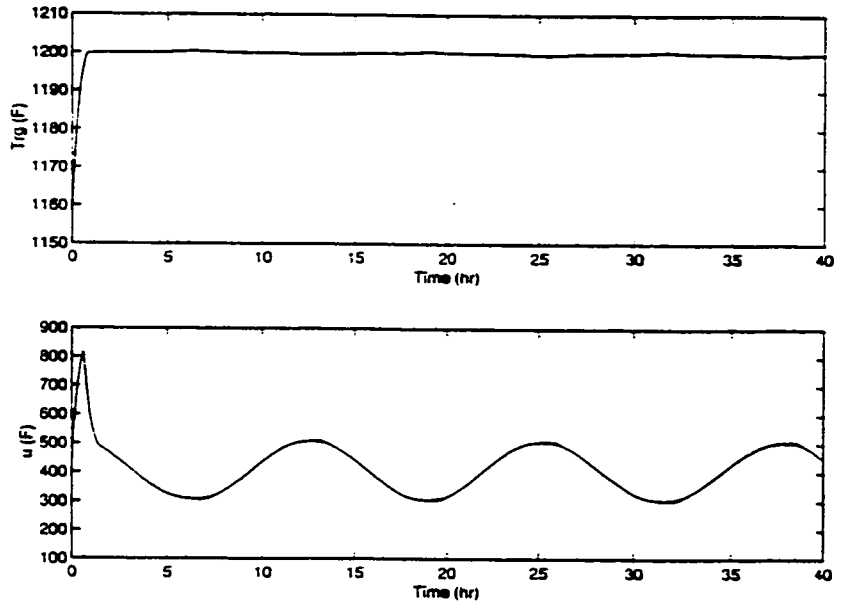

Figure 4.3: Closed-loop output and manipulated input profiles under the controller of Eq.4.35 for a $44^{o}F$ increase in the reference input.

of the other two controllers.

In the second set of simulation runs, we tested the output tracking capabilities of the nonlinear controller of Eq.4.35 for a 44^oF increase in the reference input.

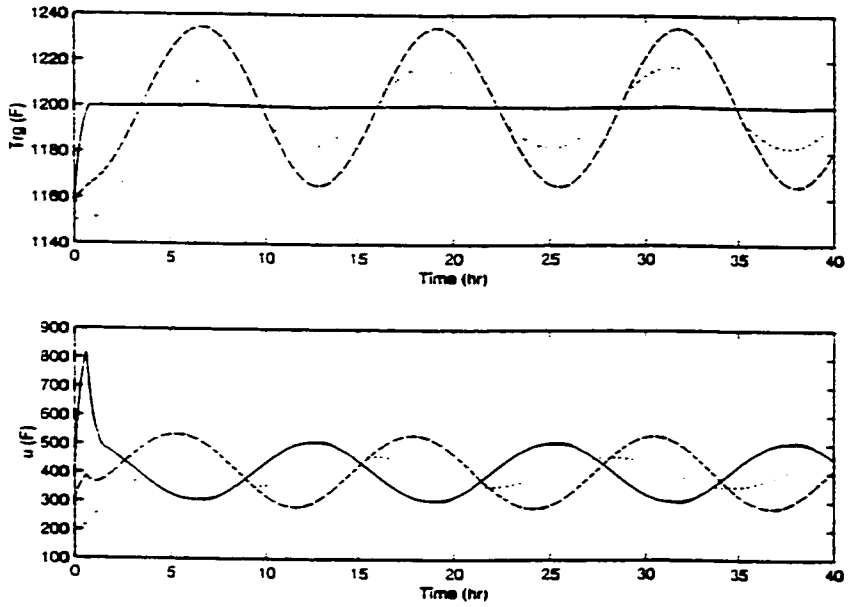

Figure 4.4: Closed-loop output and manipulated input profiles under the controller of Eq.4.35 (solid line), the controller of Eq.4.35 without accounting for the uncertainty (dashed line), and a PI controller (dotted line) for a 44^oF increase in the reference input.

Figure 4.3 shows the output and manipulated input profiles. The controller drives the output to the new reference input value compensating for the effect of the uncertainty and state delays, and satisfying the requirement of Eq.4.37. We also tested the controller of Eq.4.35 with $\tilde{c}_0(x(t), x(t-\alpha), t) = 0$ and a PI controller with $K_c = 10$ and $\tau_I = 0.1$. Figure 4.4 displays the output and manipulated input profiles of all three controllers. Again, the superiority of the proposed controller is evident. Finally, we also implemented a nonlinear controller which does not account for the presence of the state delays (no uncertainty was considered in this simulation run). Figure 4.5 shows the closed-loop output profile and manipulated input profile; this controller

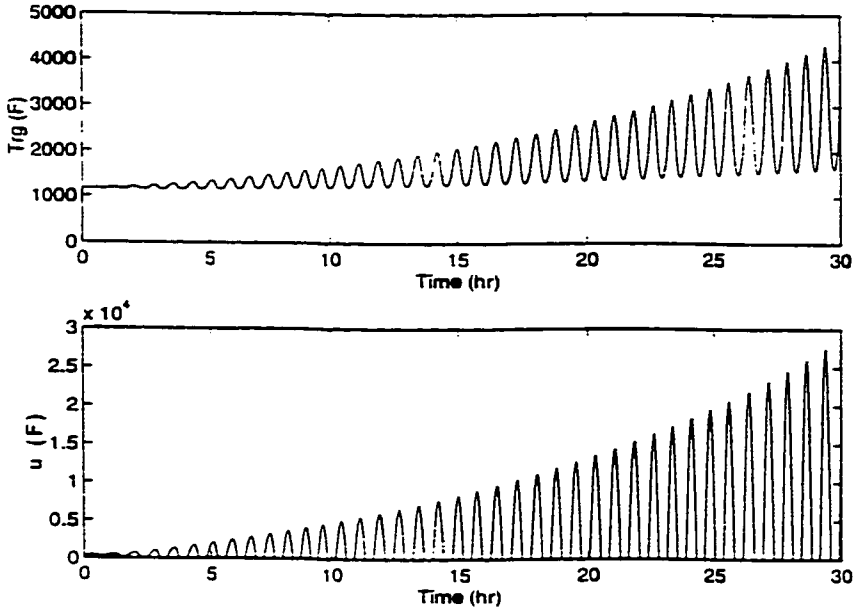

Figure 4.5: Closed-loop output and manipulated input profiles under the controller of Eq.4.35 with $\alpha = 0$; no model uncertainty is present.

leads to an unstable closed-loop system because it does not account for the presence of significant state delays.

4.6 Conclusions

We considered single-input single-output nonlinear DDE systems with uncertain variables and proposed a general methodology for the synthesis of robust nonlinear state feedback controllers that guarantee boundedness of the states and ensure that the ultimate discrepancy between the output and the external reference input in the closed-loop system can be made arbitrarily small by an appropriate choice of controller parameters. The controllers were synthesized by using a novel combination of geometric and Lyapunov-based techniques. The proposed control method was successfully applied to a fluidized catalytic cracking unit with a time-varying uncertain

variable and was shown to outperform a PI controller, a nonlinear controller that does not account for the uncertainty, and a nonlinear controller that does not account for the state delays. In the next chapter we extend these results to systems of PDEs with time-delays that arise in the modeling of transport-reaction processes (e.g., [132, 44]).

Chapter 5

Nonlinear Feedback Control of Parabolic Partial Differential Difference Equation Systems

5.1 Introduction

Quasi-linear parabolic PDDE systems arise naturally in the modeling of diffusion-convection-reaction processes with time-delays. A typical example of such processes is the tubular reactor with recycle loop, where the nonlinearities arise from the complex reaction mechanisms and the Arrhenius dependence of the reaction rates on temperature, and the time delays occur due to transportation lag in the recycle loop and dead times associated with the measurement sensor and the control actuator.

In the past, most of the research on control of diffusion-convection-reaction processes has been carried out in the context of linear/quasi-linear parabolic PDEs (see, for example, the review papers [19, 96, 45] and the references therein). Motivated by the fact that the eigenspectrum of the parabolic spatial differential operator can be partitioned into a finite-dimensional slow one and an infinite-dimensional stable fast

complement, the standard approach to synthesize feedback controllers for parabolic PDEs (e.g., [18, 30]) involves initially the application of standard Galerkin's method to the PDE system to derive ODE systems that accurately describe its dominant dynamics. These ODE systems are subsequently used as the basis for the synthesis of finite-dimensional controllers. A potential drawback of this approach is that the number of modes that should be retained to derive an ODE system which yields the desired degree of approximation may be very large, thereby leading to complex controller synthesis and high dimensionality of the resulting controllers.

To overcome these controller synthesis and implementation problems, recent research efforts have focused on the synthesis of low-order controllers for parabolic PDE systems by taking advantage of the concept of inertial manifold (IM) [144]. If exists, an IM is a positively invariant, exponentially attracting, finite-dimensional Lipschitz manifold. When the trajectories of the PDE system are on the IM, then this system is *exactly* described by a low-order ODE system (called inertial form), which can be used for the synthesis of low-order controllers. The main obstacle in implementing this approach is the computation of the closed-form expression of the IM, which, in most practical applications, is an almost impossible task. Fortunately, the development of efficient procedures for the construction of accurate approximations of the function that describes the inertial manifold (called approximate inertial manifolds (AIMs)) (see, for example, [58, 57, 46]) has allowed the construction of approximations of the inertial form of desired accuracy. These developments led to the synthesis of low-order linear output feedback controllers for boundary stabilization of parabolic PDEs [128, 93, 127], as well as the synthesis of nonlinear low-order output feedback controllers that enforce closed-loop stability and output tracking in quasi-linear parabolic PDE systems with distributed control action [46].

The conventional approach to control parabolic PDDE systems is to neglect the presence of time delays and address the controller design problem on the basis of the resulting parabolic PDE system, employing one of the aforementioned methods. However, such an approach may pose unacceptable limitations on the achievable control quality and cause serious problems in the behavior of the closed-loop system including poor performance and instability. These problems have motivated significant research on control of time-delay systems. Specifically, most of the research has focused on control of linear/nonlinear ODE systems with manipulated input delay, in which the presence of the time delay prevents the use of large controller gains, thereby leading to sluggish closed-loop response. To overcome this problem, many researchers proposed various predictor schemes which completely eliminate the time delay from the characteristic polynomial of the input/output dynamics of the closed-loop system, allowing the use of larger controller gains (see, for example, [133, 28, 61, 71, 87]). For DDE systems with state, measurement and manipulated input delays, a general method which integrates geometric concepts, Lyapunov functionals and predictor schemes was proposed in [7] for the synthesis of nonlinear output feedback controllers. In the area of control of parabolic distributed parameter systems with time-delays, most of the research has focused on the synthesis of optimal controllers (e.g., [81, 150]).

This chapter [12] focuses on single-input single-output quasi-linear parabolic PDDE systems, for which the eigenspectrum of the spatial differential operator can be partitioned into a finite-dimensional slow one and an infinite-dimensional stable fast complement. For such systems, we propose a general methodology for the synthesis of nonlinear output feedback controllers that guarantee stability and enforce output tracking in the closed-loop system. Initially, a nonlinear model reduction scheme which is based on combination of Galerkin's method with the concept of approximate

inertial manifold is employed for the derivation of DDE systems that describe the dominant dynamics of the PDDE system. Then, these DDE systems are used as the basis for the explicit construction of nonlinear output feedback controllers through combination of geometric and Lyapunov techniques. The controllers enforce the desired properties in the closed-loop parabolic PDDE system independently of the size of the state delays, provided that the separation of the slow and fast eigenvalues of the spatial differential operator is sufficiently large and an appropriate matrix is positive definite. The methodology is successfully employed to stabilize the temperature profile of a tubular reactor with recycle at a spatially nonuniform unstable steady-state.

5.2 Preliminaries

5.2.1 Description of parabolic PDDE systems

We consider parabolic partial differential difference equations systems with a state-space representation of the form:

$$\begin{aligned} \frac{\partial \bar{x}}{\partial t} &= A\frac{\partial \bar{x}}{\partial z} + B\frac{\partial^2 \bar{x}}{\partial z^2} + wb(z)u(t) + f(\bar{x}(z,t), \bar{x}(z,t-\alpha)) \\ y_c &= \int_{\bar{\alpha}}^{\bar{\beta}} c(z)k\bar{x}(z,t)dz, \quad y_m = \int_{\bar{\alpha}}^{\bar{\beta}} s(z)\omega\bar{x}(z,t-\tilde{\alpha})dz \end{aligned} \tag{5.1}$$

subject to the boundary conditions:

$$\begin{aligned} C_1\bar{x}(\bar{\alpha},t) + D_1\frac{\partial \bar{x}}{\partial z}(\bar{\alpha},t) &= R_1 \\ C_2\bar{x}(\bar{\beta},t) + D_2\frac{\partial \bar{x}}{\partial z}(\bar{\beta},t) &= R_2 \end{aligned} \tag{5.2}$$

and the initial condition:

$$\bar{x}(z,\xi) = \bar{\eta}(z,\xi), \quad \xi \in [-\alpha, 0] \tag{5.3}$$

where $\bar{x}(z,t) = [\bar{x}_1(z,t) \ \cdots \ \bar{x}_n(z,t)]^T$ denotes the vector of state variables, $z \in [\bar{\alpha}, \bar{\beta}] \subset \mathbb{R}$ is the spatial coordinate, $t \in [0, \infty)$ is the time, $u \in \mathbb{R}$ denotes the

manipulated input, $y_c \in \mathbb{R}$ denotes the controlled output, and $y_m \in \mathbb{R}$ denotes the measured output. $\frac{\partial \bar{x}}{\partial z}, \frac{\partial^2 \bar{x}}{\partial z^2}$ denote the first- and second-order spatial derivatives of $\bar{x}$, $f(\bar{x})$ is a nonlinear vector function, w, k, ω are constant vectors, A, B, C_1, D_1, C_2, D_2 are constant matrices, R_1, R_2 are column vectors, α denotes the state delay, $\tilde{\alpha}$ denotes the measured output delay (measurement sensor dead time), and $\bar{\eta}(z, \xi)$ is the initial condition.

The vector function $b(z)$ is assumed to be known and smooth, and describes how the control action $u(t)$ is distributed in the interval $[\bar{\alpha}, \bar{\beta}]$, $c(z)$ is a known smooth function of z which is determined by the desired performance specifications in the interval $[\bar{\alpha}, \bar{\beta}]$, and $s(z)$ is a known smooth function of z which describes the "shape" of the measurement sensor (e.g., point/distributed sensing). Whenever the control action enters the system at a single point z_0, with $z_0 \in [\bar{\alpha}, \bar{\beta}]$ (i.e., point actuation), the function $b(z)$ is taken to be nonzero in a finite spatial interval of the form $[z_0 - \epsilon, z_0 + \epsilon]$, where ϵ is a small positive real number, and zero elsewhere in $[\bar{\alpha}, \bar{\beta}]$. Throughout this chapter, we will use the order of magnitude notation $O(\epsilon)$. In particular, $\delta(\epsilon) = O(\epsilon)$ if there exist positive real numbers k_1 and k_2 such that: $|\delta(\epsilon)| \leq k_1 |\epsilon|$, $\forall\ |\epsilon| < k_2$. Finally, we will use the Lie derivative notation: $L_f h$ denotes the Lie derivative of a scalar field h with respect to the vector field f, $L_f^k h$ denotes the k-th order Lie derivative and $L_g L_f^{k-1} h$ denotes the mixed Lie derivative.

Referring to the system of Eq.5.1, we note: a) the spatial differential operator is linear; this assumption is valid for diffusion-convection-reaction processes for which the diffusion coefficient and the thermal conductivity can be taken to be independent of concentrations and temperature (see the reactor example of Section 5.5), b) the manipulated input enters the system in a linear and affine fashion; this is typically the case in many practical applications where, for example, the wall temperature

is chosen as the manipulated input, c) the controlled output is different than the measured output; this is done to allow more flexibility in the formulation of the control problem for diffusion-convection-reaction processes, and d) there is no manipulated input delay taken into account; this is done to simplify the notation of the theoretical development and the case of input delay is addressed in Remark 5.9.

5.2.2 Formulation of parabolic PDDE system in Hilbert space

We initially consider an infinite dimensional Hilbert space $\mathcal{H}([\bar{\alpha},\bar{\beta}];\mathbb{R}^n)$ of n-dimensional vector functions defined on $[\bar{\alpha},\bar{\beta}]$ that satisfy the boundary condition of Eq.5.2, with inner product and norm:

$$\begin{aligned}(\omega_1,\omega_2) &= \int_{\bar{\alpha}}^{\bar{\beta}}(\omega_1(z),\omega_2(z))_{\mathbb{R}^n}dz \\ ||\omega_1||_2 &= (\omega_1,\omega_1)^{\frac{1}{2}}\end{aligned} \tag{5.4}$$

where ω_1,ω_2 are two elements of $\mathcal{H}([\bar{\alpha},\bar{\beta}];\mathbb{R}^n)$ and the notation $(\cdot,\cdot)_{\mathbb{R}^n}$ denotes the standard inner product in $\mathbb{R}^n$. We formulate the parabolic PDDE system of Eq.5.1 in $\mathcal{H}([\bar{\alpha},\bar{\beta}];\mathbb{R}^n)$ by defining the state function x as:

$$x(t)=\bar{x}(z,t), \quad t>0, \quad z\in[\bar{\alpha},\bar{\beta}], \tag{5.5}$$

the operator $\mathcal{A}$ in $\mathcal{H}([\bar{\alpha},\bar{\beta}];\mathbb{R}^n)$ as:

$$\begin{aligned}\mathcal{A}x &= A\frac{\partial\bar{x}}{\partial z}+B\frac{\partial^2\bar{x}}{\partial z^2}, \\ x\in D(\mathcal{A}) &= \Big\{x\in\mathcal{H}([\bar{\alpha},\bar{\beta}];\mathbb{R}^n); \quad C_1\bar{x}(\bar{\alpha},t)+D_1\frac{\partial\bar{x}}{\partial z}(\bar{\alpha},t)=R_1; \\ &\qquad C_2\bar{x}(\bar{\beta},t)+D_2\frac{\partial\bar{x}}{\partial z}(\bar{\beta},t)=R_2\Big\}\end{aligned} \tag{5.6}$$

and the input and output operators as:

$$\mathcal{B}u=wbu, \quad \mathcal{C}x=(c,kx), \quad \mathcal{S}x=(s,\omega x) \quad . \tag{5.7}$$

The system of Eqs.5.1-5.2-5.3 takes then the following form:

$$\begin{aligned} \dot{x} &= \mathcal{A}x + \mathcal{B}u + f(x(t), x(t-\alpha)) \\ y_c &= \mathcal{C}x(t), \quad y_m = \mathcal{S}x(t-\tilde{\alpha}) \\ x(\xi) &= \bar{\eta}(\xi), \quad \xi \in [-\alpha, 0] \end{aligned} \tag{5.8}$$

where $f(x(t), x(t-\alpha)) = f(\bar{x}(z,t), \bar{x}(z,t-\alpha))$ and $\bar{\eta}(\xi) = \bar{\eta}(z,\xi)$. We assume that the nonlinear term $f(x(t), x(t-\alpha))$ is locally Lipschitz with respect to its arguments and satisfies $f(0,0) = 0$.

In the remainder of this subsection, we precisely characterize the class of parabolic PDDE systems of the form of Eq.5.1 considered in this work in terms of the properties of the eigenspectrum of $\mathcal{A}$. To this end, we consider the following eigenvalue problem:

$$\mathcal{A}\phi_j = \lambda_j \phi_j, \quad j = 1, \ldots, \infty \tag{5.9}$$

where λ_j denotes an eigenvalue and ϕ_j denotes the corresponding eigenfunction. The eigenspectrum of $\mathcal{A}$ is defined as $\sigma(\mathcal{A}) = \{\lambda_1, \lambda_2, \ldots, \}$. Assumption 5.1 that follows was introduced in [46] and states that $\sigma(\mathcal{A})$ can be partitioned into a finite set containing m eigenvalues which are close to the imaginary axis and an infinite-dimensional complement containing eigenvalues which are far in the left-half of the complex plane. This assumption is satisfied by the majority of nonlinear parabolic PDDE systems arising in the modeling of diffusion-convection-reaction processes (see, for example, the tubular reactor example of Section 5.5).

Assumption 5.1:

1. *$Re\{\lambda_1\} \geq Re\{\lambda_2\} \geq \cdots \geq Re\{\lambda_j\} \geq \cdots$, where $Re\{\lambda_j\}$ denotes the real part of λ_j.*

2. *$\sigma(\mathcal{A})$ can be partitioned as $\sigma(\mathcal{A}) = \sigma_1(\mathcal{A}) + \sigma_2(\mathcal{A})$, where $\sigma_1(\mathcal{A})$ consists of the first m (with m finite) eigenvalues, i.e. $\sigma_1(\mathcal{A}) = \{\lambda_1, \ldots, \lambda_m\}$, and $\dfrac{|Re\{\lambda_1\}|}{|Re\{\lambda_m\}|} = O(1)$.*

3. Re $\lambda_{m+1} < 0$ *and* $\dfrac{|Re\,\{\lambda_m\}|}{|Re\,\{\lambda_{m+1}\}|} = O(\epsilon)$ *where* $\epsilon < 1$ *is a small positive number.*

5.2.3 Galerkin's method

In this subsection, we review standard Galerkin's method in the context of the PDDE system of Eq.5.8. Let $\mathcal{H}_s$, $\mathcal{H}_f$ be modal subspaces of $\mathcal{A}$, defined as $\mathcal{H}_s = span\{\phi_1, \phi_2, \ldots, \phi_m\}$ and $\mathcal{H}_f = span\{\phi_{m+1}, \phi_{m+2}, \ldots,\}$ (the existence of $\mathcal{H}_s$, $\mathcal{H}_f$ follows from Assumption 5.1). Clearly, dim $\mathcal{H}_s$+dim $\mathcal{H}_f$=dim $\mathcal{H}$. Defining the orthogonal projection operators P_s and P_f such that $x_s = P_s x$, $x_f = P_f x$, the state x of the system of Eq.5.8 can be decomposed as:

$$x = x_s + x_f = P_s x + P_f x \tag{5.10}$$

Applying P_s and P_f to the system of Eq.5.8 and using the above decomposition for x, the system of Eq.5.8 can be equivalently written in the following form:

$$\begin{aligned}
\frac{dx_s}{dt} &= \mathcal{A}_s x_s(t) + \mathcal{B}_s u + f_s(x_s(t), x_s(t-\alpha), x_f(t), x_f(t-\alpha)) \\
\frac{dx_f}{dt} &= \mathcal{A}_f x_f(t) + \mathcal{B}_f u + f_f(x_s(t), x_s(t-\alpha), x_f(t), x_f(t-\alpha)) \\
y_c &= \mathcal{C} x_s(t) + \mathcal{C} x_f(t), \quad y_m = \mathcal{S} x_s(t-\tilde{\alpha}) + \mathcal{S} x_f(t-\tilde{\alpha}) \\
x_s(\xi) &= P_s x(\xi) = P_s \bar{\eta}(\xi) = \bar{\eta}_s(\xi), \quad x_f(\xi) = P_f x(\xi) = P_f \bar{\eta}(\xi) = \bar{\eta}_f(\xi), \quad \xi \in [-\alpha, 0]
\end{aligned} \tag{5.11}$$

where $\mathcal{A}_s = P_s \mathcal{A} P_s$, $\mathcal{B}_s = P_s \mathcal{B}$, $f_s = P_s f$, $\mathcal{A}_f = P_f \mathcal{A} P_f$, $\mathcal{B}_f = P_f \mathcal{B}$ and $f_f = P_f f$. In the above system, $\mathcal{A}_s$ is a diagonal matrix of dimension $m \times m$ of the form $\mathcal{A}_s = diag\{\lambda_1, \lambda_2, \ldots, \lambda_m\}$, $f_s(x_s(t), x_s(t-\alpha), x_f(t), x_f(t-\alpha))$ and $f_f(x_s(t), x_s(t-\alpha), x_f(t), x_f(t-\alpha))$ are Lipschitz vector functions, and $\mathcal{A}_f$ is an unbounded differential operator which is exponentially stable (this follows from part 3 of Assumption 5.1 and the selection of $\mathcal{H}_s, \mathcal{H}_f$). Neglecting the fast modes, the DDE system, which describes

the slow dynamics of the system of Eq.5.11, is derived as:

$$\begin{aligned} \frac{dx_s}{dt} &= \mathcal{A}_s x_s(t) + \mathcal{B}_s u + f_s(x_s(t), x_s(t-\alpha), 0, 0) \\ y_{cs} &= \mathcal{C} x_s(t), \quad y_{ms} = \mathcal{S} x_s(t-\bar{\alpha}) \\ x_s(\xi) &= \bar{\eta}_s(\xi), \quad \xi \in [-\alpha, 0] \end{aligned} \tag{5.12}$$

where the subscript s in y_{cs} and y_{ms} denotes that these outputs are associated with a slow system.

Remark 5.1: Whenever the eigenfunctions ϕ_j of the operator $\mathcal{A}$ can not be calculated analytically, one can still use Galerkin's method to perform model reduction by using "empirical eigenfunctions" of the PDDE system as basis functions in $\mathcal{H}_s$ and $\mathcal{H}_f$ (such "empirical eigenfunctions" can be extracted from detailed numerical simulations of the PDDE system using Karhunen-Loéve expansion; see [66] for details on Karhunen-Loéve expansion).

5.2.4 Spectral and stability properties of DDE systems

In this subsection, we initially formulate the DDE system of Eq.5.12 as an infinite dimensional system in an appropriate Banach space and provide the statement and solution of the eigenvalue problem for the linear delay operator (see Eq.5.16 below). The solution of the eigenvalue problem will be utilized in the design of nonlinear distributed state observers in Section 5.4. To this end, we rewrite the system of Eq.5.12 as follows:

$$\begin{aligned} \frac{dx_s}{dt} &= \bar{\mathcal{A}}_s x_s(t) + \tilde{\mathcal{A}}_s x_s(t-\alpha) + \mathcal{B}_s u + f_{ns}(x_s(t), x_s(t-\alpha), 0, 0) \\ y_{cs} &= \mathcal{C} x_s(t), \quad y_{ms} = \mathcal{S} x_s(t-\bar{\alpha}) \\ x_s(\xi) &= \bar{\eta}_s(\xi), \quad \xi \in [-\alpha, 0] \end{aligned} \tag{5.13}$$

where $\bar{\mathcal{A}}_s, \tilde{\mathcal{A}}_s$ are constant matrices and the term $f_{ns}(x_s(t), x_s(t-\alpha), 0, 0)$ includes only higher-order terms.

We formulate the system of Eq.5.13 in the Banach space $C_s([-\alpha, 0], \mathcal{H}_s)$ of continuous n-vector valued functions defined in the interval $[-\alpha, 0]$ with inner product and norm:

$$\begin{aligned} (\tilde{\omega}_1, \tilde{\omega}_2) &= \tilde{\omega}_1(0)\tilde{\omega}_2(0) + \int_{-\alpha}^{0} \tilde{\omega}_1(z+\alpha)\bar{A}_s\tilde{\omega}_2(z)dz, \\ ||\tilde{\omega}_1||_2 &= (\tilde{\omega}_1, \tilde{\omega}_1)^{\frac{1}{2}} \end{aligned} \tag{5.14}$$

where $\tilde{\omega}_1$ is an element of $C_s^*([-\alpha, 0], \mathcal{H}_s^*)$, $\mathcal{H}_s^*$ is the n-dimensional vector space of row vectors, and $\tilde{\omega}_2 \in C_s$. On C_s, the state function x_s of the system of Eq.5.13 is defined as:

$$x_{st}(\xi) = x_s(t+\xi), \quad t \geq 0, \quad \xi \in [-\alpha, 0], \tag{5.15}$$

and the operator $\mathcal{D}$ as:

$$\mathcal{D}\phi(\xi) = \left\{ \begin{array}{ll} \dfrac{d\phi(\xi)}{d\xi}, & \xi \in [-\alpha, 0) \\ \\ \bar{A}_s\phi(0) + \bar{A}_s\phi(-\alpha), & \xi = 0 \end{array} \right\} \tag{5.16}$$

$$\phi(\xi) \in D(\mathcal{D}) = \left\{\phi \in C_s^*([-\alpha, 0], \mathbb{R}^{n^*}) : \dot{\phi} \in C_s, \dot{\phi}(0) = \bar{A}_s\phi(0) + \bar{A}_s\phi(-\alpha)\right\} \tag{5.17}$$

$D(\mathcal{D})$ is a dense subset of C_s. If $\bar{\eta}_s \in D(\mathcal{D})$, then the system of Eq.5.13 can be equivalently written as:

$$\begin{aligned} \frac{dx_{st}}{dt} &= \mathcal{D}x_{st} + \mathcal{B}_s u + f_{ns}(Px_{st}, Qx_{st}, 0, 0) \\ y(t) &= CPx_{st}, \quad y_{ms} = \mathcal{S}Rx_{st} \\ x_s(\xi) &= \bar{\eta}_s(\xi), \quad \xi \in [-\alpha, 0] \end{aligned} \tag{5.18}$$

where $Px_{st} = x_{st}(0)$, $Qx_{st} = x_{st}(-\alpha)$ and $Rx_{st} = x_{st}(-\tilde{\alpha})$.

The eigenvalue problem for the operator $\mathcal{D}$ is defined as:

$$\mathcal{D}\tilde{\phi}_j = \mu_j\tilde{\phi}_j, \quad j = 1, \ldots, \infty \tag{5.19}$$

where μ_j denotes an eigenvalue and $\tilde{\phi}_j$ denotes the corresponding eigenfunction (note that $\tilde{\phi}_j$ is a vector function of dimension m); the eigenspectrum of $\mathcal{D}$, $\sigma(\mathcal{D})$, is defined

as the set of all eigenvalues of $\mathcal{D}$, i.e., $\sigma(\mathcal{D}) = \{\mu_1, \mu_2, \ldots, \}$ and is given by [63]:

$$\sigma(\mathcal{D}) \;=\; \left\{\mu : det(\mu I - \bar{A}_s - \bar{A}_s e^{-\mu\alpha}) = 0\right\} \tag{5.20}$$

The eigenfunctions can be directly computed from the formula $\bar{\phi}_j(\xi) = e^{\mu_j \xi}\bar{\phi}_j(0)$, where $\bar{\phi}_j(0)$ satisfies the equation $(\mu_j I - \bar{A}_s - \bar{A}_s e^{-\mu_j\alpha})\bar{\phi}_j(0) = 0$, where $\xi \in [-\alpha, 0]$ and $j = 1, \ldots, \infty$. The adjoint operator $\bar{\mathcal{D}}$ of $\mathcal{D}$ is defined from the relation $(\mathcal{D}\tilde{\phi}, \tilde{\psi}) = (\tilde{\phi}, \bar{\mathcal{D}}\tilde{\psi})$, where $(,)$ denotes the inner product of Eq.5.14, and its eigenspectrum, $\sigma(\bar{\mathcal{D}})$, satisfies $\sigma(\bar{\mathcal{D}}) = \sigma(\mathcal{D})$.

In the remainder of this subsection, we review the definitions of asymptotic stability and input-to-state stability for DDE systems as well as a basic theorem that provides sufficient conditions for assessing asymptotic stability. To this end, we consider the following system of nonlinear differential difference equations:

$$\dot{x}_s(t) \;=\; f(x_s(t), x_s(t-\alpha), \theta(t), \theta(t-\alpha)), \quad x_s(\xi) = \bar{\eta}_s(\xi), \quad \xi \in [-\alpha, 0] \tag{5.21}$$

where $x_s \in \mathcal{H}_s$, $\theta \in \mathcal{H}_s$, and suppose that $f(0,0,0,0) = 0$. Moreover, given a function $\theta : [-\alpha, \infty) \to \mathcal{H}_s$, $\theta_t(\xi)$ represents a function from $[-\alpha, 0]$ to $\mathcal{H}_s$ defined by $\theta_t(\xi) := \theta(t+\xi)$. We also define $|\theta_t(\xi)| := \max_{t-\alpha \le \xi \le t} ||\theta_t(\xi)||_2$, $||\theta_t|| := sup_{s \ge 0}|\theta_s(\xi)|$ and $||\theta_t||_T := sup_{0 \le s \le T}|\theta_s(\xi)|$. Finally, a function γ: $\mathbb{R}_{\ge 0} \to \mathbb{R}_{\ge 0}$ is said to be of class $\mathcal{Q}$ if it is continuous, nondecreasing and is zero at zero. It is of class K if it is continuous, strictly increasing and is zero at zero. A function $\beta : \mathbb{R}_{\ge 0} \times \mathbb{R}_{\ge 0} \to \mathbb{R}_{\ge 0}$ is said to be of class KL if, for each fixed t, the function $\beta(\cdot, t)$ is of class K and, for each fixed s, the function $\beta(s, \cdot)$ is nonincreasing and tends to zero at infinity.

Definition 5.1: *Let γ be a function of class-$\mathcal{Q}$ and δ_x, δ_θ be positive real numbers. The system of Eq.5.21 is said to be input-to-state stable if $|x_{s0}(\xi)| \le \delta_x$ and $||\theta_t|| \le \delta_\theta$ imply that the solution of the system of Eq.5.21 is defined for all times and satisfies:*

$$|x_{st}(\xi)| \;\le\; \beta(|x_{s0}(\xi)|, t) + \gamma(||\theta_t||), \;\; \forall\, t \ge 0 \tag{5.22}$$

The above definition, when $\theta(t) \equiv 0$, $\forall\, t \geq 0$ reduces to the definition of asymptotic stability for the zero solution of the DDE system of Eq.5.21.

The following theorem provides sufficient conditions for the stability of the zero solution of the system of Eq.5.21, expressed in terms of a suitable functional.

Theorem 5.1 [63]: *Consider the system of Eq.5.21 with* $\theta(t) \equiv 0$ *and let* $\gamma_1, \gamma_2, \gamma_3$ *be functions of class* $\mathcal{Q}$. *If* $\gamma_1(s), \gamma_2(s) > 0$ *for* $s > 0$ *and there is a continuous functional* $V : C_s \rightarrow R_{\geq 0}$ *such that:*

$$\begin{aligned} \gamma_1(||x_s(t)||_2) \leq V(x_{st}(\xi)) \leq \gamma_2(|x_{st}(\xi)|) \\ \dot{V}(x_{st}(\xi)) \leq -\gamma_3(||x_s(t)||_2) \end{aligned} \tag{5.23}$$

then the solution $x_s = 0$ *is stable. If* $\gamma_3(s) > 0$ *for* $s > 0$, *then the solution* $x_s = 0$ *is locally asymptotically stable. Moreover if* $\gamma_1(s) \rightarrow \infty$ *as* $s \rightarrow \infty$ *and* $\gamma_3(s) > 0$ *for* $s > 0$, *then the solution* $x_s = 0$ *is globally asymptotically stable.*

Remark 5.2: Regarding the properties of the eigenspectrums of the operators $\mathcal{A}$ and $\mathcal{D}$, we note the following similarities: a) the eigenspectrums $\sigma(\mathcal{A})$ and $\sigma(\mathcal{D})$ are both point spectrums containing eigenvalues of finite multiplicity, b) the number of eigenvalues of both $\sigma(\mathcal{A})$ and $\sigma(\mathcal{D})$ which have positive real part (i.e., they are located in the right-half of the complex plane) is always finite, and c) the real parts of all the eigenvalues of $\sigma(\mathcal{A})$ and $\sigma(\mathcal{D})$ are bounded from above (i.e., there exists a positive real number β such that $\max\{|Re\ \lambda_i|, |Re\ \mu_i|\} \leq \beta$ for all $i = 1, \ldots, \infty$). On the other hand, $\sigma(\mathcal{A})$ and $\sigma(\mathcal{D})$ exhibit significant structural differences: specifically, $\sigma(\mathcal{A})$ can be partitioned into a finite set containing eigenvalues which are close to the imaginary axis and an infinite-dimensional complement containing eigenvalues which are far in the left-half of the complex plane (Assumption 5.1), while the eigenvalues of $\sigma(\mathcal{D})$ are asymptotically distributed along nearly vertical asymptotes in the complex plane (see [63, 106] for more details). These structural differences of $\sigma(\mathcal{A})$ and

$\sigma(\mathcal{D})$ directly affect the approach that is used for controller design for parabolic PDE and DDE systems, respectively. In particular, the control of parabolic PDE systems is addressed on the basis of finite-dimensional approximations obtained through linear/nonlinear Galerkin's method, while the control of DDE systems is addressed by using combination of geometric concepts with the method of Lyapunov functionals on the basis of the DDE system (see Subsection 5.4.2 for more details).

Remark 5.3: Even though, at this stage, there is no systematic way for selecting the form of the functional $V(x_{st}(\xi))$ which is suitable for a particular application, a choice for $V(x_{st}(\xi))$, which is frequently used to show local exponential stability of a DDE system of the form of Eq.5.21 via Theorem 5.1, is:

$$V(x_{st}(\xi)) \;=\; x_s(t)^T C x_s(t) + a^2 \int_{t-\alpha}^{t} x_s(s)^T E x_s(s) ds \qquad (5.24)$$

where E, C are symmetric positive definite matrices and a is a positive real number. Clearly, the functional of Eq.5.24 satisfies $K_1 ||x_s(t)||_2^2 \leq V(x_{st}(\xi)) \leq K_2 |x_{st}(\xi)|^2$ for some positive K_1, K_2.

5.3 Nonlinear model reduction

In this section, we construct nonlinear DDE systems that accurately reproduce the dynamics of the parabolic PDDE system of Eq.5.8. The construction of the DDE systems is achieved by generalizing a nonlinear model reduction procedure introduced in [46] for parabolic PDE systems, to the class of systems of Eq.5.8. The nonlinear model reduction procedure is based on a combination of standard Galerkin's method with the concept of approximate inertial manifold.

We initially formulate the system of Eq.5.12 within a singular perturbation framework. Using that $\epsilon = \dfrac{|Re\ \lambda_1|}{|Re\ \lambda_{m+1}|}$, the system of Eq.5.11 can be written in the following

form:

$$\begin{aligned} \frac{dx_s}{dt} &= \mathcal{A}_s x_s(t) + \mathcal{B}_s u + f_s(x_s(t), x_s(t-\alpha), x_f(t), x_f(t-\alpha)) \\ \epsilon\frac{dx_f}{dt} &= \mathcal{A}_{f\epsilon} x_f(t) + \epsilon\mathcal{B}_f u + \epsilon f_f(x_s(t), x_s(t-\alpha), x_f(t), x_f(t-\alpha)) \\ x_s(\xi) &= \bar{\eta}_s(\xi), \quad x_f(\xi) = \bar{\eta}_f(\xi), \quad \xi \in [-\alpha, 0] \end{aligned} \tag{5.25}$$

where $\mathcal{A}_{f\epsilon}$ is an unbounded differential operator defined as $\mathcal{A}_{f\epsilon} = \epsilon\mathcal{A}_f$. Since ϵ is a small positive number less than unity (Assumption 5.1, part 3), the system of Eq.5.25 is in the standard singularly perturbed form [80], with x_s being the slow states and x_f being the fast states.

Introducing the fast time-scale $\tau = \frac{t}{\epsilon}$ in Eq.5.25 and setting $\epsilon = 0$, the following infinite-dimensional fast subsystem is obtained:

$$\frac{dx_f}{d\tau} = \mathcal{A}_{f\epsilon} x_f \tag{5.26}$$

which is globally exponentially stable since the operator $\mathcal{A}_{f\epsilon}$ generates an exponentially stable semigroup.

Now, we introduce the concepts of inertial manifold and approximate inertial manifold. Our definition of the concept of inertial manifold is a direct generalization of the one used in [46] (see also [144]) for parabolic PDE systems. An inertial manifold $\mathcal{M}$ for the system of Eq.5.8 is a subset of $\mathcal{H}$, which satisfies the following properties:

i) $\mathcal{M}$ is a Lipschitz manifold,

ii) $\mathcal{M}$ is a graph of a Lipschitz function $\Sigma(x_s(t), x_s(t-\alpha), u(t), \epsilon)$ mapping $[0, \infty) \times \mathcal{H}_s \times \mathbb{R}^l \times (0, \epsilon^*]$ into $\mathcal{H}_f$ and for every solution $x_s(t), x_f(t)$ of Eq.5.25, with $x_f(\xi) = \bar{\eta}_f(\xi),\ \xi \in [-\alpha, 0]$, then

$$\begin{aligned} x_f(t) &= \Sigma(x_s(t), \bar{\eta}_s(t-\alpha), u(t), \epsilon), \quad \forall\, t \in (0, \alpha], \\ x_f(t) &= \Sigma(x_s(t), x_s(t-\alpha), u(t), \epsilon), \quad \forall\, t > \alpha \end{aligned} \tag{5.27}$$

iii) $\mathcal{M}$ attracts every trajectory exponentially.

The evolution of the state x_f on $\mathcal{M}$ is given by Eq.5.27, while the evolution of the state x_s is governed by the following DDE system (called inertial form):

$$\begin{aligned}
\frac{dx_s}{dt} &= \mathcal{A}_s x_s + \mathcal{B}_s u + f_s(x_s(t), \bar{\eta}_s(t-\alpha), \Sigma(x_s(t), \bar{\eta}_s(t-\alpha), u(t), \epsilon), \bar{\eta}_f(t-\alpha)), \\
&\qquad \forall\, t \in (0, \alpha], \\
\frac{dx_s}{dt} &= \mathcal{A}_s x_s + \mathcal{B}_s u + f_s(x_s(t), x_s(t-\alpha), \Sigma(x_s(t), x_s(t-\alpha), u(t), \epsilon), \\
&\qquad \Sigma(x_s(t-\alpha), x_s(t-2\alpha), u(t-\alpha), \epsilon)), \quad \forall\, t > \alpha
\end{aligned} \tag{5.28}$$

Assuming that $u(t)$ is smooth, differentiating Eq.5.27 and utilizing Eq.5.25, $\Sigma(x_s(t), x_s(t-\alpha), u(t), \epsilon)$ can be computed as the solution of the following partial differential difference equation:

$$\begin{aligned}
\epsilon\left(\frac{\partial \Sigma}{\partial x_s}\dot{x}_s + \frac{\partial \Sigma}{\partial u}\dot{u}\right) &= \mathcal{A}_{f\epsilon}\Sigma(x_s(t), \bar{\eta}_s(t-\alpha), u(t), \epsilon) + \epsilon \mathcal{B}_f u + \epsilon f_f(x_s(t), \bar{\eta}_s(t-\alpha), \\
&\qquad \Sigma(x_s(t), \bar{\eta}_s(t-\alpha), u(t), \epsilon), \bar{\eta}_f(t-\alpha)), \quad \forall\, t \in (0, \alpha], \\
\epsilon\left(\frac{\partial \Sigma}{\partial t}\dot{x}_s + \frac{\partial \Sigma}{\partial x_s(t-\alpha)}\dot{x}_s(t-\alpha) + \frac{\partial \Sigma}{\partial u}\dot{u}\right) & \\
&= \mathcal{A}_{f\epsilon}\Sigma(x_s(t), x_s(t-\alpha), u(t), \epsilon) + \epsilon \mathcal{B}_f u \\
&\quad + \epsilon f_f(x_s(t), x_s(t-\alpha), \Sigma(x_s(t), x_s(t-\alpha), u(t), \epsilon), \\
&\quad \Sigma(x_s(t-\alpha), x_s(t-2\alpha), u(t-\alpha), \epsilon)), \quad \forall\, t > \alpha
\end{aligned} \tag{5.29}$$

which $\Sigma(x_s(t), x_s(t-\alpha), u(t), \epsilon)$ has to satisfy for all $x_s \in \mathcal{H}_s$, $u \in \mathbb{R}^l$, $\epsilon \in (0, \epsilon^*]$.

From the complex structure of Eq.5.29, it is obvious that the computation of the explicit form of $\Sigma(x_s(t), x_s(t-\alpha), u(t), \epsilon)$ is impossible in most practical applications. To circumvent this problem, a procedure based on singular perturbations (introduced in [46]) is used to compute approximations of $\Sigma(x_s(t), x_s(t-\alpha), u(t), \epsilon)$ (approximate inertial manifolds) and approximations of the inertial form, of desired accuracy. More specifically, the vectors $\Sigma(x_s(t), x_s(t-\alpha), u(t), \epsilon)$ and $u(t)$ are expanded in a power

series in ϵ:

$$\begin{aligned} u &= \bar{u}_0 + \epsilon\bar{u}_1 + \epsilon^2\bar{u}_2 + \cdots + \epsilon^k\bar{u}_k + O(\epsilon^{k+1}) \\ \Sigma(x_s(t), x_s(t-\alpha), u(t), \epsilon) &= \Sigma_0(x_s(t), x_s(t-\alpha), u(t)) \\ &\quad +\epsilon\Sigma_1(x_s(t), x_s(t-\alpha), u(t)) \\ &\quad +\epsilon^2\Sigma_2(x_s(t), x_s(t-\alpha), u(t)) + \cdots \\ &\quad +\epsilon^k\Sigma_k(x_s(t), x_s(t-\alpha), u(t)) + O(\epsilon^{k+1}) \end{aligned} \tag{5.30}$$

where $\bar{u}_\nu$ and Σ_ν, $\nu = 0, \cdots, k$ are smooth vector functions. Substituting the expressions of Eq.5.30 into Eq.5.29, and equating terms of the same power in ϵ, one can obtain approximations of $\Sigma(t, x_s(t), x_s(t-\alpha), u, \epsilon)$ up to a desired order. Substituting the $O(\epsilon^{k+1})$ approximation of $\Sigma(x_s(t), x_s(t-\alpha), u(t), \epsilon)$ and u into Eq.5.28, the following approximation of the inertial form is obtained:

$$\begin{aligned} \frac{dx_s}{dt} &= \mathcal{A}_s x_s + \mathcal{B}_s\left(\bar{u}_0 + \epsilon\bar{u}_1 + \cdots + \epsilon^k\bar{u}_k\right) \\ &\quad +f_s(x_s(t), \bar{\eta}_s(t-\alpha), \Sigma_0(x_s(t), \bar{\eta}_s(t-\alpha), u(t)) + \cdots \\ &\quad +\epsilon^k\Sigma_k(x_s(t), \bar{\eta}_s(t-\alpha), u(t)), \bar{\eta}_f(t-\alpha)), \quad \forall\, t \in (0, \alpha], \\ \frac{dx_s}{dt} &= \mathcal{A}_s x_s + \mathcal{B}_s\left(\bar{u}_0 + \epsilon\bar{u}_1 + \cdots + \epsilon^k\bar{u}_k\right) \\ &\quad +f_s(x_s(t), x_s(t-\alpha), \Sigma_0(x_s(t), x_s(t-\alpha), u(t)) + \cdots \\ &\quad +\epsilon^k\Sigma_k(x_s(t), x_s(t-\alpha), u(t)), \Sigma_0(x_s(t-\alpha), x_s(t-2\alpha), u(t-\alpha)) + \cdots \\ &\quad +\epsilon^k\Sigma_k(x_s(t-\alpha), x_s(t-2\alpha), u(t-\alpha))), \quad \forall\, t > \alpha \end{aligned} \tag{5.31}$$

In order to characterize the stability of the system of Eq.5.25 from the stability properties of the slow subsystem of Eq.5.31 and the fast subsystem of Eq.5.26, we need to impose the following exponential stability requirement on the system of Eq.5.31 with $u(t) \equiv 0$ and $\epsilon = 0$.

Assumption 5.2: *The DDE system of Eq.5.31 with $u(t) \equiv 0$ and $\epsilon = 0$ is exponentially stable, in the sense that there exists a smooth Lyapunov functional $V : \mathcal{C}_s \to \mathbb{R}_{\geq 0}$ and a set of positive real numbers $(a_1, a_2, a_3, a_4, a_5, a_6, a_7)$, such that for all $x_s \in \mathcal{H}_s$*

that satisfy $||x_s||_2 \leq a_7$, *the following conditions hold:*

$$\begin{aligned} a_1||x_s||_2^2 &\leq V(x_{st}) \leq a_2|x_{st}|^2 \\ \dot{V}(x_{st}) &\leq -a_3||x_s(t)||_2^2 - a_4||x_s(t-\alpha)||_2^2 \\ \left\|\frac{\partial V}{\partial x_s}\right\|_2 &\leq a_5||x_s(t)||_2 + a_6||x_s(t-\alpha)||_2 \end{aligned} \tag{5.32}$$

We are now in a position to state the main stability result of this section. The proof is given in Appendix C.

Theorem 5.2: *Consider the system of Eq.5.8 with* $u(t) \equiv 0$, *for which Assumption 5.1 holds. Suppose also that Assumption 5.2 holds. Then, there exist positive real numbers* μ_1, μ_2, ϵ^* *such that if* $|x_{s0}(\xi)| \leq \mu_1$, $|x_{f_0}(\xi)| \leq \mu_2$ *and* $\epsilon \in (0, \epsilon^*]$, *and the matrix:*

$$\begin{bmatrix} S_1 & -S_2^T \\ -S_2 & S_3 \end{bmatrix} \tag{5.33}$$

where S_1, S_2, S_3 *are matrices defined in Eq.C.6, is positive definite, then there exist positive real numbers* $K \geq 1, \sigma$ *such that:*

$$\begin{bmatrix} ||x_s||_2 \\ ||x_f||_2 \end{bmatrix} \leq Ke^{-\sigma t} \begin{bmatrix} |x_{s0}(\xi)| \\ |x_{f_0}(\xi)| \end{bmatrix}, \tag{5.34}$$

independently of the size of α.

Remark 5.4: The requirement that the matrix of Eq.5.33 is positive definite arises from our desire to derive a general result for assessing the stability properties of the PDDE system of Eq.5.8 in terms of the stability properties of the DDE system of Eq.5.31 independently of the size of the state delay. Of course, such a requirement is not needed when times delays are not present in the system of Eq.5.8 (see [46]). Finally, even though the stability requirement of Assumption 5.2 is imposed on the system of Eq.5.31 with $\epsilon = 0$ and $u(t) \equiv 0$, the result of Theorem 5.2 can be also shown to hold when the stability requirement of Assumption 5.2 is imposed on the system of Eq.5.31 with $\epsilon \neq 0$ and $u(t) \equiv 0$.

Remark 5.5: The expansion of $\Sigma(x_s(t), x_s(t-\alpha), u(t), \epsilon)$ in a power series in ϵ (Eq.5.30) is well-posed with respect to ϵ because as $\epsilon \to 0$, $\Sigma(x_s(t), x_s(t-\alpha), u(t), \epsilon) \to \Sigma_0(x_s(t), x_s(t-\alpha), u(t)) = 0$, and the corresponding approximate inertial form is:

$$\frac{dx_s}{dt} = \mathcal{A}_s x_s + \mathcal{B}_s \bar{u}_0 + f_s(x_s(t), x_s(t-\alpha), 0, 0) \tag{5.35}$$

which is the DDE system obtained from the standard Galerkin's method. Furthermore, for $k = 1$, the expansion of Eq.5.30 yields $\Sigma(x_s(t), x_s(t-\alpha), u(t), \epsilon) = \epsilon\Sigma_1(x_s(t), x_s(t-\alpha), \bar{u}_0(t)) = -\epsilon(\mathcal{A}_{f\epsilon})^{-1}[\mathcal{B}_f \bar{u}_0(t) + f_f(x_s(t), x_s(t-\alpha), 0, 0)]$, and the corresponding approximate inertial form is:

$$\begin{aligned}
\frac{dx_s}{dt} &= \mathcal{A}_s x_s + \mathcal{B}_s(\bar{u}_0 + \epsilon\bar{u}_1) \\
&\quad + f_s(x_s(t), \eta_s(t-\alpha), \epsilon\Sigma_1(x_s(t), \eta_s(t-\alpha), \bar{u}_0(t)), \eta_f(t-\alpha)), \quad \forall\, t \in (0, \alpha], \\
\frac{dx_s}{dt} &= \mathcal{A}_s x_s + \mathcal{B}_s(\bar{u}_0 + \epsilon\bar{u}_1) + f_s(x_s(t), x_s(t-\alpha), \epsilon\Sigma_1(x_s(t), x_s(t-\alpha), \bar{u}_0(t)), \\
&\quad \epsilon\Sigma_1(x_s(t-\alpha), x_s(t-2\alpha), \bar{u}_0(t-\alpha)), \quad \forall\, t > \alpha
\end{aligned} \tag{5.36}$$

In contrast to the system of Eq.5.35, the above system utilizes information about the structure of the fast subsystem, thereby yielding solutions which are asymptotically closer to the solutions of the open-loop system of Eq.5.8 (i.e., $\lim_{t\to\infty} ||x(t) - x_s(t)||_2 = O(\epsilon^2)$) compared to the solutions of the system of Eq.5.35 for which $\lim_{t\to\infty} ||x(t) - x_s(t)||_2 = O(\epsilon)$. Finally, the expansion of u in a power series in ϵ in Eq.5.30 is motivated by our intention to appropriately modify the synthesis of the controller such that the controlled output of the $O(\epsilon^{k+1})$ approximation of the closed-loop inertial form, y_{cs}, satisfies $\lim_{t\to\infty} |y_{cs} - v| = 0$, where v is the reference input.

5.4 Nonlinear output feedback control

In this section, we synthesize nonlinear output feedback controllers that guarantee local exponential stability and force the output of the closed-loop PDDE system to

asymptotically follow the reference input independently of the size of the state delay, provided that ϵ is sufficiently small.

5.4.1 A general result

We initially use the result of Theorem 5.1 to establish that any nonlinear output feedback controller that guarantees stability and enforces asymptotic output tracking in the DDE system of Eq.5.31, exponentially stabilizes the closed-loop PDDE system and ensures that the discrepancy between the output of the closed-loop DDE system and the output of the closed-loop PDDE system is asymptotically of $O(\epsilon^{k+1})$, provided that ϵ is sufficiently small. The nonlinear output feedback controller which enforces the desired control objectives in the system of Eq.5.31 is constructed through a standard combination of a state feedback controller with a state observer.

More specifically, we consider nonlinear state feedback control laws of the following general form:

$$\begin{aligned} u &= \bar{u}_0 + \epsilon\bar{u}_1 + \epsilon^2\bar{u}_2 + \cdots + \epsilon^k\bar{u}_k \\ &= \mathcal{A}_0(x_s(t), \bar{v}(t), x_s(t-\alpha), \bar{v}(t-\alpha)) + \cdots \\ &\quad +\epsilon^k[\mathcal{A}_k(x_s(t), \bar{v}(t), x_s(t-\alpha), \bar{v}(t-\alpha))] \\ &=: \mathcal{A}_\epsilon(x_s(t), \bar{v}(t), x_s(t-\alpha), \bar{v}(t-\alpha)) \end{aligned} \tag{5.37}$$

where $\mathcal{A}_0(x_s(t), \bar{v}(t), x_s(t-\alpha), \bar{v}(t-\alpha)), \cdots, \mathcal{A}_k(x_s(t), \bar{v}(t), x_s(t-\alpha), \bar{v}(t-\alpha))$ are smooth scalar functions, $\bar{v}(s) = [v(s)\ v^{(1)}(s)\ \cdots\ v^{(r-1)}(s)]^T$, $s \in [t-\alpha, t]$ and $v^{(k)}$ denotes the k—th time-derivative of the reference input $v \in \mathbb{R}$.

The nonlinear controllers are constructed by following a sequential procedure. Specifically, the component $\bar{u}_0 = \mathcal{A}_0(x_s(t), \bar{v}(t), x_s(t-\alpha), \bar{v}(t-\alpha))$ is initially synthesized on the basis of the $O(\epsilon)$ approximation of the inertial form; then the component $\bar{u}_1 = \mathcal{A}_1(x_s(t), \bar{v}(t), x_s(t-\alpha), \bar{v}(t-\alpha))$ is synthesized on the basis of the $O(\epsilon^2)$ approximation of the inertial form. In general, at the k-th step, the component $\bar{u}_k = \mathcal{A}_k(x_s(t), \bar{v}(t), x_s(t-\alpha), \bar{v}(t-\alpha))$ is synthesized on the basis of the

$O(\epsilon^{k+1})$ approximation of the inertial form (Eq.5.31). The explicit synthesis of $\mathcal{A}_\nu(x_s(t), \bar{v}(t), x_s(t-\alpha), \bar{v}(t-\alpha))$, $\nu = 0, \ldots, k$ to guarantee stability and force the controlled output of the $O(\epsilon^{\nu+1})$ approximation of the inertial form to asymptotically follow the reference input will be addressed in Subsection 5.4.2 below.

Since measurements of the states $\bar{x}$ (and thus x_s) are usually not available in practice, we will use the following nonlinear state observer for the implementation of the state feedback law of Eq.5.37:

$$
\begin{aligned}
\dot{\omega}_s &= \mathcal{A}_s\omega_s + \mathcal{B}_s\left(\bar{u}_0 + \epsilon\bar{u}_1 + \cdots + \epsilon^k\bar{u}_k\right) \\
&\quad + f_s(\omega_s(t), \bar{\eta}_s(t-\alpha), \Sigma_0(\omega_s(t), \bar{\eta}_s(t-\alpha), u(t)) + \cdots \\
&\quad + \epsilon^k\Sigma_k(\omega_s(t), \bar{\eta}_s(t-\alpha), u(t)), \bar{\eta}_f(t-\alpha)) + \Phi_{C_s}(0)L(y_m(t-\tilde{\alpha}) - \mathcal{S}\omega_s(t-\tilde{\alpha})) \\
&\quad + \tilde{\mathcal{A}}_s\int_0^{\alpha-\tilde{\alpha}} \Phi_{C_s}(\xi-\alpha)L(y_m(t-\xi-\tilde{\alpha}) - \mathcal{S}\omega_s(t-\xi-\tilde{\alpha}))d\xi, \quad \forall\, t \in (0, \alpha] \\
\dot{\omega}_s &= \mathcal{A}_s\omega_s + \mathcal{B}_s\left(\bar{u}_0 + \epsilon\bar{u}_1 + \cdots + \epsilon^k\bar{u}_k\right) \\
&\quad + f_s(\omega_s(t), \omega_s(t-\alpha), \Sigma_0(\omega_s(t), \omega_s(t-\alpha), u(t)) + \cdots \\
&\quad + \epsilon^k\Sigma_k(\omega_s(t), \omega_s(t-\alpha), u(t)), \Sigma_0(\omega_s(t-\alpha), \omega_s(t-2\alpha), u(t-\alpha)) + \cdots \\
&\quad + \epsilon^k\Sigma_k(\omega_s(t-\alpha), \omega_s(t-2\alpha), u(t-\alpha))) + \Phi_{C_s}(0)L(y_m(t-\tilde{\alpha}) - \mathcal{S}\omega_s(t-\tilde{\alpha})) \\
&\quad + \tilde{\mathcal{A}}_s\int_0^{\alpha-\tilde{\alpha}} \Phi_{C_s}(\xi-\alpha)L(y_m(t-\xi-\tilde{\alpha}) - \mathcal{S}\omega_s(t-\xi-\tilde{\alpha}))d\xi, \quad \forall\, t > \alpha \\
&\quad \omega_s(\xi) = \bar{\omega}_s(\xi), \quad \xi \in [-\alpha, 0]
\end{aligned}
\tag{5.38}
$$

where $\omega_s \in \mathbb{R}^m$ is the observer state, $\bar{\omega}_s(\xi)$ is a smooth vector function defined in $\xi \in [-\alpha, 0]$, and $\Phi_{C_s} = [\tilde{\phi}_1, \tilde{\phi}_2, \ldots, \tilde{\phi}_m]$. L is a constant column vector chosen so that all the eigenvalues of the operator $\tilde{\mathcal{A}}_s\omega_s(t) + \tilde{\mathcal{A}}_s\omega_s(t-\alpha) - \Phi_{C_s}(0)L\mathcal{S}\omega_s(t-\tilde{\alpha}) - \tilde{\mathcal{A}}_s\int_0^{\alpha-\tilde{\alpha}} \Phi_{C_s}(\xi-\alpha)L\mathcal{S}\omega_s(t-\xi-\tilde{\alpha})d\xi$ are in the left-half of the complex plane.

Assumption 5.3 states the desired control objectives that the output feedback controller of Eqs.5.37-5.38 enforces in the closed-loop PDDE system.

Assumption 5.3: *The nonlinear output feedback controller of the form of Eqs.5.37-5.38 exponentially stabilizes the $O(\epsilon^{k+1})$ approximation of the closed-loop inertial form*

and ensures that its output satisfy $\lim_{t\to\infty}|y_{cs}(t)-v|=0$, *independently of the size of the state delay.*

Theorem 5.3 provides precise conditions under which the nonlinear controller of Eqs.5.37-5.38 enforces exponential stability and asymptotic output tracking in the closed-loop PDDE system (the proof is given in Appendix C).

Theorem 5.3: *Consider the PDDE system of Eq.5.8, for which Assumptions 5.1 and 5.3 hold. Then, there exist positive real numbers* $\bar{\mu}_1, \bar{\mu}_2, \bar{\epsilon}^*, \bar{\sigma}$ *such that if* $|x_{s0}(\xi)| \leq \bar{\mu}_1$, $|x_{f_0}(\xi)| \leq \bar{\mu}_2$ *and* $\bar{\epsilon} \in (0, \bar{\epsilon}^*]$, *and the matrix:*

$$\begin{bmatrix} \bar{S}_1 & -\bar{S}_2^T \\ -\bar{S}_2 & \bar{S}_3 \end{bmatrix} \tag{5.39}$$

where $\bar{S}_1, \bar{S}_2, \bar{S}_3$ *are matrices defined in Appendix C (see Eq.C.6), is positive definite, then the controller of Eqs.5.37-5.38 enforces: a) local exponential stability, and b) asymptotic output tracking* ($\lim_{t\to\infty}|y_{cs}(t)-v| = O(\epsilon^{k+1})$) *in the closed-loop PDDE system, independently of the size of the state delay.*

Remark 5.6: Owing to the infinite-dimensional range of $\Sigma_k(\omega_s(t), \omega_s(t-\alpha), u(t))$, the practical implementation of the output feedback controller of Eqs.5.37-5.38 involves approximating $\Sigma_k(\omega_s(t), \omega_s(t-\alpha), u(t))$ by a finite-dimensional vector function $\Sigma_k^{\bar{m}}(\omega_s(t), \omega_s(t-\alpha), u(t))$, which can be derived [46] by keeping the first $\bar{m}$ elements of $\Sigma_k(\omega_s(t), \omega_s(t-\alpha), u(t))$ and neglecting the remaining infinite ones. Clearly, as $\bar{m} \to \infty$, $\Sigma_k^{\bar{m}}(\omega_s(t), \omega_s(t-\alpha), u(t))$ approaches $\Sigma_k(\omega_s(t), \omega_s(t-\alpha), u(t))$. This implies that by picking $\bar{m}$ to be sufficiently large, the controller of Eqs.5.37-5.38 with $\Sigma_k^{\bar{m}}(\omega_s(t), \omega_s(t-\alpha), u(t))$ instead of $\Sigma_k(\omega_s(t), \omega_s(t-\alpha), u(t))$ guarantees stability and enforces output tracking in the closed-loop parabolic PDDE system.

5.4.2 Controller synthesis

In this subsection, we will synthesize a nonlinear output feedback controller for the system of Eq.5.8 on the basis of the system of Eq.5.31, using geometric control methods and Lyapunov techniques. To this end, we need to make certain assumptions on the structure and stability properties of the system of Eq.5.13. The reader may refer to [7] for details on the nature of these assumptions. To simplify the statement of these assumptions, we introduce the notation $f_{ns}(x_s(t), x_s(t-\alpha), 0, 0) = f_1(x_s(t)) + f_2(x_s(t), x_s(t-\alpha))$, $\bar{f}_0(x_s(t)) = \bar{A}_s x_s(t) + f_1(x_s(t))$, $\mathcal{B}_s = g(x_s(t), x(t-\alpha))$, $\bar{p}_0(x_s(t), x_s(t-\alpha)) = \bar{A}_s x_s(t-\alpha) + f_2(x_s(t), x_s(t-\alpha))$ and $Cx_s(t) = h_0(x_s(t))$ which allows us to rewrite the system of Eq.5.13 in the following form:

$$\begin{aligned} \dot{x}_s &= \bar{f}_0(x_s(t)) + g(x_s(t), x_s(t-\alpha))\bar{u}_0 + \bar{p}_0(x_s(t), x_s(t-\alpha)) \\ y_{cs} &= h_0(x_s(t)) \end{aligned} \tag{5.40}$$

The first assumption is motivated by the requirement of output tracking and will play a crucial role in the synthesis of the controller.

Assumption 5.4 [7]: *Referring to the system of Eq.5.40, there exists an integer r and a change of variables:*

$$\begin{bmatrix} \zeta(s) \\ \eta(s) \end{bmatrix} = \begin{bmatrix} \zeta_1(s) \\ \zeta_2(s) \\ \vdots \\ \zeta_r(s) \\ \eta_1(s) \\ \vdots \\ \eta_{n-r}(s) \end{bmatrix} = \mathcal{X}(x_s(s)) = \begin{bmatrix} h_0(x_s) \\ L_{\bar{f}_0} h_0(x_s(s)) \\ \vdots \\ L^{r-1}_{\bar{f}_0} h_0(x_s(s)) \\ \chi_1(x_s(s)) \\ \vdots \\ \chi_{n-r}(x_s(s)) \end{bmatrix} \tag{5.41}$$

where $s \in [t-\alpha, t]$ and $\chi_1(x_s(s)), \cdots, \chi_{m-r}(x_s(s))$ are scalar functions such that the

system of Eq.5.40 takes the form:

$$\begin{aligned}
\dot{\zeta}_1 &= \zeta_2(t) + p_{01}(\zeta(t),\eta(t),\zeta(t-\alpha),\eta(t-\alpha)) \\
&\vdots \\
\dot{\zeta}_{r-1} &= \zeta_r(t) + p_{0(r-1)}(\zeta(t),\eta(t),\zeta(t-\alpha),\eta(t-\alpha)) \\
\dot{\zeta}_r &= L^r_{\bar{f}_0} h_0(\mathcal{X}^{-1}(\zeta(t),\eta(t))) + L_g L^{r-1}_{\bar{f}_0} h_0(\mathcal{X}^{-1}(\zeta(t),\eta(t)))\bar{u}_0 \\
&\quad + p_{0r}(\zeta(t),\eta(t),\zeta(t-\alpha),\eta(t-\alpha)) \\
\dot{\eta}_1 &= \Psi_{01}(\zeta(t),\eta(t),\zeta(t-\alpha),\eta(t-\alpha)) \\
&\vdots \\
\dot{\eta}_{m-r} &= \Psi_{0(m-r)}(\zeta(t),\eta(t),\zeta(t-\alpha),\eta(t-\alpha)) \\
y_{cs} &= \zeta_1
\end{aligned} \tag{5.42}$$

where $p_{01}(\zeta(t),\eta(t),\zeta(t-\alpha),\eta(t-\alpha)),\ldots,p_{0r}(\zeta(t),\eta(t),\zeta(t-\alpha),\eta(t-\alpha))$, $\Psi_{01}(\zeta(t),\eta(t),\zeta(t-\alpha),\eta(t-\alpha)),\ldots,\Psi_{0(m-r)}(\zeta(t),\eta(t),\zeta(t-\alpha),\eta(t-\alpha))$ *are nonlinear Lipschitz functions and* $L_g L^{r-1}_{\bar{f}_0} h_0(x_s) \neq 0$ *for all* $x_s(s) \in \mathbb{R}^m$ *and* $s \in [t-\alpha, t]$.

Assumption 5.4 provides the explicit form of a coordinate change (which is independent of the state delay present in the system of Eq.5.31) that transforms the nonlinear DDE system of Eq.5.31 into an interconnection of two subsystems, the ζ-subsystem which describes the input/output dynamics of the system of Eq.5.31 and the η-subsystem which includes the dynamics of the system of Eq.5.31 which are unobservable from the output. Specifically, the interconnection of Eq.5.42 is obtained by considering the change of variables of Eq.5.41 with $s = t$, differentiating it with respect to time, and using that $x(t) = \mathcal{X}^{-1}(\zeta(t),\eta(t))$ and $x(t-\alpha) = \mathcal{X}^{-1}(\zeta(t-\alpha),\eta(t-\alpha))$ (note that this is possible because the coordinate change of Eq.5.41 is assumed to be valid for $s \in [t-\alpha, t]$). The coordinate transformation of Eq.5.41 is not restrictive from an application point of view (one can easily verify that Assumption 5.4 holds, see for example the two applications studied in Chapter 3). The assumption that $L_g L^{r-1}_{\bar{f}} h(x) \neq 0$ for all $x(s) \in \mathbb{R}^n$ and $s \in [t-\alpha, t]$ is necessary in order to guarantee that the controller which will be synthesized is well-posed in the sense that it does not generate infinite control action for any values of the states of the process (compare

with the structure of the controller given in Theorem 5.4).

Assumption 5.5 that follows imposes a standard stability requirement on the $\eta-$subsystem of the system of Eq.5.42 which will allow addressing the controller synthesis task on the basis of the low-order ζ-subsystem.

Assumption 5.5 [7]: *The dynamical system:*

$$\begin{aligned} \dot{\eta}_1 &= \Psi_{01}(\zeta(t), \eta(t), \zeta(t-\alpha), \eta(t-\alpha)) \\ &\vdots \\ \dot{\eta}_{m-r} &= \Psi_{0(m-r)}(\zeta(t), \eta(t), \zeta(t-\alpha), \eta(t-\alpha)) \end{aligned} \tag{5.43}$$

is input-to-state stable with respect to the input $\zeta_t(\xi)$.

Loosely speaking, the above assumption states that if the state of the $\zeta-$subsystem is bounded, then the state of the $\eta-$subsystem will also remain bounded. In practice, Assumption 5.5 can be verified by linearizing the system of Eq.5.43 with $\zeta_t(\xi) = 0$ around the operating steady-state and computing the eigenvalues of the resulting linear system. If all of these eigenvalues are in the left-half of the complex plane, then [143] Assumption 5.5 is satisfied locally (i.e., for sufficiently small initial conditions and $\zeta_t(\xi)$). An application of this approach for checking Assumption 5.5 is discussed previously in Subsection 3.2.2.

Using Assumption 5.5, the controller synthesis problem can be now addressed on the basis of the $\zeta-$subsystem. Specifically, applying the following preliminary feedback law:

$$\begin{aligned} \bar{u}_0 = \frac{1}{L_g L_{\bar{f}_0}^{r-1} h_0(\mathcal{X}^{-1}(\zeta,\eta))} &(\tilde{u}_0 - L_{\bar{f}_0}^r h_0(\mathcal{X}^{-1}(\zeta,\eta)) \\ &- p_{0r}(\zeta(t), \eta(t), \zeta(t-\alpha), \eta(t-\alpha))) \end{aligned} \tag{5.44}$$

where $\tilde{u}_0$ is an auxiliary input, to the system of Eq.5.42 in order to cancel all the nonlinear terms that can be cancelled by using a feedback which utilizes measurements

of $x_s(s)$ for $s \in [t-\alpha, t]$, we obtain the following modified system:

$$\begin{aligned}
\dot{\zeta}_1 &= \zeta_2 + p_{01}(\zeta(t), \eta(t), \zeta(t-\alpha), \eta(t-\alpha)) \\
&\vdots \\
\dot{\zeta}_{r-1} &= \zeta_r + p_{0(r-1)}(\zeta(t), \eta(t), \zeta(t-\alpha), \eta(t-\alpha))) \\
\dot{\zeta}_r &= \tilde{u}_0 \\
\dot{\eta}_1 &= \Psi_{01}(\zeta(t), \eta(t), \zeta(t-\alpha), \eta(t-\alpha)) \\
&\vdots \\
\dot{\eta}_{m-r} &= \Psi_{0(m-r)}(\zeta(t), \eta(t), \zeta(t-\alpha), \eta(t-\alpha)) \\
y_{cs} &= \zeta_1
\end{aligned} \tag{5.45}$$

Introducing the notation:

$$\tilde{A}_0 = \begin{bmatrix} 0 & 1 & 0 & \cdots & 0 & 0 \\ 0 & 0 & 1 & \cdots & 0 & 0 \\ 0 & 0 & 0 & \cdots & 0 & 0 \\ \vdots & \vdots & \vdots & \ddots & \vdots & \vdots \\ 0 & 0 & 0 & \cdots & 0 & 0 \end{bmatrix}, \quad b_0 = \begin{bmatrix} 0 \\ 0 \\ 0 \\ \vdots \\ 1 \end{bmatrix},$$

$$p_0(\zeta(t), \eta(t), \zeta(t-\alpha), \eta(t-\alpha)) = \begin{bmatrix} p_{01}(\zeta(t), \eta(t), \zeta(t-\alpha), \eta(t-\alpha)) \\ p_{02}(\zeta(t), \eta(t), \zeta(t-\alpha), \eta(t-\alpha)) \\ \vdots \\ p_{0(r-1)}(\zeta(t), \eta(t), \zeta(t-\alpha), \eta(t-\alpha)) \\ 0 \end{bmatrix} \tag{5.46}$$

the ζ-subsystem of the system of Eq.5.45 can be written in the following compact form:

$$\begin{aligned}
\dot{\zeta} &= \tilde{A}_0 \zeta + b_0 \tilde{u}_0 + p_0(\zeta(t), \eta(t), \zeta(t-\alpha), \eta(t-\alpha)) \\
y_{cs} &= \zeta_1
\end{aligned} \tag{5.47}$$

The controller synthesis task has been now reduced to the one of synthesized $\tilde{u}_0$ to stabilize the ζ-subsystem and force the output y_{cs} to asymptotically follow the reference input, v. To develop a solution to this problem, we will need to make the following assumption on the growth of the vector $p_0(\zeta(t), \eta(t), \zeta(t-\alpha), \eta(t-\alpha))$.

Assumption 5.6 [7]: *Let* $\tilde{e}_0(s) = [(h(x_s(s)) - v(s)) \; (L_{\tilde{f}_0} h_0(x_s(s)) - v^{(1)}(s)) \; \cdots \; (L_{\tilde{f}_0}^{r-1} h_0(x_s(s)) - v^{(r-1)}(s))]^T$, $s \in [t-\alpha, t]$ *where* $v^{(k)}$ *denotes the* $k-th$ *time-derivative of the reference input* v. *There exist positive real numbers* a_1, a_2 *such that the following*

bound can be written:

$$|p_0(\bar{e}_0(t)+\bar{v}(t),\eta(t),\bar{e}_0(t-\alpha)+\bar{v}(t-\alpha),\eta(t-\alpha))|^2_{\mathbb{R}^m} \leq a_{01}\bar{e}_0^2(t)+a_{02}\bar{e}_0^2(t-\alpha) \tag{5.48}$$

where $|\cdot|_{\mathbb{R}^m}$ *denotes the standard Euclidean norm in* $\mathbb{R}^m$.

The above assumption on the growth of the vector $p_0(\bar{e}_0(t)+\bar{v}(t),\eta(t),\bar{e}_0(t-\alpha)+\bar{v}(t-\alpha),\eta(t-\alpha))$ does not need to hold globally (i.e., for any $\bar{e}_0(t),\eta(t)$), and thus, it is satisfied by most practical problems (see, for example, the applications studied in Chapter 3 of this dissertation).

Theorem 5.4 provides the synthesis formula of the output feedback controller and conditions that guarantee closed-loop stability in the case of considering an $O(\epsilon^2)$ approximation of the exact slow system for the synthesis of the controller. The derivation of synthesis formulas for higher-order approximations of the output feedback controller is notationally complicated, although conceptually straightforward, and thus will be omitted for reasons of brevity (the proof of the theorem is similar to the one of Theorem 5.3 and will be omitted for brevity).

Theorem 5.4: *Consider the nonlinear parabolic PDDE system of Eq.5.13 with* $\alpha > 0$ *and* $\tilde{\alpha} > 0$, *for which Assumption 5.1 and 5.3 holds. Suppose also that the DDE system of Eq.5.31 satisfies Assumptions 5.4, 5.5 and 5.6 and the matrix equations:*

$$\tilde{A}_\nu^T P_\nu + P_\nu \tilde{A}_\nu - 2P_\nu^T b_\nu R_{\nu 2}^{-1} b_\nu^T P_\nu + (a_\nu^2 + a_{\nu 1})I + P_\nu^2 = -R_{\nu 1} \tag{5.49}$$

where $a_\nu^2 > a_{\nu 2}$, *and* $R_{\nu 1}, R_{\nu 2}$ *are positive definite matrices, have unique positive definite solutions for* P_ν *for* $\nu = 0, 1$. *Then, there exist positive real numbers* $\tilde{\mu}_1, \tilde{\mu}_2, \tilde{\epsilon}^*, \tilde{\sigma}$ *such that if* $|x_{s0}(\xi)| \leq \tilde{\mu}_1$, $|x_{f_0}(\xi)| \leq \tilde{\mu}_2$ *and* $\tilde{\epsilon} \in (0, \tilde{\epsilon}^*]$, *and a matrix of the form:*

$$\begin{bmatrix} \tilde{S}_1 & -\tilde{S}_2^T \\ -\tilde{S}_2 & \tilde{S}_3 \end{bmatrix} \tag{5.50}$$

is positive definite (the explicit form of $\tilde{S}_1, \tilde{S}_2, \tilde{S}_3$ is omitted for brevity), the distributed output feedback controller:

$$
\begin{aligned}
\dot{\omega}_s &= \mathcal{A}_s\omega_s + \mathcal{B}_s u + f_s(\omega_s(t), \bar{\eta}_s(t-\alpha), \Sigma_0(\omega_s(t), \bar{\eta}_s(t-\alpha), u(t)) \\
&\quad +\epsilon\Sigma_1(\omega_s(t), \bar{\eta}_s(t-\alpha), u(t)), \bar{\eta}_f(t-\alpha)) + \Phi_{\mathcal{C}_s}(0)L(y_m(t-\tilde{\alpha}) - \mathcal{S}\omega_s(t-\tilde{\alpha})) \\
&\quad +\tilde{A}_s\int_0^{\alpha-\tilde{\alpha}} \Phi_{\mathcal{C}_s}(\xi-\alpha)L(y_m(t-\xi-\tilde{\alpha}) - \mathcal{S}\omega_s(t-\xi-\tilde{\alpha}))d\xi, \quad \forall\, t \in (0, \alpha] \\
\dot{\omega}_s &= \mathcal{A}_s\omega_s + \mathcal{B}_s u + f_s(\omega_s(t), \omega_s(t-\alpha), \Sigma_0(\omega_s(t), \omega_s(t-\alpha), u(t)) \\
&\quad +\epsilon\Sigma_1(\omega_s(t), \omega_s(t-\alpha), u(t)), \Sigma_0(\omega_s(t-\alpha), \omega_s(t-2\alpha), u(t-\alpha)) \\
&\quad +\epsilon\Sigma_1(\omega_s(t-\alpha), \omega_s(t-2\alpha), u(t-\alpha))) + \Phi_{\mathcal{C}_s}(0)L(y_m(t-\tilde{\alpha}) - \mathcal{S}\omega_s(t-\tilde{\alpha})) \\
&\quad +\tilde{A}_s\int_0^{\alpha-\tilde{\alpha}} \Phi_{\mathcal{C}_s}(\xi-\alpha)L(y_m(t-\xi-\tilde{\alpha}) - \mathcal{S}\omega_s(t-\xi-\tilde{\alpha}))d\xi, \quad \forall\, t > \alpha \\
&\quad \omega_s(\xi) = \bar{\omega}_s(\xi), \quad \xi \in [-\alpha, 0), \quad \omega_s(0) = \bar{\omega}_{s0} \\
u &= \frac{1}{L_g L_{\tilde{f}_0}^{r-1} h_0(\omega_s)} \Big(-R_{02}^{-1} b_0^T P_0 \bar{e}_0 + v^{(r)}(t) - L_{\tilde{f}_0}^r h_0(\omega_s) \\
&\quad -p_{0r}(\omega_s(t), \bar{v}(t), \omega_s(t-\alpha), \bar{v}(t-\alpha))) + \epsilon\frac{1}{L_g L_{\tilde{f}_1}^{r-1} h_1(\omega_s)} \Big(-R_{12}^{-1} b_1^T P_1 \bar{e}_1 \\
&\quad +v^{(r)}(t) - L_{\tilde{f}_1}^r h_1(\omega_s) - p_{1r}(\omega_s(t), \bar{v}(t), \omega_s(t-\alpha), \bar{v}(t-\alpha))\Big)
\end{aligned}
\tag{5.51}
$$

where $\bar{e}_0 = [(h_0(\omega_s(t)) - v) \;\; (L_{\tilde{f}_0} h_0(\omega_s(t)) - v^{(1)}) \;\; \cdots \;\; (L_{\tilde{f}_0}^{r-1} h_0(\omega_s(t)) - v^{(r-1)})]^T$ and $\bar{e}_1 = [(h_1(\omega_s(t)) - v) \;\; (L_{\tilde{f}_1} h_1(\omega_s(t)) - v^{(1)}) \;\; \cdots \;\; (L_{\tilde{f}_1}^{r-1} h_1(\omega_s(t)) - v^{(r-1)})]^T$ enforces: a) local exponential stability, and b) asymptotic output tracking ($\lim_{t\to\infty} |y_{cs}(t) - v| = O(\epsilon^2)$) in the closed-loop PDDE system, independently of the size of the state delay.

Remark 5.7: Note that the exponential stability of the closed-loop system under the controller of Eq.5.51 guarantees robustness with respect to sufficiently small initialization errors on the observer states, uncertainty in the model parameters and external disturbances.

Remark 5.8: The nonlinear distributed output feedback controller of Eq.5.51 is an infinite dimensional one owing to the infinite dimensional nature of the observer of Eq.5.38. Therefore, finite-dimensional approximation of these controllers have to be

derived for on-line implementation. This task can be performed by utilizing standard discretization techniques such as finite differences. We note that it is well-established (e.g., [134]) that as the number of discretization points increases, the closed-loop system resulting from the DDE model plus an approximate finite-dimensional controller converges to the closed-loop system resulting from the DDE model plus the infinite-dimensional controller, guaranteeing the well-posedness of the approximate finite-dimensional controller.

Remark 5.9: When manipulated input delay is present in the system of Eq.5.13, the proposed approach can still be employed for controller design. The only difference is that the output feedback controller of Eq.5.51 will be designed on the basis of an auxiliary output constructed within a state-space Smith predictor framework; the reader may refer to [7] for details.

5.5 Application to a tubular reactor with recycle

We consider the non-isothermal tubular reactor shown in Figure 5.1, where an irreversible first-order reaction of the form $A \rightarrow B$ takes place. The reaction is exothermic and a cooling jacket is used to remove heat from the reactor. The outlet of the reactor is fed to a separator where the unreacted species A is separated from the product B. The unreacted amount of species A is then fed back to the reactor through a recycle loop. Under standard modeling assumptions, the dynamic model of the process can be derived from mass and energy balances and takes the following dimensionless form:

$$\begin{aligned}
\frac{\partial \bar{x}_1}{\partial t} &= -\frac{\partial \bar{x}_1}{\partial z} + \frac{1}{Pe_T}\frac{\partial^2 \bar{x}_1}{\partial z^2} + B_T B_C exp^{\frac{\gamma \bar{x}_1}{1+\bar{x}_1}}(1+\bar{x}_2) + \beta_T(b(z)u(t) - \bar{x}_1) \\
\frac{\partial \bar{x}_2}{\partial t} &= -\frac{\partial \bar{x}_2}{\partial z} + \frac{1}{Pe_C}\frac{\partial^2 \bar{x}_2}{\partial z^2} - B_C exp^{\frac{\gamma \bar{x}_1}{1+\bar{x}_1}}(1+\bar{x}_2)
\end{aligned} \tag{5.52}$$

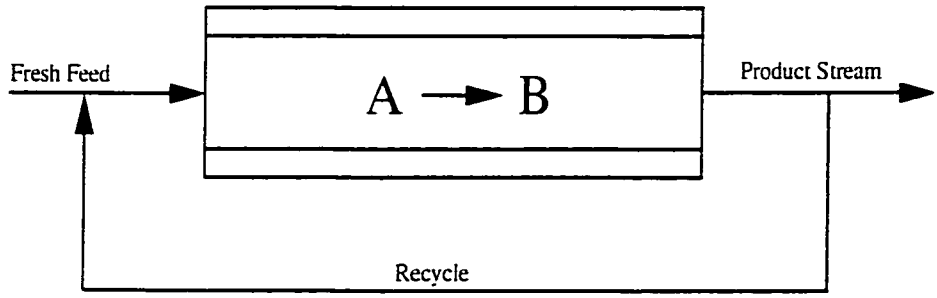

Figure 5.1: A tubular reactor with recycle.

subject to the boundary conditions:

$$\begin{aligned} z = 0\,, \qquad \frac{\partial \bar{x}_1}{\partial z} &= Pe_T(\bar{x}_1 - (1-r)x_{1f} - r\bar{x}_1(1, t-\alpha))\,, \\ \frac{\partial \bar{x}_2}{\partial z} &= Pe_C(\bar{x}_2 - (1-r)x_{2f} - r\bar{x}_2(1, t-\alpha))\,; \\ z = 1\,, \qquad \frac{\partial \bar{x}_1}{\partial z} &= 0\,, \qquad \frac{\partial \bar{x}_2}{\partial z} = 0 \end{aligned} \tag{5.53}$$

where $\bar{x}_1$ and $\bar{x}_2$ denote dimensionless temperature and concentration of species A in the reactor, respectively, Pe_T and Pe_C are the heat and thermal Peclet numbers, respectively, B_T and B_C denote a dimensionless heat of reaction and a dimensionless pre-exponential factor, respectively, r is the recirculation coefficient (it varies from zero to one, with one corresponding to total recycle and zero fresh feed and zero corresponding to no recycle), α is the recycle loop dead time, γ is a dimensionless activation energy, β_T is a dimensionless heat transfer coefficient, u is a dimensionless jacket temperature (chosen to be the manipulated input), and $b(z)$ is the actuator distribution function.

In order to transform the boundary condition of Eq.5.53 to a homogeneous one, we insert the non-homogeneous part of the boundary condition into the differential equation and obtain the following PDDE representation of the process:

$$\begin{aligned}
\frac{\partial \bar{x}_1}{\partial t} &= -\frac{\partial \bar{x}_1}{\partial z} + \frac{1}{Pe_T}\frac{\partial^2 \bar{x}_1}{\partial z^2} + B_T B_C exp^{\frac{\gamma \bar{x}_1}{1+\bar{x}_1}}(1+\bar{x}_2) + \beta_T(b(z)u(t) - \bar{x}_1) \\
&\quad +\delta(z-0)((1-r)x_{1f} + r\bar{x}_1(1, t-\alpha)) \\
\frac{\partial \bar{x}_2}{\partial t} &= -\frac{\partial \bar{x}_2}{\partial z} + \frac{1}{Pe_C}\frac{\partial^2 \bar{x}_2}{\partial z^2} - B_C exp^{\frac{\gamma \bar{x}_1}{1+\bar{x}_1}}(1+\bar{x}_2) \\
&\quad +\delta(z-0)((1-r)x_{2f} + r\bar{x}_2(1, t-\alpha))
\end{aligned} \tag{5.54}$$

where $\delta(\cdot)$ is the standard Dirac function, subject to the homogeneous boundary conditions:

$$\begin{aligned}
z = 0\,, \quad & \frac{\partial \bar{x}_1}{\partial z} = Pe_T \bar{x}_1\,, \quad & \frac{\partial \bar{x}_2}{\partial z} = Pe_C \bar{x}_2\,; \\
z = 1\,, \quad & \frac{\partial \bar{x}_1}{\partial z} = 0\,, & \frac{\partial \bar{x}_2}{\partial z} = 0
\end{aligned} \tag{5.55}$$

The following values for the process parameters were used in our calculations:

$$\begin{aligned}
&Pe_T = 7.0, \quad && Pe_C = 7.0, \quad && B_C = 0.1, \quad && B_T = 2.5, \\
&\beta_T = 2.0, \quad && \gamma = 10.0, \quad && r = 0.5, \quad && \alpha = 0.1
\end{aligned} \tag{5.56}$$

For the above values, the operating steady-state of the open-loop system is unstable (the linearization around the steady-state possesses one real unstable eigenvalue, $\mu = 0.0328$, and infinitely many stable eigenvalues), thereby implying the need to operate the process under feedback control. We note that in the absence of recycle-loop (i.e., $r = 0$), the above process parameters correspond to a stable steady-state for the open-loop system.

The spatial differential operator of the system of Eq.5.54 is of the form:

$$\mathcal{A}x = \begin{bmatrix} \mathcal{A}_1 x_1 & 0 \\ 0 & \mathcal{A}_2 x_2 \end{bmatrix} = \begin{bmatrix} \frac{1}{Pe_T}\frac{\partial^2 \bar{x}_1}{\partial z^2} - \frac{\partial \bar{x}_1}{\partial z} & 0 \\ 0 & \frac{1}{Pe_C}\frac{\partial^2 \bar{x}_2}{\partial z^2} - \frac{\partial \bar{x}_2}{\partial z} \end{bmatrix} \tag{5.57}$$

The solution of the eigenvalue problem for $\mathcal{A}_i$ can be obtained by utilizing standard techniques from linear operator theory (see, for example, [122]) and is of the form:

$$\begin{aligned}
\lambda_{ij} &= \frac{\bar{a}_{ij}^2}{Pe} + \frac{Pe}{4}, \quad i = 1,2, \quad j = 1,\ldots,\infty \\
\phi_{ij}(z) &= B_{ij} e^{Pe\frac{z}{2}} \left(cos(\bar{a}_{ij} z) + \frac{Pe}{2\bar{a}_{ij}} sin(\bar{a}_{ij} z) \right), \quad i = 1,2, \quad j = 1,\ldots,\infty \\
\bar{\phi}_{ij}(z) &= e^{-Pez} \phi_{ij}(z), \quad i = 1,2, \quad j = 1,\ldots,\infty
\end{aligned} \tag{5.58}$$

where $Pe = Pe_T = Pe_C$, and $\lambda_{ij}, \phi_{ij}, \bar{\phi}_{ij}$, denote the eigenvalues, eigenfunctions and adjoint eigenfunctions of $\mathcal{A}_i$, respectively. $\bar{a}_{ij}, B_{ij}$ can be calculated from the following formulas:

$$\begin{aligned}
tan(\bar{a}_{ij}) &= \frac{Pe\bar{a}_{ij}}{\bar{a}_{ij}^2 - \left(\frac{Pe}{2}\right)^2}, \quad i = 1,2, \quad j = 1,\ldots,\infty \\
B_{ij} &= \left\{ \int_0^1 \left(cos(\bar{a}_{ij} z) + \frac{Pe}{2\bar{a}_{ij}} sin(\bar{a}_{ij} z) \right)^2 dz \right\}^{-\frac{1}{2}}, \quad i = 1,2, \quad j = 1,\ldots,\infty
\end{aligned} \tag{5.59}$$

A direct computation of the first nine eigenvalues of $\mathcal{A}$ yields: $\lambda_{11} = \lambda_{21} = -2.36$, $\lambda_{12} = \lambda_{22} = -4.60$, $\lambda_{13} = \lambda_{23} = -9.13$, $\lambda_{14} = \lambda_{24} = -16.30$, $\lambda_{15} = \lambda_{25} = -26.22$, $\lambda_{16} = \lambda_{26} = -38.94$, $\lambda_{17} = \lambda_{27} = -54.47$, $\lambda_{18} = \lambda_{28} = -72.81$, and $\lambda_{19} = \lambda_{29} = -93.96$.

A 400-th order Galerkin truncation of the system of Eq.5.54-5.56 was used in our simulations in order to accurately describe the process (further increase on the order of the Galerkin truncation was found to give negligible improvement on the accuracy of the results). Figure 5.2 shows the open-loop profile of $\bar{x}_1$ along the length of the reactor which corresponds to the operating unstable steady-state. Therefore, the control problem is to manipulate the wall temperature, $u(t)$, in order to stabilize the reactor at the open-loop unstable steady-state. The controlled output was defined as $y_c(t) = \int_0^1 e^{-Pez} \phi_{11}(z) \bar{x}_1 dz$, the actuator distribution function was taken to be

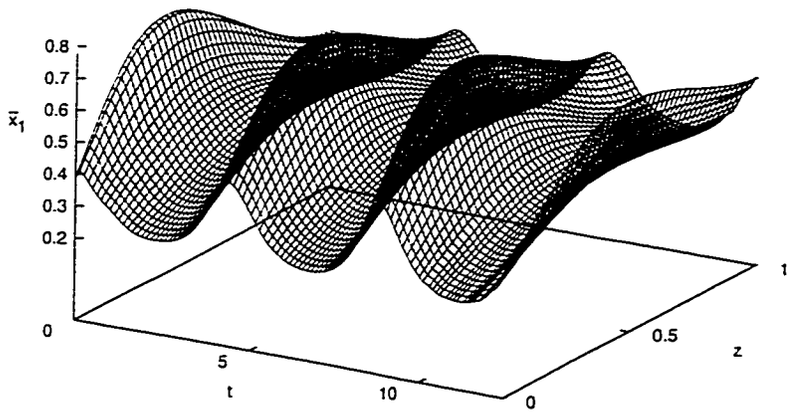

Figure 5.2: Spatiotemporal evolution of $\bar{x}_1$ in the open-loop system.

$b(z) = 1$ (uniform wall temperature in space), and the measurement sensor shape function was assumed to be of the form $s(z) = e^{-Pez}\phi_{11}(z)$ (distributed sensing).

Two sets of simulation runs were performed to: a) evaluate the improvement on the performance of the controller which is achieved when the controller is synthesized on the basis of DDE models derived from combination of Galerkin's method with approximate inertial manifolds (first set of simulations), and b) compare the performance of the proposed nonlinear controllers with nonlinear controllers which are designed on the basis of approximate ODE models which do not account for the time delay in the recycle loop (second set of simulations). In all the simulations runs, the process was initially ($t = 0$) assumed to be at the unstable steady state, and the reference input value was set at $v = 0.12$.

In the first set of simulations, we assumed the time-delay of the recycle loop to be $\alpha = 0.1$. We initially employed the standard Galerkin's method to derive an

approximate DDE system which was used for the synthesis of a nonlinear output feedback controller. It was found that the *lowest − order* DDE model obtained from standard Galerkin's method which leads to the synthesis of a controller that stabilizes the closed-loop system is 10 (i.e., $m = 10$, $\bar{m} = 0$). Figures 5.3 and 5.4

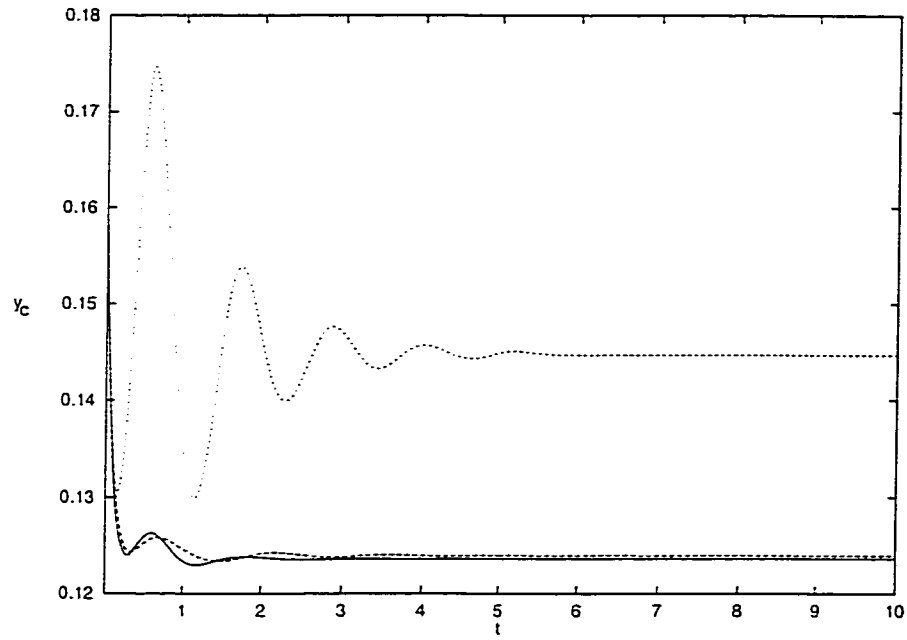

Figure 5.3: Closed-loop output profiles under a controller of the form of Eq.5.51 with $m = 10$, $\bar{m} = 12$ (solid line), a controller of the form of Eq.5.51 with $m = 10$, $\bar{m} = 0$ (short-dashed line), and a controller of the form of Eq.5.51 with $m = 22$, $\bar{m} = 0$ (long-dashed line).

(short-dashed lines) show the evolution of the output of the closed-loop system and the profile of the manipulated input under a nonlinear output feedback controller of the form of Eq.5.51 synthesized on the basis of the approximate model comprised of ten differential difference equations (the controller parameters are $\epsilon = 0$, $\Phi_{C_s}(0) = [1\ 1\ \ldots\ 1\ 1]^T_{10\times 1}$ and $L = 2$). It is clear that this controller stabilizes the system far away from the desired reference input value. Figure 5.6 (short-dashed line) shows the corresponding closed-loop steady-state profile of $\bar{x}_1$, which is clearly not close to the desired one (dotted line). We subsequently used the proposed combination of

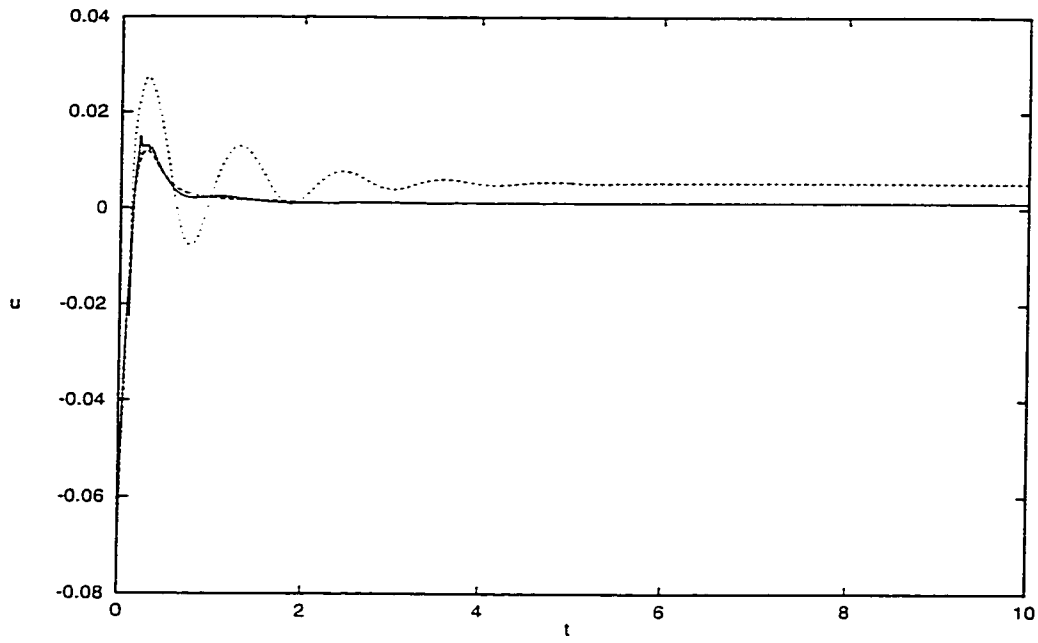

Figure 5.4: Manipulated input profiles under a controller of the form of Eq.5.51 with $m = 10$, $\bar{m} = 12$ (solid line), a controller of the form of Eq.5.51 with $m = 10$, $\bar{m} = 0$ (short-dashed line), and a controller of the form of Eq.5.51 with $m = 22$, $\bar{m} = 0$ (long-dashed line).

Galerkin's method with approximate inertial manifolds to derive a DDE system which was used for the synthesis of a nonlinear output feedback controller. We constructed a 10-th order DDE model which uses a 12-th order approximation for the state x_f (i.e. $m = 10$, $\bar{m} = 12$) and used it for the design of a nonlinear output feedback controller of the form of Eq.5.51 (the controller parameters are $\epsilon = 0.0606$, $\Phi_{\mathcal{C}_s}(0) = [1\ 1\ \ldots\ 1\ 1]^T_{10\times 1}$ and $L = 2$). Figures 5.3 and 5.4 (solid lines) show the evolution of the output of the closed-loop system and the profile of the manipulated input, while Figure 5.5 shows the spatiotemporal evolution of $\bar{x}_1$ and Figure 5.6 (solid line) shows the final steady-state profile of $\bar{x}_1$. This controller clearly regulates the system very close to the reference input value. Finally, we also implemented on the process a nonlinear output feedback controller of the form of Eq.5.51 which was synthesized on the basis of a DDE model obtained with $m = 22$ and $\bar{m} = 0$ (the controller

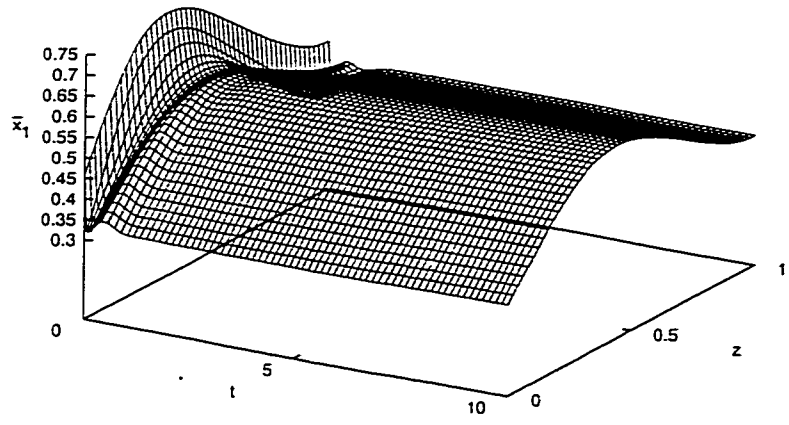

Figure 5.5: Spatiotemporal evolution of $\bar{x}_1$ under a controller of the form of Eq.5.51 with $m = 10$, $\bar{m} = 12$.

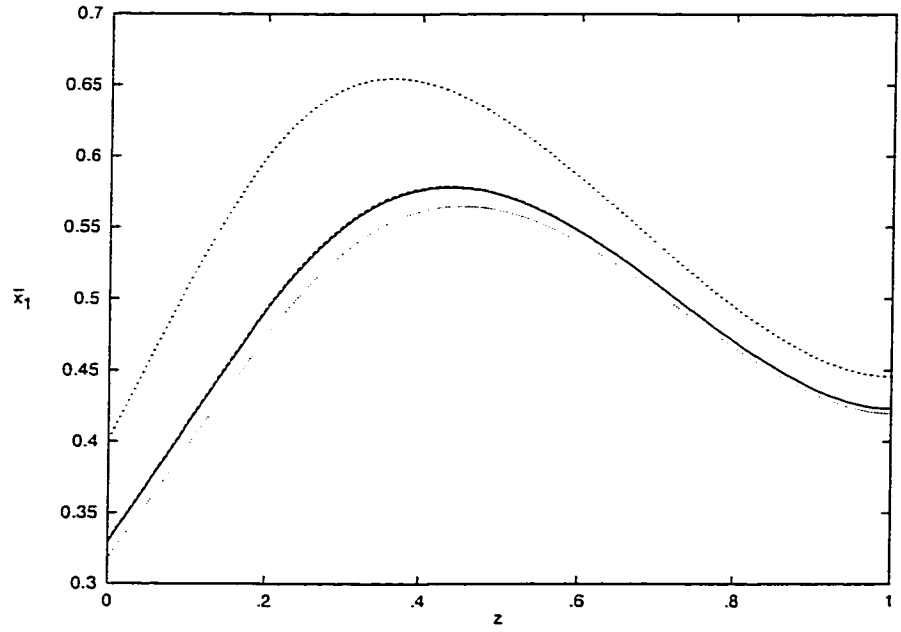

Figure 5.6: Final steady-state profile of $\bar{x}_1$ under a controller of the form of Eq.5.51 with $m = 10$, $\bar{m} = 12$ (solid line), a controller of the form of Eq.5.51 with $m = 10$, $\bar{m} = 0$ (short-dashed line), a controller of the form of Eq.5.51 with $m = 22$, $\bar{m} = 0$ (long-dashed line), and profile of the desired operating steady state (dotted line).

parameters are $\epsilon = 0$, $\Phi_{c_s}(0) = [1\ 1\ \ldots\ 1\ 1]^T_{22\times 1}$ and $L = 2$). Figures 5.3 and 5.4 (long-dashed lines) show the corresponding closed-loop output and manipulated input profiles, while Figure 5.6 (long-dashed line) shows the profile of $\bar{x}_1$. The performance of this controller is very close to the one of the controller synthesized on the basis of the DDE model obtained with $m = 10$ and $\bar{m} = 12$, indicating the effectiveness of the proposed approach for the synthesis of high-performance controllers based on low-order DDE systems.

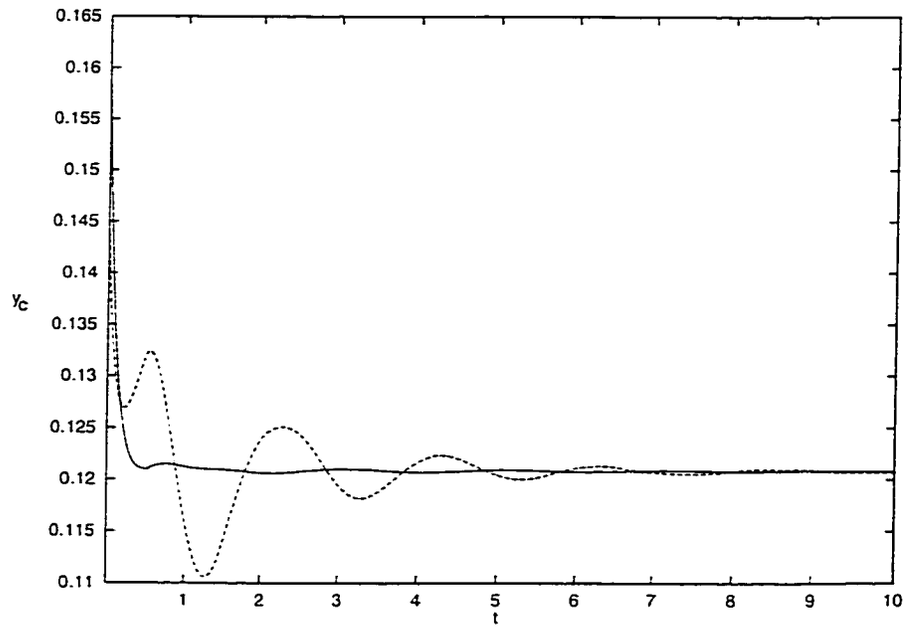

Figure 5.7: Closed-loop output profiles under a controller of the form of Eq.5.51, with $\alpha = 0.5$, and $m = 22$, $\bar{m} = 24$ (solid line), a controller of the form of Eq.5.51, with $\alpha = 0$, and $m = 22$, $\bar{m} = 24$ (long-dashed line), and a controller of the form of Eq.5.51, with $\alpha = 0.5$, and $m = 22$, $\bar{m} = 0$ (short-dashed line).

In the second set of simulation runs, our objective is to demonstrate that the closed-loop performance of the proposed nonlinear controllers is superior to the one of nonlinear controllers which are designed on the basis of approximate ODE models which do not account for the time delay in the recycle loop. To this end, we assumed a larger time-delay for the recycle loop, $\alpha = 0.5$. We initially used the proposed

combination of Galerkin's method with approximate inertial manifolds to construct a 22-nd order DDE model which uses a 24-th order approximation for the state x_f (i.e. $m = 20$, $\bar{m} = 24$) and used it for the design of a nonlinear output feedback controller of the form of Eq.5.51 (the controller parameters are $\epsilon = 0.0163$, $\Phi_{C_s}(0) = [1\ 1\ \ldots\ 1\ 1]^T_{22\times 1}$ and $L = 2$). Figures 5.7 and 5.8 (solid lines) show the evolution of

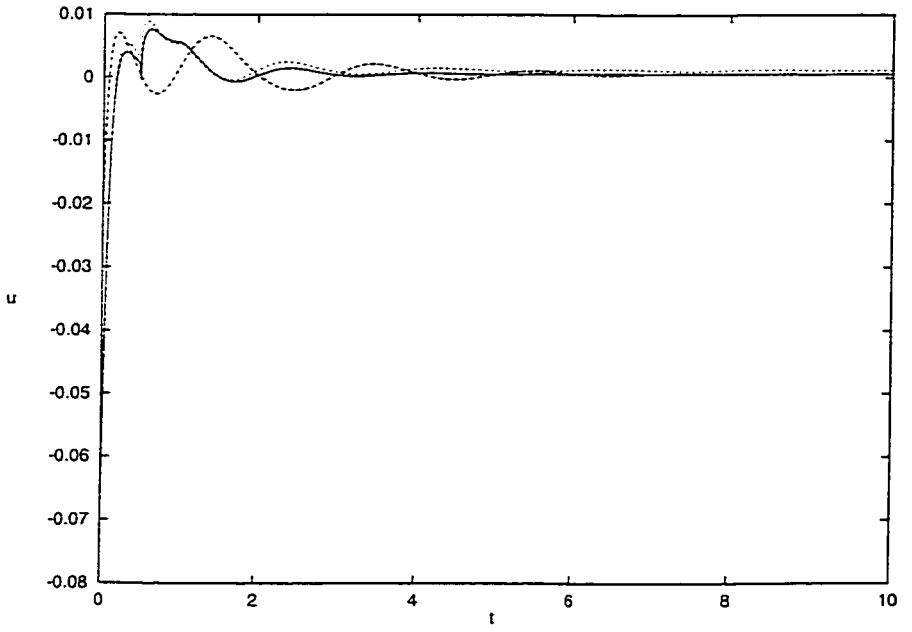

Figure 5.8: Manipulated input profiles under a controller of the form of Eq.5.51, with $\alpha = 0.5$, and $m = 22$, $\bar{m} = 24$ (solid line), a controller of the form of Eq.5.51, with $\alpha = 0$, and $m = 22$, $\bar{m} = 24$ (long-dashed line), and a controller of the form of Eq.5.51, with $\alpha = 0.5$, and $m = 22$, $\bar{m} = 0$ (short-dashed line).

the output of the closed-loop system and the profile of the manipulated input, while Figure 5.9 shows the spatiotemporal evolution of $\bar{x}_1$ and Figure 5.10 (solid line) shows the final steady-state profile of $\bar{x}_1$. This controller clearly drives quickly the output very close to the reference input value, exhibiting a very good transient response. Note that owing to the larger time-delay (0.5 versus 0.1), the order of the DDE model needed to derive a stabilizing controller is higher (22 versus 10). To demonstrate the effect of the time delay on the closed-loop performance, we implemented on the

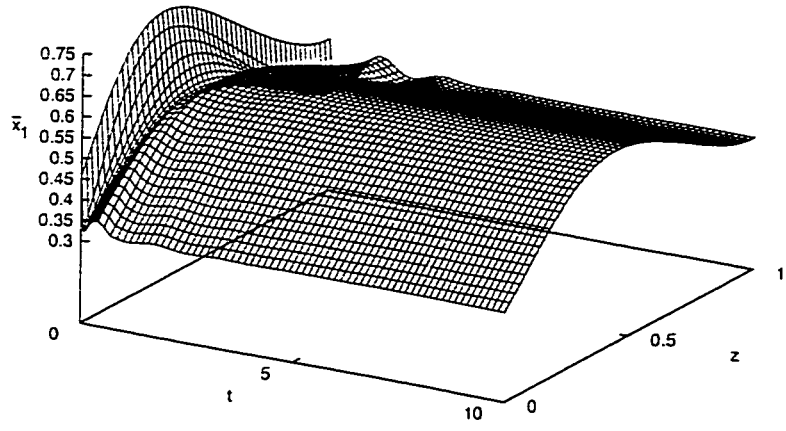

Figure 5.9: Spatiotemporal evolution of $\bar{x}_1$ under a controller of the form of Eq.5.51, with $\alpha = 0.5$, and $m = 22$, $\bar{m} = 24$.

process the nonlinear output feedback controller used in the previous simulation run with $\alpha = 0$ (i.e., the time-delay is not accounted for in the controller; the other controller parameters are the same as in the previous run). Figures 5.7 and 5.8 (long-dashed lines) show the evolution of the output of the closed-loop system and the profile of the manipulated input, while Figure 5.10 (long-dashed line) shows the final steady-state profile of $\bar{x}_1$. This controller yields a very poor transient response before driving the output close to the new reference input value. Finally, we used Galerkin's method to construct a 22-th order DDE model x_f (i.e. $m = 22$, $\bar{m} = 0$) and used it for the design of a nonlinear output feedback controller of the form of Eq.5.51. Figures 5.7 and 5.8 (short-dashed lines) show the evolution of the output of the closed-loop system and the profile of the manipulated input, while Figure 5.10 (short-dashed line) shows the corresponding closed-loop steady-state profile of $\bar{x}_1$, which is not close to the desired one (dotted line). It is clear that this controller stabilizes the system away

from the desired reference input value.

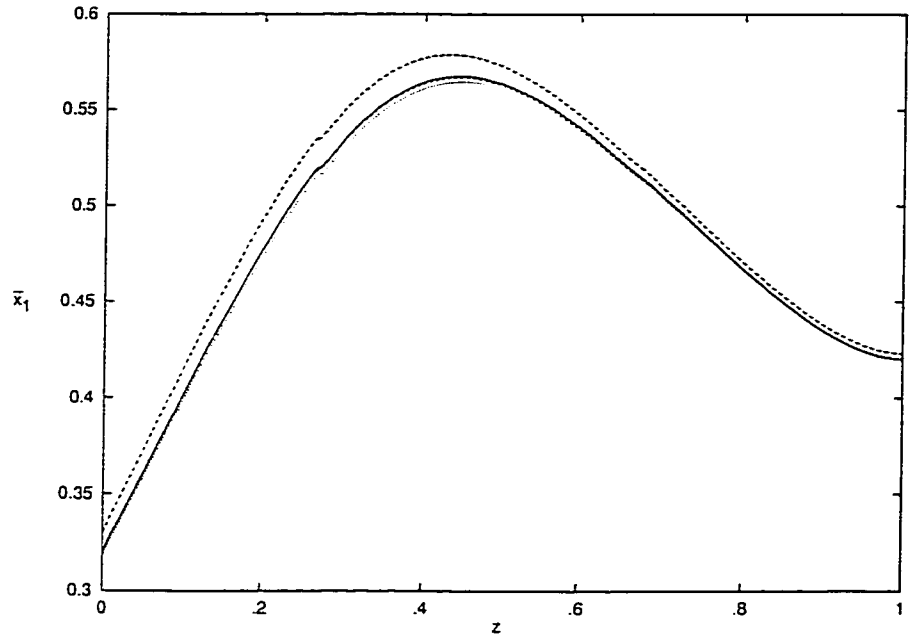

Figure 5.10: Final steady-state profile of $\bar{x}_1$ under a controller of the form of Eq.5.51, with $\alpha = 0.5$, and $m = 22$, $\bar{m} = 24$ (solid line), a controller of the form of Eq.5.51, with $\alpha = 0$, and $m = 22$, $\bar{m} = 24$ (long-dashed line), and a controller of the form of Eq.5.51, with $\alpha = 0.5$, and $m = 22$, $\bar{m} = 0$ (short-dashed line), and profile of the desired operating steady state (dotted line).

The results of the above simulation study clearly indicate the effectiveness of the proposed approach for the synthesis of nonlinear feedback controllers based on low-order DDE systems, as well as the importance of accounting for the effect of time-delays in the controller design.

5.6 Conclusions

In this chapter, we introduced a methodology for the synthesis of nonlinear output feedback controllers for nonlinear parabolic PDDE systems. Initially, a nonlinear model reduction scheme which is based on combination of Galerkin's method with the concept of approximate inertial manifold was employed for the derivation of DDE

systems that accurately capture the dominant dynamics of the PDDE system. These DDE systems were subsequently used as the basis for the explicit construction of nonlinear output feedback controllers through combination of geometric and Lyapunov techniques. The controllers guarantee stability and enforce output tracking in the closed-loop parabolic PDDE system, independently of the size of the state delays, provided that the separation of the slow and fast eigenvalues of the spatial differential operator is sufficiently large and an appropriate matrix is positive definite. The methodology was successfully employed to stabilize the temperature profile of a tubular reactor with recycle at a spatially nonuniform unstable steady-state.

Chapter 6

Nonlinear Dynamics and Control of a Tubular Reactor with Recycle

6.1 Introduction

Tubular reactors are widely used for the production of a variety of industrial products and are characterized by strong coupling of diffusive, convective and reactive mechanisms. This coupling is the source of the rich open-loop dynamic behavior exhibited by tubular reactors including multiple steady states, traveling waves, and periodic, quasi-periodic and chaotic behavior; the reader may refer to [124, 125] and the classic paper [70] for results and references in this area.

In tubular reactors where highly exothermic reactions take place, a typical feature is the occurrence of a small region inside the reactor where the temperature is very high (usually referred to as 'hot-spot'). One way to reduce the 'hot-spot' temperature is to use a recycle loop around the reactor that returns the unreacted reactant back to the reactor. The use of recycle loop typically results in a significant reduction of the 'hot-spot' temperature, while it allows maintaining the reactor conversion at the desired level. This is possible because the recycle loop reduces the fresh material fed

into the reactor while increasing the residence time of the fresh material inside the reactor. Unfortunately, the use of recycle loop introduces a feedback mechanism into the process and brings the reactor closer to the verge of unstable behavior; thereby implying the need to operate tubular reactors with recycle under feedback control. The dynamics of tubular reactors with recycle in which the diffusive phenomena are negligible compared to the convective ones and a highly exothermic reaction takes place have been extensively studied in a series of papers written by Berezowski [22, 23, 24, 25, 141, 26] (see also [159, 158]) and the occurrence of multiple steady states and chaotic behavior has been established.

When diffusive and convective phenomena are equally important and the recycle loop dead-time is explicitly included in the process model, tubular reactors with recycle are modeled by systems of parabolic PDDEs. The main feature of such systems is that the eigenspectrum of the parabolic spatial differential operator can be partitioned into a finite-dimensional slow one and an infinite-dimensional stable fast complement, which implies that the dominant dynamics of these systems can be approximately described by a small number of degrees of freedom. Motivated by this, we recently proposed a general methodology [12] for the synthesis of nonlinear output feedback controllers that guarantee stability and enforce output tracking in the closed-loop system. The key step of this method is the use of a nonlinear model reduction scheme which is based on combination of Galerkin's method with the concept of approximate inertial manifold is employed for the derivation of DDE systems that describe the dominant dynamics of the PDDE system. These DDE systems are then used as the basis for the explicit construction of nonlinear output feedback controllers through combination of geometric and Lyapunov techniques. The controllers enforce the stability and tracking in the closed-loop system independently of the size of the

state delay.

This chapter [11] presents a study on the dynamics and control of a tubular reactor with recycle loop where an exothermic reaction of the form $A \rightarrow B$ takes place. Initially, a detailed mathematical model for the process which consists of two nonlinear PDDEs and accounts for diffusion, convection and chemical reaction, as well as for dead-time in the recycle loop is presented. Then, the dynamics of the process for different values of the recycle ration is studied and is found that the introduction of the recycle loop reduces the 'hot-spot' temperature inside the reactor, while maintaining the desired rate of production of the species B. In addition, the use of the recycle loop introduces a feedback mechanism into the process which renders the open-loop steady state unstable. To stabilize the process, we use the method developed in chapter 5 to synthesize a nonlinear output feedback controller based on an approximate DDE model obtained through application of nonlinear Galerkin's method to the detailed process model. The performance of the controller for different values of the recycle ratio is successfully tested through simulations and is found to be superior to the one achieved by nonlinear controllers synthesized based on approximate models obtained from linear Galerkin's method.

6.2 Tubular reactor with recycle: Description and modeling

We consider the non-isothermal tubular reactor without catalyst packing, shown previously in Figure 5.1, where an irreversible first-order reaction of the form $A \rightarrow B$ takes place. The reaction is exothermic and a cooling jacket is used to remove heat from the reactor. The outlet of the reactor is fed into a separator where the unreacted species A is separated from the product B. The unreacted amount of species A is

then fed back to the reactor through a recycle loop. Under the standard assumptions of constant density (ρ) and heat capacity (c_p) of the reacting fluid, and constant axial fluid velocity (v), the dynamic model of the process can be derived from mass and energy balances and takes the following form:

$$\begin{aligned} \frac{\partial T}{\partial \bar{t}} &= -v\frac{\partial T}{\partial \bar{z}} + \frac{k}{\rho c_p}\frac{\partial^2 T}{\partial \bar{z}^2} + \frac{-\Delta H}{\rho c_p} exp\Big(-\frac{E}{RT}\Big) C_A - \frac{hA_s}{\rho c_p}(T - T_c) \\ \frac{\partial C_A}{\partial \bar{t}} &= -v\frac{\partial C_A}{\partial \bar{z}} + D_A\frac{\partial^2 C_A}{\partial z^2} - k_o exp\Big(-\frac{E}{RT}\Big) C_A \end{aligned} \tag{6.1}$$

where T and C_A denote the temperature and concentration of species A in the reactor, respectively, k and D_A are the thermal conductivity and mass diffusivity of the reacting fluid, respectively, k_o, E and $(-\Delta H)$ represent the pre-exponential constant, activation energy, and the heat of the reaction, respectively, h is the heat transfer coefficient between the reactor and the cooling jacket, A_s is the surface area of the reactor walls, and T_c is the jacket temperature. Assuming negligible reaction in the recycle loop and instantaneous mixing of fresh feed and recycle feed at the reactor inlet, the boundary conditions of the system of Eq.6.1 take the form:

$$\begin{aligned} \bar{z} = 0 : \quad & \frac{\partial T}{\partial \bar{z}} = \frac{\rho c_p v}{K}(T - (1-r)T_f - rT(L, t-\alpha)), \\ & \frac{\partial C_A}{\partial \bar{z}} = \frac{v}{D_A}(C_A - (1-r)C_{Af} - rC_A(L, t-\alpha)); \\ \bar{z} = L : \quad & \frac{\partial T}{\partial \bar{z}} = 0, \qquad \frac{\partial C_A}{\partial \bar{z}} = 0 \end{aligned} \tag{6.2}$$

where T_f and C_{Af} denote the inlet temperature and concentration of species A in the reactor, L is the length of the reactor, r is the recycle ratio and α is the recycle loop dead time. Note that r varies from zero to one, with one corresponding to total recycle and zero fresh feed and zero corresponding to no recycle.

In order to simplify the presentation of our results, we introduce the following dimensionless variables:

$$
\begin{aligned}
t &= \frac{\bar{t}v}{L}, \quad z = \frac{\bar{z}}{L}, \quad Pe_1 = \frac{\rho c_p v L}{k}, \quad Pe_2 = \frac{vL}{D_A}, \quad \bar{x}_1 = \frac{T - T_0}{T_0}, \\
\bar{x}_2 &= \frac{C_A - C_{A0}}{C_{A0}}, \quad x_{1f} = \frac{T_f - T_0}{T_0}, \quad x_{2f} = \frac{C_{Af} - C_{A0}}{C_{A0}}, \quad u = \frac{T_c - T_0}{T_0}, \\
\gamma &= \frac{E}{RT_0}, \quad \beta_T = \frac{hA_s L}{C_{A0}} \quad B_T = \frac{-(\Delta H)C_{A0}}{\rho c_p T_0}, \quad B_C = \frac{k_0 exp(-\frac{E}{RT_0})L}{v}
\end{aligned}
\tag{6.3}
$$

to write the system of Eqs.6.1-6.2 in the following form:

$$
\begin{aligned}
\frac{\partial \bar{x}_1}{\partial t} &= -\frac{\partial \bar{x}_1}{\partial z} + \frac{1}{Pe_1}\frac{\partial^2 \bar{x}_1}{\partial z^2} + \beta_T(u(z,t) - \bar{x}_1) + B_T B_C exp\Big(\frac{\gamma \bar{x}_1}{1+\bar{x}_1}\Big)(1+\bar{x}_2) \\
\frac{\partial \bar{x}_2}{\partial t} &= -\frac{\partial \bar{x}_2}{\partial z} + \frac{1}{Pe_2}\frac{\partial^2 \bar{x}_2}{\partial z^2} - B_C exp\Big(\frac{\gamma \bar{x}_1}{1+\bar{x}_1}\Big)(1+\bar{x}_2)
\end{aligned}
\tag{6.4}
$$

subject to the following boundary conditions:

$$
\begin{aligned}
z = 0 : \quad & \frac{\partial \bar{x}_1}{\partial z} = Pe_1(\bar{x}_1 - (1-r)x_{1f} - r\bar{x}_1(1, t-\alpha)) \, , \\
& \frac{\partial \bar{x}_2}{\partial z} = Pe_2(\bar{x}_2 - (1-r)x_{2f} - r\bar{x}_2(1, t-\alpha)) \, ; \\
z = 1 : \quad & \frac{\partial \bar{x}_1}{\partial z} = 0 \, , \qquad \frac{\partial \bar{x}_2}{\partial z} = 0
\end{aligned}
\tag{6.5}
$$

Furthermore, in order to simplify the computation of the eigenvalues and eigenfunctions of the spatial differential operator which will be used in our calculations, we insert the non-homogeneous part of the boundary conditions of Eq.6.5 into the differential equation and obtain the following parabolic PDDE model for the process:

$$
\begin{aligned}
\frac{\partial \bar{x}_1}{\partial t} &= -\frac{\partial \bar{x}_1}{\partial z} + \frac{1}{Pe_1}\frac{\partial^2 \bar{x}_1}{\partial z^2} + \beta_T(u(z,t) - \bar{x}_1) + B_T B_C exp\Big(\frac{\gamma \bar{x}_1}{1+\bar{x}_1}\Big)(1+\bar{x}_2) \\
&\quad + \delta(z-0)((1-r)x_{1f} + r\bar{x}_1(1, t-\alpha)) \\
\frac{\partial \bar{x}_2}{\partial t} &= -\frac{\partial \bar{x}_2}{\partial z} + \frac{1}{Pe_2}\frac{\partial^2 \bar{x}_2}{\partial z^2} - B_C exp\Big(\frac{\gamma \bar{x}_1}{1+\bar{x}_1}\Big)(1+\bar{x}_2) \\
&\quad + \delta(z-0)((1-r)x_{2f} + r\bar{x}_2(1, t-\alpha))
\end{aligned}
\tag{6.6}
$$

where $\delta(\cdot)$ is the standard Dirac function, subject to the homogeneous boundary

conditions:

$$\begin{aligned} z=0\,, \qquad & \frac{\partial \bar{x}_1}{\partial z} = Pe_1 \bar{x}_1\,, \qquad & \frac{\partial \bar{x}_2}{\partial z} = Pe_2 \bar{x}_2\,; \\ z=1\,, \qquad & \frac{\partial \bar{x}_1}{\partial z} = 0\,, & \frac{\partial \bar{x}_2}{\partial z} = 0 \end{aligned} \tag{6.7}$$

Finally, we present the solution to the eigenvalue problem of the spatial differential operator of the process i.e.,:

$$\begin{aligned} \mathcal{A}x &= \begin{bmatrix} \mathcal{A}_1 \bar{x}_1 & 0 \\ 0 & \mathcal{A}_2 \bar{x}_2 \end{bmatrix} \\ &= \begin{bmatrix} \dfrac{1}{Pe_1}\dfrac{\partial^2 \bar{x}_1}{\partial z^2} - \dfrac{\partial \bar{x}_1}{\partial z} & 0 \\ 0 & \dfrac{1}{Pe_2}\dfrac{\partial^2 \bar{x}_2}{\partial z^2} - \dfrac{\partial \bar{x}_2}{\partial z} \end{bmatrix} \end{aligned} \tag{6.8}$$

The solution of the eigenvalue problem for $\mathcal{A}_i$, where $i = 1, 2$, can be obtained by utilizing standard techniques from linear operator theory (see, for example, [122]) and is of the form:

$$\begin{aligned} \lambda_{ij} &= \frac{\bar{a}_{ij}^2}{Pe_i} + \frac{Pe_i}{4}, \\ \phi_{ij}(z) &= B_{ij} e^{Pe_i \frac{z}{2}} \left(cos(\bar{a}_{ij} z) + \frac{Pe_i}{2\bar{a}_{ij}} sin(\bar{a}_{ij} z) \right), \\ \bar{\phi}_{ij}(z) &= e^{-Pe_i z} \phi_{ij}(z), \quad i = 1, 2, \quad j = 1, \ldots, \infty \end{aligned} \tag{6.9}$$

where $\lambda_{ij}, \phi_{ij}, \bar{\phi}_{ij}$, denote the eigenvalues, eigenfunctions and adjoint eigenfunctions of $\mathcal{A}_i$, respectively. $B_{ij}, \bar{a}_{ij}$ can be calculated analytically from the following formulas:

$$\begin{aligned} B_{ij} &= \left\{ \int_0^1 \left(cos(\bar{a}_{ij} z) + \frac{Pe_i}{2\bar{a}_{ij}} sin(\bar{a}_{ij} z) \right)^2 dz \right\}^{-\frac{1}{2}}, \\ tan(\bar{a}_{ij}) &= \frac{Pe_i \bar{a}_{ij}}{\bar{a}_{ij}^2 - \left(\frac{Pe_i}{2} \right)^2}, \quad i = 1, 2, \quad j = 1, \ldots, \infty \end{aligned} \tag{6.10}$$

Remark 6.1: It is important to point out that our study focuses on tubular reactors in which the diffusion and convection phenomena in the axial direction are both

important, and thus, the model of Eqs.6.6-6.7 constitutes a *parabolic* PDDE system. This feature, together with the explicit modeling of the dead-time associated with the recycle loop, distinguishes our work from previous studies on the analysis of the dynamics of tubular reactors with recycle [22, 23, 24, 25, 141, 26].

6.3 Effect of recycle ratio on open-loop dynamics

The objective of this section is to study the effect of the recycle ratio on the behavior and dynamics of the tubular reactor. To this end, we use standard Galerkin's method to derive an accurate high-order discretization of the PDDE system of Eqs.6.6-6.7. Specifically, the first 200 eigenfunctions of Eq.6.9 were used as basis functions in Galerkin's method to discretize the process model in space and reduce it into a large set (400 equations) of differential difference equations (DDEs). The time-integration of the resulting set of DDEs was performed by utilizing explicit Euler. It was verified that further increase in the number of eigenfunctions and reduction in the step of time-integration results in negligible improvements in the accuracy of the computed solution. The following values for the process parameters were used in our calculations:

$$\begin{aligned} Pe_1 &= 7.0, \quad Pe_2 = 7.0, \quad B_C = 0.1, \quad B_T = 2.5, \\ &\beta_T = 2.0, \quad \gamma = 10.0, \quad \alpha = 2.5 \end{aligned} \tag{6.11}$$

Since our objective is to study the effect of recycle ratio on open-loop dynamics and the behavior of the closed-loop system, the above parameters were chosen so that when the recycle loop is not used (i.e., $r = 0$), the open-loop system possesses a unique globally asymptotically stable spatially non-uniform steady state; this fact was verified both analytically and numerically through extensive simulations of the open-loop system for different initial conditions. Furthermore, for the above values of the process parameters, the diffusive and convective phenomena are equally impor-

tant. Figure 6.1 (solid line) shows the resulting steady state profile of $\bar{x}_1$; note the occurrence of a 'hot-spot' close to the inlet of the reactor. Subsequently, we intro-

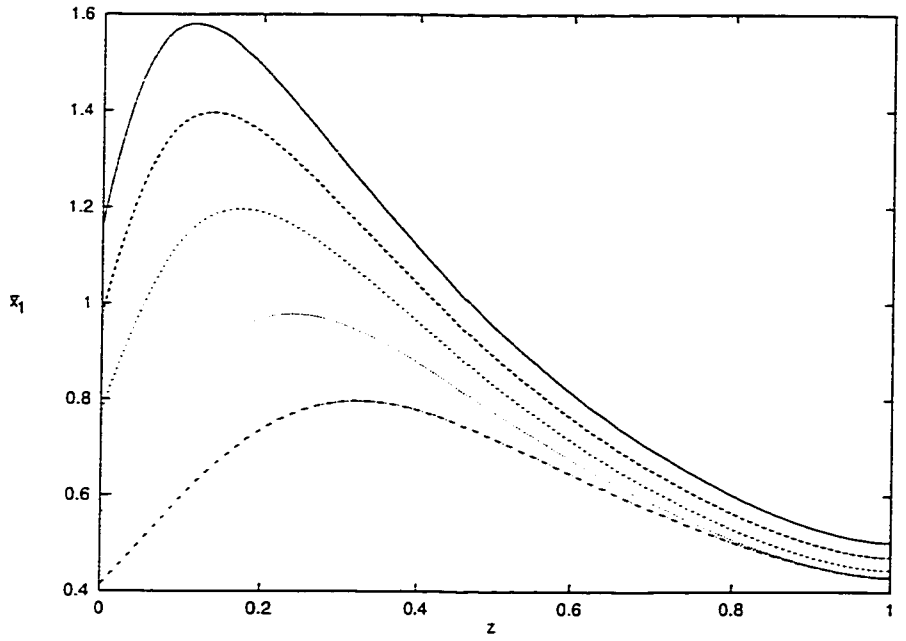

Figure 6.1: Steady state profile of $\bar{x}_1$ for different values of r: $r = 0.0$ (solid line), $r = 0.1$ (long-dashed line), $r = 0.2$ (short-dashed line), $r = 0.3$ (dotted line), and $r = 0.38$ (dashed-dotted line).

duced the recycle-loop to the process; the flow rate of the fresh feed to the process is reduced depending on the recycle flow rate so that the total flow rate to the reactor remains constant. Figure 6.1 shows the steady state profile of $\bar{x}_1$ for various recycle ratios, $r = 0.1$ (long-dashed line), $r = 0.2$ (short-dashed line), $r = 0.3$ (dotted line), and $r = 0.38$ (dashed-dotted line), for which the process is stable.

As the recycle ratio increases, the amount of fresh feed entering the reactor decreases, and thus, the temperature of the 'hot-spot' inside the reactor decreases and the location of the 'hot-spot' moves towards the center of the reactor. We also observe that even though the 'hot-spot' temperature decreases, the use of the recycle loop allows maintaining the production rate of the process constant; a very important benefit from a practical standpoint. Unfortunately, as the recycle ratio increases,

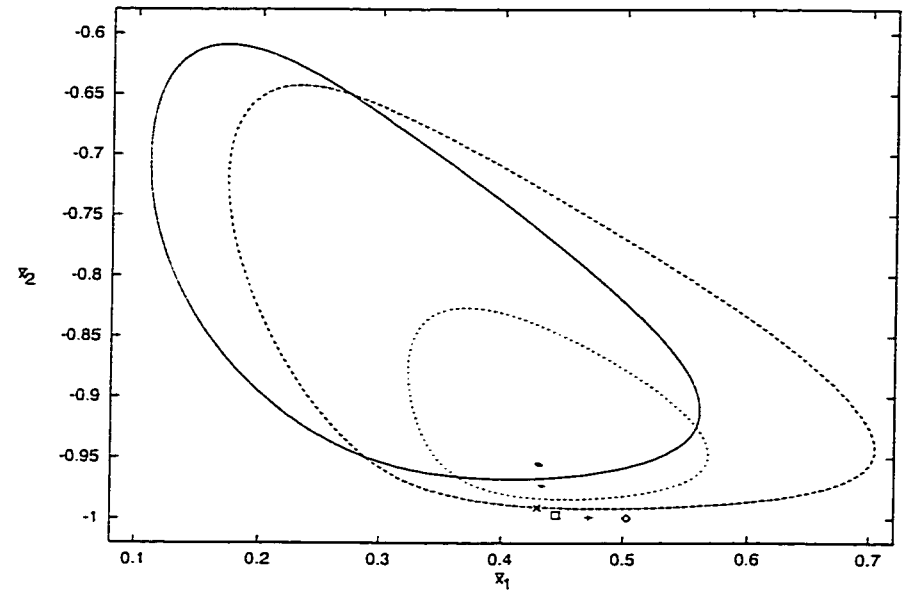

Figure 6.2: Profile of $\bar{x}_1(1,t)$ versus $\bar{x}_2(1,t)$ for different values of r: $r = 0$ ($\diamond$), $r = 0.1$ ($+$), $r = 0.2$ ($\square$), $r = 0.3$ ($\times$) (stable operating points), $r = 0.4$ (solid line), $r = 0.45$ (solid line), $r = 0.5$ (short-dashed line), $r = 0.6$ (long-dashed line), and $r = 0.7$ (solid line) (stable limit cycles).

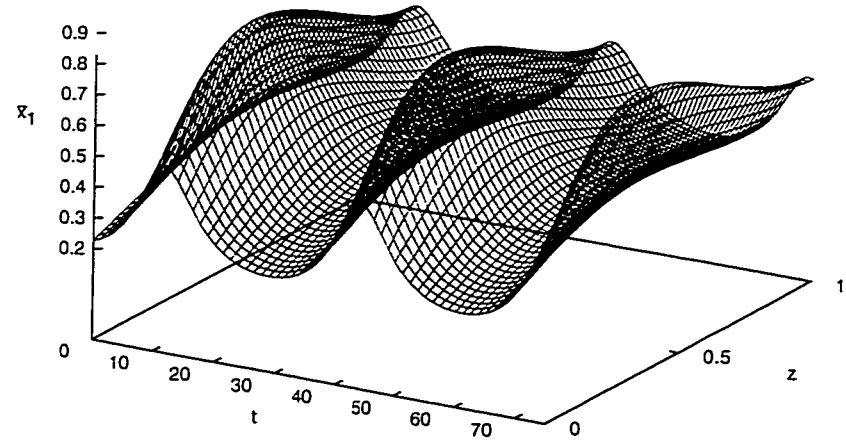

Figure 6.3: Open-loop spatiotemporal profile of $\bar{x}_1$, $r = 0.5$.

the stable steady state of the open-loop process gets closer to the instability limit. In particular, when the recycle ratio is equal to $r = 0.39$, the spatially non-uniform steady state becomes unstable and a globally asymptotically stable periodic (limit cycle) spatially non-uniform state appears. Figure 6.2 shows $\bar{x}_1(1,t)$ versus $\bar{x}_2(1,t)$ for different values of the recycle ratio. Clearly, when $r \geq 0.39$ the reactor moves to the periodic spatially non-uniform state; this can be also seen in Figure 6.3 where the open-loop spatiotemporal profile of $\bar{x}_1$ for $r = 0.5$ is shown. The open-loop instability of the steady state that yields a very high production rate with relatively low 'hot-spot' temperature motivates implementing a nonlinear feedback controller on the reactor to enforce stability and achieve operation for $r \geq 0.39$.

6.4 Nonlinear control of a tubular reactor with recycle

In this section, we synthesize and implement a nonlinear output feedback controller on the tubular reactor with recycle. The controller is synthesized on the basis of the process model and guarantees exponential stability in the closed-loop system and enforces the controlled output to asymptotically follow the reference input, independently of the size of the recycle loop dead-time. Specifically, the following methodology is used for controller synthesis: Initially, a nonlinear model reduction scheme which is based on combination of Galerkin's method with approximate inertial manifolds is employed for the derivation of DDE systems that describe the dominant dynamics of the PDDE system of Eqs.6.6-6.7. Then, these DDE systems are used as the basis for the explicit construction of nonlinear output feedback controllers through combination of geometric and Lyapunov techniques. All the details of the model reduction and controller synthesis results including rigorous proofs are given in [8] and will be omitted in this note for brevity.

The control problem is to manipulate the jacket temperature to stabilize the reactor at a spatially-nonuniform steady state where the production of species B is desirable and the 'hot-spot' temperature is acceptable, for values of r for which the open-loop system is unstable. To achieve this control objective, the controlled output was defined as $y_c(t) = \int_0^1 e^{-Pez}\phi_{11}(z)\bar{x}_1 dz$, and the manipulated variable was chosen as $u(z,t) = b(z)u(t)$ where the actuator distribution function was taken to be $b(z) = 1$ (uniform wall temperature in space). Furthermore, since the objective is stabilization at an unstable steady state, we assumed that there is available a large number of point measurements of the temperature throughout the reactor so that $y_c(t)$ is known with sufficient accuracy.

Two sets of simulation runs were performed to evaluate the improvement on the performance of the controller which is achieved when the controller is synthesized on the basis of DDE models derived from combination of Galerkin's method with approximate inertial manifolds, for $r = 0.5$ and $r = 0.7$ (in both cases the open-loop system exhibits unstable (oscillatory) behavior). In all the simulation runs, the process was initially ($t = 0$) assumed to be at a spatially non-uniform state and the reference input value was set at $v = 0.12$ (this is a value of $y(t)$ which corresponds to a steady state with the desired characteristics). Moreover, in order to perform meaningful comparisons, the same tuning parameters are used in the various controllers implemented on the reactor for $r = 0.5$ and $r = 0.7$. Following the presentation in our previous work [8] and in order to simplify the presentation of the following results, we will denote the dimension of the DDE system used for controller design with, m, and the dimension of the approximate inertial manifold used to improve the accuracy of this model with $\bar{m}$.

In the first set of simulations, we pick $r = 0.5$ which corresponds to an unstable

open-loop state. In order to provide a basis for comparing the performance of controllers designed based on DDE models derived by using combination of Galerkin's method with approximate inertial manifolds, we initially employed the standard Galerkin's method to derive an approximate DDE system which was used for the synthesis of a nonlinear output feedback controller. It was found that the lowest-order DDE model obtained from standard Galerkin's method which leads to the synthesis of a controller that stabilizes the closed-loop system is 10 (i.e., $m = 10$, $\bar{m} = 0$); lower-order controllers were unable to stabilize the closed-loop system. Figures 6.4 and 6.5 (short-dashed lines) show the evolution of the output of the closed-loop system and

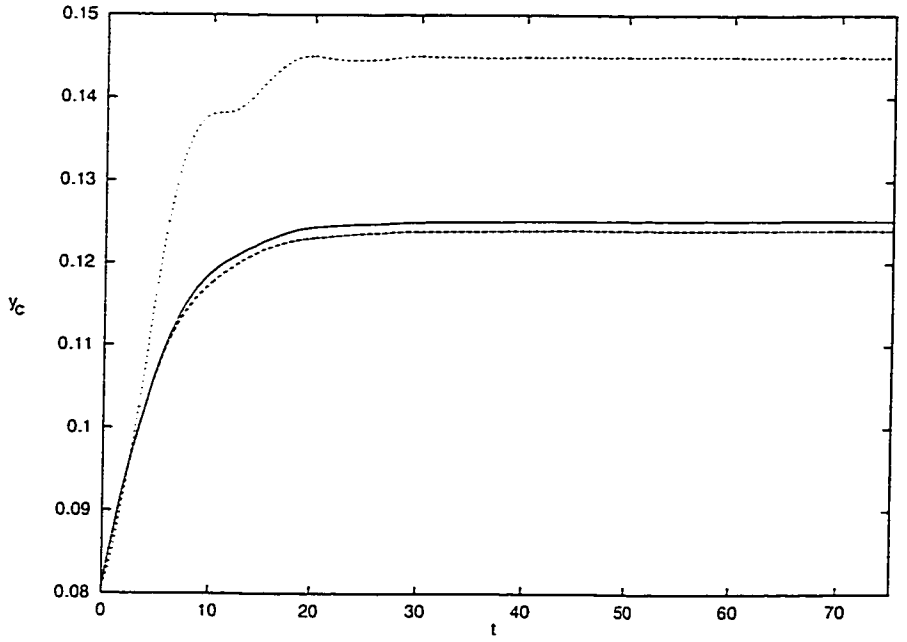

Figure 6.4: Closed-loop output profiles of the process with $r = 0.5$, under a controller with $m = 10$, $\bar{m} = 12$ (solid line), a controller with $m = 10$, $\bar{m} = 0$ (short-dashed line), and a controller with $m = 18$, $\bar{m} = 0$ (long-dashed line).

the profile of the manipulated input under a nonlinear output feedback controller synthesized on the basis of the model comprised of ten differential difference equations. Even though this controller stabilizes the closed-loop system, it fails to drive

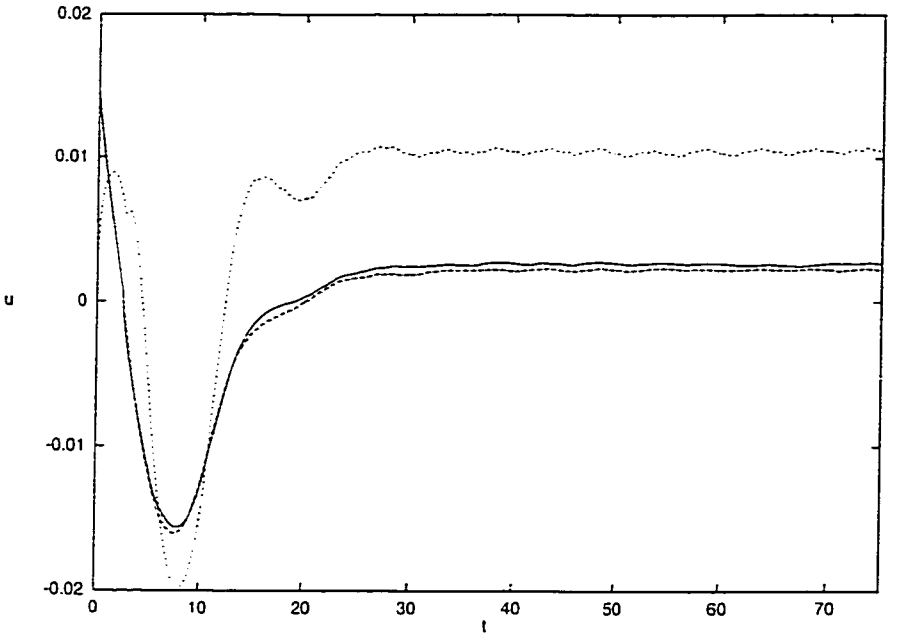

Figure 6.5: Manipulated input profiles for the process with recycle ratio $r = 0.5$, under a controller with $m = 10$, $\bar{m} = 12$ (solid line), a controller with $m = 10$, $\bar{m} = 0$ (short-dashed line), and a controller with $m = 18$, $\bar{m} = 0$ (long-dashed line).

the output at the desired reference input value, $v = 0.12$. Figure 6.6 (short-dashed line) shows the corresponding closed-loop steady state profile of $\bar{x}_1$, which is clearly not close to the desired one (dotted line). We subsequently used a combination of Galerkin's method with approximate inertial manifolds to derive a 10-th order DDE model which uses a 12-th order approximation for the approximate inertial manifold, (i.e., $m = 10$, $\bar{m} = 12$). Figures 6.4 and 6.5 (solid lines) show the evolution of the output of the closed-loop system and the profile of the manipulated input, while Figure 6.7 shows the spatiotemporal evolution of $\bar{x}_1$ and Figure 6.6 (solid line) shows the steady state profile of $\bar{x}_1$. This controller clearly regulates the system very close to the reference input value. Finally, we also implemented on the process a nonlinear output feedback controller which was synthesized on the basis of a DDE model obtained with $m = 18$ and $\bar{m} = 0$. Figures 6.3 and 6.4 (long-dashed lines) show the

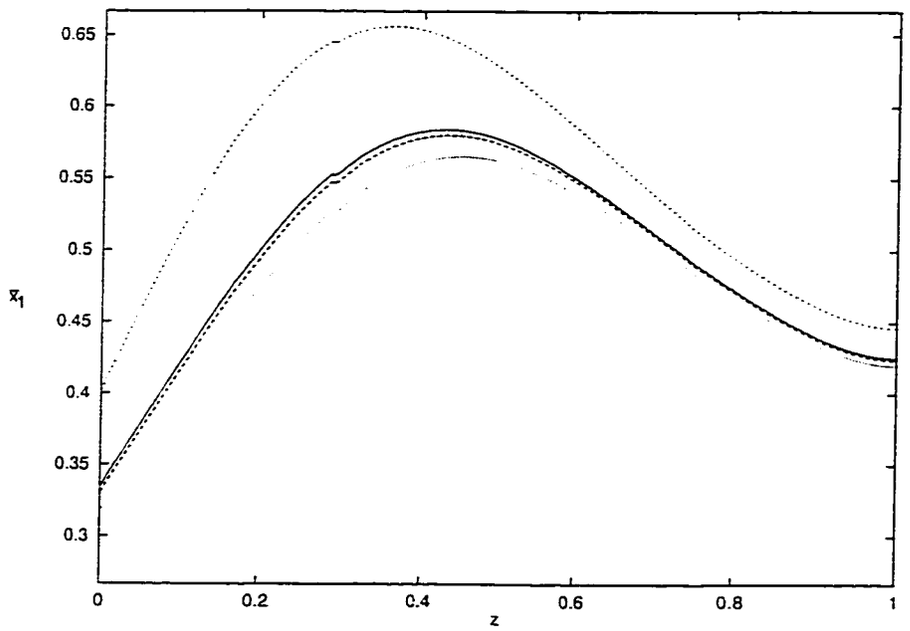

Figure 6.6: Steady state profile of $\bar{x}_1$ of the process with $r = 0.5$, under a controller with $m = 10$, $\bar{m} = 12$ (solid line), a controller with $m = 10$, $\bar{m} = 0$ (short-dashed line), and a controller with $m = 18$, $\bar{m} = 0$ (long-dashed line), and profile of the desired operating steady state (dotted line).

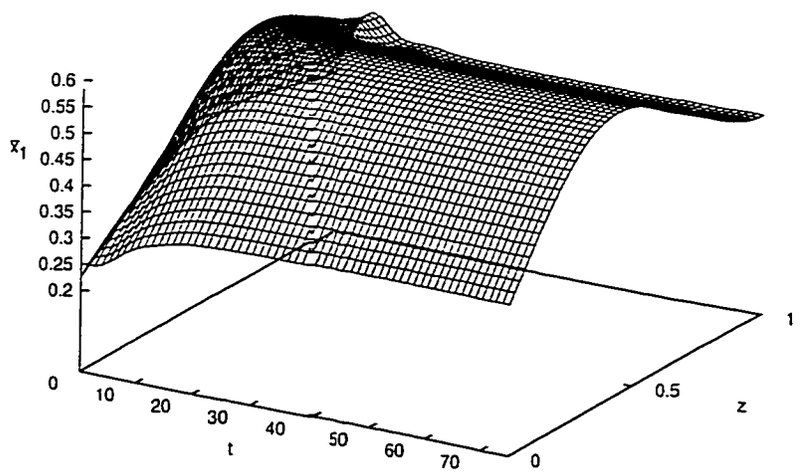

Figure 6.7: Spatiotemporal evolution of $\bar{x}_1$ under a controller with $m = 10$, $\bar{m} = 12$; $r = 0.5$

corresponding closed-loop output and manipulated input profiles, while Figure 6.6 (long-dashed line) shows the profile of $\bar{x}_1$. The performance of this controller is very close to the one of the controller synthesized on the basis of the DDE model obtained with $m = 10$ and $\bar{m} = 12$.

In the second simulation runs, we changed the recycle ratio of the process to $r = 0.7$; this value also corresponds to oscillatory open-loop behavior. As in the previous case, we first implemented on the process a nonlinear output feedback controller designed on the basis of a DDE model obtained using Galerkin's method with $m = 10$ and $\bar{m} = 0$ (again, 10 is the lower order for which stabilization of the closed-loop system is accomplished). Figures 6.8, 6.9 and 6.10 (short-dashed lines) show the

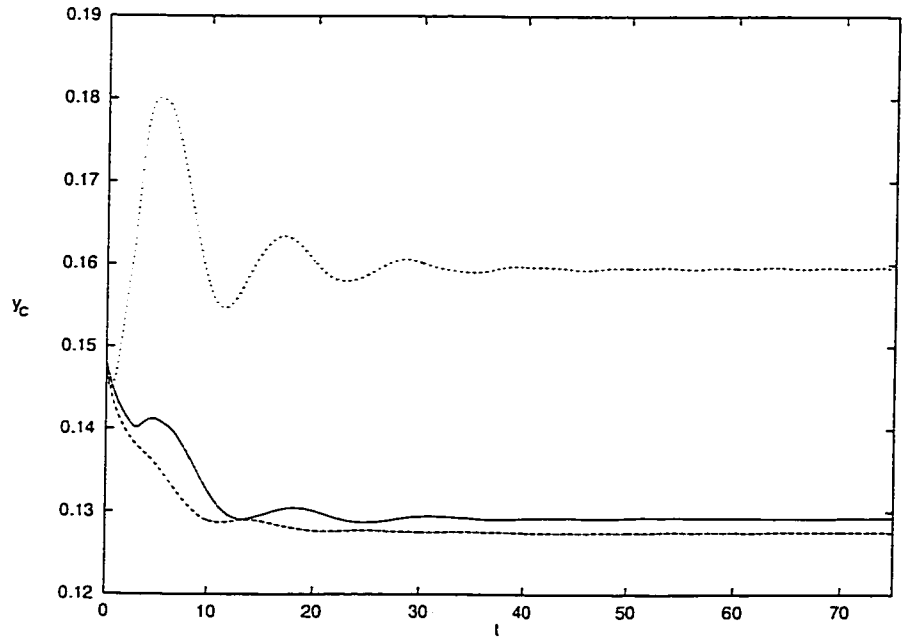

Figure 6.8: Closed-loop output profiles of the process with $r = 0.7$, under a controller with $m = 10$, $\bar{m} = 12$ (solid line), a controller with $m = 10$, $\bar{m} = 0$ (short-dashed line), and a controller with $m = 18$, $\bar{m} = 0$ (long-dashed line).

evolution of the output of the closed-loop system, the profile of the manipulated input and the closed-loop steady state profile of $\bar{x}_1$, respectively. Again, this controller

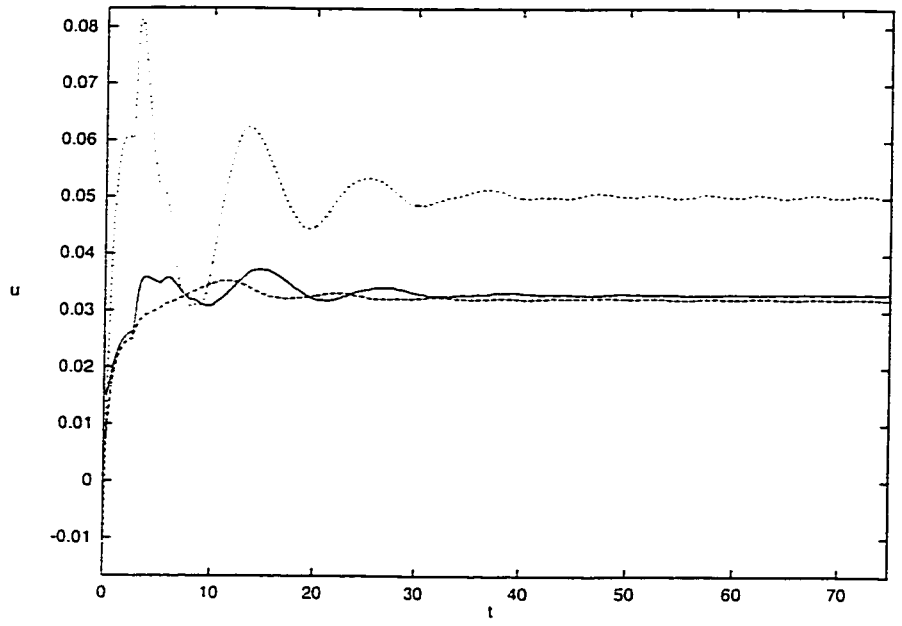

Figure 6.9: Manipulated input profiles under a controller with $m = 10$, $\bar{m} = 12$ (solid line), a controller with $m = 10$, $\bar{m} = 0$ (short-dashed line), and a controller with $m = 18$, $\bar{m} = 0$ (long-dashed line); $r = 0.7$.

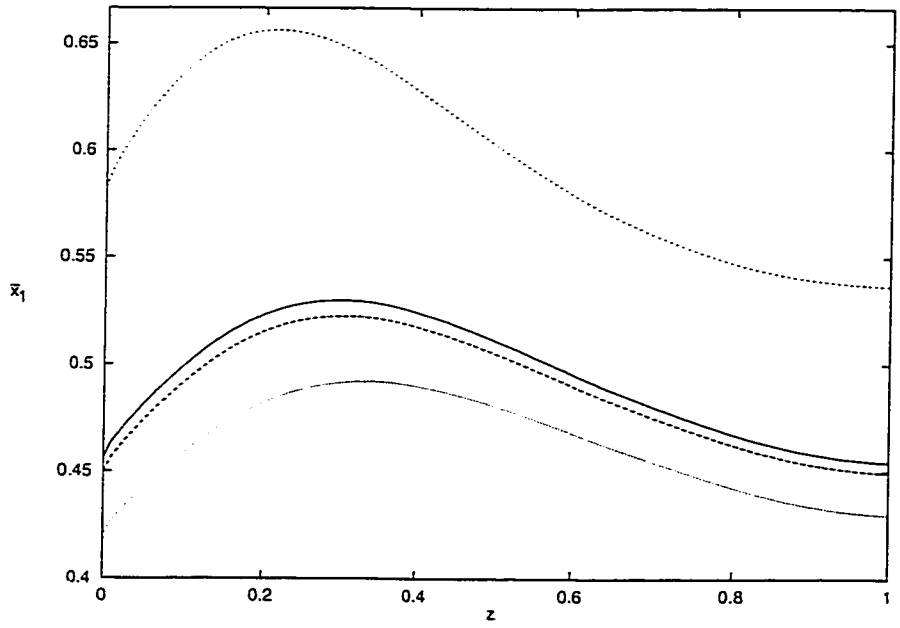

Figure 6.10: Steady state profile of $\bar{x}_1$ under a controller with $m = 10$, $\bar{m} = 12$ (solid line), a controller with $m = 10$, $\bar{m} = 0$ (short-dashed line), and a controller with $m = 18$, $\bar{m} = 0$ (long-dashed line), and profile of the desired operating steady state (dotted line); $r = 0.7$.

exhibits a very poor performance, stabilizing the system far from the desired steady state. Then, we used a 12-th order approximation for the approximate inertial manifold to improve the accuracy of the 10-th order DDE model obtained from Galerkin's method (i.e., $m = 10$, $\bar{m} = 12$) and used the resulting model for the synthesis of a nonlinear output feedback controller. Figures 6.8, 6.9 and 6.10 (solid lines) show the profiles of the controlled output, the manipulated input, and $\bar{x}_1$ at steady state, respectively, and Figure 6.11 shows the spatiotemporal evolution of $\bar{x}_1$. This controller clearly regulates the system very close to the desired steady state. Finally, for

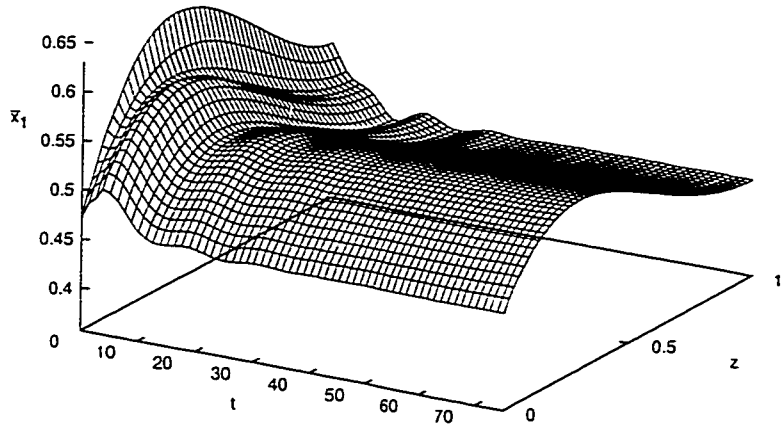

Figure 6.11: Spatiotemporal evolution of $\bar{x}_1$ under a controller with $m = 10$, $\bar{m} = 12$; $r = 0.7$.

the sake of comparison, we tested a nonlinear output feedback controller which was synthesized on the basis of a DDE model obtained with $m = 18$ and $\bar{m} = 0$. Figures 6.8, 6.9 and 6.10 (long-dashed lines) show the profiles of the controlled output, manipulated input and $\bar{x}_1$ at steady state. Clearly, the performance of this controller is very close to the one of the controller synthesized on the basis of the DDE model obtained with $m = 10$ and $\bar{m} = 12$.

From the simulation results, it is evident that the combination of Galerkin's method with approximate inertial manifolds leads to the synthesis of high-performance controllers based on low-order DDE systems. We finally note that we have found similar results for many other values of $r \geq 0.39$; these results are not shown here for brevity.

Remark 6.2: Regarding the effect of the recycle-loop dead time on the open-loop dynamics and the performance of the closed-loop system, we found through simulations that: a) the stability of the spatially non-uniform steady state for $r < 0.39$ and the stability of the periodic state of the open-loop system for $r \geq 0.39$ are independent of the value of the dead time in the recycle-loop, α, b) the recycle ratio, $r = 0.39$, for which the globally stable open-loop steady state becomes unstable is independent of α, and c) the closed-loop response as the α increases becomes significantly more sluggish, which means that retuning of the controller is needed to achieve the desired rate of convergence to the steady state in the closed-loop system for larger α.

Remark 6.3: We note that the approach followed here for the construction of low-order DDE approximations of the model of Eqs.6.6-6.7 and the synthesis of nonlinear feedback controllers is not directly applicable to the case of tubular reactors in which the diffusive phenomena are negligible compared to the convective phenomena (like the reactors studied in [22, 23, 24, 25, 141, 26]). The reason is that tubular reactors with negligible convective phenomena are modeled by first-order hyperbolic PDE systems in which the eigenvalues of the spatial differential operator cluster along vertical or nearly vertical asymptotes in the complex plane, and therefore, the controller synthesis problem has to be directly addressed on the basis of the PDE system (see [42] and [74] for results on nonlinear control of hyperbolic PDEs and 'hot-spot' suppression in convection-reaction processes, respectively).

6.5 Conclusions

In this chapter, we presented a study on the dynamics and control of a tubular reactor with recycle loop where an exothermic reaction of the form $A \rightarrow B$ takes place. Initially, a detailed mathematical model for the process which consists of two nonlinear PDDEs and accounts for diffusion, convection and chemical reaction, as well as for dead-time in the recycle loop was presented. Then, the dynamics of the process for different values of the recycle ration was studied and was found that the introduction of the recycle loop reduces the 'hot-spot' temperature inside the reactor, while maintaining the desired rate of production of the species B. In addition, the use of the recycle loop introduces a feedback mechanism into the process which renders the open-loop steady state unstable. To stabilize the process, we used the method developed in chapter 5 to synthesize a nonlinear output feedback controller based on an approximate DDE model obtained through application of nonlinear Galerkin's method to the detailed process model. The performance of the controller for different values of the recycle ratio was successfully tested through simulations and was found to be superior to the one achieved by nonlinear controllers synthesized based on approximate models obtained from linear Galerkin's method.

Chapter 7

Integrating Nonlinear Output Feedback Control and Optimal Actuator/Sensor Placement for Transport Reaction Processes

7.1 Introduction

Transport-reaction processes with significant diffusive and dispersive mechanism are typically characterized by severe nonlinearities and spatial variations, and are naturally described by quasi-linear parabolic PDEs. Nonlinearities usually arise from complex reaction mechanism and Arrhenius dependence of the reaction rate on temperature, and spatial variations occur due to the presence of significant diffusion and convection phenomena. Typical examples of transport-reaction processes are tubular reactors, packed-bed reactors, and chemical vapor deposition reactors.

Parabolic PDE systems typically involve spatial differential operators whose eigenspectrum can be partitioned into a finite-dimensional slow one and an infinite-dimen-

sional stable fast one [59, 18]. This implies that the dynamic behavior of such systems can be approximately described by finite-dimensional systems. Therefore, the standard approach to the control of parabolic PDEs involves the application of Galerkin's method to the PDE system to derive ODE systems that describe the dynamics of the dominant (slow) modes of the PDE system, which are subsequently used as the basis for the synthesis of finite-dimensional controllers (e.g., [18, 122]). A potential drawback of this approach is that the number of modes that should be retained to derive an ODE system that yields the desired degree of approximation may be very large, leading to complex controller design and high dimensionality of the resulting controllers. Motivated by this, recent efforts on control of parabolic PDE systems have focused on the problem of synthesizing low-order controllers on the basis of ODE models obtained through combination of Galerkin's method with approximate inertial manifolds (see the recent book [36] for details and references).

Even though the developed methods allow to systematically design nonlinear controllers for transport reaction processes, there is no work on the integration of nonlinear controllers with optimal placement of control actuators and measurement sensors for transport reaction processes so that the desired control objectives are achieved with minimal energy use. Regarding the problem of optimal placement of control actuators, the conventional approach is to select the actuator locations based on open-loop considerations to ensure that the necessary controllability requirements are satisfied. More recently, efforts have been made on the problem of integrating feedback control and optimal actuator placement for certain classes of linear distributed parameter systems including investigation of controllability measures and actuator placement in oscillatory systems [13], optimal placement of actuators for linear feedback control in parabolic PDEs [157, 54] and in actively controlled structures [120, 33].

On the other hand, the problem of selecting optimal locations for measurement sensors in distributed parameter systems has received very significant attention over the last twenty years. The essence of this problem is to use a finite number of measurements to compute the best estimate of the entire distributed state for all positions and times employing a state observer in the presence of measurement noise. Early efforts for the solution to this problem focused on linear systems [161, 31, 91, 116, 112] and the application of the results to optimal state estimation in tubular reactors [49, 92, 64, 3, 149]. The central idea to the solution involves the use of a spatial discretization scheme to obtain a lumped approximation of the original distributed parameter system followed by the formulation and solution of an optimal state estimation problem which involves computing sensor locations so that an appropriate functional that includes penalty on the estimation error and the measurement noise is minimized. Significant research efforts have also been made on the problem of optimal placement of controllers and sensors for distributed parameter systems [17, 4, 68, 51, 104, 117]. An excellent review of results on sensors and controllers location in distributed systems can be found in [89]. Despite the progress on optimal sensor placement and the availability of results on the integration of linear feedback control with actuator placement for linear parabolic PDEs, there are no results on the integration of nonlinear output feedback control with optimal placement of control actuators and measurement sensors for transport-reaction processes described by nonlinear parabolic PDEs.

In this chapter [6, 9, 10] we propose a general and practical methodology for the integration of nonlinear output feedback control with optimal placement of control actuators and measurement sensors for transport-reaction processes described by a broad class of quasi-linear parabolic PDEs for which the eigenspectrum of the spa-

tial differential operator can be partitioned into a finite-dimensional slow one and an infinite-dimensional stable fast complement. Initially, Galerkin's method is employed to derive finite-dimensional approximations of the PDE system which are used for the synthesis of stabilizing nonlinear state feedback controllers via geometric techniques. The optimal actuator location problem is subsequently formulated as the one of minimizing a meaningful cost functional that includes penalty on the response of the closed-loop system and the control action and is solved by using standard unconstrained optimization techniques. Then, under the assumption that the number of measurement sensors is equal to the number of slow modes, we employ a procedure proposed in [40] for obtaining estimates for the states of the approximate finite-dimensional model from the measurements. The estimates are combined with the state feedback controllers to derive output feedback controllers. The optimal location of the measurement sensors is computed by minimizing a cost function of the estimation error in the closed-loop infinite-dimensional system. It is rigorously established that the proposed output feedback controllers enforce stability in the closed-loop infinite-dimensional system and that the solution to the optimal actuator/sensor problem, which is obtained on the basis of the closed-loop finite-dimensional system, is near-optimal in the sense that it approaches the optimal solution for the infinite-dimensional system as the separation of the slow and fast eigenmodes increases. The proposed methodology is successfully applied to a diffusion-reaction process and a non-isothermal packed-bed reactor with recycle to derive nonlinear output feedback controllers and compute optimal actuator/sensor locations for stabilization of unstable steady-states.

7.2 Preliminaries

7.2.1 Description of parabolic PDE systems

We consider transport-reaction processes described by quasi-linear parabolic PDE systems of the form:

$$\begin{aligned} \frac{\partial \bar{x}}{\partial t} &= A\frac{\partial \bar{x}}{\partial z} + B\frac{\partial^2 \bar{x}}{\partial z^2} + wb(z)u + f(\bar{x}) \\ y_c^i &= \int_\alpha^\beta c^i(z)k\bar{x}(z,t)dz, \qquad i = 1,\ldots,l \\ y_m^\kappa &= \int_\alpha^\beta s^\kappa(z)\omega\bar{x}(z,t)dz \qquad \kappa = 1,\ldots,p \end{aligned} \tag{7.1}$$

subject to the boundary conditions:

$$\begin{aligned} C_1\bar{x}(\alpha,t) + D_1\frac{\partial \bar{x}}{\partial z}(\alpha,t) &= R_1 \\ C_2\bar{x}(\beta,t) + D_2\frac{\partial \bar{x}}{\partial z}(\beta,t) &= R_2 \end{aligned} \tag{7.2}$$

and the initial condition:

$$\bar{x}(z,0) = \bar{x}_0(z) \tag{7.3}$$

where $\bar{x}(z,t) = [\bar{x}_1(z,t) \cdots \bar{x}_n(z,t)]^T \in \mathbb{R}^n$ denotes the vector of state variables, $z \in [\alpha,\beta] \subset \mathbb{R}$ is the spatial coordinate, $t \in [0,\infty)$ is the time, $u = [u^1\ u^2 \cdots u^l]^T \in \mathbb{R}^l$ denotes the vector of manipulated inputs, $y_c^i \in \mathbb{R}$ denotes the i-th controlled output, and $y_m^\kappa \in \mathbb{R}$ denotes the κ-th measured output. $\frac{\partial \bar{x}}{\partial z}, \frac{\partial^2 \bar{x}}{\partial z^2}$ denote the first- and second-order spatial derivatives of $\bar{x}$, $f(\bar{x})$ is a nonlinear vector function, w, k are constant vectors, A, B, C_1, D_1, C_2, D_2 are constant matrices, R_1, R_2 are column vectors, and $\bar{x}_0(z)$ is the initial condition. $b(z)$ is a known smooth vector function of z of the form $b(z) = [b^1(z)\ b^2(z) \cdots b^l(z)]$, where $b^i(z)$ describes how the control action $u^i(t)$ is distributed in the interval $[\alpha,\beta]$, $c^i(z)$ is a known smooth function of z which is determined by the desired performance specifications in the interval $[\alpha,\beta]$, and $s^\kappa(z)$ is a known smooth function of z which depends on the shape (point or

distributing sensing) of the measurement sensors in the interval $[\alpha, \beta]$. Whenever the control action enters the system at a single point z_0, with $z_0 \in [\alpha, \beta]$ (i.e. point actuation), the function $b^i(z)$ is taken to be nonzero in a finite spatial interval of the form $[z_0 - \epsilon, z_0 + \epsilon]$, where ϵ is a small positive real number, and zero elsewhere in $[\alpha, \beta]$. Figure 7.1 shows the location of the manipulated inputs, controlled outputs, and measured outputs in the case of a prototype example. Throughout the paper, we will use the order of magnitude notation $O(\epsilon)$. In particular, $\delta(\epsilon) = O(\epsilon)$ if there exist positive real numbers k_1 and k_2 such that: $|\delta(\epsilon)| \leq k_1 |\epsilon|$, $\forall\, |\epsilon| < k_2$.

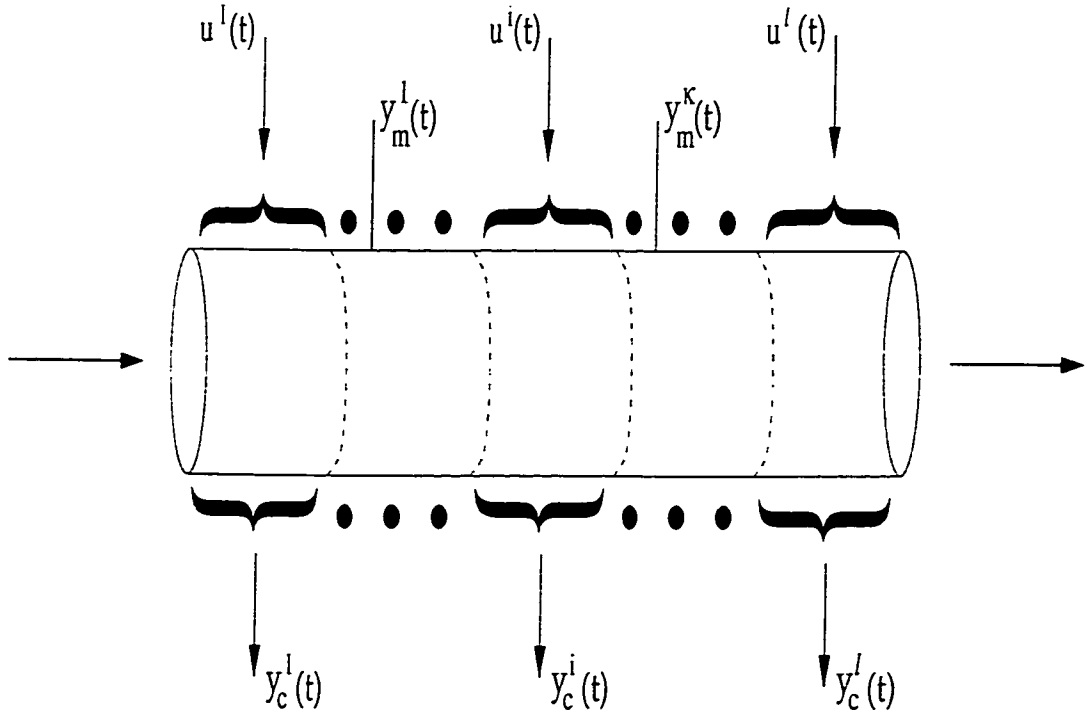

Figure 7.1: Location of the manipulated inputs, controlled outputs, and measured outputs in the case of a prototype example.

Referring to the system of Eq.7.1, several remarks are in order: a) the spatial differential operator is linear; this assumption is valid for diffusion-convection-reaction processes where the diffusion coefficient and the conductivity can be taken independent of temperature and concentrations, b) the manipulated input enters the system

in a linear and affine fashion; this is typically the case in many practical applications where, for example, the wall temperature is chosen as the manipulated input, and c) the nonlinearities appear in an additive fashion (e.g., complex reaction rates, Arrhenius dependence of reaction rates on temperature).

In the remainder of this section, we precisely characterize the class of parabolic PDE systems of the form of Eq.7.1 which we consider in the manuscript. To this end, we formulate the parabolic PDE system of Eq.7.1 as an infinite dimensional system in the Hilbert space $\mathcal{H}([\alpha,\beta];\mathbb{R}^n)$ (this will also simplify the notation of the paper, since the boundary conditions of Eq.7.2 will be directly included in the formulation; see Eq.7.8 below), with $\mathcal{H}$ being the space of n-dimensional vector functions defined on $[\alpha,\beta]$ that satisfy the boundary condition of Eq.7.2, with inner product and norm:

$$\begin{aligned} (\omega_1,\omega_2) &= \int_\alpha^\beta (\omega_1(z),\omega_2(z))_{\mathbb{R}^n} dz \\ ||\omega_1||_2 &= (\omega_1,\omega_1)^{\frac{1}{2}} \end{aligned} \tag{7.4}$$

where ω_1,ω_2 are two elements of $\mathcal{H}([\alpha,\beta];\mathbb{R}^n)$ and the notation $(\cdot,\cdot)_{\mathbb{R}^n}$ denotes the standard inner product in $\mathbb{R}^n$. Defining the state function x on $\mathcal{H}([\alpha,\beta];\mathbb{R}^n)$ as:

$$x(t) = \bar{x}(z,t), \quad t>0, \quad z\in[\alpha,\beta], \tag{7.5}$$

the operator $\mathcal{A}$ in $\mathcal{H}([\alpha,\beta];\mathbb{R}^n)$ as:

$$\begin{aligned} \mathcal{A}x &= A\frac{\partial \bar{x}}{\partial z} + B\frac{\partial^2 \bar{x}}{\partial z^2}, \\ x\in D(\mathcal{A}) &= \left\{ \begin{array}{c} x\in\mathcal{H}([\alpha,\beta];\mathbb{R}^n) \\ C_1\bar{x}(\alpha,t) + D_1\dfrac{\partial \bar{x}}{\partial z}(\alpha,t) = R_1 \\ C_2\bar{x}(\beta,t) + D_2\dfrac{\partial \bar{x}}{\partial z}(\beta,t) = R_2 \end{array} \right\} \end{aligned} \tag{7.6}$$

and the input, controlled output, and measured output operators as:

$$\mathcal{B}u = wbu, \qquad \mathcal{C}x = (c,kx), \qquad \mathcal{S}x = (s,\omega x) \tag{7.7}$$

the system of Eqs.7.1-7.2-7.3 takes the form:

$$\begin{aligned} \dot{x} &= \mathcal{A}x + \mathcal{B}u + f(x), \quad x(0) = x_0 \\ y_c &= \mathcal{C}x, \quad y_m = \mathcal{S}x \end{aligned} \tag{7.8}$$

where $f(x(t)) = f(\bar{x}(z,t))$ and $x_0 = \bar{x}_0(z)$. We assume that the nonlinear terms $f(x)$ are locally Lipschitz with respect to their arguments and satisfy $f(0) = 0$. For $\mathcal{A}$, the eigenvalue problem is defined as:

$$\mathcal{A}\phi_j = \lambda_j \phi_j, \quad j = 1, \ldots, \infty \tag{7.9}$$

where λ_j denotes an eigenvalue and ϕ_j denotes an eigenfunction; the eigenspectrum of $\mathcal{A}$, $\sigma(\mathcal{A})$, is defined as the set of all eigenvalues of $\mathcal{A}$, i.e. $\sigma(\mathcal{A}) = \{\lambda_1, \lambda_2, \ldots, \}$. Assumption 7.1 that follows states that the eigenspectrum of $\mathcal{A}$ can be partitioned into a finite-dimensional part consisting of m slow eigenvalues and a stable infinite-dimensional complement containing the remaining fast eigenvalues, and that the separation between the slow and fast eigenvalues of $\mathcal{A}$ is large.

Assumption 7.1:

1. *$Re\,\{\lambda_1\} \geq Re\,\{\lambda_2\} \geq \cdots \geq Re\,\{\lambda_j\} \geq \cdots$, where $Re\,\{\lambda_j\}$ denotes the real part of λ_j.*

2. *$\sigma(\mathcal{A})$ can be partitioned as $\sigma(\mathcal{A}) = \sigma_1(\mathcal{A}) + \sigma_2(\mathcal{A})$, where $\sigma_1(\mathcal{A})$ consists of the first m (with m finite) eigenvalues, i.e. $\sigma_1(\mathcal{A}) = \{\lambda_1, \ldots, \lambda_m\}$, and $\dfrac{|Re\,\{\lambda_1\}|}{|Re\,\{\lambda_m\}|} = O(1)$.*

3. *$Re\,\lambda_{m+1} < 0$ and $\dfrac{|Re\,\{\lambda_m\}|}{|Re\,\{\lambda_{m+1}\}|} = O(\epsilon)$ where $\epsilon < 1$ is a small positive number.*

The assumption of finite number of unstable eigenvalues is always satisfied for nonlinear parabolic PDE systems [59], while the assumption of discrete eigenspectrum and the assumption of existence of only a few dominant modes that describe the dy-

namics of the nonlinear parabolic PDE system are usually satisfied by the majority of diffusion-convection-reaction processes (see the examples of Sections 6 and 7).

7.2.2 Galerkin's method

We will now review the application of standard Galerkin's method to the system of Eq.7.8 to derive an approximate finite-dimensional system. Let $\mathcal{H}_s$, $\mathcal{H}_f$ be modal subspaces of $\mathcal{A}$, defined as $\mathcal{H}_s = span\{\phi_1, \phi_2, \ldots, \phi_m\}$ and $\mathcal{H}_f = span\{\phi_{m+1}, \phi_{m+2}, \ldots,\}$ (the existence of $\mathcal{H}_s$, $\mathcal{H}_f$ follows from Assumption 7.1). Defining the orthogonal projection operators P_s and P_f such that $x_s = P_s x$, $x_f = P_f x$, the state x of the system of Eq.7.8 can be decomposed as:

$$x = x_s + x_f = P_s x + P_f x \tag{7.10}$$

Applying P_s and P_f to the system of Eq.7.8 and using the above decomposition for x, the system of Eq.7.8 can be equivalently written in the following form:

$$\begin{aligned} \frac{dx_s}{dt} &= \mathcal{A}_s x_s + \mathcal{B}_s u + f_s(x_s, x_f) \\ \frac{\partial x_f}{\partial t} &= \mathcal{A}_f x_f + \mathcal{B}_f u + f_f(x_s, x_f) \\ y_c &= \mathcal{C} x_s + \mathcal{C} x_f, \qquad y_m = \mathcal{S} x_s + \mathcal{S} x_f, \\ x_s(0) &= P_s x(0) = P_s x_0, \qquad x_f(0) = P_f x(0) = P_f x_0 \end{aligned} \tag{7.11}$$

where $\mathcal{A}_s = P_s \mathcal{A} P_s$, $\mathcal{B}_s = P_s \mathcal{B}$, $f_s = P_s f$, $\mathcal{A}_f = P_f \mathcal{A} P_f$, $\mathcal{B}_f = P_f \mathcal{B}$ and $f_f = P_f f$ and the notation $\frac{\partial x_f}{\partial t}$ is used to denote that the state x_f belongs in an infinite-dimensional space. In the above system, $\mathcal{A}_s$ is a diagonal matrix of dimension $m \times m$ of the form $\mathcal{A}_s = diag\{\lambda_j\}$, $f_s(x_s, x_f)$ and $f_f(x_s, x_f)$ are Lipschitz vector functions, and $\mathcal{A}_f$ is an unbounded differential operator which is exponentially stable (following from part 3 of Assumption 7.1 and the selection of $\mathcal{H}_s, \mathcal{H}_f$). Neglecting the fast and stable infinite-dimensional x_f-subsystem in the system of Eq.7.11, the following m-dimensional slow

system is obtained:

$$\begin{aligned} \frac{d\tilde{x}_s}{dt} &= \mathcal{A}_s\tilde{x}_s + \mathcal{B}_s u + f_s(\tilde{x}_s, 0) \\ \tilde{y}_c &= \mathcal{C}\tilde{x}_s, \qquad \tilde{y}_m = \mathcal{S}\tilde{x}_s \end{aligned} \tag{7.12}$$

where the tilde symbol in $\tilde{x}_s$, $\tilde{y}_c$ and $\tilde{y}_m$ denotes that the state $\tilde{x}_s$, the controlled output $\tilde{y}_c$, and the measured output $\tilde{y}_m$ are associated with the approximation of the slow x_s-subsystem.

Remark 7.1: We note that the above model reduction procedure which led to the approximate ODE system of Eq.7.11 can also be used, when empirical eigenfunctions of the system of Eq.7.8 computed through Karhunen-Loéve expansion (see [36] for details) are used as basis functions in $\mathcal{H}_s$ and $\mathcal{H}_f$ instead of the eigenfunctions of $\mathcal{A}$.

7.3 Problem statement and solution framework

In this paper, we address the problem of computing optimal locations of point control actuators and point measurement sensors associated with nonlinear output feedback control laws of the following general form:

$$u = \mathcal{F}(y_m) \tag{7.13}$$

where $\mathcal{F}(y_m)$ is a nonlinear vector function and y_m denotes the vector of measured outputs, so that the following properties are enforced in the closed-loop system: a) exponential stability, and b) the optimal actuator/sensor locations, which are obtained on the basis of the closed-loop finite-dimensional system, are near-optimal in the sense that it approaches the optimal solution for the infinite-dimensional system as the separation of the slow and fast eigenmodes increases. To address this problem, we will initially synthesize stabilizing nonlinear state feedback controllers via geometric techniques on the basis of finite-dimensional approximations of the PDE system obtained via Galerkin's method. The optimal actuator location problem will be subsequently

formulated as the one of minimizing a meaningful cost functional that includes penalty on the response of the closed-loop system and the control action and will be solved by using standard unconstrained optimization techniques. Then, under the assumption that the number of measurement sensors is equal to the number of slow modes, we will employ a procedure proposed in [40] for obtaining estimates for the states of the approximate finite-dimensional model from the measurements. The estimates will be combined with the state feedback controllers to derive output feedback controllers. The optimal location of the measurement sensors will be computed by minimizing a cost function of the estimation error in the closed-loop infinite-dimensional system. It will be established by using singular perturbation techniques that the desired properties are enforced in the closed-loop system, provided that the separation of the slow and fast eigenmodes increases.

7.4 Integrating nonlinear control and optimal actuator placement

7.4.1 Nonlinear state feedback controller synthesis

In this section, we assume that measurements of the states of the PDE system of Eq.7.12 are available and address the problem of synthesizing nonlinear static state feedback control laws of the general form:

$$u = \mathcal{F}(z_a, \tilde{x}_s) \tag{7.14}$$

where $\mathcal{F}(z_a, \tilde{x}_s)$ is a nonlinear vector function and z_a denotes the vector of the actuator locations, that guarantee exponential stability of the closed-loop finite-dimensional system. To this end, we will need the following assumption (see Remark 7.2 below for a discussion on this assumption).

Assumption 7.2: *$l = m$ (i.e., the number of control actuators is equal to the number of slow modes), and the inverse of the matrix $\mathcal{B}_s$ exists.*

Proposition 7.1 that follows provides the explicit formula for the state feedback controller that achieves the control objective (the proof of this proposition is trivial and is omitted for brevity).

Proposition 7.1: *Consider the finite-dimensional system of Eq.7.12 for which Assumption 7.2 holds. Then, the state feedback controller:*

$$u = \mathcal{B}_s^{-1}\left((\Lambda_s - \mathcal{A}_s)\tilde{x}_s - f_s(\tilde{x}_s, 0)\right) \tag{7.15}$$

where Λ_s is a stable matrix, guarantees global exponential stability of the closed-loop finite-dimensional system.

Remark 7.2: The structure of the closed-loop finite-dimensional system under the controller of Eq.7.15 has the following form:

$$\dot{\tilde{x}}_s = \Lambda_s \tilde{x}_s \tag{7.16}$$

and thus, the response of this system depends only on the stable matrix Λ_s and the initial condition, $x_s(0)$, and is independent of the actuator locations.

Remark 7.3: The requirement $l = m$ is sufficient and not necessary, and it is made to simplify the solution of the controller synthesis problem. Full linearization of the closed-loop finite-dimensional system through coordinate change and nonlinear feedback can be achieved for any number of manipulated inputs (i.e., for any $l \in [1, m]$), provided that an appropriate set of involutivity conditions is satisfied by the corresponding vector fields of the system of Eq.7.12 (see [69] for details).

7.4.2 Computation of optimal location of control actuators

In this subsection, we compute the actuator locations so that the state feedback controller of Eq.7.15 is near-optimal for the full PDE system of Eq.7.11 with respect to a meaningful cost functional which is defined over the infinite time-interval and imposes penalty on the response of the closed-loop system and the control action. To this end, we initially focus on the ODE system of Eq.7.12 and consider the following cost functional:

$$J_s = \int_0^\infty ((\tilde{x}_s^T(x_s(0),t), Q_s\tilde{x}_s(x_s(0),t)) + u^T(\tilde{x}_s(x_s(0),t), z_a)Ru(\tilde{x}_s(x_s(0),t), z_a))dt \tag{7.17}$$

where Q_s and R are positive definite matrices. The cost of Eq.7.17 is well-defined and meaningful since it imposes penalty on the response of the closed-loop finite-dimensional system and the control action. However, a potential problem of this cost is its dependence on the choice of a particular initial condition, $x_s(0)$, and thus, the solution to the optimal placement problem based on this cost may lead to actuator locations that perform very poorly for a large set of initial conditions. To eliminate this dependence and obtain optimality over a broad set of initial conditions, we follow [101] and consider an average cost over a set of m linearly independent initial conditions, $x_s^i(0)$, $i = 1, \ldots, m$, of the following form:

$$\begin{aligned} \hat{J}_s = \frac{1}{m}\sum_{i=1}^{m}\int_0^\infty ((\tilde{x}_s^T(x_s^i(0),t), Q_s\tilde{x}_s(x_s^i(0),t)) \\ +u^T(\tilde{x}_s(x_s^i(0),t), z_a)Ru(\tilde{x}_s(x_s^i(0),t), z_a))dt \end{aligned} \tag{7.18}$$

Referring to the above cost, we first note that the penalty on the response of the closed-loop system:

$$\hat{J}_{xs} = \frac{1}{m}\sum_{i=1}^{m}\int_0^\infty (\tilde{x}_s^T(x_s^i(0),t), Q_s\tilde{x}_s(x_s^i(0),t))dt \tag{7.19}$$

is finite because the solution of the closed-loop system of Eq.7.16 is exponentially stable by appropriate choice of Λ_s. Moreover, $\hat{J}_{xs}$ is independent of the actuator locations (Remark 7.4), and thus, the optimal actuator placement problem reduces to the one of minimizing the following cost which only includes penalty on the control action:

$$\hat{J}_{us} = \frac{1}{m}\sum_{i=1}^{m}\int_0^\infty u^T(\bar{x}_s(x_s^i(0),t),z_a)Ru(\bar{x}_s(x_s^i(0),t),z_a)dt$$

$\hat{J}_{us}$ is a function of multiple variables, $z_a = [z_{a1}\ z_{a2}\ \cdots\ z_{al}]$, and thus, it obtains its local minimum values when its gradient with respect to the actuator locations is equal to zero, i.e.:

$$\frac{\partial \hat{J}_{us}}{\partial z_a} = \left[\frac{\partial \hat{J}_{us}}{\partial z_{a1}}\ \cdots\ \frac{\partial \hat{J}_{us}}{\partial z_{al}}\right]^T = [\,0\ \cdots\ 0\,]^T \tag{7.20}$$

and $\nabla_{z_a z_a}\hat{J}_{us}(z_{am}) > 0$ where $\nabla_{z_a z_a}\hat{J}_{us}$ is the Hessian matrix of $\hat{J}_{us}$ and z_{am} is a solution of the system of nonlinear algebraic equations of Eq.7.20 (which includes l equations with l unknowns). The solution z_{am} for which the above conditions are satisfied and $\hat{J}_{us}$ obtains its smallest value (global minimum) corresponds to the optimal actuator locations for the closed-loop finite-dimensional system. Theorem 7.1 that follows establishes that these locations are near-optimal for the closed-loop infinite-dimensional system (the proof of this theorem can be found in the Appendix).

Theorem 7.1: *Consider the infinite-dimensional system of Eq.7.11 for which Assumption 7.1 holds, and the finite-dimensional system of Eq.7.12, for which Assumption 7.2 holds. Then, there exist positive real numbers μ_1, μ_2 and ϵ^* such that if $|x_s(0)| \leq \mu_1$, $||x_f(0)||_2 \leq \mu_2$, and $\epsilon \in (0, \epsilon^*]$, then the controller of Eq.7.13:*
(a) guarantees exponential stability of the closed-loop infinite-dimensional system, and
(b) the optimal locations of the point actuators obtained for the closed-loop finite-dimensional system are near-optimal for the closed-loop infinite-dimensional system

in the sense that:

$$\hat{J} = \frac{1}{m}\sum_{i=1}^{m}\int_0^{\infty}((x_s^T(x_s^i(0),t),Q_s x_s(x_s^i(0),t)) + (x_f^T(x_s^i(0),t),Q_f x_f(x_f^i(0),t)) + u^T(x_s(x_s^i(0),t),z_a)Ru(x_s(x_s^i(0),t),z_a))dt \longrightarrow \hat{J}_s \quad as \quad \epsilon \longrightarrow 0 \tag{7.21}$$

where Q_f is an unbounded positive definite operator and $\hat{J}$ is the average cost function associated with the controller of Eq.7.15 and the infinite-dimensional system of Eq.7.11.

Remark 7.4: Note that even though the response of the closed-loop finite-dimensional system of Eq.7.16 is independent of the actuator locations, the response of the closed-loop infinite-dimensional system does depend on the actuators locations. However, this dependence is scaled by ϵ, and therefore, it decreases as we increase the number of modes included in the finite-dimensional system used for controller design.

Remark 7.5: In general, the solution to the system of Eq.7.20 can be computed through combination of numerical integration techniques and multivariable Newton's method.

Remark 7.6: The results of this section can be generalized to the case where the finite-dimensional approximation of the system of Eq.7.11 is obtained through combination of Galerkin's method with approximate inertial manifolds [36].

7.5 Integrating nonlinear output feedback control and optimal actuator/sensor placement

The nonlinear controller of Eq.7.15 was derived under the assumption that measurements of the state variables, $\bar{x}(z,t)$, are available at all positions and times. However, from a practical point of view these measurements are available for only a finite

number of positions, and also there are many practical applications where these measurements are not even available (for example, concentrations of certain species in a chemical reactor may not be measured on-line). Motivated by this practical problems, we address in this section: a) the synthesis of nonlinear output feedback controllers that use measurements of the process outputs, y_m, to enforce stability in the closed-loop infinite-dimensional system, and b) the computation of optimal locations of the measurement sensors. Specifically, we consider output feedback control laws of the general form:

$$u(t) = \mathcal{F}(y_m) \tag{7.22}$$

where $\mathcal{F}(y_m)$ is a nonlinear vector function and y_m is the vector of measured outputs. A discussion that explains the choice of static versus dynamic output feedback is given in Remark 7.7. The synthesis of the controller of Eq.7.22 will be achieved by combining the state feedback controller of Eq.7.15 with a procedure proposed in [40] for obtaining estimates for the states of the approximate ODE model of Eq.7.12 from the measurements. To this end, we need to impose the following requirement on the number of measured outputs in order to obtain estimates of the states x_s of the finite-dimensional system of Eq.7.12, from the measurements y_m^κ, $\kappa = 1, \ldots, p$.

Assumption 7.3: *$p = m$ (i.e., the number of measurements is equal to the number of slow modes), and the inverse of the operator S exist, so that $\hat{x}_s = S^{-1} y_m$.*

We note that the requirement that the inverse of the operator S exists can be achieved by appropriate choice of the location of the measurement sensors (i.e., functions $s^\kappa(z)$). The optimal locations for the measurement sensors can be computed by minimizing an average cost function of the estimation error of the closed-loop infinite-

dimensional system of the form:

$$\hat{J}(e) = \frac{1}{m}\sum_{i=1}^{m}\int_0^{\infty}(||x_s(x_s^i(0),t) - \hat{x}_s(x_s^i(0),t)||_2)dt \tag{7.23}$$

where x_s is the slow state of the closed-loop infinite-dimensional system of Eq.7.11, $\hat{x}_s = \mathcal{S}^{-1}y_m$, and $e(t) = ||x_s - \hat{x}_s||_2$ is the estimation error. In contrast to the solution of the optimal location problem for the control actuators, the solution to this optimization problem requires the solution of the closed-loop infinite-dimensional system in order to compute x_s, and $\hat{x}_s$ (from the measurements y_m^κ, $\kappa = 1, 2, \ldots, p$), and thus, it is more computationally demanding.

Theorem 7.2 that follows establishes that the proposed output feedback controller enforces stability in the closed-loop infinite-dimensional system and that the solution to the optimal actuator/sensor problem, which is obtained on the basis of the closed-loop finite-dimensional system, is near-optimal in the sense that it approaches the optimal solution for the infinite-dimensional system as the separation of the slow and fast eigenmodes increases. The proof of this theorem can be found in Appendix D.

Theorem 7.2: *Consider the full system of Eq.7.11 for which Assumption 7.1 hold, and the finite-dimensional system of Eq.7.12, for which Assumption 7.2 and 7.3 hold, under the nonlinear output feedback controller:*

$$\begin{aligned} \hat{x}_s &= \mathcal{S}^{-1}y_m \\ u &= \mathcal{B}_s^{-1}\left((\Lambda_s - \mathcal{A}_s)\hat{x}_s - f_s(\hat{x}_s, 0)\right) \end{aligned} \tag{7.24}$$

Then, there exist positive real numbers μ_1, μ_2 and ϵ^* such that if $|x_s(0)| \leq \mu_1$, $||x_f(0)||_2 \leq \mu_2$, and $\epsilon \in (0, \epsilon^*]$, then the controller of Eq.7.24:

(a) guarantees exponential stability of the closed-loop system, and

(b) the locations of the point actuators and measurement sensors are near-optimal in the sense that the cost function associated with the controller of Eq.7.24 and the

system of Eq.7.11 satisfies:

$$\hat{J} = \frac{1}{m}\sum_{i=1}^{m}\int_0^{\infty}((x_s^T(x_s^i(0),t),Q_s x_s(x_s^i(0),t))+(x_f^T(x_s^i(0),t),Q_f x_f(x_f^i(0),t)) +u^T(x_s(x_s^i(0)),t,z_a)Ru(x_s(x_s^i(0)),t,z_a))dt \longrightarrow \hat{J}_s \quad as \quad \epsilon \longrightarrow 0 \tag{7.25}$$

where $\hat{J}$ and $\hat{J}_s$ are the average cost functions of the infinite-dimensional system of Eq.7.11 and the finite-dimensional system of Eq.7.12, respectively, under the output feedback controller of Eq.7.24.

Remark 7.7: We note that the controller of Eq.7.24 uses static feedback of the measured outputs y_m^{κ}, $\kappa = 1,\ldots,p$, and thus, it feeds back both x_s and x_f (this is in contrast to the state feedback controller of Eq.7.15 which only uses feedback of the slow state x_s). However, even though the use of x_f feedback could lead to destabilization of the stable fast subsystem, the large separation of the slow and fast modes of the spatial differential operator (i.e., assumption that ϵ is sufficiently small) and the fact that the controller does not include terms of the form $O(\frac{1}{\epsilon})$ do not allow such a destabilization to occur.

In the remainder of the manuscript, we show two applications of the proposed approach for optimal actuator/sensor placement to a typical diffusion-reaction process and a non-isothermal tubular reactor with recycle.

7.6 Application to a diffusion-reaction process

7.6.1 Process description - Control problem formulation

Consider a long, thin rod in a reactor (Figure 7.2). The reactor is fed with pure species A and a zeroth order exothermic catalytic reaction of the form $A \rightarrow B$ takes place on the rod. Since the reaction is exothermic, a cooling medium which is in contact with the rod is used for cooling. Under the assumptions of constant density and heat

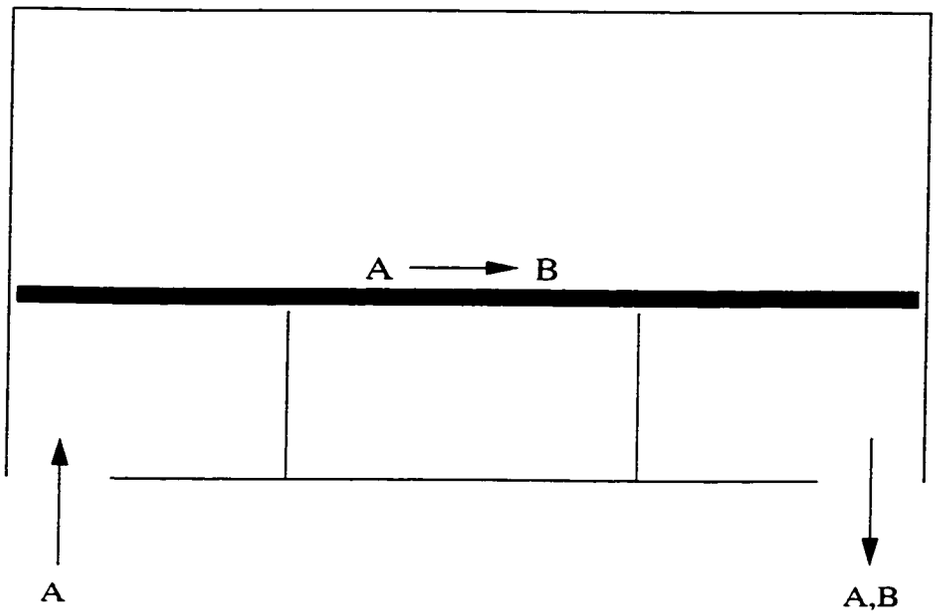

Figure 7.2: Catalytic rod.

capacity of the rod, constant conductivity of the rod, and constant temperature at both ends of the rod, the mathematical model which describes the spatiotemporal evolution of the dimensionless rod temperature consists of the following parabolic PDE:

$$\frac{\partial \bar{x}}{\partial t} = \frac{\partial^2 \bar{x}}{\partial z^2} + \beta_T e^{-\frac{\gamma}{1+\bar{x}}} + \beta_U (b(z)u(t) - \bar{x}) - \beta_T e^{-\gamma} \tag{7.26}$$

subject to the Dirichlet boundary conditions:

$$\bar{x}(0,t) = 0, \quad \bar{x}(\pi,t) = 0 \tag{7.27}$$

and the initial condition:

$$\bar{x}(z,0) = \bar{x}_0(z) \tag{7.28}$$

where $\bar{x}$ denotes the dimensionless temperature in the reactor, β_T denotes a dimensionless heat of reaction, γ denotes a dimensionless activation energy, β_U denotes a dimensionless heat transfer coefficient, and u denotes the manipulated input (temper-

ature of the cooling medium). The following typical values were given to the process parameters:

$$\beta_T = 50.0, \quad \beta_U = 2.0, \quad \gamma = 4.0 \tag{7.29}$$

For the above values, the operating steady state $\bar{x}(z,t) = 0$ is an unstable one (Figure 7.3 shows the profile of evolution of open-loop rod temperature starting from initial

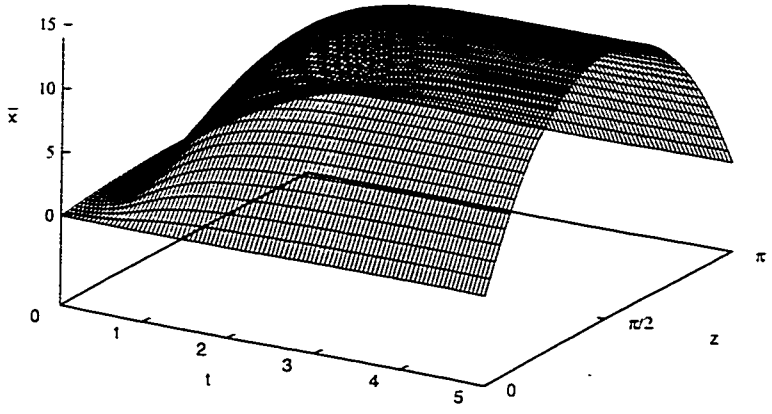

Figure 7.3: Profile of evolution of rod temperature in the open-loop system.

conditions close to the steady state $\bar{x}(z,t) = 0$; the process moves to another stable steady state characterized by a maximum in the temperature profile, *hot-spot*, in the middle of the rod).

A 30-th order Galerkin truncation of the system of Eq.7.26-7.28 was used in our simulations in order to accurately describe the process (further increase on the order of the Galerkin truncation was found to give negligible improvement on the accuracy of the results). The control objective is to stabilize the rod temperature profile at the unstable steady state $\bar{x}(z,t) = 0$. The eigenvalue problem for the spatial differential

operator of the process:

$$\mathcal{A}x = \frac{\partial^2 \bar{x}}{\partial z^2}, \quad x \in D(\mathcal{A}) = \{x \in \mathcal{H}([0,\pi];\mathbb{R});\ \bar{x}(0,t) = 0, \quad \bar{x}(\pi,t) = 0\} \tag{7.30}$$

can be solved analytically and its solution is of the form:

$$\lambda_j = -j^2, \quad \phi_j(z) = \bar{\phi}_j(z) = \sqrt{\frac{2}{\pi}} sin(j\ z), \quad j = 1, \ldots, \infty \tag{7.31}$$

where $\lambda_j, \phi_j, \bar{\phi}_j$, denote the eigenvalues, eigenfunctions and adjoint eigenfunctions of $\mathcal{A}_i$, respectively. In the remainder of this section, we use the proposed method to compute the optimal locations in the case of using two and three control actuators and measurement sensors.

7.6.2 Two actuator/sensor example

Initially, we assume that two point control actuators and measurement sensors are used to stabilize the system. Therefore, following Assumptions 7.2 and 7.3, we use Galerkin's method to derive a second order ODE approximation of the PDE of Eq.7.26 which is used for controller design and optimal actuator/sensor placement. The form of the approximate ODE system is given below:

$$\begin{aligned} \begin{bmatrix} \dot{\tilde{x}}_{s1} \\ \dot{\tilde{x}}_{s2} \end{bmatrix} &= \begin{bmatrix} \lambda_1 - \beta_U & 0 \\ 0 & \lambda_2 - \beta_U \end{bmatrix} \begin{bmatrix} \tilde{x}_{s1} \\ \tilde{x}_{s2} \end{bmatrix} \\ &+\beta_U \begin{bmatrix} \bar{\phi}_1(z_{a1}) & \bar{\phi}_1(z_{a2}) \\ \bar{\phi}_2(z_{a1}) & \bar{\phi}_2(z_{a2}) \end{bmatrix} \begin{bmatrix} u_1 \\ u_2 \end{bmatrix} + \beta_T \begin{bmatrix} f_1(\tilde{x}_s, 0) \\ f_2(\tilde{x}_s, 0) \end{bmatrix} \end{aligned} \tag{7.32}$$

where z_{a1} and z_{a2} are the locations of the two point actuators and the explicit forms of the terms $f_1(\tilde{x}_s, 0)$ and $f_2(\tilde{x}_s, 0)$ are omitted for brevity. The measured output $y_m(t) \in \mathbb{R}^2$ is defined as:

$$\begin{bmatrix} y_{m1} \\ y_{m2} \end{bmatrix} = \begin{bmatrix} x(z_{s1}, t) \\ x(z_{s2}, t) \end{bmatrix} \tag{7.33}$$

where z_{s1} and z_{s2} are the locations of the two point sensors. For the system of Eq.7.32, the nonlinear state feedback controller of Eq.7.15 takes the form:

$$\begin{aligned} u &= B^{-1}(z_a)F(\tilde{x}_s) = \frac{1}{\beta_U}\begin{bmatrix} \bar{\phi}_1(z_{a1}) & \bar{\phi}_1(z_{a2}) \\ \bar{\phi}_2(z_{a1}) & \bar{\phi}_2(z_{a2}) \end{bmatrix}^{-1} \\ &\times \left(\begin{bmatrix} -\alpha - \lambda_1 + \beta_U & 0 \\ 0 & -\beta - \lambda_2 + \beta_U \end{bmatrix} \begin{bmatrix} (\tilde{x}_{s1}, \phi_1) \\ (\tilde{x}_{s2}, \phi_2) \end{bmatrix} + \beta_T \begin{bmatrix} (f_1(\tilde{x}_s, 0), \phi_1) \\ (f_2(\tilde{x}_s, 0), \phi_2) \end{bmatrix} \right) \end{aligned} \tag{7.34}$$

Substituting the above controller into the system of Eq.7.32, we obtain the following closed-loop ODE system:

$$\begin{bmatrix} \dot{\tilde{x}}_{s1} \\ \dot{\tilde{x}}_{s2} \end{bmatrix} = \begin{bmatrix} -\alpha & 0 \\ 0 & -\beta \end{bmatrix} \begin{bmatrix} \tilde{x}_{s1} \\ \tilde{x}_{s2} \end{bmatrix} \tag{7.35}$$

where α and β are positive real numbers. Since the response of the above system depends only on the parameters α, β and the initial condition x_s, and is independent of the actuator locations, we compute the optimal actuator locations by minimizing the following cost functional, which only includes penalty on the control action:

$$\hat{J}_{us} = \frac{1}{2}\sum_{i=1}^{2}\int_0^\infty F^T(\tilde{x}_s(x_s^i(0), t))(B^{-1}(z_a))^T R B^{-1}(z_a) F(\tilde{x}_s(x_s^i(0), t))dt \tag{7.36}$$

Using the following values for the parameters $\alpha = \beta = 1$, $x_s^1(0) = \phi_1$, and $x_s^2(0) = \phi_2$, and taking R, Q_s, Q_f to be unit matrices of appropriate dimensions, the optimal actuator locations were found to be: $z_{a1} = 0.39\pi$ and $z_{a2} = 0.66\pi$.

Finally, we compute the optimal sensor locations by minimizing the following cost functional of the estimation error:

$$\hat{J}(e) = \frac{1}{2}\sum_{i=1}^{2}\int_0^\infty (||x_s(x_s^i(0)) - \hat{x}_s(x_s^i(0))||_2))dt \tag{7.37}$$

where x_s is obtained from the simulation of the full-order closed-loop system of Eq.7.11, and $\hat{x}_s$ is obtained from the measured outputs of the full-order closed-loop

system as shown below:

$$\begin{bmatrix} \hat{x}_{s1} \\ \hat{x}_{s2} \end{bmatrix} = \begin{bmatrix} \phi_1(z_{s1}) & \phi_2(z_{s1}) \\ \phi_1(z_{s2}) & \phi_2(z_{s2}) \end{bmatrix}^{-1} \begin{bmatrix} y_{m1}(z_{s1},t) \\ y_{m2}(z_{s2},t) \end{bmatrix}, \tag{7.38}$$

We found the optimal location of measurement sensors to be: $z_{s1} = 0.31\pi$ and $z_{s2} = 0.72\pi$. Finally, by combining the state feedback controller of Eq.7.34 with the measurements, and the optimal actuator/sensor locations, we derive the following nonlinear output feedback controller:

$$\begin{aligned} \begin{bmatrix} \hat{x}_{s1} \\ \hat{x}_{s2} \end{bmatrix} &= \begin{bmatrix} \phi_1(z_{s1}) & \phi_2(z_{s1}) \\ \phi_1(z_{s2}) & \phi_2(z_{s2}) \end{bmatrix}^{-1} \begin{bmatrix} y_{m1}(z_{s1},t) \\ y_{m2}(z_{s2},t) \end{bmatrix} \\ u &= \frac{1}{\beta_U} \begin{bmatrix} \bar{\phi}_1(z_{a1}) & \bar{\phi}_1(z_{a2}) \\ \bar{\phi}_2(z_{a1}) & \bar{\phi}_2(z_{a2}) \end{bmatrix}^{-1} \left(\begin{bmatrix} -\alpha - \lambda_1 + \beta_U & 0 \\ 0 & -\beta - \lambda_2 + \beta_U \end{bmatrix} \right. \\ &\quad \left. \times \begin{bmatrix} (\hat{x}_{s1}, \phi_1) \\ (\hat{x}_{s2}, \phi_2) \end{bmatrix} + \beta_T \begin{bmatrix} (f_1(\hat{x}_s, 0), \phi_1) \\ (f_2(\hat{x}_s, 0), \phi_2) \end{bmatrix} \right) \end{aligned} \tag{7.39}$$

We performed several simulation runs to evaluate the performance of the proposed method for computing optimal locations of control actuators and measurement sensors. We initially apply the state feedback controller of Eq.7.34 to the 30-th order Galerkin truncation of the system of Eq.7.26-7.28 and investigate the influence of the different actuator locations on the various cost functions. Table 7.1 shows the values

Table 7.1: Results for two control actuators.

Case	Actuator Locations	$\hat{J}_u$	$\hat{J}_x$	$\hat{J}$
Optimal	$.39\pi, .66\pi$	.8075	.5332	1.3407
Linearized	$.32\pi, .68\pi$	.8980	.5414	1.4416
3	$.20\pi, .80\pi$	5.2109	1.7957	7.0066
4	$.30\pi, .70\pi$	.9065	.5608	1.5473

of the costs $\hat{J}_u$, $\hat{J}_x$, and $\hat{J}$ of the full-order closed-loop system under the state feedback controller of Eq.7.34, in the case of optimal actuator placement, and for the sake of

comparison, the values of these costs in the case of alternative actuator placements including optimal actuator placement based on the linearized system (second line). The cost for the control action used to stabilize the system at $\bar{x}(z,t) = 0$ when the actuators are optimally placed, is clearly smaller than the case of actuator placement based on the linearized system (by 10.1%), case 3 (by 84.5%), and case 4 (by 10.3%). Figures 7.4 and 7.5 show the norm of the control action, $||u||$, for $x(0) = \phi_1$ (Figure 7.4) and $x(0) = \phi_2$ (Figure 7.5), for the optimal case (solid line), the linearized case (long-dashed line), case 3 (short-dashed line), and case 4 (dotted line). Clearly, the control action used for stabilization in the case of optimal actuator placement is smaller than all the other cases.

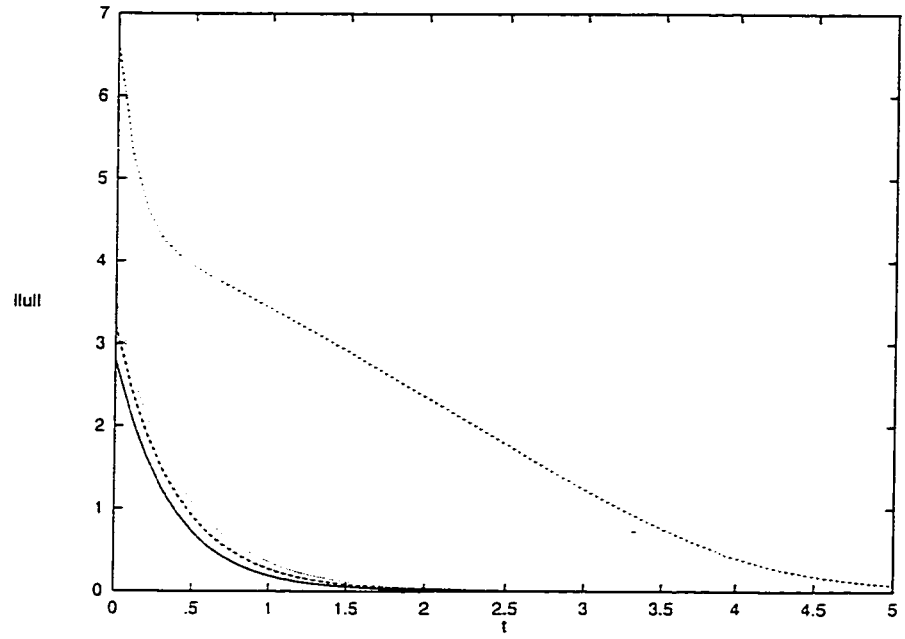

Figure 7.4: Closed-loop norm of the control effort, $||u||$, for the two actuator/sensor example, for $x_s(0) = \phi_1$, for the optimal case (solid line), the linearized case (long-dashed line), case 3 (short-dashed line), and case 4 (dotted line).

We also tested the proposed optimal sensor locations $z_{s1} = 0.31\pi$ and $z_{s2} = 0.72\pi$. To this end, we implement the nonlinear output feedback controller of Eq.7.39 on the

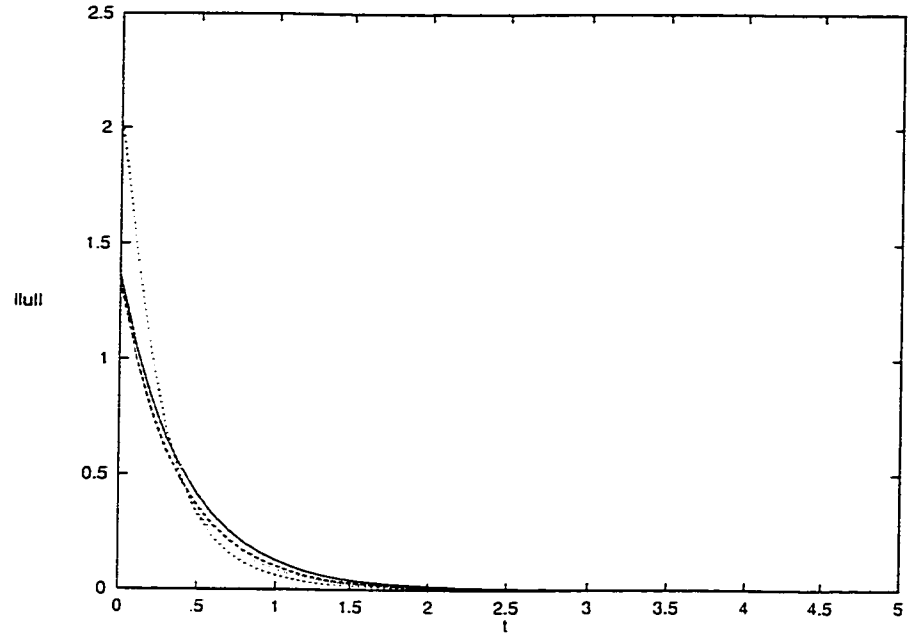

Figure 7.5: Closed-loop norm of the control effort, $||u||$, for the two actuator/sensor example, for $x_s(0) = \phi_2$, for the optimal case (solid line), the linearized case (long-dashed line), case 3 (short-dashed line), and case 4 (dotted line).

30-th order Galerkin truncation of the system of Eq.7.26-7.28 with actuator locations $z_{a1} = 0.39\pi$ and $z_{a2} = 0.66\pi$ and different sensor locations. Table 7.2 shows the

Table 7.2: Results for two control actuators and measurement sensors.

Case	Sensor locations	$\hat{J}(e)$	$\hat{J}_u$	$\hat{J}_x$	$\hat{J}$
Optimal	$.31\pi, .72\pi$	5.947e-4	.7998	.5150	1.3149
2	$.48\pi, .71\pi$	1.613e-3	.8384	.5720	1.4104
3	$.31\pi, .49\pi$	3.604e-3	.8579	.5963	1.4542

values of the costs $\hat{J}(e), \hat{J}_u, \hat{J}_x$, and $\hat{J}$ of the full-order closed-loop system under the output feedback controller of Eq.7.39, in the case of optimal sensor placement, and for the sake of comparison, the values of these costs in the case of two other sensor locations. The estimation error of the sensor locations of $z_{s1} = .31\pi$ and $z_{s2} = .72\pi$ computed by the proposed approach is clearly smaller than the other two cases. In

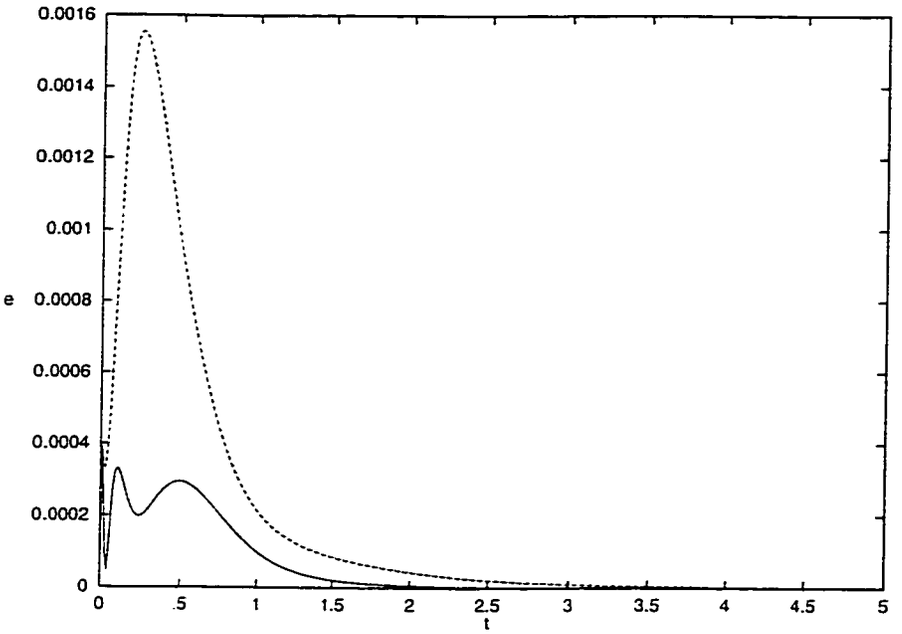

Figure 7.6: Closed-loop norm of the estimation error $||e||$ versus time, for the two actuator/sensor example, and for the optimal actuator/sensor locations, for $x_s(0) = \phi_1$ (solid line) and $x_s(0) = \phi_2$ (dashed line).

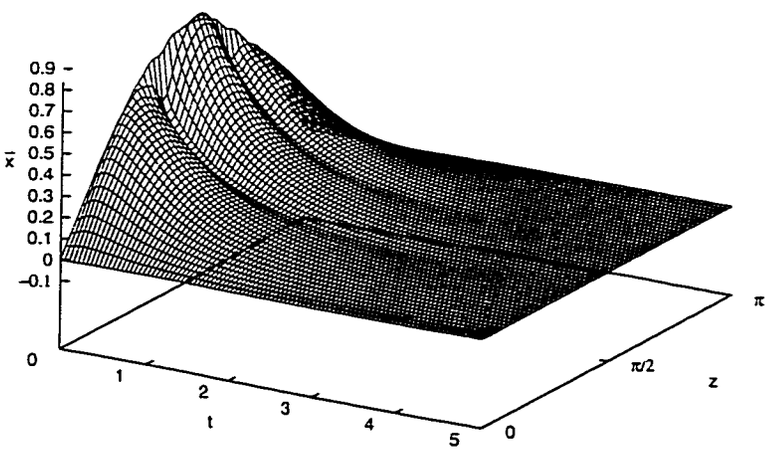

Figure 7.7: Profile of evolution of the temperature of the rod, for the two actuator/sensor example, under output feedback control, for the optimal actuator/sensor locations, for $x_s(0) = \phi_1$.

Figure 7.6, we display the closed-loop norm of the estimation error versus time, for the optimal actuator/sensor locations, for $x_s(0) = \phi_1$ (solid line) and $x_s(0) = \phi_2$ (dashed line). We can see that for both initial conditions the estimation error is very small. Finally, Figures 7.7 and 7.8 show the profiles of the evolution of the temperature of

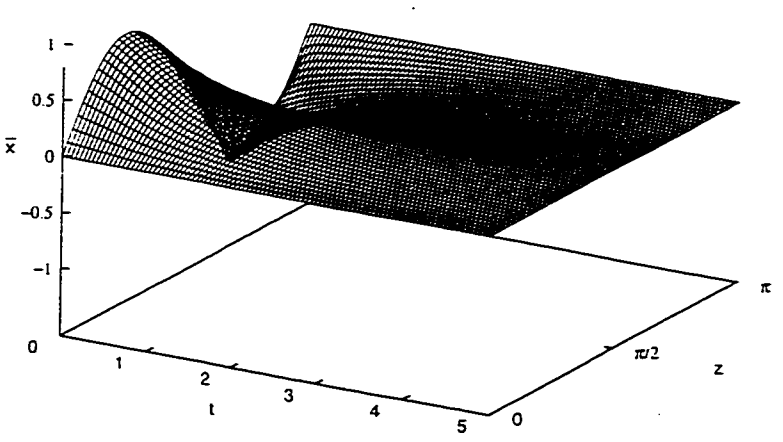

Figure 7.8: Profile of evolution of the temperature of the rod, for the two actuator/sensor example, under output feedback control, for the optimal actuator/sensor locations, for $x_s(0) = \phi_2$.

the rod, under output feedback control, for the optimal actuator/sensor locations, for $x_s(0) = \phi_1$ (Figure 7.7), and for $x_s(0) = \phi_2$ (Figure 7.8). We can see that the proposed controller with optimal actuator/sensor locations, stabilizes the system to the spatially uniform operating steady state very quickly, for both cases.

7.6.3 Three actuator/sensor example

In the second set of the simulation runs, we assume that three control actuators and measurement sensors are available for stabilization. Following Assumption 7.2, we use Galerkin's method to derive a third-order approximation of the PDE system which

is used for controller design and optimal actuator/sensor placement. To reduce the space of the paper, we proceed with the presentation of the results.

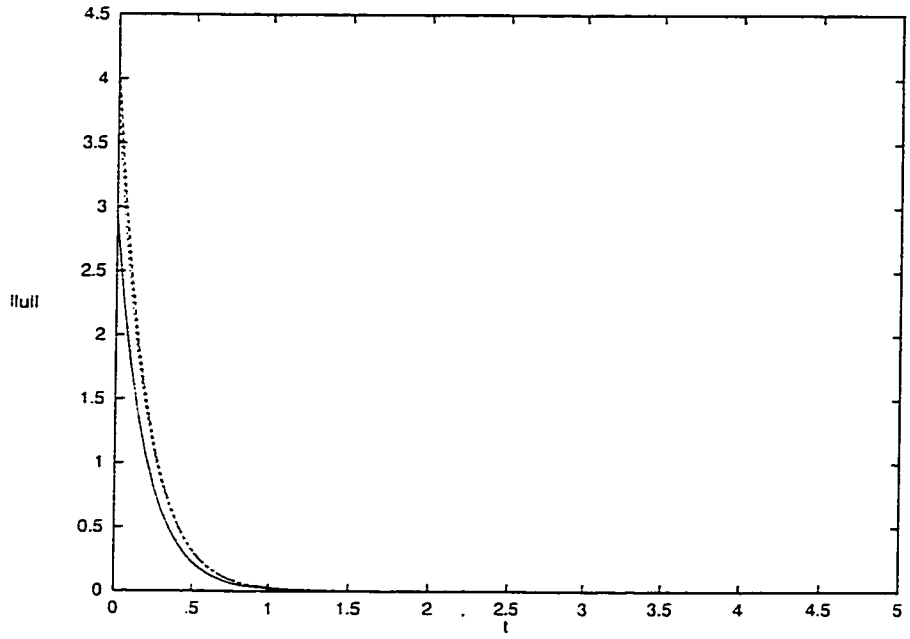

Figure 7.9: Closed-loop norm of the control effort, $||u||$, for the three actuator/sensor example, for $x_s(0) = \phi_1$, for the optimal case (solid line), the case 2 (long-dashed line), case 3 (short-dashed line), and case 4 (dotted line).

Initially, we synthesized and implemented a state feedback controller on the 30-th order Galerkin truncation of the system of Eq.7.26-7.28 in order to compute the optimal actuator locations. Table 7.3 shows the values of the costs $\hat{J}_u$, $\hat{J}_x$, and $\hat{J}$ of

Table 7.3: Results for three control actuators.

Case	Actuator Locations	$\hat{J}_u$	$\hat{J}_x$	$\hat{J}$
Optimal	$.17\pi, .50\pi, .81\pi$	1.365	.506	1.871
2	$.10\pi, .50\pi, .90\pi$	2.034	.557	2.591
3	$.20\pi, .60\pi, .90\pi$	4.072	.804	4.876

the full-order closed-loop system under state feedback control, in the case of optimal actuator placement, and for the sake of comparison, the values of these costs in the

case of alternative actuator placements. Clearly, in the case of optimal actuator placement at $z_{a1} = .17\pi$, $z_{a2} = .50\pi$, and $z_{a3} = .81\pi$, the cost of the control action used to stabilize the system at $\bar{x}(z,t) = 0$ is smaller than case 2 (by 32.9%), and case 3 (by 66.5%). Figures 7.9, 7.10, and 7.11 show the norm of the control action, $||u||$,

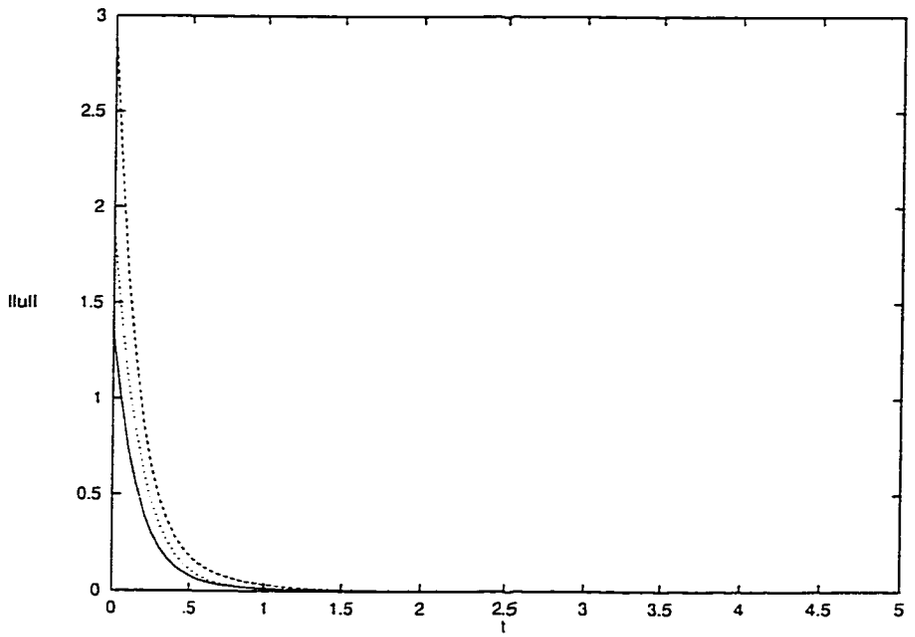

Figure 7.10: Closed-loop norm of the control effort, $||u||$, for the three actuator/sensor example, for $x_s(0) = \phi_2$, for the optimal case (solid line), the case 2 (long-dashed line), case 3 (short-dashed line), and case 4 (dotted line).

for $x(0) = \phi_1$ (Figure 7.9), $x(0) = \phi_2$ (Figure 7.10), and $x(0) = \phi_3$ (Figure 7.11), for the optimal case (solid line), case 2 (long-dashed line), and case 3 (short-dashed line). In the case of optimal actuator placement, the control action spent is smaller.

Subsequently, we synthesized and implemented a nonlinear output feedback controller on the 30-th order Galerkin truncation of the system of Eq.7.26-7.28 with actuator locations $z_{a1} = 0.17\pi$, $z_{a2} = 0.50\pi$ and $z_{a3} = 0.81\pi$ and computed the optimal sensor locations. Table 7.4 shows the values of the costs $\hat{J}(e), \hat{J}_u, \hat{J}_x$, and $\hat{J}$ of the full-order closed-loop system under output feedback control, in the case of opti-

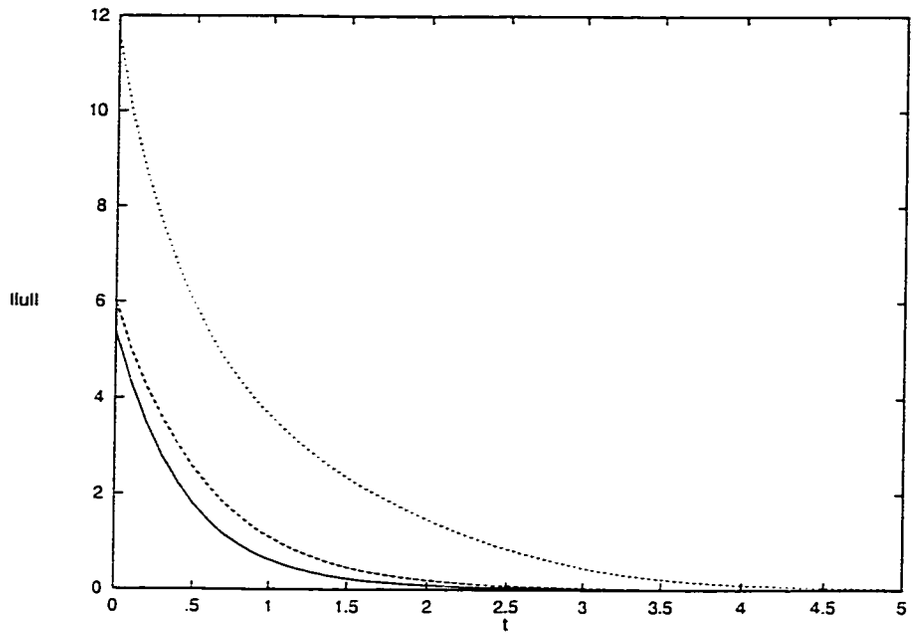

Figure 7.11: Closed-loop norm of the control effort, $||u||$, for the three actuator/sensor example, for $x_s(0) = \phi_3$, for the optimal case (solid line), the case 2 (long-dashed line), and case 3 (short-dashed line).

mal sensor placement, and for the sake of comparison, the values of these costs in the case of two other sensor locations. The estimation error of the proposed sensor

Table 7.4: Results for three control actuators and measurement sensors.

Case	Location of sensors	$\hat{J}(e)$	$\hat{J}_u$	$\hat{J}_x$	$\hat{J}$
Optimal	$.13\pi, .40\pi, .73\pi$	3.590e-6	1.532	.421	1.953
2	$.13\pi, .43\pi, .74\pi$	4.730e-6	1.552	.431	1.983
3	$.13\pi, .42\pi, .72\pi$	7.435e-6	1.588	.446	2.043

locations at $.13\pi$, $.40\pi$, and 73π, is clearly smaller than the other two cases. Figure 7.12 shows the closed-loop norm of the estimation error versus time, for the optimal actuator/sensor locations, for $x_s(0) = \phi_1$ (solid line), for $x_s(0) = \phi_2$ (dashed line), and for $x_s(0) = \phi_3$ (dotted line). We can see that for all three initial conditions the estimation error is very small. Finally, Figures 7.13, 7.14, and 7.15 display the

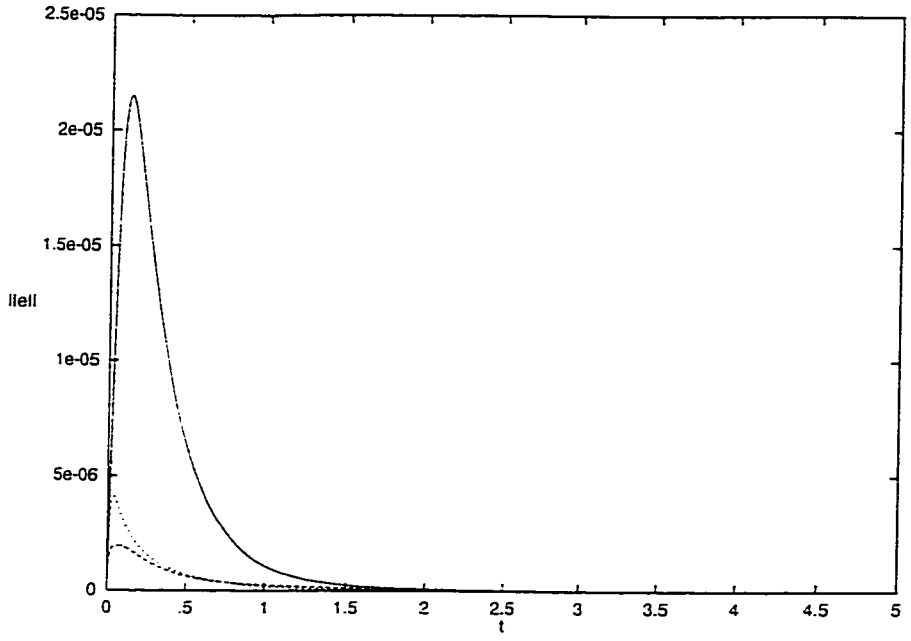

Figure 7.12: Closed-loop norm of the estimation error $||e||$ versus time, for the three actuator/sensor example, and for the optimal actuator/sensor locations, for $x_s(0) = \phi_1$ (solid line), $x_s(0) = \phi_1$ (long-dashed line) and $x_s(0) = \phi_3$ (short-dashed line).

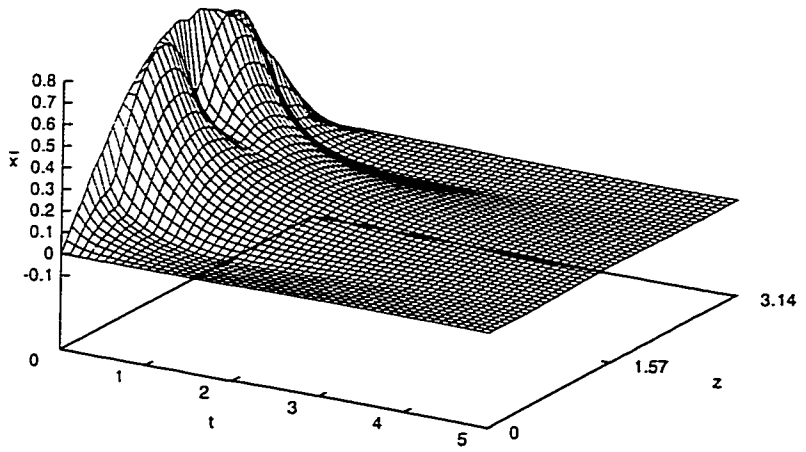

Figure 7.13: Profile of evolution of the temperature of the rod, for the three actuator/sensor example, under output feedback control, for the optimal actuator/sensor locations, for $x_s(0) = \phi_1$.

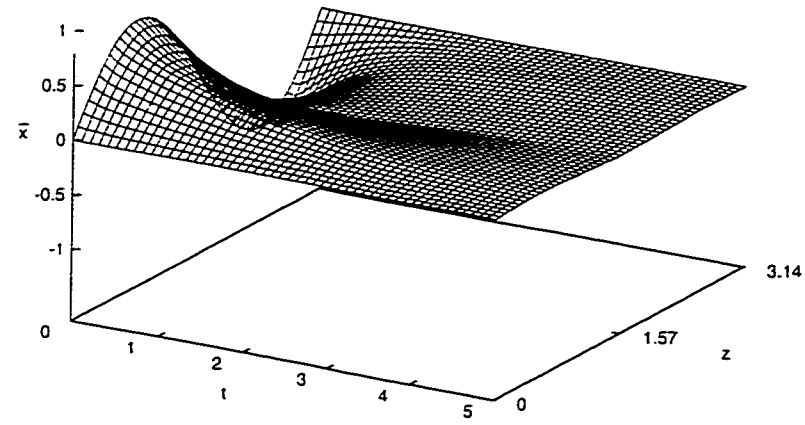

Figure 7.14: Profile of evolution of the temperature of the rod, for the three actuator/sensor example, under output feedback control, for the optimal actuator/sensor locations, for $x_s(0) = \phi_2$.

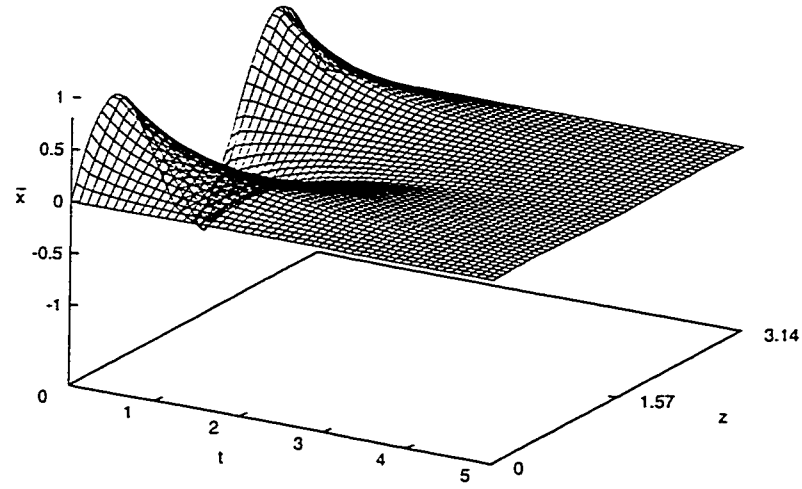

Figure 7.15: Profile of evolution of the temperature of the rod, for the three actuator/sensor example, under output feedback control, for the optimal actuator/sensor locations, for $x_s(0) = \phi_3$.

profiles of the evolution of the temperature of the rod, under output feedback control, for the optimal actuator/sensor locations, for $x_s(0) = \phi_1$ (Figure 7.13), for $x_s(0) = \phi_2$ (Figure 7.14), and for $x_s(0) = \phi_3$ (Figure 7.15). We can see that the proposed controller with optimal actuator/sensor locations, stabilizes the system to the spatially uniform operating steady state very quickly, for all three cases.

7.7 Application to a non-isothermal tubular reactor with recycle

We again consider the non-isothermal tubular reactor shown previously in Figure 5.1, where an irreversible first-order reaction of the form $A \rightarrow B$ takes place. The reaction is exothermic and a cooling jacket is used to remove heat from the reactor. The outlet of the reactor is fed to a separator where the unreacted species A is separated from the product B. The unreacted amount of species A is then fed back to the reactor through a recycle loop. Under standard modeling assumptions, the dynamic model of the process can be derived from mass and energy balances and takes the following dimensionless form:

$$\begin{aligned}
\frac{\partial \bar{x}_1}{\partial t} &= -\frac{\partial \bar{x}_1}{\partial z} + \frac{1}{Pe_T}\frac{\partial^2 \bar{x}_1}{\partial z^2} + B_T B_C exp^{\frac{\gamma \bar{x}_1}{1+\bar{x}_1}}(1+\bar{x}_2) + \beta_T(b(z)u(t) - \bar{x}_1) \\
\frac{\partial \bar{x}_2}{\partial t} &= -\frac{\partial \bar{x}_2}{\partial z} + \frac{1}{Pe_C}\frac{\partial^2 \bar{x}_2}{\partial z^2} - B_C exp^{\frac{\gamma \bar{x}_1}{1+\bar{x}_1}}(1+\bar{x}_2)
\end{aligned} \tag{7.40}$$

subject to the boundary conditions:

$$\begin{aligned}
\frac{\partial \bar{x}_1(0,t)}{\partial z} &= Pe_T(\bar{x}_1(0,t) - (1-r)\bar{x}_{1f}(t) - r\bar{x}_1(1,t)) , \\
\frac{\partial \bar{x}_2(0,t)}{\partial z} &= Pe_C(\bar{x}_2(0,t) - (1-r)\bar{x}_{2f}(t) - r\bar{x}_2(1,t)) ; \\
\frac{\partial \bar{x}_1(1,t)}{\partial z} &= 0 , \qquad \frac{\partial \bar{x}_2(1,t)}{\partial z} = 0
\end{aligned} \tag{7.41}$$

where $\bar{x}_1$ and $\bar{x}_2$ denote dimensionless temperature and concentration of species A in the reactor, respectively, $\bar{x}_{1f}$ and $\bar{x}_{2f}$ denote dimensionless inlet temperature and inlet concentration of species A in the reactor, respectively, Pe_T and Pe_C are the heat and thermal Peclet numbers, respectively, B_T and B_C denote a dimensionless heat of reaction and a dimensionless pre-exponential factor, respectively, r is the recirculation coefficient (it varies from zero to one, with one corresponding to total recycle and zero fresh feed and zero corresponding to no recycle), γ is a dimensionless activation energy, β_T is a dimensionless heat transfer coefficient, u is a dimensionless jacket temperature (chosen to be the manipulated input), and $b(z)$ is the actuator distribution function. Note here that for the purposes of this analysis, we will assume that there is no recycle loop dead time.

In order to transform the boundary condition of Eq.7.41 to a homogeneous one, we insert the non-homogeneous part of the boundary condition into the differential equation and obtain the following PDE representation of the process:

$$\begin{aligned}
\frac{\partial \bar{x}_1}{\partial t} &= -\frac{\partial \bar{x}_1}{\partial z} + \frac{1}{Pe_T}\frac{\partial^2 \bar{x}_1}{\partial z^2} + B_T B_C exp^{\frac{\gamma \bar{x}_1}{1+\bar{x}_1}}(1+\bar{x}_2) + \beta_T(b(z)u(t) - \bar{x}_1) \\
&\quad +\delta(z-0)((1-r)\bar{x}_{1f} + r\bar{x}_1(1,t)) \\
\frac{\partial \bar{x}_2}{\partial t} &= -\frac{\partial \bar{x}_2}{\partial z} + \frac{1}{Pe_C}\frac{\partial^2 \bar{x}_2}{\partial z^2} - B_C exp^{\frac{\gamma \bar{x}_1}{1+\bar{x}_1}}(1+\bar{x}_2) \\
&\quad +\delta(z-0)((1-r)\bar{x}_{2f} + r\bar{x}_2(1,t))
\end{aligned} \tag{7.42}$$

where $\delta(\cdot)$ is the standard Dirac function, subject to the homogeneous boundary conditions:

$$\begin{aligned}
\frac{\partial \bar{x}_1(0,t)}{\partial z} &= Pe_T \bar{x}_1(0,t)\,, \qquad \frac{\partial \bar{x}_2(0,t)}{\partial z} = Pe_C \bar{x}_2(0,t)\,; \\
\frac{\partial \bar{x}_1(1,t)}{\partial z} &= 0\,, \qquad \frac{\partial \bar{x}_2(1,t)}{\partial z} = 0
\end{aligned} \tag{7.43}$$

The following values for the process parameters were used in our calculations:

$$Pe_T = 7.0, \quad Pe_C = 7.0, \quad B_C = 0.1, \quad B_T = 2.5, \quad \beta_T = 2.0, \quad \gamma = 10.0, \quad r = 0.5 \tag{7.44}$$

For the above values, the operating steady-state of the open-loop system is unstable (the linearization around the steady-state possesses one real unstable eigenvalue, $\mu = 0.0328$, and infinitely many stable eigenvalues), thereby implying the need to operate the process under feedback control. We note that in the absence of recycle-loop (i.e., $r = 0$), the above process parameters correspond to a stable steady-state for the open-loop system.

The spatial differential operator of the system of Eq.7.42 is of the form:

$$\mathcal{A}\bar{x} = \begin{bmatrix} \mathcal{A}_1\bar{x}_1 & 0 \\ 0 & \mathcal{A}_2\bar{x}_2 \end{bmatrix} = \begin{bmatrix} \frac{1}{Pe_T}\frac{\partial^2\bar{x}_1}{\partial z^2} - \frac{\partial\bar{x}_1}{\partial z} & 0 \\ 0 & \frac{1}{Pe_C}\frac{\partial^2\bar{x}_2}{\partial z^2} - \frac{\partial\bar{x}_2}{\partial z} \end{bmatrix} \tag{7.45}$$

The solution of the eigenvalue problem for $\mathcal{A}_i$ can be obtained by utilizing standard techniques from linear operator theory (see, for example, [122]) and is of the form:

$$\begin{aligned} \lambda_{ij} &= \frac{\bar{a}_{ij}^2}{Pe} + \frac{Pe}{4}, \quad i = 1,2, \quad j = 1,\ldots,\infty \\ \phi_{ij}(z) &= B_{ij}e^{Pe\frac{z}{2}}\left(cos(\bar{a}_{ij}z) + \frac{Pe}{2\bar{a}_{ij}}sin(\bar{a}_{ij}z)\right), \quad i = 1,2, \quad j = 1,\ldots,\infty \\ \bar{\phi}_{ij}(z) &= e^{-Pez}\phi_{ij}(z), \quad i = 1,2, \quad j = 1,\ldots,\infty \end{aligned} \tag{7.46}$$

where $Pe = Pe_T = Pe_C$, and $\lambda_{ij}, \phi_{ij}, \bar{\phi}_{ij}$, denote the eigenvalues, eigenfunctions and adjoint eigenfunctions of $\mathcal{A}_i$, respectively. $\bar{a}_{ij}$, B_{ij} can be calculated from the following formulas:

$$tan(\bar{a}_{ij}) = \frac{Pe\bar{a}_{ij}}{\bar{a}_{ij}^2 - \left(\frac{Pe}{2}\right)^2}, \quad i = 1,2, \quad j = 1,\ldots,\infty$$

$$B_{ij} = \left\{ \int_0^1 \left(cos(\bar{a}_{ij}z) + \frac{Pe}{2\bar{a}_{ij}} sin(\bar{a}_{ij}z) \right)^2 dz \right\}^{-\frac{1}{2}}, \quad i = 1, 2, \quad j = 1, \ldots, \infty \tag{7.47}$$

A 400-th order Galerkin truncation of the system of Eq.7.42-7.44 was used in our simulations in order to accurately describe the process (further increase on the order of the Galerkin truncation was found to give negligible improvement on the accuracy of the results). Figure 7.16 shows the open-loop profile of $\bar{x}_1$ along the length of the

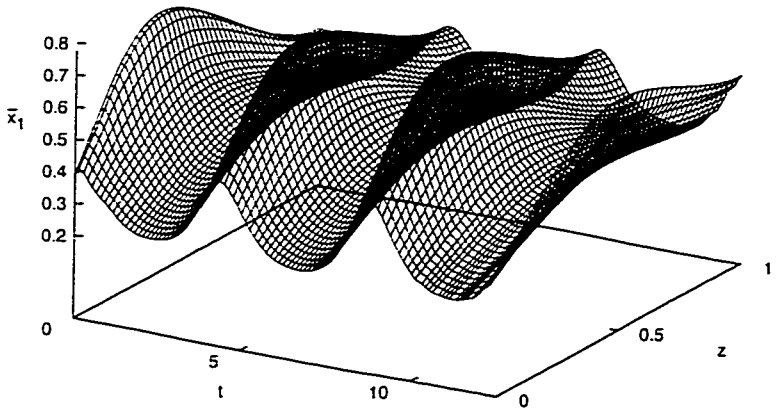

Figure 7.16: Spatiotemporal evolution of $\bar{x}_1$ in the open-loop system.

reactor, which corresponds to the operating unstable steady-state. Therefore, the control problem is to manipulate the wall temperature, $u(t)$, in order to stabilize the reactor at the desired operating steady-state, and the control output was defined as $y_c(t) = \int_0^1 e^{-Pez} \phi_{11}(z) x_{11} dz$. The process was initially ($t = 0$) assumed to be at the unstable steady state, and the desired reference input value was set at $v = 0.12$.

Based on simulations of the open-loop process dynamics, we take as the slow modes

of the process the first eight temperature modes plus the first thirty concentration modes and use Galerkin's method to derive a 38th-order ODE system employed for controller synthesis. We use one point control actuator to stabilize the system (note that this is possible since the assumption $m = l$ is sufficient and not necessary; see also discussion in Remark 7.3), and the actuator distribution function was taken to be $b(z) = \delta(z - z_{act})$ (one point control actuator placed at $z = z_{act}$). Since it is not feasible in practice to measure the concentration of species A in the reactor at 30 spatial positions, we use eight point temperature sensors to obtain estimates of the first eight modes of the reactor temperature (i.e., the measurement sensor shape function takes the form $s(z) = [\delta(z - z_{s1}) \quad \delta(z - z_{s2}) \quad \dots \quad \delta(z - z_{s8})]^T$) and design a nonlinear Luenberger-type state observer consisting of 30 ordinary differential equations to obtain estimates of the first 30 concentration modes from the temperature measurements (see, for example, [35] for details on how such an observer can be designed).

Since the process is initially ($t = 0$) assumed to be at the unstable steady state, we will compute the optimal location of control actuator and measurement sensors with respect to this initial condition. Furthermore, since the reference input value is set at $v = 0.12$, we define the costs J, J_x, and J_u as follows:

$$\begin{aligned} J = J_x + J_u &= \int_0^\infty ((x_s - x_{sf})^T Q_s (x_s - x_{sf}) + (x_f - x_{ff})^T Q_f (x_f - x_{ff}))dt \\ &\quad + \int_0^\infty (u - u_f)^T R (u - u_f) dt \end{aligned} \tag{7.48}$$

where x_{sf}, x_{ff}, and u_f are the values of x_s, x_f, and u, respectively, at the desired operating steady state, to ensure that the costs become zero when the process is stabilized at the steady state. Table 7.5 shows the values of the costs J_u, J_x, and J for state feedback control, in the case of optimal actuator placement, and for the sake of comparison, the values of these costs in the case of alternative actuator placement.

Table 7.5: Results for different actuator location.

Case	Actuator Location	$J_u(10^{-5})$	$J_x(10^{-5})$	$J(10^{-5})$
Optimal	0	9.647	36.536	46.183
2	.1	21.540	36.536	58.076
3	.2	60.062	36.536	96.598
4	.3	229.42	36.536	265.95
5	.4	1,672.8	36.536	1,709.3

Figure 7.17 show the control action u, for the optimal case (solid line), case 2 (long-dashed line), case 3 (short-dashed line), case 4 (dotted line), and case 5 (dashed-dotted line). Clearly, the control action spent to stabilize the system at the desired operating profile in the case of optimal actuator placement at $z_{act} = 0$, is significantly less than the other four cases.

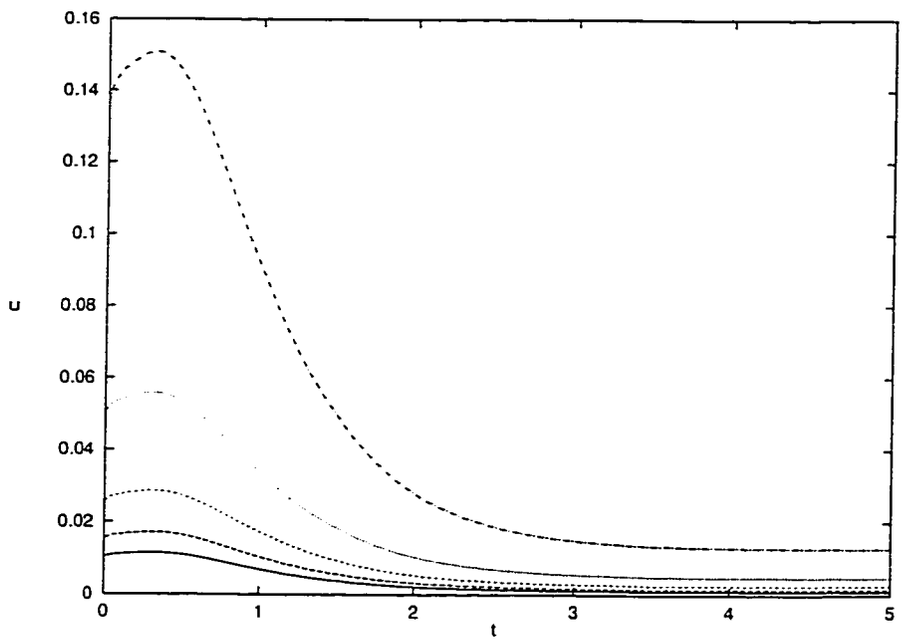

Figure 7.17: Closed-loop control effort, u, for the optimal actuator location at $z_{act} = 0$ (solid line), for the actuator location at $z_{act} = .1$ (long-dashed line), at $z_{act} = .2$ (short-dashed line), at $z_{act} = .3$ (dotted line), and at $z_{act} = .4$ (dashed-dotted line).

We now proceed with the output feedback implementation of the state feedback

controller. To this end, we pick the sensors locations so that the resulting output feedback controller guarantees stability of the closed-loop system and the estimation error in the closed-loop system is very small. Table 7.6 shows values of the costs J_u, J_x,

Table 7.6: Results for different sensor locations.

Case	Sensor Locations	$J_u(10^{-5})$	$J_x(10^{-5})$	$J(10^{-5})$
1	.05, .15, .30, .45, .55, .70, .85, .95	10.280	39.717	49.997
2	.07, .20, .32, .44, .56, .68, .80, .93	10.029	38.099	48.128
3	.05, .20, .35, .45, .55, .65, .80, .95	10.096	39.011	49.107
4	.06, .18, .31, .43, .56, .68, .81, .93	9.748	36.446	46.194

and J for four different sensor locations. Figures 7.18 and 7.19 show the profile of the control action u, and the final steady-state profile of $\bar{x}_1$, for case 1 (solid line), case 2 (long-dashed line), case 3 (short-dashed line), and case 4 (dotted line). Clearly, in all

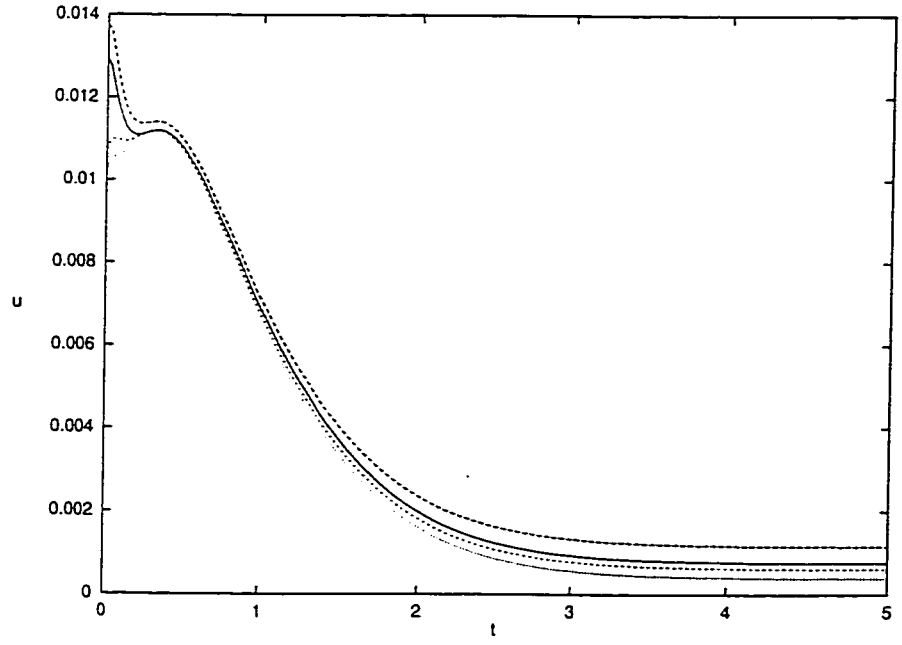

Figure 7.18: Profile of the closed-loop control effort, u, for four different sensor locations; case 1 (solid line), case 2 (long-dashed line), case 3 (short-dashed line), and case 4 (dotted line).

these cases, the stabilization of the unstable steady state is achieved with comparable

cost, thereby indicating 8 temperature sensors distributed appropriately along the length of the reactor suffice to obtain a stabilizing controller. To demonstrate the

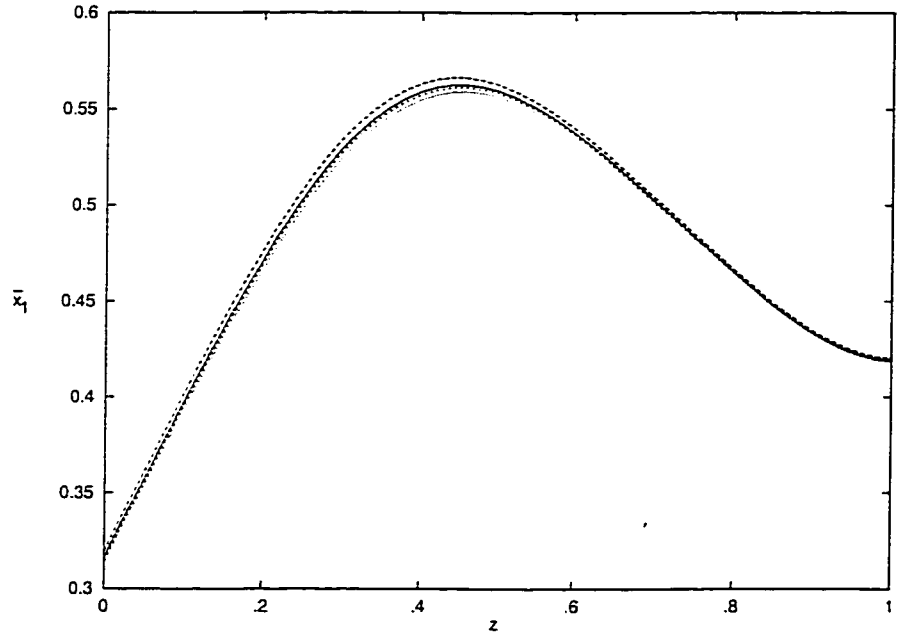

Figure 7.19: Final steady-state profile of $\bar{x}_1$, for four different sensor locations; case 1 (solid line), case 2 (long-dashed line), case 3 (short-dashed line), and case 4 (dotted line).

performance of the controller, Figure 7.20 shows the evolution of the closed-loop reactor temperature for the optimal actuator locations and for the sensor location of case 1. The controller stabilizes the process very close to the desired operating profile.

Remark 7.8: Referring to the above examples, we note that the optimal sensor locations depend significantly on the choice of boundary conditions and the location of the control actuators. When the process states at the boundaries are fixed at a constant value (Dirichlet-type boundary conditions), the sensors are placed away from the boundaries since we cannot gain much information about the system behavior by placing the sensors close to the boundaries. On the other hand, if the boundary

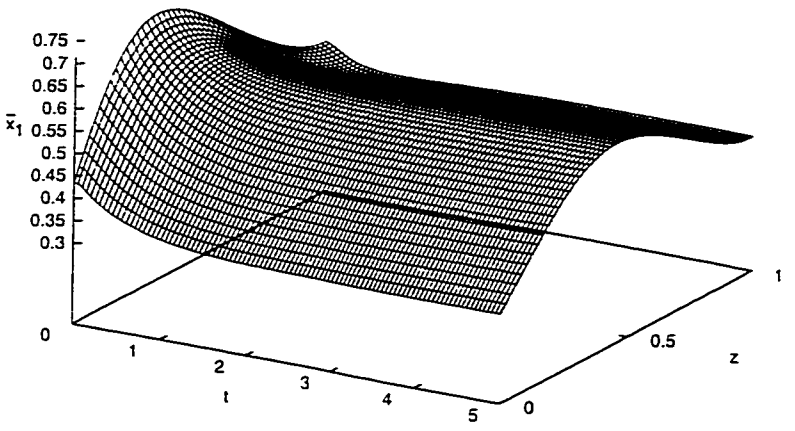

Figure 7.20: Spatiotemporal evolution of $\bar{x}_1$ under the nonlinear output feedback controller with the optimally placed actuator, and the configuration for the sensors locations of case 1.

conditions are of mixed type (Robin-type boundary conditions), the states of the system close to the boundaries constantly change with time, and thus, measurements close to the boundaries provide more information about the dynamics of the system. In addition, the sensors should be placed away from the actuator locations in order to obtain more information about the dynamics of the system, since on and near the control actuators the state of the system is affected more by the dynamics of the controller and less by the natural dynamics of the process.

7.8 Conclusions

In this chapter, we proposed a general and practical methodology for the integration of nonlinear output feedback control with optimal placement of control actuators and measurement sensors for transport-reaction processes described by a broad class of

quasi-linear parabolic PDEs. Given a class of stabilizing nonlinear state feedback controllers which were derived on the basis of finite-dimensional approximations of the PDE, the optimal actuator location problem was formulated as the one of minimizing a meaningful cost functional that includes penalty on the response of the closed-loop system and the control action and was solved by using standard unconstrained optimization techniques. Then, under the assumption that the number of measurement sensors is equal to the number of slow modes, estimates for the states of the approximate finite-dimensional model from the measurements were computed and used to derive nonlinear output feedback controllers. The optimal location of the measurement sensors was computed by minimizing a cost function of the estimation error in the closed-loop infinite-dimensional system. It was rigorously established that the proposed output feedback controllers enforce stability in the closed-loop infinite-dimensional system and that the solution to the optimal actuator/sensor problem, which is obtained on the basis of the closed-loop finite-dimensional system, is near-optimal in the sense that it approaches the optimal solution for the infinite-dimensional system as the separation of the slow and fast eigenmodes increases. The proposed methodology was successfully applied to a diffusion-reaction process and a non-isothermal tubular reactor with recycle to derive nonlinear output feedback controllers and compute optimal actuator/sensor locations for stabilization of unstable steady-states.

Chapter 8

Conclusions

The present doctoral thesis has focused on the development of a general and practical framework, for the synthesis of nonlinear control systems for nonlinear differential difference equation systems that systematically addresses the problems of modification of the input/output behavior, elimination of measurable disturbances, and attenuation of unmeasured disturbances and unknown parameters. The proposed control algorithms were applied to industrially important chemical processes. Specifically, the main contributions of this dissertation can be summarized as follows:

1. **Control of nonlinear DDE systems.** A methodology was developed for the synthesis of nonlinear output feedback controllers that enforce stability and output tracking in the closed-loop system, independently of the size of the state delays. The method is based on novel integration of geometric, Lyapunov and spectral decomposition techniques.

2. **Control of nonlinear DDE systems with uncertainty.** Utilizing a combination of geometric control concepts and Lyapunov's direct method, a methodology was developed for the synthesis of robust nonlinear controllers that guarantees boundedness of the state and achieves asymptotic output tracking with arbi-

trary degree of asymptotic attenuation of the effect of uncertain variables on the output of the closed-loop system, independently of the size of the state delays.

3. **Control of nonlinear PDDE systems.** An approach was proposed for nonlinear control of quasi-linear parabolic partial differential difference equation systems whose dynamics can be separated into slow and fast ones. Taking advantage of the low-dimensional nature of the dominant dynamics of such systems, we developed a procedure, based on a combination of Galerkin's method with approximate inertial manifolds, for the construction of low-order DDE systems that accurately reproduce the dominant dynamics of the PDDE system. These DDE systems were used as the basis for the synthesis of nonlinear output feedback controllers that guarantee stability and enforce output tracking in the closed-loop system.

4. **Application to chemical process control.** The developed control methods were successfully applied to industrially important chemical processes including a reactor-separator process with recycle, a fluidized catalytic cracking unit and a tubular reactor with recycle.

Finally, in the context of my doctoral thesis, I also proposed a general and practical methodology for the integration of nonlinear output feedback control with optimal placement of control actuators and measurement sensors for transport-reaction processes described by a broad class of quasi-linear parabolic PDEs.

Appendix A

Proofs of Chapter 2

Definitions

- $L_f h$ denotes the Lie derivative of a scalar field h with respect to the vector field f. $L_f^k h$ denotes the k-th order Lie derivative and $L_g L_f^{k-1} h$ denotes the mixed Lie derivative.
- A function $\gamma : \mathbb{R}_{\geq 0} \to \mathbb{R}_{\geq 0}$ is said to be of class $\mathcal{Q}$ if it is continuous, zero at zero and nondecreasing. It is of class K if it is continuous, strictly increasing and is zero at zero.
- A function $\beta : \mathbb{R}_{\geq 0} \times \mathbb{R}_{\geq 0} \to \mathbb{R}_{\geq 0}$ is said to be of class KL if, for each fixed t, the function $\beta(\cdot, t)$ is of class K and, for each fixed s, the function $\beta(s, \cdot)$ is nonincreasing and tends to zero at infinity.

Proof of Theorem 2.2:

Under the controller of Eq.2.21, the closed-loop system takes the form:

$$\begin{aligned} \dot{\omega} &= \mathcal{F}(\omega, h(x(t-\alpha)), v) \\ \dot{x} &= Ax(t) + Bx(t-\alpha) + f(x(t), x(t-\alpha)) \\ &\quad + g(x(t), x(t-\alpha))\mathcal{P}(\omega, h(x(t-\alpha)), t), \\ &\quad x(\xi) = \bar{\eta}(\xi), \quad \xi \in [-\alpha, 0), \quad x(0) = \bar{\eta}_0 \end{aligned} \tag{A.1}$$

Introducing the extended state vector $\hat{\omega} = [\omega^T \; x^T]^T$, the above system can be written in the following compact form:

$$\dot{\hat{\omega}} \;=\; \bar{\mathcal{F}}(\hat{\omega}(t), \hat{\omega}(t-\alpha)) \tag{A.2}$$

where the specific form of the vector $\bar{\mathcal{F}}(\hat{\omega}(t), \hat{\omega}(t-\alpha))$ can be easily obtained by comparing Eq.A.1 and Eq.A.2, and it is omitted here for brevity. From the fact that the controller of Eq.2.21 enforces local exponential stability and asymptotic output tracking in the closed-loop system when $\alpha = 0$, we have that the system:

$$\dot{\hat{\omega}} \;=\; \bar{\mathcal{F}}(\hat{\omega}(t), \hat{\omega}(t)) \tag{A.3}$$

is locally exponentially stable. For $t \geq 2\alpha$, the system of Eq.A.2 can be rewritten as:

$$\begin{aligned} \dot{\hat{\omega}} \;&=\; \bar{\mathcal{F}}(\hat{\omega}(t), \hat{\omega}(t)) + [\bar{\mathcal{F}}(\hat{\omega}(t), \hat{\omega}(t-\alpha)) - \bar{\mathcal{F}}(\hat{\omega}(t), \hat{\omega}(t))] \\ &=\; \bar{\mathcal{F}}(\hat{\omega}(t), \hat{\omega}(t)) - \int_{t-\alpha}^{t} \frac{\partial \bar{\mathcal{F}}}{\partial \hat{\omega}}(\hat{\omega}(\theta), \hat{\omega}(\theta), t) \bar{\mathcal{F}}(\hat{\omega}(\theta-\alpha), \hat{\omega}(\theta)) d\theta \end{aligned} \tag{A.4}$$

We consider the function $V = \hat{\omega}^T(t)\hat{\omega}(t)$ as a Lyapunov function candidate for the system of Eq.A.4. Computing the time-derivative of V along the trajectory of the system of Eq.A.4, we obtain:

$$\dot{V} \;=\; 2\hat{\omega}(t)\bar{\mathcal{F}}(\hat{\omega}(t), \hat{\omega}(t)) - 2\int_{t-\alpha}^{t} \hat{\omega}(t) \frac{\partial \bar{\mathcal{F}}}{\partial \hat{\omega}}(\hat{\omega}(\theta), \hat{\omega}(\theta), t) \bar{\mathcal{F}}(\hat{\omega}(\theta-\alpha), \hat{\omega}(\theta)) d\theta \tag{A.5}$$

From the smoothness of the function $\bar{\mathcal{F}}$, we have that there exists an L such that $\left| \frac{\partial \bar{\mathcal{F}}}{\partial \hat{\omega}}(\hat{\omega}(\theta), \hat{\omega}(\theta), t) \right|_{\mathbb{R}^n} \leq L$, and the bound on $\dot{V}$ of Eq.A.5, takes the form:

$$\begin{aligned} \dot{V} \;&\leq\; 2\hat{\omega}(t)\bar{\mathcal{F}}(\hat{\omega}(t), \hat{\omega}(t)) + 2L^2 \int_{t-\alpha}^{t} |\hat{\omega}(t)\hat{\omega}(\theta-\alpha)|_{\mathbb{R}^n} d\theta \\ &\leq\; 2\hat{\omega}(t)\bar{\mathcal{F}}(\hat{\omega}(t), \hat{\omega}(t)) + 2L^2 |\hat{\omega}(t)|_{\mathbb{R}^n} \int_{t-\alpha}^{t} |\hat{\omega}(\theta-\alpha)|_{\mathbb{R}^n} d\theta \end{aligned} \tag{A.6}$$

Now, given a positive real number $\bar{q} > 1$, we consider the set of all $\hat{\omega}(t)$ that satisfy:

$$\hat{\omega}^2(t-\xi) \leq \bar{q}^2 \hat{\omega}^2(t), \quad 0 \leq \xi \leq 2\alpha \tag{A.7}$$

for which, we have that:

$$\dot{V} \leq 2\hat{\omega}(t)\bar{\mathcal{F}}(\hat{\omega}(t),\hat{\omega}(t)) + 2L^2\alpha\bar{q}|\hat{\omega}(t)|^2_{\mathbb{R}^n} \tag{A.8}$$

From the fact that the controller of Eq.2.21 enforces local exponential stability and asymptotic output tracking in the closed-loop system when $\alpha = 0$, we have that the system:

$$\dot{\hat{\omega}} = \bar{\mathcal{F}}(\hat{\omega}(t),\hat{\omega}(t)) \tag{A.9}$$

is locally exponentially stable, which implies that:

$$2\hat{\omega}(t)\bar{\mathcal{F}}(\hat{\omega}(t),\hat{\omega}(t)) \leq -a|\hat{\omega}(t)|^2_{\mathbb{R}^n} \tag{A.10}$$

where a is a positive real number. Substituting the above bound into Eq.A.8, we obtain:

$$\begin{aligned} \dot{V} &\leq -a|\hat{\omega}(t)|^2_{\mathbb{R}^n} + 2L^2\alpha\bar{q}|\hat{\omega}(t)|^2_{\mathbb{R}^n} \\ &\leq -(a - 2L^2\alpha\bar{q})|\hat{\omega}(t)|^2_{\mathbb{R}^n} \end{aligned} \tag{A.11}$$

For $\alpha < \frac{a}{2L^2\bar{q}}$, we have that $\dot{V} \leq 0$, and using Theorem 4.2 from [63], we directly obtain that the system of Eq.A.1 is exponentially stable. The proof that $\lim_{t\to\infty} |y - v|_{\mathbb{R}} = 0$ is conceptually similar and will be omitted for brevity. $\triangle$

Proof of Theorem 2.3:

Substitution of the controller of Eq.2.37 into the system of Eq.2.2 with $\tilde{\alpha} = 0$, yields the following system:

$$\begin{aligned} \dot{x} &= Ax + Bx(t-\alpha) + f(x, x(t-\alpha)) \\ &\quad + g(x, x(t-\alpha))\mathcal{A}(x(t), \bar{v}(t), x(t-\alpha), \bar{v}(t-\alpha)) \\ y &= h(x) \end{aligned} \tag{A.12}$$

Using that $f(x(t), x(t-\alpha)) = f_1(x(t)) + f_2(x(t), x(t-\alpha))$, $\tilde{f}(x(t)) = Ax(t) + f_1(x(t))$, and $\bar{p}(x(t), x(t-\alpha)) = Bx(t-\alpha) + f_2(x(t), x(t-\alpha))$, the above system can be written

as:

$$\begin{aligned} \dot{x} &= \bar{f}(x(t)) + g(x(t), x(t-\alpha))\mathcal{A}(x(t), \bar{v}(t), x(t-\alpha), \bar{v}(t-\alpha)) + \bar{p}(x(t), x(t-\alpha)) \\ y &= h(x) \end{aligned} \tag{A.13}$$

Applying the coordinate transformation of Eq.2.27 to the above system and setting, for ease of notation, $x(s) = \mathcal{X}^{-1}(\zeta(s), \eta(s))$, $s \in [t-\alpha, t]$, we obtain:

$$\begin{aligned} \dot{\zeta}_1 &= \zeta_2 + p_1(\zeta(t), \eta(t), \zeta(t-\alpha), \eta(t-\alpha)) \\ &\vdots \\ \dot{\zeta}_{r-1} &= \zeta_r + p_{r-1}(\zeta(t), \eta(t), \zeta(t-\alpha), \eta(t-\alpha)) \\ \dot{\zeta}_r &= L_{\bar{f}}^r h(x) + L_g L_{\bar{f}}^{r-1} h(x) \mathcal{A}(x(t), \bar{v}(t), x(t-\alpha), \bar{v}(t-\alpha)) \\ &\quad + p_r(\zeta(t), \eta(t), \zeta(t-\alpha), \eta(t-\alpha)) \\ \dot{\eta}_1 &= \Psi_1(\zeta(t), \eta(t), \zeta(t-\alpha), \eta(t-\alpha)) \\ &\vdots \\ \dot{\eta}_{n-r} &= \Psi_{n-r}(\zeta(t), \eta(t), \zeta(t-\alpha), \eta(t-\alpha)) \\ y &= \zeta_1 \end{aligned} \tag{A.14}$$

Introducing, the variables $e_i = \zeta_i - v^{(i-1)}$, $i = 1, \cdots, r$, the system of Eq.A.14 takes the form:

$$\begin{aligned} \dot{e}_1 &= e_2 + p_1(\bar{e}(t) + \bar{v}(t), \eta(t), \bar{e}(t-\alpha) + \bar{v}(t-\alpha), \eta(t-\alpha)) \\ &\vdots \\ \dot{e}_{r-1} &= e_r + p_{r-1}(\bar{e}(t) + \bar{v}(t), \eta(t), \bar{e}(t-\alpha) + \bar{v}(t-\alpha), \eta(t-\alpha)) \\ \dot{e}_r &= L_{\bar{f}}^r h(x) - v^{(r)} + L_g L_{\bar{f}}^{r-1} h(x) \mathcal{A}(x(t), \bar{v}(t), x(t-\alpha), \bar{v}(t-\alpha)) \\ &\quad + p_r(\bar{e}(t) + \bar{v}(t), \eta(t), \bar{e}(t-\alpha) + \bar{v}(t-\alpha), \eta(t-\alpha)) \\ \dot{\eta}_1 &= \Psi_1(\bar{e}(t) + \bar{v}(t), \eta(t), \bar{e}(t-\alpha) + \bar{v}(t-\alpha), \eta(t-\alpha)) \\ &\vdots \\ \dot{\eta}_{n-r} &= \Psi_{n-r}(\bar{e}(t) + \bar{v}(t), \eta(t), \bar{e}(t-\alpha) + \bar{v}(t-\alpha), \eta(t-\alpha)) \end{aligned} \tag{A.15}$$

where $\bar{e} = [e_1\ e_2\ \cdots\ e_r]^T$. For the above system, we assume, without loss of generality, that when $\eta = 0$, $\bar{e} = 0$ is an equilibrium solution.

We now consider the $\bar{e}$-subsystem of the system of Eq.A.15:

$$\begin{aligned}
\dot{e}_1 &= e_2 + p_1(\bar{e}(t)+\bar{v}(t),\eta(t),\bar{e}(t-\alpha)+\bar{v}(t-\alpha),\eta(t-\alpha)) \\
&\vdots \\
\dot{e}_{r-1} &= e_r + p_{r-1}(\bar{e}(t)+\bar{v}(t),\eta(t),\bar{e}(t-\alpha)+\bar{v}(t-\alpha),\eta(t-\alpha)) \\
\dot{e}_r &= L_{\tilde{f}}^r h(x) - v^{(r)} + L_g L_{\tilde{f}}^{r-1} h(x)\mathcal{A}(x(t),\bar{v}(t),x(t-\alpha),\bar{v}(t-\alpha)) \\
&\quad + p_r(\bar{e}(t)+\bar{v}(t),\eta(t),\bar{e}(t-\alpha)+\bar{v}(t-\alpha),\eta(t-\alpha))
\end{aligned} \tag{A.16}$$

Using the explicit form of the controller formula of Eq.2.37 and the definition for the matrix $\bar{A}$ and the vectors b, p of Eq.2.32, the above system can be written in the following compact form:

$$\dot{\bar{e}} = \bar{A}\bar{e} - bR_2^{-1}b^T P\bar{e} + p(\bar{e}(t)+\bar{v}(t),\eta(t),\bar{e}(t-\alpha)+\bar{v}(t-\alpha),\eta(t-\alpha)) \tag{A.17}$$

We will now show that if Eq.2.36 has a unique positive definite solution for P and the state of the η-subsystem of Eq.A.15 is bounded, then the system of Eq.A.17 is exponentially stable, which implies that $\lim_{t\to\infty}|y-v|_{\mathbb{R}} = 0$. To establish this result, we consider the following smooth functional $V : \mathcal{C} \to \mathbb{R}_{\geq 0}$:

$$V(\bar{e}_t(\xi)) = \bar{e}^T P\bar{e} + a^2\int_{t-\alpha}^{t}\bar{e}^T(s)\bar{e}(s)ds \tag{A.18}$$

which clearly satisfies, $K_1|\bar{e}(t)|^2_{\mathbb{R}^r} \leq V(\bar{e}_t(\xi)) \leq K_2|\bar{e}_t(\xi)|^2$, for some positive constants K_1 and K_2. Computing the time-derivative of V along the trajectories of the system of Eq.A.17, we obtain:

$$\begin{aligned}
\dot{V} &= \dot{\bar{e}}^T P\bar{e} + \bar{e}^T P\dot{\bar{e}} + a^2(\bar{e}^T(t)\bar{e}(t) - \bar{e}^T(t-\alpha)\bar{e}(t-\alpha)) \\
&\leq (\bar{e}^T\bar{A}^T - \bar{e}^T P^T bR_2^{-1}b^T + p^T(\bar{e}(t)+\bar{v}(t),\eta(t),\bar{e}(t-\alpha)+\bar{v}(t-\alpha),\eta(t-\alpha)))P\bar{e} \\
&\quad + \bar{e}^T P(\bar{A}\bar{e} - bR_2^{-1}b^T P\bar{e} + p(\bar{e}(t)+\bar{v}(t),\eta(t),\bar{e}(t-\alpha)+\bar{v}(t-\alpha),\eta(t-\alpha))) \\
&\quad + a^2(\bar{e}^T(t)\bar{e}(t) - \bar{e}^T(t-\alpha)\bar{e}(t-\alpha)) \\
&\leq \bar{e}^T(\bar{A}^T P + P\bar{A} - 2P^T bR_2^{-1}b^T P + a^2 I_{n\times n})\bar{e} \\
&\quad + 2p^T(\bar{e}(t)+\bar{v}(t),\eta(t),\bar{e}(t-\alpha)+\bar{v}(t-\alpha),\eta(t-\alpha))P\bar{e} \\
&\quad - a^2\bar{e}^T(t-\alpha)\bar{e}(t-\alpha)
\end{aligned} \tag{A.19}$$

where $I_{n\times n}$ denotes the identity matrix of dimension $n \times n$. Using the inequality $2x^T y \leq x^T x + y^T y$ where x and y are column vectors, we obtain:

$$\begin{aligned}\dot{V} &\leq \bar{e}^T(\tilde{A}^T P + P\tilde{A} - 2P^T b R_2^{-1} b^T P + a^2 I_{n\times n})\bar{e} \\ &\quad + p^2(\bar{e}(t) + \bar{v}(t), \eta(t), \bar{e}(t-\alpha) + \bar{v}(t-\alpha), \eta(t-\alpha)) \\ &\quad + \bar{e}^T P^2 \bar{e} - a^2 \bar{e}^T(t-\alpha)\bar{e}(t-\alpha) \\ &\leq \bar{e}^T(\tilde{A}^T P + P\tilde{A} - 2P^T b R_2^{-1} b^T P + a^2 I_{n\times n} + P^2)\bar{e} \\ &\quad + p^2(\bar{e}(t) + \bar{v}(t), \eta(t), \bar{e}(t-\alpha) + \bar{v}(t-\alpha), \eta(t-\alpha)) \\ &\quad - a^2 \bar{e}^T(t-\alpha)\bar{e}(t-\alpha)\end{aligned} \tag{A.20}$$

Since the state of the η-subsystem of Eq.A.15 is supposed to be bounded and assuming quadratic growth for the term $p^2(\bar{e}(t) + \bar{v}(t), \eta(t), \bar{e}(t-\alpha) + \bar{v}(t-\alpha), \eta(t-\alpha))$ (Assumption 2.3), we have that there exist positive real numbers a_1, a_2 such that the following bound can be written:

$$|p(\bar{e}(t) + \bar{v}(t), \eta(t), \bar{e}(t-\alpha) + \bar{v}(t-\alpha), \eta(t-\alpha))|^2_{\mathbb{R}^r} \leq a_1 \bar{e}^2(t) + a_2 \bar{e}^2(t-\alpha) \tag{A.21}$$

Substituting the above inequality on the bound for $\dot{V}$ in Eq.A.20, we obtain:

$$\begin{aligned}\dot{V} &\leq \bar{e}^T(\tilde{A}^T P + P\tilde{A} - 2P^T b R_2^{-1} b^T P + a^2 I_{n\times n} + P^2)\bar{e} \\ &\quad + a_1 \bar{e}^2(t) + a_2 \bar{e}^2(t-\alpha) - a^2 \bar{e}^T(t-\alpha)\bar{e}(t-\alpha) \\ &\leq \bar{e}^T(\tilde{A}^T P + P\tilde{A} - 2P^T b R_2^{-1} b^T P + (a^2 + a_1) I_{n\times n} + P^2)\bar{e} \\ &\quad - (a^2 - a_2)\bar{e}^2(t-\alpha)\end{aligned} \tag{A.22}$$

Now, if $a^2 > a_2$ and there exists a positive definite symmetric matrix P which solves the following matrix equation:

$$\tilde{A}^T P + P\tilde{A} - 2P^T b R_2^{-1} b^T P + (a^2 + a_1) I_{n\times n} + P^2 = -R_1 \tag{A.23}$$

where R_1 is a positive definite matrix, then:

$$\begin{aligned}\dot{V} &\leq -\bar{e}^T R_1 \bar{e} - a_3 \bar{e}^2(t-\alpha) \\ &\leq -\lambda_{min}(R_1)\bar{e}^2 - a_3 \bar{e}^2(t-\alpha)\end{aligned} \tag{A.24}$$

where a_3 is a positive real number and $\lambda_{min}(R_1)$ denotes the smallest eigenvalue of the matrix R_1. Since V and $\dot{V}$ satisfy the assumptions of Theorem 2.1, we have

that there exist positive real numbers K, a such that the state of the $\bar{e}-$subsystem of Eq.A.16 is exponentially stable i.e., it satisfies:

$$|\bar{e}(t)|_{\mathbb{R}^r} \leq Ke^{-at}|\bar{e}(0)|_{\mathbb{R}^r} \tag{A.25}$$

for every value of the delay, α, and thus, $\lim_{t\to\infty}|y-v|_{\mathbb{R}} = 0$.

To complete the proof of the theorem, we need to show that there exists a positive real number δ such that if $\max\{|x_0(\xi)|, ||\bar{v}||\} \leq \delta$, then the state of the closed-loop system is exponentially stable and the output of the closed-loop system satisfies $\lim_{t\to\infty}|y-v|_{\mathbb{R}^n} = 0$. To establish this result, we will analyze the behavior of the DDE system of Eq.A.15 using a two-step small-gain theorem type argument [143]. In the first step, we will use a contradiction argument to show that the evolution of the states $\bar{e}, \eta$, starting from sufficiently small initial conditions i.e., $|\bar{e}_0(\xi)| \leq \delta_{\bar{e}}$ and $|\eta_0(\xi)| \leq \delta_\eta$ (where $(\delta_{\bar{e}}, \delta_\eta)$ are positive real numbers which can be explicitly computed as functions of δ from the coordinate change of Eq.2.27), satisfies the following inequalities:

$$|\bar{e}(t)| \leq \bar{\delta}_{\bar{e}}\,, \quad |\eta(t)| \leq \bar{\delta}_\eta, \quad \forall\, t\,\epsilon[0,\infty) \tag{A.26}$$

where $\bar{\delta}_{\bar{e}} > K\delta_{\bar{e}}$ and $\bar{\delta}_\eta > \delta_\eta$ are positive real numbers which will be specified below. In the second step, we will use the boundedness result obtained from the first step and the exponentially decaying bound of Eq.A.25 to prove that the state of the η-subsystem of Eq.A.15 decays exponentially to zero.

From Assumption 2.3, we have that the $\eta-$subsystem of the system of Eq.A.15 is input-to-state stable, which implies that there exist a function $\bar{\gamma}_{\bar{e}}$ of class Q, a function β_η of class KL and positive real numbers $\bar{\delta}_{\bar{e}}, \delta_\eta$ such that if $|\eta_0(\xi)| < \delta_\eta$ and $||\bar{e}_t|| < \bar{\delta}_{\bar{e}}$, then:

$$|\eta(t)| \leq |\eta_t(\xi)| \leq \beta(|\eta_0(\xi)|, t) + \bar{\gamma}_{\bar{e}}(||\bar{e}_t||), \;\; \forall\, t \geq 0 \tag{A.27}$$

We will proceed by contradiction. Set $\bar{\delta}_\eta > \beta_\eta(\delta_\eta, 0) + \bar{\gamma}_{\bar{e}}(K\delta_{\bar{e}})$ and let $\bar{T}$ be the smallest time such that there is a $\hat{\delta}$ so that $t \in (\bar{T}, \bar{T} + \hat{\delta})$ implies either $|\bar{e}(t)| > \bar{\delta}_{\bar{e}}$ or $|\bar{\eta}(t)| > \bar{\delta}_\eta$. Then, for each $t \in [0, \bar{T}]$ the conditions of Eq.A.26 hold.

Consider the functions $\bar{e}^{\bar{T}}(t)$, $\eta^{\bar{T}}(t)$ defined as follows:

$$\bar{e}^{\bar{T}}(t) = \left\{ \begin{array}{ll} \bar{e}(t) & t \in [0, \bar{T}] \\ 0 & t \in (\bar{T}, \infty) \end{array} \right\}, \quad \eta^{\bar{T}}(t) = \left\{ \begin{array}{ll} \eta(t) & t \in [0, \bar{T}] \\ 0 & t \in (\bar{T}, \infty) \end{array} \right\} \tag{A.28}$$

Now, using Eq.A.27 we have that:

$$\begin{aligned} \sup_{0 \leq t \leq \bar{T}} (\beta_\eta(|\eta_0(\xi)|, t) + \bar{\gamma}_{\bar{e}}(||\bar{e}_t||)) &\leq \beta_\eta(\delta_\eta, 0) + \bar{\gamma}_{\bar{e}}(K\delta_{\bar{e}}) \\ \sup_{0 \leq t \leq \bar{T}} \left(K|\bar{e}(0)|_{\mathbb{R}^r} e^{-at} \right) &\leq K|\bar{e}(0)|_{\mathbb{R}^r} \leq K\delta_{\bar{e}} \end{aligned} \tag{A.29}$$

and that:

$$\begin{aligned} ||\bar{e}^{\bar{T}}|| &\leq K\delta_{\bar{e}} < \bar{\delta}_{\bar{e}} \\ ||\eta^{\bar{T}}|| &\leq \beta_\eta(\delta_\eta, 0) + \bar{\gamma}_{\bar{e}}(K\delta_{\bar{e}}) < \bar{\delta}_\eta \end{aligned} \tag{A.30}$$

By continuity, we have that there exist some positive real number $\bar{k}$ such that $||\bar{e}^{\bar{T}+\bar{k}}(t)|| \leq \bar{\delta}_{\bar{e}}$ and $||\eta^{\bar{T}+\bar{k}}(t)|| \leq \bar{\delta}_\eta$, $\forall\ t \in [0, \bar{T} + \bar{k}]$. This contradicts the definition of $\bar{T}$. Hence, Eq.A.26 holds $\forall\ t \geq 0$.

Since the states, $(\bar{e}, \eta)$, of the closed-loop system of Eq.A.15 are bounded and $\bar{e}(t)$ decays exponentially to zero, a direct application of the result of Theorem 2 in [143] implies that the η-subsystem of Eq.A.15 is also exponentially stable, and thus, the system of Eq.A.15 is exponentially stable and its output satisfies $\lim_{t \to \infty} |y - v|_{\mathbb{R}^n} = 0$.

$\triangle$

Proof of Theorem 2.4:

We initially construct that dynamical system which describes the dynamics of the estimation error, $e_t = \omega_t - x_t$. Differentiating e_t and using the systems of Eq.2.10 and Eq.2.50, we obtain:

$$\begin{aligned} \frac{de_t}{dt} &= \mathcal{A}e_t + f(P(e_t + x_t), Q(e_t + x_t)) - f(Px_t, Qx_t) \\ &\quad + \Phi_H L(\Psi_H, e_t + x_t)(y(t) - h(P(e_t + x_t))) \end{aligned} \tag{A.31}$$

Computing the linearization of the above system and applying the spectral decomposition procedure, we obtain:

$$\begin{aligned} \frac{de_t^p}{dt} &= \mathcal{A}_p e_t^p - \Phi_H L(w(Pe_t^p + Pe_t^n)) \\ \frac{\partial e_t^n}{\partial t} &= \mathcal{A}_n e_t^n \\ e_t^p(0) &= P_p e(0) = P_p(\bar{\omega} - \bar{\eta}), \quad e_t^n(0) = P_n e(0) = P_n(\bar{\omega} - \bar{\eta}) \end{aligned} \tag{A.32}$$

because $P_n \Phi_H L(\Psi_H, \omega_t)(y(t) - h(P\omega_t)) \equiv 0$ by construction, and $w = \dfrac{\partial h}{\partial x}(0)$. Since all the eigenvalues of the operator $\mathcal{A}_n$ lie in the left-half of the complex, this implies that the subsystem:

$$\frac{\partial e_t^n}{\partial t} = \mathcal{A}_n e_t^n \tag{A.33}$$

is exponentially stable. Therefore, the infinite-dimensional system of Eq.A.32 possesses identical stability properties with the finite-dimensional system:

$$\frac{de_t^p}{dt} = \mathcal{A}_p e_t^p + \Phi_H L w P e_t^p \tag{A.34}$$

From the observability Assumption 2.4, however, we have that the above system is exponentially stable, which implies that the error system is exponentially to zero, and thus, the estimation error, $e_t = \omega_t - x_t$, tends locally exponentially to zero.

Nonlinear state observer simplification:

The abstract dynamical system of Eq.2.50 can be simplified by utilizing the fact that:

$$\begin{aligned} \mathcal{A}\omega_t(\xi) &+ \Phi_H L(\Psi_H, \phi)(y(t) - h(P\omega_t(\xi))) \\ &= \left\{ \begin{array}{ll} \dfrac{d\phi(\xi)}{d\xi} + \Phi_H(\xi) L(\Psi_H, \phi)(y(t) - h(P\omega_t(\xi))), & \xi \in [-\alpha, 0) \\ A\omega_t(0) + B\phi(-\alpha) - \Phi_H(0) L(\Psi_H, \phi) h(P\omega_t(\xi)), & \xi = 0 \end{array} \right\} \end{aligned} \tag{A.35}$$

which implies that is equivalent to the following system of partial differential equations:

$$\frac{\partial\tilde{\omega}}{\partial t}(\xi,t) = \frac{\partial\tilde{\omega}}{\partial\xi}(\xi,t) + \Phi_H(\xi)L(\Psi_H,\tilde{\omega}(\xi,t))(y(t)-h(\tilde{\omega}(0,t))) \tag{A.36}$$

$$\frac{\partial\tilde{\omega}}{\partial t}(0,t) = A\tilde{\omega}(0,t) + B\tilde{\omega}(-\alpha,t) + \Phi_H(0)L(\Psi_H,\tilde{\omega}(\xi,t))(y(t)-h(\tilde{\omega}(0,t))) \tag{A.37}$$

where $\tilde{\omega}(\xi,t) = \omega_t(\xi)$. A further simplification can be performed by integrating the hyperbolic PDE of Eq.A.36 along its characteristics to obtain a nonlinear integro-differential equation system for the observer. The characteristics of Eq.A.36 are the family of lines with slope $\frac{dt}{d\xi} = -1$, i.e., the set of lines satisfying $t+\xi = c$, where c is a constant. Integrating the Eq.A.36 along its characteristics, we obtain:

$$\frac{d\tilde{\omega}}{d\xi}(c-\xi,\xi) = -\Phi(\xi)L(\Psi_H,\tilde{\omega}(\xi,t))h(\tilde{\omega}(0,c-\xi)) + \Phi(\xi)L(\Psi_H,\tilde{\omega}(\xi,t))y(c-\xi) \tag{A.38}$$

so that:

$$\begin{aligned}\tilde{\omega}(c-\theta,\theta) &= \tilde{\omega}(c,0) - \int_0^\theta \Phi(\xi)L(\Psi_H,\tilde{\omega}(\xi,t))(h(\tilde{\omega}(0,c-\xi)) - y(c-\xi))d\xi, \\ &\quad \theta\in[-\alpha,0],\end{aligned} \tag{A.39}$$

or:

$$\tilde{\omega}(t,\theta) = \tilde{\omega}(t+\theta,0) - \int_0^\theta \Phi(\xi)L(\Psi_H,\tilde{\omega}(\xi,t)))(h(\tilde{\omega}(0,t+\theta-\xi)) - y(t+\theta-\xi))d\xi \tag{A.40}$$

Finally,

$$\begin{aligned}\tilde{\omega}(t,-\alpha) &= \tilde{\omega}(t-\alpha,0) - \int_0^{-\alpha}\Phi(\xi)L(\Psi_H,\tilde{\omega}(\xi,t))(h(\tilde{\omega}(0,t-\alpha-\xi)) \\ &\quad -y(t-\alpha-\xi))d\xi \\ &= \tilde{\omega}(t-\alpha,0) + \int_0^{\alpha}\Phi(\xi-\alpha)L(\Psi_H,\tilde{\omega}(\xi,t))(h(\tilde{\omega}(0,t-\xi)) \\ &\quad -y(t-\xi))d\xi\end{aligned} \tag{A.41}$$

Substituting $\tilde{\omega}(t+\theta,0)=\omega(t+\theta)$ into Eq.A.37, we obtain the following system:

$$\begin{aligned}\dot{\omega} &= A\omega(t)+B\omega(t-\alpha)+f(\omega(t),\omega(t-\alpha))+g(\omega(t),\omega(t-\alpha))u \\ &\quad +\Phi_H(0)L(\Psi_H,\tilde{\omega}(\xi,t))(y(t)-h(\omega(t))) \\ &\quad +B\int_0^{\alpha}\Phi_H(\xi-\alpha)L(\Psi_H,\tilde{\omega}(\xi,t))[y(t-\xi)-h(\omega(t-\xi))]d\xi\end{aligned} \tag{A.42}$$

which is identical to the one of Eq.2.51. △

Proof of Theorem 2.5:

Under the output feedback controller of Eq.2.57, the closed-loop system takes the form:

$$\begin{aligned}\dot{\omega} &= A\omega(t)+B\omega(t-\alpha)+f(\omega(t),\omega(t-\alpha)) \\ &\quad +\Phi_H(0)L(\Psi_H,\tilde{\omega}(\xi,t))(y(t)-h(\omega(t))) \\ &\quad +B\int_0^{\alpha}\Phi_H(\xi-\alpha)L(\Phi_H,\tilde{\omega}(\xi,t))[y(t-\xi)-h(\omega(t-\xi))]d\xi \\ &\quad +g(\omega(t),\omega(t-\alpha))\frac{1}{L_gL_{\tilde{f}}^{r-1}h(\omega)}\left(-R_2^{-1}b^TP\bar{e}(t)+v^{(r)}(t)-L_{\tilde{f}}^{r}h(\omega)\right. \\ &\quad \left.-p_r(\omega(t),\bar{v}(t),\omega(t-\alpha),\bar{v}(t-\alpha))\right) \\ \dot{x} &= Ax(t)+Bx(t-\alpha)+f(x(t),x(t-\alpha)) \\ &\quad +g(x(t),x(t-\alpha))\frac{1}{L_gL_{\tilde{f}}^{r-1}h(\omega)}\left(-R_2^{-1}b^TP\bar{e}(t)+v^{(r)}(t)-L_{\tilde{f}}^{r}h(\omega)\right. \\ &\quad \left.-p_r(\omega(t),\bar{v}(t),\omega(t-\alpha),\bar{v}(t-\alpha))\right)\end{aligned} \tag{A.43}$$

Since we are interested in proving local exponential stability of the above system, we compute its linearization around the zero solution and use that $f(0,0)=0$ and $f(x(t),x(t-\alpha))$ includes higher-order terms, and $g(0,0)=c$, where c is a constant vector, to obtain the following linear system:

$$\begin{aligned}\dot{\omega} &= A\omega(t)+B\omega(t-\alpha)+\Phi_H(0)L(wx(t)-w\omega(t)) \\ &\quad +B\int_0^{\alpha}\Phi_H(\xi-\alpha)L[wx(t-\xi)-w\omega(t-\xi)]d\xi \\ &\quad +cu_{lin}(\omega(t),\bar{v}(t),\omega(t-\alpha),\bar{v}(t-\alpha)) \\ \dot{x} &= Ax(t)+Bx(t-\alpha)+cu_{lin}(\omega(t),\bar{v}(t),\omega(t-\alpha),\bar{v}(t-\alpha))\end{aligned} \tag{A.44}$$

where L is the linearization of the nonlinear vector $L(\Psi_H, \bar{\omega}(\xi,t))$ around the zero solution, $w = \dfrac{\partial h}{\partial x}(0)$, and u_{lin} is the linearization of the term:

$$\frac{1}{L_g L_{\bar{f}}^{r-1} h(\omega)} \left(-R_2^{-1} b^T P \bar{e}(t) + v^{(r)}(t) - L_{\bar{f}}^r h(\omega)) - p_r(\omega(t), \bar{v}(t), \omega(t-\alpha), \bar{v}(t-\alpha)) \right) \tag{A.45}$$

around the zero solution.

Introducing the error vector $e_r = x - \omega$, the closed-loop system of Eq.A.44 can be written as:

$$\begin{aligned} \dot{e_r} &= Ae_r(t) + Be_r(t-\alpha) + \Phi_H(0) L w e_r(t) + B\int_0^\alpha \Phi_H(\xi-\alpha) L w e_r(t-\xi) d\xi \\ \dot{x} &= Ax(t) + Bx(t-\alpha) + c u_{lin}(x(t) + e_r(t), \bar{v}(t), x(t-\alpha) + e_r(t-\alpha), \bar{v}(t-\alpha)) \end{aligned} \tag{A.46}$$

From the observability Assumption 2.3, we have that the error system:

$$\dot{e_r} = Ae_r(t) + Be_r(t-\alpha) + \Phi_H(0) L w e_r(t) + B\int_0^\alpha \Phi_H(\xi-\alpha) L w e_r(t-\xi) d\xi \tag{A.47}$$

is exponentially stable. Moreover, from the construction of the state feedback controller, we have that the system:

$$\begin{aligned} \dot{x} &= Ax(t) + Bx(t-\alpha) + c u_{lin}(x(t), \bar{v}(t), x(t-\alpha), \bar{v}(t-\alpha)) \\ y &= wx(t) \end{aligned} \tag{A.48}$$

is exponentially stable and the output asymptotically follows the reference input (proof of Theorem 2.2). Therefore, we have that the linear system of Eq.A.46 is an interconnection of two exponentially stable subsystems, which implies that it is also exponentially stable. Using the result of Theorem 1.1 in [63, Chapter 10] (which allows inferring the local stability properties of a nonlinear system based on its linearization) we obtain that the nonlinear closed-loop system of Eq.A.43 is locally exponentially stable and the discrepancy between the output and the reference input asymptotically tends to zero. $\triangle$

Appendix B

Proof of Chapter 4

Proof of Theorem 4.2:

Consider the DDE system of Eq.2.26 under the robust controller of Eq.4.19:

$$\begin{aligned} \dot{x} &= \bar{f}_{nom}(x(t)) + g(x(t), x(t-\alpha))\mathcal{R}(x(t), x(t-\alpha), t) + \tilde{p}(x(t), x(t-\alpha), \theta(t-\alpha_\theta)) \\ y &= h(x) \end{aligned} \tag{B.1}$$

Applying the coordinate transformation of Eq.4.8 to the above system and setting, for ease of notation, $x(s) = \mathcal{X}^{-1}(\zeta(s), \eta(s), \theta(s))$, $s \in [t-\alpha, t]$, $t \in [0, \infty)$ we obtain:

$$\begin{aligned} \dot{\zeta}_1 &= \zeta_2(t) + \tilde{p}_1(\zeta(t), \eta(t), \zeta(t-\alpha), \eta(t-\alpha), \theta(t-\alpha_\theta)) \\ &\vdots \\ \dot{\zeta}_{r-1} &= \zeta_r(t) + \tilde{p}_{r-1}(\zeta(t), \eta(t), \zeta(t-\alpha), \eta(t-\alpha), \theta(t-\alpha_\theta)) \\ \dot{\zeta}_r &= L^r_{\bar{f}_{nom}} h(x(s)) + L_g L^{r-1}_{\bar{f}_{nom}} h(x(s))\mathcal{R}(x(t), x(t-\alpha), t) \\ &\quad + \tilde{p}_r(\zeta(t), \eta(t), \zeta(t-\alpha), \eta(t-\alpha), \theta(t-\alpha_\theta)) \\ \dot{\eta}_1 &= \Psi_1(\zeta(t), \eta(t), \zeta(t-\alpha), \eta(t-\alpha), \theta(t-\alpha_\theta)) \\ &\vdots \\ \dot{\eta}_{n-r} &= \Psi_{n-r}(\zeta(t), \eta(t), \zeta(t-\alpha), \eta(t-\alpha), \theta(t-\alpha_\theta)) \\ y &= \zeta_1(t) \end{aligned} \tag{B.2}$$

Introducing, the variables $e_i(t) = \zeta_i(t) - v^{(i-1)}$, $i = 1, \cdots, r$, and the notation $\bar{v}(s) = [v(s)\ v^{(1)}(s)\ \cdots\ v^{(r-1)}(s)]^T$, $s \in [t-\alpha, t]$ where $v^{(k)}$ denotes the k-th time derivative of the reference input v, which is assumed to be a sufficiently smooth function of

time, and $\tilde{p}_r(\zeta(t),\eta(t),\zeta(t-\alpha),\eta(t-\alpha),\theta(t-\alpha_\theta)) = p_r(\zeta(t),\eta(t),\zeta(t-\alpha),\eta(t-\alpha)) + \delta_r(\zeta(t),\eta(t),\zeta(t-\alpha),\eta(t-\alpha),\theta(t-\alpha_\theta))$, the system of Eq.B.2 takes the form:

$$\begin{aligned}
\dot{e}_1 &= e_2(t) + \tilde{p}_1(\bar{e}(t)+\bar{v}(t),\eta(t),\bar{e}(t-\alpha)+\bar{v}(t-\alpha),\eta(t-\alpha),\theta(t-\alpha_\theta)) \\
&\vdots \\
\dot{e}_{r-1} &= e_r(t) + \tilde{p}_{r-1}(\bar{e}(t)+\bar{v}(t),\eta(t),\bar{e}(t-\alpha)+\bar{v}(t-\alpha),\eta(t-\alpha),\theta(t-\alpha_\theta)) \\
\dot{e}_r &= L^r_{\tilde{f}_{nom}} h(x(s)) - v^{(r)} + L_g L^{r-1}_{\tilde{f}_{nom}} h(x(s))\mathcal{R}(x(t),x(t-\alpha),t) \\
&\quad + p_r(\bar{e}(t)+\bar{v}(t),\eta(t),\bar{e}(t-\alpha)+\bar{v}(t-\alpha),\eta(t-\alpha)) \\
&\quad + \delta_r(\bar{e}(t)+\bar{v}(t),\eta(t),\bar{e}(t-\alpha)+\bar{v}(t-\alpha),\eta(t-\alpha),\theta(t-\alpha_\theta)) \\
\dot{\eta}_1 &= \Psi_1(\bar{e}(t)+\bar{v}(t),\eta(t),\bar{e}(t-\alpha)+\bar{v}(t-\alpha),\eta(t-\alpha),\theta(t-\alpha_\theta)) \\
&\vdots \\
\dot{\eta}_{n-r} &= \Psi_{n-r}(\bar{e}(t)+\bar{v}(t),\eta(t),\bar{e}(t-\alpha)+\bar{v}(t-\alpha),\eta(t-\alpha),\theta(t-\alpha_\theta))
\end{aligned} \tag{B.3}$$

where $\bar{e}(t) = [e_1(t)\ e_2(t)\ \cdots\ e_r(t)]^T$ and $\eta(t) = [\eta_1(t)\ \eta_2(t)\ \cdots\ \eta_{n-r}(t)]^T$. For the above system, we assume, without loss of generality, that $[\bar{e}\ \eta] = [0\ 0]$ is an equilibrium solution.

We now consider the $\bar{e}$-subsystem of the system of Eq.B.3:

$$\begin{aligned}
\dot{e}_1 &= e_2(t) + \tilde{p}_1(\bar{e}(t)+\bar{v}(t),\eta(t),\bar{e}(t-\alpha)+\bar{v}(t-\alpha),\eta(t-\alpha),\theta(t-\alpha_\theta)) \\
&\vdots \\
\dot{e}_{r-1} &= e_r(t) + \tilde{p}_{r-1}(\bar{e}(t)+\bar{v}(t),\eta(t),\bar{e}(t-\alpha)+\bar{v}(t-\alpha),\eta(t-\alpha),\theta(t-\alpha_\theta)) \\
\dot{e}_r &= L^r_{\tilde{f}_{nom}} h(x(s)) - v^{(r)} + L_g L^{r-1}_{\tilde{f}_{nom}} h(x(s))\mathcal{R}(x(t),x(t-\alpha),t) \\
&\quad + p_r(\bar{e}(t)+\bar{v}(t),\eta(t),\bar{e}(t-\alpha)+\bar{v}(t-\alpha),\eta(t-\alpha)) \\
&\quad + \delta_r(\bar{e}(t)+\bar{v}(t),\eta(t),\bar{e}(t-\alpha)+\bar{v}(t-\alpha),\eta(t-\alpha),\theta(t-\alpha_\theta))
\end{aligned} \tag{B.4}$$

Using the explicit form of the controller formula of Eq.4.19 and the definition for the matrix $\tilde{A}$ and the vectors $b, \bar{p}(\bar{e}(t)+\bar{v}(t),\eta(t),\bar{e}(t-\alpha)+\bar{v}(t-\alpha),\eta(t-\alpha),\theta(t-\alpha_\theta))$, the above system can be written in the following compact form:

$$\begin{aligned}
\dot{\bar{e}} &= \tilde{A}\bar{e}(t) + b\Big(-R_2^{-1}b^T P\bar{e} - \bar{\chi}\tilde{c}_0(\bar{e}(t)+\bar{v}(t),\eta(t),\bar{e}(t-\alpha)+\bar{v}(t-\alpha),\eta(t-\alpha),t) \\
&\quad \times w(\bar{e}(t),\phi)) + \bar{p}(\bar{e}(t)+\bar{v}(t),\eta(t),\bar{e}(t-\alpha)+\bar{v}(t-\alpha),\eta(t-\alpha),\theta(t-\alpha_\theta)) \\
&\quad + b\delta_r(\bar{e}(t)+\bar{v}(t),\eta(t)\bar{e}(t-\alpha)+\bar{v}(t-\alpha),\eta(t-\alpha),\theta(t-\alpha_\theta))
\end{aligned} \tag{B.5}$$

We will now show that if Eq.4.18 holds and the state of the η-subsystem of Eq. B.3 is bounded, then the system of Eq. B.5 ensures that the ultimate discrepancy between the output and the external reference inputs in the closed-loop system can be made arbitrarily small by an appropriate choice of controller parameters, which implies that $\lim_{t\to\infty} sup|y(t) - v(t)|_{\mathbb{R}} \leq d$. To establish this result, we consider the following smooth functional $V : \mathcal{C} \to \mathbb{R}_{\geq 0}$:

$$V(\bar{e}_t(\xi)) \;=\; \bar{e}^T(t)P\bar{e}(t) + a^2\int_{t-\alpha}^{t} \bar{e}^T(s)\bar{e}(s)ds \tag{B.6}$$

where P is a positive definite symmetric matrix, a is a positive scalar, and V clearly satisfies, $K_1\|\bar{e}(t)\|^2_{\mathbb{R}^r} \leq V(\bar{e}_t(\xi)) \leq K_2|\bar{e}_t(\xi)|^2$, for some positive constants K_1 and K_2.

From Assumption 4.3, we have that

$$\begin{aligned}|\delta_r(\bar{e}(t) + \bar{v}(t), \eta(t), \bar{e}(t-\alpha) + \bar{v}(t-\alpha), \eta(t-\alpha), \theta(t-\alpha_\theta))|_{\mathbb{R}} \\ \leq\; \tilde{c}_0(\bar{e}(t) + \bar{v}(t), \eta(t), \bar{e}(t-\alpha) + \bar{v}(t-\alpha), \eta(t-\alpha), t)\end{aligned} \tag{B.7}$$

Computing the time-derivative of V along the trajectories of the system of Eq.B.5, we obtain:

$$\begin{aligned}\dot{V} \;&=\; \dot{\bar{e}}(t)^T P\bar{e}(t) + \bar{e}^T(t)P\dot{\bar{e}}(t) + a^2\Big(\bar{e}^T(t)\bar{e}(t) - \bar{e}^T(t-\alpha)\bar{e}(t-\alpha)\Big) \\ &\leq\; \Big(\bar{e}^T(t)\tilde{A}^T - \bar{e}^T(t)PbR_2^{-1}b^T \\ &\quad -\bar{\chi}w(\bar{e}(t),\phi)^T\tilde{c}_0^T(\bar{e}(t) + \bar{v}(t), \eta(t), \bar{e}(t-\alpha) + \bar{v}(t-\alpha), \eta(t-\alpha), t)b^T \\ &\quad +\bar{p}^T(\bar{e}(t) + \bar{v}(t), \eta(t), \bar{e}(t-\alpha) + \bar{v}(t-\alpha), \eta(t-\alpha), \theta(t-\alpha_\theta)) \\ &\quad +\delta_r(\bar{e}(t) + \bar{v}(t), \eta(t), \bar{e}(t-\alpha) + \bar{v}(t-\alpha), \eta(t-\alpha), \theta(t-\alpha_\theta))b^T\Big)\, P\bar{e}(t) \\ &\quad +\bar{e}^T(t)P\left(\tilde{A}\bar{e}(t) - bR_2^{-1}b^TP\bar{e}(t)\right. \\ &\quad -b\bar{\chi}\tilde{c}_0(\bar{e}(t) + \bar{v}(t), \eta(t), \bar{e}(t-\alpha) + \bar{v}(t-\alpha), \eta(t-\alpha), t)w(\bar{e}(t),\phi) \\ &\quad +\bar{p}(\bar{e}(t) + \bar{v}(t), \eta(t), \bar{e}(t-\alpha) + \bar{v}(t-\alpha), \eta(t-\alpha), \theta(t-\alpha_\theta)) \\ &\quad \left.+b\delta_r(\bar{e}(t) + \bar{v}(t), \eta(t), \bar{e}(t-\alpha) + \bar{v}(t-\alpha), \eta(t-\alpha), \theta(t-\alpha_\theta))\right) \\ &\quad +a^2(\bar{e}^T(t)\bar{e}(t) - \bar{e}^T(t-\alpha)\bar{e}(t-\alpha))\end{aligned}$$

$$
\begin{aligned}
&\leq \bar{e}^T(t)\left(\tilde{A}^T P + P\tilde{A} - 2P^T b R_2^{-1} b^T P + a^2 I_{n\times n}\right)\bar{e}(t) \\
&\quad +2\bar{p}^T\left(\bar{e}(t)+\bar{v}(t),\eta(t),\bar{e}(t-\alpha)+\bar{v}(t-\alpha),\eta(t-\alpha),\theta(t-\alpha_\theta)\right)P\bar{e}(t) \\
&\quad +2\left(-\bar{\chi}\tilde{c}_0(\bar{e}(t)+\bar{v}(t),\eta(t),\bar{e}(t-\alpha)+\bar{v}(t-\alpha),\eta(t-\alpha),t)w(\bar{e}(t),\phi)\right. \\
&\quad \left.+\delta_r(\bar{e}(t)+\bar{v}(t),\eta(t),\bar{e}(t-\alpha)+\bar{v}(t-\alpha),\eta(t-\alpha),\theta(t-\alpha_\theta))\right)b^T P\bar{e}(t) \\
&\quad -a^2\bar{e}^T(t-\alpha)\bar{e}(t-\alpha)
\end{aligned}
\tag{B.8}
$$

where $I_{n\times n}$ denotes the identity matrix of dimension $n \times n$.

Using the inequality $2x^T y \leq x^T x + y^T y$ where x and y are column vectors, we obtain:

$$
\begin{aligned}
\dot{V} &\leq \bar{e}^T(t)(\tilde{A}^T P + P\tilde{A} - 2P^T b R_2^{-1} b^T P + a^2 I_{n\times n} + P^2)\bar{e}(t) \\
&\quad +\bar{p}^2(\bar{e}(t)+\bar{v}(t),\eta(t),\bar{e}(t-\alpha)+\bar{v}(t-\alpha),\eta(t-\alpha),\theta(t-\alpha_\theta)) \\
&\quad -2\bar{\chi}\tilde{c}_0(\bar{e}(t)+\bar{v}(t),\eta(t),\bar{e}(t-\alpha)+\bar{v}(t-\alpha),\eta(t-\alpha),t)\frac{|b^T P\bar{e}|_{\mathbb{R}}^2}{|b^T P\bar{e}|_{\mathbb{R}}+\phi} \\
&\quad +2\delta_r(\bar{e}(t)+\bar{v}(t),\eta(t),\bar{e}(t-\alpha)+\bar{v}(t-\alpha),\eta(t-\alpha),\theta(t-\alpha_\theta))b^T P\bar{e} \\
&\quad -a^2\bar{e}^T(t-\alpha)\bar{e}(t-\alpha) \\
&\leq \bar{e}^T(t)(\tilde{A}^T P + P\tilde{A} - 2P^T b R_2^{-1} b^T P + a^2 I_{n\times n} + P^2)\bar{e}(t) \\
&\quad +\bar{p}^2(\bar{e}(t)+\bar{v}(t),\eta(t),\bar{e}(t-\alpha)+\bar{v}(t-\alpha),\eta(t-\alpha),\theta(t-\alpha_\theta)) \\
&\quad -\frac{2\bar{\chi}\tilde{c}_0(\bar{e}(t)+\bar{v}(t),\eta(t),\bar{e}(t-\alpha)+\bar{v}(t-\alpha),\eta(t-\alpha),t)|b^T P\bar{e}|_{\mathbb{R}}^2}{|b^T P\bar{e}|_{\mathbb{R}}+\phi} \\
&\quad +\frac{2\delta_r(\bar{e}(t)+\bar{v}(t),\eta(t),\bar{e}(t-\alpha)+\bar{v}(t-\alpha),\eta(t-\alpha),\theta(t-\alpha_\theta))|b^T P\bar{e}|_{\mathbb{R}}^2}{|b^T P\bar{e}|_{\mathbb{R}}+\phi} \\
&\quad +\frac{2\phi\delta_r(\bar{e}(t)+\bar{v}(t),\eta(t),\bar{e}(t-\alpha)+\bar{v}(t-\alpha),\eta(t-\alpha),\theta(t-\alpha_\theta))|b^T P\bar{e}|_{\mathbb{R}}}{|b^T P\bar{e}|_{\mathbb{R}}+\phi} \\
&\quad -a^2\bar{e}^T(t-\alpha)\bar{e}(t-\alpha) \\
&\leq \bar{e}^T(t)(\tilde{A}^T P + P\tilde{A} - 2P^T b R_2^{-1} b^T P + a^2 I_{n\times n} + P^2)\bar{e}(t) \\
&\quad +\bar{p}^2(\bar{e}(t)+\bar{v}(t),\eta(t),\bar{e}(t-\alpha)+\bar{v}(t-\alpha),\eta(t-\alpha),\theta(t-\alpha_\theta)) \\
&\quad -\frac{2(\bar{\chi}-1)\tilde{c}_0(\bar{e}(t)+\bar{v}(t),\eta(t),\bar{e}(t-\alpha)+\bar{v}(t-\alpha),\eta(t-\alpha),t)|b^T P\bar{e}|_{\mathbb{R}}^2}{|b^T P\bar{e}|_{\mathbb{R}}+\phi} \\
&\quad +\frac{2\phi\delta_r(\bar{e}(t)+\bar{v}(t),\eta(t),\bar{e}(t-\alpha)+\bar{v}(t-\alpha),\eta(t-\alpha),\theta(t-\alpha_\theta))|b^T P\bar{e}|_{\mathbb{R}}}{|b^T P\bar{e}|_{\mathbb{R}}+\phi} \\
&\quad -a^2\bar{e}^T(t-\alpha)\bar{e}(t-\alpha)
\end{aligned}
\tag{B.9}
$$

Assumption 4.4 implies that there exist positive real numbers a_1, a_2 such that the following bound holds:

$$\begin{aligned}\|\bar{p}(\bar{e}(t)+\bar{v}(t),\eta(t),\bar{e}(t-\alpha)+\bar{v}(t-\alpha),\eta(t-\alpha),\theta(t-\alpha_\theta))\|^2_{\mathbb{R}^r} \\ \leq a_1\bar{e}^2(t)+a_2\bar{e}^2(t-\alpha)\end{aligned} \tag{B.10}$$

Substituting the above inequality on the bound for $\dot{V}$ in Eq.B.9, we obtain:

$$\begin{aligned}\dot{V} \leq\ & \bar{e}^T(t)(\tilde{A}^TP+P\tilde{A}-2P^TbR_2^{-1}b^TP+(a^2+a_1)I_{n\times n}+P^2)\bar{e}(t) \\ & -(a^2-a_2)\bar{e}^2(t-\alpha) \\ & -2(\bar{\chi}-1)\tilde{c}_0(\bar{e}(t)+\bar{v}(t),\eta(t),\bar{e}(t-\alpha)+\bar{v}(t-\alpha),\eta(t-\alpha),t)|b^TP\bar{e}|_{\mathbb{R}} \\ & +2\phi\delta_r(\bar{e}(t)+\bar{v}(t),\eta(t),\bar{e}(t-\alpha)+\bar{v}(t-\alpha),\eta(t-\alpha),\theta(t-\alpha_\theta))\end{aligned} \tag{B.11}$$

Now, if $a^2-a_2=a_3$ where a_3 is a positive real number, and there exists a positive definite symmetric matrix P which solves the following matrix equation:

$$\tilde{A}^TP+P\tilde{A}-2P^TbR_2^{-1}b^TP+(a^2+a_1)I_{n\times n}+P^2=-R_1 \tag{B.12}$$

where R_1 is a positive definite matrix, then:

$$\begin{aligned}\dot{V} \leq\ & -\bar{e}^T(t)R_1\bar{e}(t)-a_3\bar{e}^2(t-\alpha) \\ & -2(\bar{\chi}-1)\tilde{c}_0(\bar{e}(t)+\bar{v}(t),\eta(t),\bar{e}(t-\alpha)+\bar{v}(t-\alpha),\eta(t-\alpha),t)|b^TP\bar{e}|_{\mathbb{R}} \\ & +2\phi\delta_r(\bar{e}(t)+\bar{v}(t),\eta(t),\bar{e}(t-\alpha)+\bar{v}(t-\alpha),\eta(t-\alpha),\theta(t-\alpha_\theta))\end{aligned} \tag{B.13}$$

Using the inequality $-\bar{e}^T(t)R_1\bar{e}(t)\leq-\lambda_{min}(R_1)\bar{e}^2(t)$ and since $\delta_r(\bar{e}(t)+\bar{v}(t),\eta(t),\bar{e}(t-\alpha)+\bar{v}(t-\alpha),\eta(t-\alpha),\theta(t-\alpha_\theta))\leq\tilde{c}_0(\bar{e}(t)+\bar{v}(t),\eta(t),\bar{e}(t-\alpha)+\bar{v}(t-\alpha),\eta(t-\alpha),t)$, we obtain:

$$\begin{aligned}\dot{V} \leq\ & -\lambda_{min}(R_1)\bar{e}^2(t)-a_3\bar{e}^2(t-\alpha) \\ & -2(\bar{\chi}-1)\tilde{c}_0(\bar{e}(t)+\bar{v}(t),\eta(t),\bar{e}(t-\alpha)+\bar{v}(t-\alpha),\eta(t-\alpha),t)|b^TP\bar{e}|_{\mathbb{R}} \\ & +2\phi\tilde{c}_0(\bar{e}(t)+\bar{v}(t),\eta(t),\bar{e}(t-\alpha)+\bar{v}(t-\alpha),\eta(t-\alpha),t)\end{aligned} \tag{B.14}$$

Therefore, we have that $\dot{V}$ satisfies the following property:

$$\dot{V}\leq-\lambda_{min}(R_1)\bar{e}^2(t)-a_3\bar{e}^2(t-\alpha),\qquad a_4\|\bar{e}(t)\|_{\mathbb{R}^r}\geq|b^TP\bar{e}(t)|_{\mathbb{R}}\geq\frac{\phi}{\bar{\chi}-1} \tag{B.15}$$

where a_4 is a positive real number. The above property implies that the ultimate bound on the state $\bar{e}(t)$ of the system of Eq.B.3 depends only on the parameter ϕ and is independent of the state η and the vector of uncertain variables θ. Specifically, from Theorem 4.1 we have that the above inequality implies that there exist positive real numbers K, β and a class $\mathcal{K}$ function γ_ϕ, such that the state of the $\bar{e}-$subsystem of Eq.B.4 satisfies:

$$|\bar{e}_t(\xi)| \leq Ke^{-\beta t}|\bar{e}_0(\xi)| + \gamma_\phi(\phi) \tag{B.16}$$

for every value of the delay, α. Now, since $|\bar{e}_1(t)|_{\mathbb{R}} \leq \|\bar{e}(t)\|_{\mathbb{R}^r} \leq |\bar{e}_t(\xi)|$, for any positive number d, there exists a ϕ^* such that if $\phi \in (0, \phi^*]$, it follows that $\lim_{t\to\infty} sup\,|y(t) - v(t)|_{\mathbb{R}} \leq d$.

To complete the proof of the theorem, we need to show that there exists a positive real number δ such that if $\max\{|x_0(\xi)|, ||\bar{v}_t||, ||\theta_t||\} \leq \delta$, then the state of the closed-loop system is ultimately bounded and the output of the closed-loop system satisfies $\lim_{t\to\infty} sup|y(t) - v(t)|_{\mathbb{R}} \leq d$. This result can be established by analyzing the behavior of the DDE system of Eq.B.3 using a small gain theorem type argument similar to the one used in the proof of Theorem 1 in [48]; the details of this part of the proof will be omitted for brevity. $\triangle$

Appendix C

Proofs of Chapter 5

Proof of Theorem 5.2:

The system of Eq.5.25, with $u \equiv 0$, can be equivalently written as:

$$\begin{aligned}\frac{dx_s}{dt} &= \mathcal{A}_s x_s + f_s(x_s(t), x_s(t-\alpha), 0, 0) + [f_s(x_s(t), x_s(t-\alpha), x_f(t), x_f(t-\alpha)) \\ &\quad - f_s(x_s, x_s(t-\alpha), 0, 0)] \\ \epsilon\frac{dx_f}{dt} &= \mathcal{A}_{f\epsilon} x_f + \epsilon f_f(x_s(t), x_s(t-\alpha), x_f(t), x_f(t-\alpha))\end{aligned} \tag{C.1}$$

Let μ_1^*, μ_2^* with $\mu_1^* \geq a_5$ and $\mu_2^* \geq b_5$ be two positive real numbers such that if $||x_s||_2 \leq \mu_1^*$ and $\|x_f\|_2 \leq \mu_2^*$, then there exist positive real numbers $(k_1, k_2, k_3, k_4, k_5, k_6)$ such that

$$\begin{aligned}&||f_s(x_s(t), x_s(t-\alpha), x_f(t), x_f(t-\alpha)) - f_s(x_s(t), x_s(t-\alpha), 0, 0)||_2 \\ &\qquad \leq k_1\|x_f(t)\|_2 + k_2\|x_f(t-\alpha)\|_2 \\ &\|f_f(x_s(t), x_s(t-\alpha), x_f(t), x_f(t-\alpha))\|_2 \\ &\qquad \leq k_3\|x_s(t)\|_2 + k_4||x_s(t-\alpha)||_2 + k_5\|x_f(t)\|_2 + k_6\|x_f(t-\alpha)\|_2\end{aligned} \tag{C.2}$$

Furthermore, since the fast subsystem of Eq.5.26 is exponentially stable, there exists a smooth Lyapunov functional $W : \mathcal{C}_f \to \mathbb{R}_{\geq 0}$ and a set of positive real numbers $(b_1, b_2, b_3, b_4, b_5, b_6, b_7)$, such that for all $x_f \in \mathcal{H}_f$ that satisfy $\|x_f\|_2 \leq b_7$, the following

conditions hold:

$$\begin{aligned} b_1||x_f(t)||_2^2 &\leq W(x_{f_t}) \leq b_2|x_{f_t}|^2 \\ \dot{W}(x_{f_t}) &= \frac{1}{\epsilon}\frac{\partial W}{\partial x_f}\mathcal{A}_{f\epsilon}x_f(t) \leq -\frac{b_3}{\epsilon}||x_f(t)||_2^2 - b_4||x_f(t-\alpha)||_2^2 \\ \left\|\frac{\partial W}{\partial x_f}\right\|_2 &\leq b_5||x_f(t)||_2 + b_6||x_f(t-\alpha)||_2 \end{aligned} \tag{C.3}$$

Pick $\mu_1 < a_7 < \mu_1^*$ and $\mu_2 < b_7 < \mu_2^*$. and consider the smooth time-varying function $L : \mathcal{C}_s \times \mathcal{C}_f \to \mathbb{R}_{\geq 0}$:

$$L(x_{s_t}, x_{f_t}) = V(x_{s_t}) + W(x_{f_t}) \tag{C.4}$$

where $V(x_{s_t})$ was defined in Assumption 5.2, as a Lyapunov function candidate for the system of Eq.C.1. From Eq.5.32 and Eq.C.3, we have that $L(x_{s_t}, x_{f_t})$ is positive definite, proper (tends to $+\infty$ as $|x_{s_t}| \to \infty$, or $|x_{f_t}| \to \infty$) and decrescent, with respect to its arguments. Computing the time-derivative of L along the trajectories of the system of Eq.C.1, and using the bounds of Eq.5.32 and Eq.C.3 and the estimates of Eq.C.2, the following expressions can be obtained:

$$\begin{aligned} \dot{L}(x_{s_t}, x_f) &= \frac{\partial V}{\partial x_s}\dot{x}_s + \frac{\partial W}{\partial x_f}\dot{x}_f \\ &= \frac{\partial V}{\partial x_s}[\mathcal{A}_s x_s + f_s(x_s(t), x_s(t-\alpha), 0, 0)] \\ &\quad + \frac{\partial V}{\partial x_s}[f_s(x_s(t), x_s(t-\alpha), x_f(t), x_f(t-\alpha)) - f_s(x_s(t), x_s(t-\alpha), 0, 0)] \\ &\quad + \frac{1}{\epsilon}\frac{\partial W}{\partial x_f}\mathcal{A}_{f\epsilon}x_f + \frac{\partial W}{\partial x_f}f_f(x_s(t), x_s(t-\alpha), x_f(t), x_f(t-\alpha)) \\ &\leq -a_3||x_s(t)||_2^2 - a_4||x_s(t-\alpha)||_2^2 + (a_5||x_s(t)||_2 + a_6||x_s(t-\alpha)||_2) \\ &\quad \times (k_1||x_f(t)||_2 + k_2||x_f(t-\alpha)||_2) - \frac{b_3}{\epsilon}\|x_f\|_2^2 - b_4||x_f(t-\alpha)||_2^2 \\ &\quad + (b_5||x_f(t)||_2 + b_6||x_f(t-\alpha)||_2)(k_3||x_s(t)||_2 \\ &\quad + k_4||x_s(t-\alpha)||_2 + k_5\|x_f(t)\|_2 + k_6\|x_f(t-\alpha)\|_2) \end{aligned}$$

$$
\begin{aligned}
\leq & -\left[\begin{array}{cc} \|x_s(t)\|_2 & \|x_f(t)\|_2 \end{array}\right]\left[\begin{array}{cc} a_3 & -\frac{a_5k_1+b_5k_3}{2} \\ -\frac{a_5k_1+b_5k_3}{2} & \frac{b_3}{\epsilon}-b_5k_5 \end{array}\right]\left[\begin{array}{c} \|x_s(t)\|_2 \\ \|x_f(t)\|_2 \end{array}\right] \\
& +2\left[\begin{array}{cc} \|x_s(t)\|_2 & \|x_f(t)\|_2 \end{array}\right]\left[\begin{array}{cc} \frac{a_5k_2}{2} & \frac{b_6k_3}{2} \\ \frac{a_6k_1+b_5k_4}{2} & \frac{b_5k_6+b_6k_5}{2} \end{array}\right]\left[\begin{array}{c} \|x_s(t-\alpha)\|_2 \\ \|x_f(t-\alpha)\|_2 \end{array}\right] \\
& -\left[\begin{array}{cc} \|x_s(t-\alpha)\|_2 & \|x_f(t-\alpha)\|_2 \end{array}\right]\left[\begin{array}{cc} a_4 & -\frac{a_6k_2+b_6k_4}{2} \\ -\frac{a_6k_2+b_6k_4}{2} & b_4-b_6k_6 \end{array}\right] \\
& \times\left[\begin{array}{c} \|x_s(t-\alpha)\|_2 \\ \|x_f(t-\alpha)\|_2 \end{array}\right] \\
\leq & -\left[\begin{array}{cc} \|x_s(t)\|_2 & \|x_f(t)\|_2 \end{array}\right] S_1\left[\begin{array}{c} \|x_s(t)\|_2 \\ \|x_f(t)\|_2 \end{array}\right]+2\left[\begin{array}{cc} \|x_s(t)\|_2 & \|x_f(t)\|_2 \end{array}\right] S_2 \\
& \times\left[\begin{array}{c} \|x_s(t-\alpha)\|_2 \\ \|x_f(t-\alpha)\|_2 \end{array}\right]-\left[\begin{array}{cc} \|x_s(t-\alpha)\|_2 & \|x_f(t-\alpha)\|_2 \end{array}\right] S_3\left[\begin{array}{c} |x_s(t-\alpha)| \\ \|x_f(t-\alpha)\|_2 \end{array}\right] \\
\leq & -\left[\begin{array}{cccc} \|x_s(t)\|_2 & \|x_f(t)\|_2 & \|x_s(t-\alpha)\|_2 & \|x_f(t-\alpha)\|_2 \end{array}\right]\left[\begin{array}{cc} S_1 & -S_2^T \\ -S_2 & S_3 \end{array}\right] \\
& \times\left[\begin{array}{c} \|x_s(t)\|_2 \\ \|x_f(t)\|_2 \\ \|x_s(t-\alpha)\|_2 \\ \|x_f(t-\alpha)\|_2 \end{array}\right]
\end{aligned}
\tag{C.5}
$$

where S_1, S_2, S_3 are constant matrices of the following form:

$$
\begin{aligned}
S_1 &= \left[\begin{array}{cc} a_3 & -\frac{a_5k_1+b_5k_3}{2} \\ -\frac{a_5k_1+b_5k_3}{2} & \frac{b_3}{\epsilon}-b_5k_5 \end{array}\right], \quad S_2=\left[\begin{array}{cc} \frac{a_5k_2}{2} & \frac{b_6k_3}{2} \\ \frac{a_6k_1+b_5k_4}{2} & \frac{b_5k_6+b_6k_5}{2} \end{array}\right], \\
S_3 &= \left[\begin{array}{cc} a_4 & -\frac{a_6k_2+b_6k_4}{2} \\ -\frac{a_6k_2+b_6k_4}{2} & b_4-b_6k_6 \end{array}\right]
\end{aligned}
\tag{C.6}
$$

Picking $\epsilon^* = \dfrac{(a_3-\sqrt{\delta})b_3}{(a_3-\sqrt{\delta})(b_5k_5+\sqrt{\delta})+\left(\frac{a_5k_1+b_5k_3}{2}\right)^2}$, where $\delta \in \mathbb{R}_{>0}$, we have that if $\epsilon \in (0, \epsilon^*]$ the matrix S_1 is positive definite. Then, under the assumption that the

matrix:

$$\begin{bmatrix} S_1 & -S_2^T \\ -S_2 & S_3 \end{bmatrix} \tag{C.7}$$

is positive definite, one can show (see [63] for details) that there exists a $\delta_1 \in \mathbb{R}_{>0}$ such that

$$\dot{L}(x_{st}, x_{f_t}) \leq -\delta_1(||x_s(t)||_2^2 + \|x_f(t)\|_2^2 + ||x_s(t-\alpha)||_2^2 + \|x_f(t-\alpha)\|_2^2) \tag{C.8}$$

which from the properties of L directly implies that the state of the system of Eq.C.1 is exponentially stable, i.e. there exists positive real numbers $K \geq 1, \sigma$ such that the relation of Eq.5.34 holds. $\triangle$

Proof of Theorem 5.3:

Substituting the output feedback controller of Eq.5.37-2.51 into the system of Eq.5.25 and defining $\Sigma_0(\omega_s(t), \bar{\eta}_s(t-\alpha), u(t)) + \cdots + \epsilon^k \Sigma_k(\omega_s(t), \bar{\eta}_s(t-\alpha), u(t)), \bar{\eta}_f(t-\alpha) =: \Sigma^k(\omega_s(t), \bar{\eta}_s(t-\alpha), u(t))$, we get:

$$\begin{aligned}
\dot{\omega}_s &= \mathcal{A}_s\omega_s + \mathcal{B}_s\mathcal{A}_c(\omega_s(t), \bar{v}(t), \omega_s(t-\alpha), \bar{v}(t-\alpha)) \\
&\quad + f_s(\omega_s(t), \bar{\eta}_s(t-\alpha), \Sigma^k(\omega_s(t), \bar{\eta}_s(t-\alpha), u(t)), \bar{\eta}_f(t-\alpha)) \\
&\quad + \Phi_{\mathcal{C}_s}(0) L(y_m(t-\tilde{\alpha}) - \mathcal{S}\omega_s(t-\tilde{\alpha})) \\
&\quad + \tilde{\mathcal{A}}_s \int_0^{\alpha-\tilde{\alpha}} \Phi_{\mathcal{C}_s}(\xi-\alpha) L(y_m(t-\xi-\tilde{\alpha}) - \mathcal{S}\omega_s(t-\xi-\tilde{\alpha}))d\xi, \quad \forall\, t \in (0, \alpha] \\
\dot{\omega}_s &= \mathcal{A}_s\omega_s + \mathcal{B}_s\mathcal{A}_c(\omega_s(t), \bar{v}(t), \omega_s(t-\alpha), \bar{v}(t-\alpha)) \\
&\quad + f_s(\omega_s(t), \omega_s(t-\alpha), \Sigma^k(\omega_s(t), \omega_s(t-\alpha), u(t)), \\
&\quad \Sigma^k(\omega_s(t-\alpha), \omega_s(t-2\alpha), u(t-\alpha))) + \Phi_{\mathcal{C}_s}(0) L(y_m(t-\tilde{\alpha}) - \mathcal{S}\omega_s(t-\tilde{\alpha})) \\
&\quad + \tilde{\mathcal{A}}_s \int_0^{\alpha} \Phi_{\mathcal{C}_s}(\xi-\alpha) L(y_m(t-\xi-\tilde{\alpha}) - \mathcal{S}\omega_s(t-\xi-\tilde{\alpha}))d\xi, \quad \forall\, t > \alpha \\
\frac{dx_s}{dt} &= \mathcal{A}_s x_s(t) + \mathcal{B}_s\mathcal{A}_c(\omega_s(t), \bar{v}(t), \omega_s(t-\alpha), \bar{v}(t-\alpha)) \\
&\quad + f_s(x_s(t), x_s(t-\alpha), x_f(t), x_f(t-\alpha))
\end{aligned}$$

$$
\begin{aligned}
\epsilon\frac{dx_f}{dt} &= \mathcal{A}_{f\epsilon}x_f(t) + \epsilon\mathcal{B}_f\mathcal{A}_\epsilon(\omega_s(t),\bar{v}(t),\omega_s(t-\alpha),\bar{v}(t-\alpha)) \\
&\quad +\epsilon f_f(x_s(t),x_s(t-\alpha),x_f(t),x_f(t-\alpha)) \\
y_{cs} &= Cx_s(t) + Cx_f(t)
\end{aligned} \tag{C.9}
$$

The fast dynamics of the above closed-loop system are described by the following system:

$$
\frac{dx_f}{d\tau} = \mathcal{A}_{f\epsilon}x_f \tag{C.10}
$$

which is exponentially stable (Assumption 5.2). The $O(\epsilon^{k+1})$ approximation of the closed-loop inertial form is:

$$
\begin{aligned}
\dot{\omega}_s &= \mathcal{A}_s\omega_s + \mathcal{B}_s\mathcal{A}_\epsilon(\omega_s(t),\bar{v}(t),\omega_s(t-\alpha),\bar{v}(t-\alpha)) \\
&\quad +f_s(\omega_s(t),\bar{\eta}_s(t-\alpha),\Sigma^k(\omega_s(t),\bar{\eta}_s(t-\alpha),u(t)),\bar{\eta}_f(t-\alpha)) \\
&\quad +\Phi_{C_s}(0)L(y_{ms}(t-\tilde{\alpha}) - \mathcal{S}\omega_s(t-\tilde{\alpha})) \\
&\quad +\tilde{\mathcal{A}}_s\int_0^{\alpha-\tilde{\alpha}}\Phi_{C_s}(\xi-\alpha)L(y_{ms}(t-\xi-\tilde{\alpha}) - \mathcal{S}\omega_s(t-\xi-\tilde{\alpha}))d\xi,\ \forall\, t\in[0,\alpha] \\
\dot{\omega}_s &= \mathcal{A}_s\omega_s + \mathcal{B}_s\mathcal{A}_\epsilon(\omega_s(t),\bar{v}(t),\omega_s(t-\alpha),\bar{v}(t-\alpha)) \\
&\quad +f_s(\omega_s(t),\omega_s(t-\alpha),\Sigma^k(\omega_s(t),\omega_s(t-\alpha),u(t)), \\
&\quad \Sigma^k(\omega_s(t-\alpha),\omega_s(t-2\alpha),u(t-\alpha))) + \Phi_{C_s}(0)L(y_{ms}(t-\tilde{\alpha}) - \mathcal{S}\omega_s(t-\tilde{\alpha})) \\
&\quad +\tilde{\mathcal{A}}_s\int_0^{\alpha-\tilde{\alpha}}\Phi_{C_s}(\xi-\alpha)L(y_{ms}(t-\xi-\tilde{\alpha}) - \mathcal{S}\omega_s(t-\xi-\tilde{\alpha}))d\xi, \quad \forall\, t>\alpha \\
\frac{dx_s}{dt} &= \mathcal{A}_s x_s(t) + \mathcal{B}_s\mathcal{A}_\epsilon(\omega_s(t),\bar{v}(t),\omega_s(t-\alpha),\bar{v}(t-\alpha)) + f_s(x_s(t),x_s(t-\alpha), \\
&\quad \Sigma^k(x_s(t),x_s(t-\alpha),u(t)),\Sigma^k(x_s(t-\alpha),x_s(t-2\alpha),u(t-\alpha))) \\
y_{cs} &= Cx_s(t) + \epsilon C(\Sigma_0(x_s(t),x_s(t-\alpha),u(t)) + \cdots + \epsilon^k\Sigma_k(x_s(t),x_s(t-\alpha),u(t)))
\end{aligned} \tag{C.11}
$$

From Assumption 5.3, we have that the above system is exponentially stable and the output asymptotically follows the reference input ($\lim_{t\to\infty}|y_{cs}(t) - v| = 0$). To conclude the proof of the theorem, we need to utilize the result of Theorem 5.2. Specifically, the exponential stability of the systems of Eqs.C.10-C.11 implies that there exist positive real numbers $\bar{\mu}_1, \bar{\mu}_2, \bar{\epsilon}^*$ such that if $|x_{s0}(\xi)| \leq \bar{\mu}_1$, $|x_{f0}(\xi)| \leq \bar{\mu}_2$ and $\epsilon \in (0, \bar{\epsilon}^*]$, and

the matrix

$$\begin{bmatrix} \bar{S}_1 & -\bar{S}_2^T \\ -\bar{S}_2 & \bar{S}_3 \end{bmatrix} \tag{C.12}$$

is positive definite, then the closed-loop system of Eq.C.9 is exponentially stable and the closed-loop output satisfies $\lim_{t\to\infty} |y_c(t) - v| = O(\epsilon^{k+1})$. We note that $\bar{S}_1, \bar{S}_2, \bar{S}_3$ are constant matrices whose structure is similar to the one shown in Eq.C.6; the computation of their explicit forms requires defining the appropriate bounds for the nonlinearities of the system of Eq.C.9 and is omitted for brevity. $\triangle$

Appendix D

Proofs of Chapter 7

Proof of Theorem 7.1:

The proof of this theorem will be obtained in two steps. In the first step, we will show exponentially stability and closeness of solutions for the closed-loop system of Eq.2.47, provided that the initial conditions and ϵ are sufficiently small. In the second step, we will exploit the closeness of solutions result to show that the cost associated with the closed-loop PDE system approaches the optimal cost associated with the closed-loop finite-dimensional system under state feedback control, when the initial conditions and ϵ are sufficiently small, thereby establishing that the location of the control actuators obtained by using the finite-dimensional system is near-optimal.

Exponential Stability - Closeness of Solutions:

Using that $\epsilon = \frac{|Re\ \lambda_1|}{|Re\ \lambda_{m+1}|}$ and under the controller of Eq.5.37, the closed-loop system of Eq.2.47 takes the form:

$$\begin{aligned} \frac{dx_s}{dt} &= \Lambda_s x_s + f_s(x_s, x_f) - f_s(x_s, 0) \\ \epsilon\frac{\partial x_f}{\partial t} &= \mathcal{A}_{f\epsilon} x_f + \epsilon \bar{f}_f(x_s, x_f) \end{aligned} \tag{D.1}$$

where $\mathcal{A}_{f\epsilon}$ is an unbounded differential operator defined as $\mathcal{A}_{f\epsilon} = \epsilon\mathcal{A}_f$, and $\bar{f}_f(x_s, x_f) = \mathcal{B}_f\mathcal{B}_s^{-1}((\mathcal{A}_s - \Lambda_s)x_s + f_s(x_s, 0)) + f_f(x_s, x_f)$. Since ϵ is a small positive number less

than unity (Assumption 7.1, part 3), the system of Eq.D.1 is in the standard singularly perturbed form, with x_s being the slow states and x_f being the fast states. Introducing the fast time-scale $\tau = \frac{t}{\epsilon}$ and setting $\epsilon = 0$, we obtain the following infinite-dimensional fast subsystem from the system of Eq.D.1:

$$\frac{\partial \tilde{x}_f}{\partial \tau} = \mathcal{A}_{f\epsilon}\tilde{x}_f \tag{D.2}$$

where the tilde symbol in $\tilde{x}_f$, denotes that the state $\tilde{x}_f$ is associated with the approximation of the fast x_f-subsystem. From the fact that $Re\ \lambda_{m+1} < 0$ and the definition of ϵ, we have that the above system is globally exponentially stable. Setting $\epsilon = 0$ in the system of Eq.D.1 and using that the operator $\mathcal{A}_{f\epsilon}$ is invertible, we have that:

$$\tilde{x}_f = 0 \tag{D.3}$$

and thus the closed-loop of the finite-dimensional slow system takes the form:

$$\frac{d\tilde{x}_s}{dt} = \Lambda_s \tilde{x}_s \tag{D.4}$$

The above slow subsystem is globally exponentially stable since Λ_s is a stable matrix. From the fact that the slow subsystem of Eq.D.4 and the fast subsystem of Eq.D.2 are globally exponentially stable, there exist positive real numbers μ_1, μ_2, and ϵ^* such that if $|x_s(t)| \leq \mu_1$, $\|x_f(t)\|_2 \leq \mu_2$, and $\epsilon \in (0, \epsilon^*]$, then the system of Eq.D.1 is exponentially stable and the solution $x_s(t), x_f(t)$ of the system of Eq.D.1 satisfies for all $t \in [t_b, \infty)$:

$$\begin{aligned} x_s(t) &= \tilde{x}_s(t) + O(\epsilon) \\ x_f(t) &= \tilde{x}_f(t) + O(\epsilon) \end{aligned} \tag{D.5}$$

where t_b is the time required for $x_f(t)$ to approach $\tilde{x}_f(t)$. $\tilde{x}_s(t)$ and $\tilde{x}_f(t)$ are the solutions of the slow and fast subsystems of Eq.D.2 and Eq.D.4 respectively ([46], Proposition 1).

Near-optimality of the actuator locations:

The cost for the closed-loop infinite-dimensional system can be written as follows:

$$\begin{aligned}\hat{J} &= \frac{1}{m}\sum_{i=1}^{m}\int_0^{t_b}((x_s^T(x_s^i(0),t),Q_s x_s(x_s^i(0),t))+(x_f^T(x_s^i(0),t),Q_f x_f(x_f^i(0),t))\\ &\quad +u^T(x_s(x_s^i(0),t),z_a)Ru(x_s(x_s^i(0),t),z_a))dt\\ &+ \frac{1}{m}\sum_{i=1}^{m}\int_{t_b}^{\infty}((x_s^T(x_s^i(0),t),Q_s x_s(x_s^i(0),t))+(x_f^T(x_s^i(0),t),Q_f x_f(x_f^i(0),t))\\ &\quad +u^T(x_s(x_s^i(0),t),z_a)Ru(x_s(x_s^i(0),t),z_a))dt\end{aligned} \tag{D.6}$$

It follows then from the continuity properties of the state $x(t)$ and the control $u(t)$ that for all $t \geq t_b$ and $i = 1,\ldots,m$:

$$\begin{aligned}&x_s(x_s^i(0),t) \longrightarrow \bar{x}_s(x_s^i(0),t), \qquad x_f(x_f^i(0),t) \longrightarrow 0,\\ &u(x_s(x_s^i(0),t),z_a) \longrightarrow u(\bar{x}_s(x_s^i(0),t),z_a) \qquad as \quad \epsilon \longrightarrow 0\end{aligned} \tag{D.7}$$

and hence:

$$\begin{aligned}&\frac{1}{m}\sum_{i=1}^{m}\int_{t_b}^{\infty}(x_s^T(x_s^i(0),t)Q_s x_s(x_s^i(0),t)+(x_f^T(x_f^i(0),t)Q_f x_f(x_f^i(0),t)\\ &\qquad +u^T(x_s(x_s^i(0),t),z_a)Ru(x_s(x_s^i(0),t),z_a))dt\\ &\longrightarrow \frac{1}{m}\sum_{i=1}^{m}\int_{t_b}^{\infty}(\bar{x}_s^T(x_s^i(0),t)Q_s\bar{x}_s(x_s^i(0),t)\\ &\qquad +u^T(\bar{x}_s(x_s^i(0),t),z_a)Ru(\bar{x}_s(x_s^i(0),t),z_a))dt \quad as \quad \epsilon \longrightarrow 0\end{aligned} \tag{D.8}$$

From the exponential stability of the closed-loop system, we have that there exists a positive real number M that bounds the integrand of Eq.D.6. Using the fact that $t_b = O(\epsilon)$, we then have:

$$\begin{aligned}&\frac{1}{m}\sum_{i=1}^{m}\int_0^{t_b}(x_s^T(x_s^i(0),t)Q_s x_s(x_s^i(0),t)+(x_f^T(x_f^i(0),t)Q_f x_f(x_f^i(0),t)\\ &\qquad +u^T(x_s(x_s^i(0),t),z_a)Ru(x_s(x_s^i(0),t),z_a))dt \;\leq\; \int_0^{t_b}M dt\\ &\qquad\qquad \leq\; M\epsilon\\ &\qquad\qquad =\; O(\epsilon)\end{aligned} \tag{D.9}$$

Similarly, from the stability of the closed-loop finite-dimensional system of Eq.2.48 and the fact that $t_b = O(\epsilon)$, we have that there exists a positive real number M' such

that:

$$\begin{aligned}
&\frac{1}{m}\sum_{i=1}^{m}\int_0^{t_b}(\tilde{x}_s^T(x_s^i(0),t)Q_s\tilde{x}_s(x_s^i(0),t) \\
+u^T(\tilde{x}_s(x_s^i(0),t),z_a)Ru(\tilde{x}_s(x_s^i(0),t),z_a))dt &\leq \int_0^{t_b} M'\,dt \\
&\leq M'\epsilon \\
&= O(\epsilon)
\end{aligned} \tag{D.10}$$

Combining Eqs.D.8-D.10, we obtain:

$$\begin{aligned}
&\frac{1}{m}\sum_{i=1}^{m}\int_{t_b}^{\infty}(x_s^T(x_s^i(0),t)Q_sx_s(x_s^i(0),t)+(x_f^T(x_f^i(0),t)Q_fx_f(x_f^i(0),t) \\
&\qquad +u^T(x_s(x_s^i(0),t),z_a)Ru(x_s(x_s^i(0),t),z_a))dt \\
\longrightarrow\ &\frac{1}{m}\sum_{i=1}^{m}\int_{t_b}^{\infty}(\tilde{x}_s^T(x_s^i(0),t)Q_s\tilde{x}_s(x_s^i(0),t) \\
&\qquad +u^T(\tilde{x}_s(x_s^i(0),t),z_a)Ru(\tilde{x}_s(x_s^i(0),t),z_a))dt \quad as \quad \epsilon\longrightarrow 0
\end{aligned} \tag{D.11}$$

This completes the proof of the theorem. △

Proof of Theorem 7.2:

Under the output feedback controller of Eq.7.24, the closed-loop system takes the form:

$$\begin{aligned}
\frac{dx_s}{dt} &= \Lambda_s x_s+(\mathcal{A}_s-\Lambda_s)x_f+f_s(x_s,x_f)-f_s(x_s+x_f,0) \\
\epsilon\frac{\partial x_f}{\partial t} &= \mathcal{A}_{f\epsilon}x_f+\epsilon\mathcal{B}_f\mathcal{B}_s^{-1}((\mathcal{A}_s-\Lambda_s)(x_s+x_f)+f_s(x_s+x_f,0))+\epsilon f_f(x_s,x_f)
\end{aligned} \tag{D.12}$$

Using that ϵ is a small positive number less than unity (Assumption 7.1, part 3), and introducing the fast time-scale $\tau=\dfrac{t}{\epsilon}$ and setting $\epsilon=0$, we obtain the following infinite-dimensional fast subsystem which describes the fast dynamics of the system of Eq.D.12:

$$\frac{\partial\tilde{x}_f}{\partial\tau} = \mathcal{A}_{f\epsilon}\tilde{x}_f \tag{D.13}$$

which is globally exponentially stable. Setting $\epsilon=0$ in the system of Eq.D.12 and

using that the operator $\mathcal{A}_{f\epsilon}$ is invertible, we have that:

$$\tilde{x}_f = 0 \tag{D.14}$$

and thus the closed-loop of the finite-dimensional slow system takes the form:

$$\frac{d\tilde{x}_s}{dt} = \Lambda_s \tilde{x}_s \tag{D.15}$$

From the fact that the slow subsystem of Eq.D.15 and the fast subsystem of Eq.D.2 are globally exponentially stable, there exist positive real numbers μ_1, μ_2, and ϵ^* such that if $|x_s(t)| \leq \mu_1$, $\|x_f(t)\|_2 \leq \mu_2$, and $\epsilon \in (0, \epsilon^*]$, then the system of Eq.D.1 is exponentially stable and the solution $x_s(t), x_f(t)$ of the system of Eq.D.12 satisfies the estimates of Eq.D.5.

Given the stability and closeness of solutions results for the closed-loop system, the near-optimality of the control actuators and measurement sensors in the sense described in Eq.7.25 can be established by using similar calculations to the ones in part 2 of the proof of Theorem 7.1. $\triangle$

Bibliography

[1] F. Allgöwer and F. J. Doyle. Nonlinear process control - which way to the promised land? In *Proceedings of 5th International Conference on Chemical Process Control.*, pages 24–25, Tahoe City, CA, 1997.

[2] F. Allgöwer, A. Rehm, and E. D. Gilles. An engineering perspective on nonlinear H^{∞} control. In *Proceedings of 33rd IEEE Conference on Decision and Control*, pages 2537–2542, Orlando, FL, 1994.

[3] J. Alvarez, J. A. Romagnoli, and G. Stefanopoulos. Variable measurement structures for the control of a tubular reactor. *Chem. Eng. Sci.*, 36:1695–1712, 1981.

[4] M. Amouroux, G. Di Pillo, and L. Grippo. Optimal selection of sensors and control location for a class of distributed parameter systems. *Ric. Automatica*, 7:92–, 1976.

[5] C. Antoniades and P. D. Christofides. Robust state estimation and control of nonlinear time delay processes. In *AIChE Annual Meeting, paper 228c, Miami, FL*, 1998.

[6] C. Antoniades and P. D. Christofides. Analyzing the interaction of design and control in transport-reaction processes. In *AIChE Annual Meeting, paper 219a, Dallas, TX*, 1999.

[7] C. Antoniades and P. D. Christofides. Feedback control of nonlinear differential difference equation systems. *Chem. Eng. Sci.*, 54:5677–5709, 1999.

[8] C. Antoniades and P. D. Christofides. Robust control of nonlinear time-delay systems. *Appl. Math. & Comp. Sci.*, 9:101–127, 1999.

[9] C. Antoniades and P. D. Christofides. Computation of optimal actuator locations for nonlinear controller in transport-reaction processes. *Comp. & Chem. Eng.*, 24:577–583, 2000.

[10] C. Antoniades and P. D. Christofides. Integrating nonlinear output feedback control and optimal actuator/sensor placement for transport-reaction processes. *Chem. Eng. Sci.*, submitted,., 2000.

[11] C. Antoniades and P. D. Christofides. Nonlinear dynamics and control of a tubular reactor with recycle. *Nonlinear Analysis: Theory, Methods and Applications*, submitted,, 2000.

[12] C. Antoniades and P. D. Christofides. Nonlinear feedback control of parabolic partial differential difference equation systems. *Int. J. Contr.*, 73:1572–1591, 2000.

[13] A. Arbel. Controllability measures and actuator placement in oscillatory systems. *Int. J. Contr.*, 33:565–574, 1981.

[14] A. Arbel, I. H. Rinard, and R. Shinnar. Dynamics and control of fluidized catalytic crackers. 1. Modeling of the current generation of the FCC's. *Ind. Eng. Chem. Res.*, 34:1228–1243, 1995.

[15] A. Arbel, I. H. Rinard, and R. Shinnar. Dynamics and control of fluidized catalytic crackers. 3. Designing the control system: Choice of manipulated and

measured variables for partial control. *Ind. Eng. Chem. Res.*, 35:2215–2233, 1996.

[16] Y. Arkun and J. P. Calvet. Robust stabilization of input/output linearizable systems under uncertainty and disturbances. *AIChE J.*, 38:1145–1154, 1992.

[17] M. Athans. Toward a practical theory of distributed parameter systems. *IEEE Trans. Automat. Contr.*, AC-15:245–247, 1970.

[18] M. J. Balas. Feedback control of linear diffusion processes. *Int. J. Contr.*, 29:523–533, 1979.

[19] M. J. Balas. Trends in large scale structure control theory: Fondest hopes, wildest dreams. *IEEE Trans. Automat. Contr.*, 27:522–535, 1982.

[20] J. F. Bartee, K. F. Bloss, and C. Georgakis. Design of nonlinear reference system control structures. In *AIChE Annual Meeting, San Francisco, CA*, 1989.

[21] W. B. Bequette. Nonlinear control of chemical processes: A review. *Ind. Eng. Chem. Res.*, 30:1391–1413, 1991.

[22] M. Berezowski. A sufficient condition for the existence of single steady states in chemical reactors with recycle. *Chem. Eng. Sci.*, 45:1325–1329, 1990.

[23] M. Berezowski. Method for analyzing global stability of pseudo-homogeneous chemical reactors with recycle. *Chem. Eng. Sci.*, 46:1781–1785, 1991.

[24] M. Berezowski. Dynamic profiles of chemical reactors with recycle. *Chem. Eng. Sci.*, 48:2799–2806, 1993.

[25] M. Berezowski. Stabilization of unstable steady states of adiabatic tubular reactors with recycle. *Chem. Eng. Sci.*, 50:1989–1996, 1995.

[26] M. Berezowski. Chaotic dynamics in homogeneous tubular reactors with recycle. *Chem. Eng. Sci.*, 53:4023–4029, 1998.

[27] K. P. M. Bhat and H. N. Koivo. Modal characterizations of controllability and observability in time delay systems. *IEEE Trans. Automat. Contr.*, 21:292–293, 1976.

[28] C. Brosilow. Structure and design of Smith predictors from the viewpoint of inferential control. In *Proceedings of Joint American Control Conference*, 1976.

[29] Y. Y. Cao, Y. X. Sun W. J. Wu, and C. Cheng. Delay-dependent robust stabilization of uncertain systems with multiple state delays. In *Proceedings of IFAC-IFIP-IMACS Conference*, pages 383–387, Belfort, France, 1997.

[30] C. C. Chen and H. C. Chang. Accelerated disturbance damping of an unknown distributed system by nonlinear feedback. *AIChE J.*, 38:1461–1476, 1992.

[31] W. H. Chen and J. H. Seinfeld. Optimal location of process measurements. *Int. J. Control*, 21:1003–1014, 1975.

[32] D. Chmielewski and V. Manousiouthakis. Constrained infinite-time nonlinear quadratic-optimal control with application to chemical reactors. In *Proceedings of Conference on Control Applications*, Honolulu, HA, 1998.

[33] K. Choe and H. Baruh. Actuator placement in structural control. *J. Guidance*, 15:40–48, 1992.

[34] P. D. Christofides. Output feedback control of nonlinear two-time-scale systems. In *Proceedings of American Control Conference*, pages 1729–1733, Albuquerque, NM, 1997.

[35] P. D. Christofides. Output feedback control of nonlinear two-time-scale processes. *Ind. & Eng. Chem. Res.*, 37:1893–1909, 1998.

[36] P. D. Christofides. *Nonlinear and Robust Control of PDE Systems: Methods and Applications to Transport-Reaction Processes,* to appear. Birkhäuser, Boston, 2000.

[37] P. D. Christofides. Robust output feedback control of nonlinear singularly perturbed systems. *Automatica*, 36:45–52, 2000.

[38] P. D. Christofides and C. Antoniades. Control of nonlinear differential difference equation systems. In *AIChE Annual Meeting, paper 191i, Los Angeles, CA*, 1997.

[39] P. D. Christofides and C. Antoniades. Control of nonlinear differential difference equation systems. In *Proceedings of Mathematical Theory of Networks and Systems-98 Conference*, pages 41–44, Padova, Italy, 1998.

[40] P. D. Christofides and J. Baker. Robust output feedback control of quasi–linear parabolic PDE systems. *Syst. & Contr. Lett.*, 36:307–316, 1999.

[41] P. D. Christofides and P. Daoutidis. Compensation of measurable disturbances in two-time-scale nonlinear systems. *Automatica*, 32:1553–1573, 1996.

[42] P. D. Christofides and P. Daoutidis. Feedback control of hyperbolic PDE systems. *AIChE J.*, 42:3063–3086, 1996.

[43] P. D. Christofides and P. Daoutidis. Feedback control of two-time-scale nonlinear systems. *Int. J. Contr.*, 63:965–994, 1996.

[44] P. D. Christofides and P. Daoutidis. Nonlinear control of diffusion-convection-reaction processes. *Comp. Chem. Engng.*, 20(s):1071–1076, 1996.

[45] P. D. Christofides and P. Daoutidis. Control of nonlinear distributed parameter systems: Recent results and future research directions. In *Proceedings of 5th International Conference on Chemical Process Control.*, pages 302–306, Tahoe City, CA, 1997.

[46] P. D. Christofides and P. Daoutidis. Finite-dimensional control of parabolic PDE systems using approximate inertial manifolds. *J. Math. Anal. Appl.*, 216:398–420, 1997.

[47] P. D. Christofides and P. Daoutidis. Robust control of multivariable two-time-scale nonlinear systems. *J. Proc. Contr.*, 7:313–328, 1997.

[48] P. D. Christofides, A. R. Teel, and P. Daoutidis. Robust semi-global output tracking for nonlinear singularly perturbed systems. *Int. J. Contr.*, 65:639–666, 1996.

[49] G. Colantuoni and L. Padmanabhan. Optimal sensor locations for tubular-flow reactor systems. *Chem. Eng. Sci.*, 32:1035–1049, 1977.

[50] M. Corless. Control of uncertain nonlinear systems. *J. Dyn. Sys., Meas. & Contr.*, 115:362–372, 1993.

[51] M. Courdesses. Optimal sensors and controllers allocation in output feedback control. In *Proc. Symp. on Advances in Measurement & Control*, pages 735–740, Athens, 1978.

[52] P. Daoutidis and P. D. Christofides. Dynamic feedforward/output feedback control of nonlinear processes. *Chem. Eng. Sci.*, 50:1889–2007, 1995.

[53] P. Daoutidis and C. Kravaris. Dynamic output feedback control of multivariable nonlinear processes. *Chem. Eng. Sci.*, 49:433–447, 1994.

[54] M. A. Demetriou. Numerical investigation on optimal actuator/sensor location of parabolic PDEs. In *Proceedings of the American Control Conference*, pages 1722–1726, San Diego, CA, 1999.

[55] M. M. Denn. *Process Modeling.* Longam Inc., New York, 1986.

[56] J. Doyle, K. Glover, P. P. Khargonekar, and B. A. Francis. State space solutions to standard H_2 and H^∞ control problems. *IEEE Trans. Automat. Contr.*, 34:831–847, 1993.

[57] C. Foias, M. S. Jolly, I. G. Kevrekidis, G. R. Sell, and E. S. Titi. On the computation of inertial manifolds. *Phys. Lett. A*, 131:433–437, 1989.

[58] C. Foias, G. R. Sell, and E. S. Titi. Exponential tracking and approximation of inertial manifolds for dissipative equations. *J. Dynamics and Differential Equations*, 1:199–244, 1989.

[59] A. Friedman. *Partial Differential Equations.* Holt, Rinehart & Winston, New York, 1976.

[60] C. E. Garcia and M. Morari. Internal model control. 1: A unifying review and some new results. *Ind. & Eng. Chem. Proc. Des. Devel.*, 21:308–322, 1982.

[61] C. E. Garcia and M. Morari. Internal model control. 2: Design procedure for multivariable systems. *Ind. & Eng. Chem. Proc. Des. Devel.*, 24:472–484, 1985.

[62] G. Gu, P. P. Khargonekar, and E. B. Lee. Approximation of infinite dimensional systems. *IEEE Trans. Automat. Contr.*, 34:610–618, 1989.

[63] J. K. Hale and S. M. Verduyn Lunel. *Introduction to Functional Differential Equations.* Springer-Verlag, New York, 1993.

[64] T. J. Harris, J. F. MacGregor, and J. D. Wright. Optimal sensor location with an application to a packed bed tubular reactor. *AIChE J.*, 26:910–916, 1980.

[65] M. A. Henson and D. E. Seborg. Time delay compensation for nonlinear processes. *Ind. Eng. Chem. Res.*, 33:1493–1500, 1994.

[66] P. Holmes, J. L. Lumley, and G. Berkooz. *Turbulence, Coherent Structures, Dynamical Systems and Symmetry.* Cambridge University Press, New York, 1996.

[67] I. Huq, M. Morari, and R. C. Sorensen. Modifications to model IV fluid catalytic cracking units to improve dynamic performance. *AIChE J.*, 41:1481–1499, 1995.

[68] A. Ichikawa and E. P. Ryan. Filtering and control of distributed parameter systems with point observations and inputs. In *Proc. 2nd IFAC Symp. on Control of D.P.S.*, pages 347–357, Coventry, 1977.

[69] A. Isidori. *Nonlinear Control Systems: An Introduction.* Springer-Verlag, Berlin-Heidelberg, second edition, 1989.

[70] K. F. Jensen and W. H. Ray. The bifurcation behavior of tubular reactor. *Chem. Eng. Sci.*, 37:199–222, 1982.

[71] N. F. Jerome and W. H. Ray. High performance multivariable control strategies for systems having time delays. *AIChE J.*, 32:914–931, 1986.

[72] I. Kanellakopoulos, P. V. Kokotovic, and R. Marino. An extended direct scheme for robust adaptive nonlinear control. *Automatica*, 27:247–255, 1991.

[73] N. Kapoor and P. Daoutidis. Windup compensation for nonlinear systems with input constraints. In *AIChE Ann. Mtg., paper 4b, Chicago, IL*, 1996.

[74] I. Karafyllis and P. Daoutidis. Control of hot spots in tubular reactors. In *AIChE Annual Meeting, paper 193i, Los Angeles, CA*, 1997.

[75] N. Kazantzis and C. Kravaris. A nonlinear Luenberger-type observer with application to catalytic activity estimation. In *Proceedings of American Control Conference*, pages 1756–1760, Seattle, WA, 1995.

[76] T. A. Kendi and F. J. Doyle. An anti-windup scheme for input-output linearization. In *Proceedings of 3rd European Control Conference*, pages 2653–2658, Rome, Italy, 1995.

[77] H. K. Khalil. Robust servomechanism output feedback controller for feedback linearizable systems. *Automatica*, 30:1587–1599, 1994.

[78] H. K. Khalil. *Nonlinear Systems*. Prentice Hall, New Jersey, second edition, 1996.

[79] H. N. Koivo and A. J. Koivo. Control and estimation of systems with time-delays. In *Distributed Parameter Systems*, W. H. Ray and D. G. Lainiotis (eds.), New York, NY, 1978.

[80] P. V. Kokotovic, H. K. Khalil, and J. O'Reilly. *Singular Perturbations in Control: Analysis and Design*. Academic Press, London, 1986.

[81] A. Kowalewski. Optimal control of distributed parabolic systems with multiple time-delay lags. *Int. J. Contr.*, 69:361–381, 1998.

[82] C. Kravaris and Y. Arkun. Geometric nonlinear control - an overview. In *Proceedings of 4th International Conference on Chemical Process Control*, pages 477–515, Y. Arkun and W. H. Ray Eds., Padre Island, TX, 1991.

[83] C. Kravaris and C. B. Chung. Nonlinear state feedback synthesis by global input/output linearization. *AIChE J.*, 33:592–604, 1987.

[84] C. Kravaris and J. C. Kantor. Geometric methods for nonlinear process control 1. Background. *Ind. Eng. Chem. Res.*, 29:2295–2310, 1990.

[85] C. Kravaris and J. C. Kantor. Geometric methods for nonlinear process control 2. Controller synthesis. *Ind. Eng. Chem. Res.*, 29:2310–2323, 1990.

[86] C. Kravaris and S. Palanki. Robust nonlinear state feedback under structured uncertainty. *AIChE J.*, 34:1119–1127, 1988.

[87] C. Kravaris and R. A. Wright. Dead-time compensation for nonlinear processes. *AIChE J.*, 35:1535–1542, 1989.

[88] M. Krstic, I. Kanellakopoulos, and P. Kokotovic. *Nonlinear and Adaptive Control Design.* Wiley-Interscience, New York, 1995.

[89] C. S. Kubrusly and H. Malebranche. Sensors and controllers location in distributed systems-a survey. *Automatica*, 21:117–128, 1985.

[90] A. Kumar, P. D. Christofides, and P. Daoutidis. Singular perturbation modeling and control of nonlinear two-time-scale processes with non-explicit time-scale multiplicity. *Chem. Eng. Sci.*, 53:1491–1504, 1998.

[91] S. Kumar and J. H. Seinfeld. Optimal location of measurements for distributed parameter estimation. *IEEE Trans. Automat. Contr.*, AC-23:690–698, 1978.

[92] S. Kumar and J. H. Seinfeld. Optimal location of measurements in tubular reactors. *Chem. Eng. Sci.*, 33:1507–1516, 1978.

[93] N. Kunimatsu and H. Sano. Compensator design of semilinear parabolic systems. *Int. J. Contr.*, 60:243–263, 1994.

[94] M. J. Kurtz and M. A. Henson. Constrained output feedback control of a multivariable polymerization reactor. In *Proceedings of American Control Conference*, pages 2950–2954, Albuquerque, NM, 1997.

[95] M. J. Kurtz and M. A. Henson. Linear model predictive control of input-output linearized processes with constraints. In *Proceedings of 5th International Conference on Chemical Process Control.*, pages 335–338, Tahoe City, CA, 1997.

[96] I. Lasiecka. Control of systems governed by partial differential equations: A historical perspective. In *Proceedings of 34th IEEE Conference on Decision and Control*, pages 2792–2797, New Orleans, LA, 1995.

[97] J. H. Lee. Recent advances in model predictive control and other related areas. In *Proceedings of 5th International Conference on Chemical Process Control.*, pages 201–216, Tahoe City, CA, 1997.

[98] B. Lehman, I. Widjaya, and K. Shujaee. Vibrational control of chemical reactions in a CSTR with delayed recycle stream. *J. Math. Anal. Appl.*, 193:28–59, 1995.

[99] G. Leitmann. On one approach to the control of uncertain systems. *J. Dyn. Sys., Meas. & Contr.*, 115:373–380, 1993.

[100] J. Levine and P. Rouchon. Quality control of binary distillation columns via nonlinear aggregated models. *Automatica*, 27:463–480, 1991.

[101] W. S. Levine and M. Athans. On the determination of the optimal constant output feedback gains for linear multivariable system. *IEEE Trans. Automat. Contr.*, 15:44–48, 1978.

[102] H. Li, S. I. Niculescu, L. Dugard, and J. M. Dion. Robust decentralized H^∞ control of interconnected uncertain time delay systems. In *Proceedings of IFAC-IFIP-IMACS Conference*, pages 347–352, Belfort, France, 1997.

[103] W. Lu, E. B. Lee, and Q. T. Zhang. Balanced approximation of two-dimensional and delay-differential equations. *Int. J. Contr.*, 46:2199–2218, 1987.

[104] C. G. Malandrakis. Optimal sensor and controller allocation for a class of distributed parameter systems. *Int. J. Syst. Sci.*, 10:1283–, 1979.

[105] A. Manitius and H. Tran. Computation of closed-loop eigenvalues associated with the optimal regulator problem for functional differential equations. *IEEE Trans. Autom. Contr.*, 30:1245–1248, 1985.

[106] A. Manitius, H. Tran, G. Payre, and R. Roy. Computation of eigenvalues associated with functional differential equations. *SIAM J. Sci. Stat. Comput.*, 8:222–247, 1987.

[107] R. Marino and P. Tomei. Global adaptive output feedback control of nonlinear systems, part 1: Linear parameterization. *IEEE Trans. Autom. Contr.*, 38:17–32, 1993.

[108] R. C. McFarlane, R. C. Reineman, J. F. Bartee, and C. Georgakis. Dynamic simulator for a model iv fluid catalytic cracking unit. *Comp. & Chem. Eng.*, 17:275–293, 1993.

[109] J. J. Monge and C. Georgakis. The effect of operating variables on the dynamics of catalytic cracking processes. *Chem. Eng. Comm.*, 60:1–15, 1987.

[110] C. H. Moog, R. Castro, and M. Velasco. The dynamic disturbance decoupling problem for time-delay nonlinear systems. In *Proceedings of 35th Conference on Decision & Control*, pages 821–822, Kobe, Japan, 1996.

[111] C. F. Moore, C. L. Smith, and P. W. Murril. Improved algorithm for direct digital control. *Instr. & Contr. Syst.*, 43:70–79, 1970.

[112] M. Morari and M. J. O'Dowd. Optimal sensor location in the presence of nonstationary noise. *Automatica*, 16:463–480, 1980.

[113] G. J. Nazaroff. Stability and stabilization of linear differential delay systems. *IEEE Trans. Autom. Contr.*, 18:317–318, 1973.

[114] B. A. Ogunnaike and W. H. Ray. Multivariable controller design for linear systems having multiple time delays. *AIChE J.*, 25:1042–1057, 1979.

[115] B. A. Ogunnaike and R. A. Wright. Industrial applications of nonlinear control. In *Proceedings of 5th International Conference on Chemical Process Control.*, pages 46–59, Tahoe City, CA, 1997.

[116] S. Omatu, S. Koide, and T. Soeda. Optimal sensor location problem for a linear distributed parameter system. *IEEE Trans. Automat. Contr.*, AC-23:665–673, 1978.

[117] S. Omatu and J. H. Seinfeld. Optimization of sensor and actuator location in a distributed parameter system. *J. Franklin Inst.*, 315:407–421, 1983.

[118] J. R. Partington. Approximation of delay system by Fourier-Laguerre series. *Automatica*, 27:569–572, 1991.

[119] S. Phoojaruenchanachai and K. Furuta. Memoryless stabilization of uncertain linear systems incluting time-varying state delays. *IEEE Trans. Automat. Contr.*, 37:1022–1026, 1992.

[120] S. S. Rao, T. S. Pan, and V. B. Venkayya. Optimal placement of actuators in actively controlled structures using genetic algorithms. *AIAA J.*, 29:942–943, 1991.

[121] J. B. Rawlings, E. S. Meadows, and K. R. Muske. Nonlinear model predictive control: A tutorial and survey. In *Proceedings of International Symposium on Advanced Control of Chemical Processes*, pages 203–214, Kyoto, Japan, 1994.

[122] W. H. Ray. *Advanced Process Control.* McGraw-Hill, New York, 1981.

[123] P. Renard, D. Dochain, G. Bastin, H. Naveau, and E. J. Nyns. Adaptive control of anaerobic digestion processes: A pilot-scale application. *Biotech. Bioeng.*, 31:287–294, 1988.

[124] R. B. Root and R. A. Schmitz. An experimental study of steady state multiplicity in a loop reactor. *AIChE J.*, 15:670–679, 1969.

[125] R. B. Root and R. A. Schmitz. An experimental study of unstable states in a loop reactor. *AIChE J.*, 16:356–358, 1970.

[126] D. W. Ross and I. Flugge-Lotz. An optimal control problem for systems described by differential-difference equations. *SIAM J. Opt. Contr.*, 7:609–623, 1969.

[127] H. Sano and N. Kunimatsu. Feedback control of semi-linear diffusion systems: Inertial manifolds for closed-loop systems. *IMA J. Math. Contr. Inform.*, 11:75–92, 1994.

[128] H. Sano and N. Kunimatsu. An application of inertial manifold theory to boundary stabilization of semi-linear diffusion systems. *J. Math. Anal. Appl.*, 196:18–42, 1995.

[129] S. S. Sastry and A. Isidori. Adaptive control of linearizable systems. *IEEE Trans. Automat. Contr.*, 34:1123–1131, 1989.

[130] K. K. Shyu and J. J. Yan. Robust stability of uncertain time-delay systems and its stabilization by variable styructure control. *Int. J. Contr.*, 57:237–246, 1993.

[131] P. Singstad, H. Nordhus, K. Strand, M. Lien, L. B. Lyngmo, and O. Moen. Multivariable nonlinear control of industrial LDPE reactors. In *Proceedings of American Control Conference*, pages 615–620, Chicago, Il, 1992.

[132] M. Skliar and W. F. Ramirez. Source identification in the distributed parameter systems. *Appl. Math. & Comp. Sci.*, 8:733–754, 1998.

[133] O. J. M. Smith. Closer control of loops with dead time. *Chem. Eng. Prog.*, 53:217–225, 1957.

[134] M. A. Soliman and W. H. Ray. Optimal feedback control for linear quadratic systems having time delays. *Int. J. Contr.*, 15:609–627, 1972.

[135] M. Soroush. Nonlinear output feedback control of a polymerization reactor. In *Proceedings of American Control Conference*, pages 2672–2676, Seattle, WA, 1995.

[136] M. Soroush. Nonlinear state observer design with application to reactors. *Chem. Eng. Sci.*, 52:387–404, 1997.

[137] M. Soroush and C. Kravaris. Nonlinear control of a batch polymerization reactor: an experimental study. *AIChE J.*, 38:1429–1443, 1992.

[138] M. Soroush and C. Kravaris. Nonlinear control of a polymerization CSTR with singular characteristic matrix. *AIChE J.*, 40:980–990, 1994.

[139] M. Soroush and M. Nikravesh. Shortest-prediction-horizon nonlinear model predictive control. In *Proceedings of 13th IFAC World Congress*, pages 19–24, (Vol. M), San Francisco, CA, 1996.

[140] G. Stephanopoulos. *Chemical Process Control: An Introduction to Theory and Practice.* Prentice Hall, Englewood Cliffs, New Jersey, 1984.

[141] S. Subramanian and V. Balakotaiah. Classification of steady-state and dynamic behaviour of distributed reactor models. *Chem. Eng. Sci.*, 51:401–421, 1996.

[142] A. Teel, R. Kadiyala, P. V. Kokotovic, and S. Sastry. Indirect techniques for adaptive input-output linearization of nonlinear systems. *Int. J. Contr.*, 53:193–222, 1991.

[143] A. R. Teel. Connections between Razumikhin-type theorems and the ISS nonlinear small-gain theorem. *IEEE Trans. Autom. Contr.*, 43:960–965, 1998.

[144] R. Temam. *Infinite-Dimensional Dynamical Systems in Mechanics and Physics.* Springer-Verlag, New York, 1988.

[145] A. Thowsen. Uniform ultimate boundedness of solutions of uncertain dynamic delay systems with state-dependent and memoryless feedback control. *Int. J. Contr.*, 37:1135–1143, 1983.

[146] A. Trofino, H. Li, L. Dugard, J. M. Dion, and S. I. Niculescu. Constrained robust guaranteed cost control for uncertain linear time delay systems. In *Proceedings of 36th Conference on Decision & Control*, pages 1615–1620, San Diego, CA, 1997.

[147] K. Vit. Smith-like predictor for control of parameter-distributed processes. *Int. J. Contr.*, 30:179–191, 1979.

[148] B. Wahlberg. System identification using laguerre models. *IEEE Trans. Autom. Contr.*, 36:551–562, 1991.

[149] W. Waldraff, D. Dochain, S. Bourrel, and A. Magnus. On the use of observability measures for sensor location in tubular reactor. *J. Proc. Contr.*, 8:497–505, 1998.

[150] P. K. C. Wang. Optimal control of parabolic systems with boundary conditions involving time-delays. *SIAM J. Contr.*, 13:274–293, 1975.

[151] M. C. Wellons and T. F. Edgar. The generalized analytical predictor. *Ind. & Eng. Chem. Res.*, 26:1523–1532, 1987.

[152] S. K. P. Wong and D. E. Seborg. A theoretical analysis of smith and analytical predictors. *AIChE J.*, 32:1597–1605, 1986.

[153] S. K. P. Wong and D. E. Seborg. Control strategy for single-input single-output nonlinear systems with time delays. *Int. J. Contr.*, 48:2303–2327, 1988.

[154] R. A. Wright and C. Kravaris. Nonlinear control of pH processes using the strong acid equivalent. *Ind. Eng. Chem. Res.*, 30:1561–1572, 1991.

[155] R. A. Wright, M. Soroush, and C. Kravaris. Strong acid equivalent control of pH processes: An experimental study. *Ind. Eng. Chem. Res.*, 30:2439–2448, 1991.

[156] B. Xu and Y. Liu. An improved Razumikhin-type theorem and its applications. *IEEE Trans. Autom. Contr.*, 39:839–841, 1994.

[157] K. Xu, P. Warnitchai, and T. Igusa. Optimal placement and gains of sensors and actuators for feedback control. *J. Guid. Contr. Dyn*, 17:929–934, 1994.

[158] V. Z . Yakhinin, A. B. Rovinsky, and M. Menzinger. Convective instability induced by differential transport in the tubular packed bed reactor. *Chem. Eng. Sci.*, 50:2853–2859, 1995.

[159] V. Z. Yakhinin, A. B. Rovinsky, and M. Menzinger. Absolute stability of tubular packed bed reactor with recycle. *Chem. Eng. Sci.*, 50:1591–1593, 1995.

[160] D. Yanakiev and I. Kanellakopoulos. Longitudinal control of automated chvs with significant actuator delays. In *Proceedings of 36th Conference on Decision & Control*, pages 4756–4763, San Diego, California, 1997.

[161] T. K. Yu and J. H. Seinfeld. Observability and optimal measurement location in linear distributed parameter systems. *Int. J. Contr*, 18:785–799, 1973.